

Some pages of this thesis may have been removed for copyright restrictions.

If you have discovered material in AURA which is unlawful e.g. breaches copyright, (either yours or that of a third party) or any other law, including but not limited to those relating to patent, trademark, confidentiality, data protection, obscenity, defamation, libel, then please read our [Takedown Policy](#) and [contact the service](#) immediately

ELECTRODEPOSITION OF CORROSION RESISTANT
ZINC ALLOY COATINGS

ABDELHAFID ABIBSI

Doctor of Philosophy

THE UNIVERSITY OF ASTON IN BIRMINGHAM

NOVEMBER 1988

This copy of the thesis has been supplied on condition that anyone who consults it is understood to recognise that its copyright rests with its author and that no quotation from the thesis and no information derived from it may be published without the author's prior written consent.

The University of Aston in Birmingham

Title: Electrodeposition of Corrosion Resistant Zn alloy Coatings

Author: Abdelhafid Abibsi

Degree: Doctor of Philosophy

Date: November 1988

SUMMARY

With the increase use of de-icing salts on roads for safety, the need for improved corrosion resistance of the traditional galvanized automobile bodies has never been greater. In the present work, Zn alloy coatings (Zn-Ni and Zn-Co) were studied as an alternative to pure Zn coatings.

The production of these deposits involved formulation of various acidic (pH of about 5.5) chloride based solutions. These showed anomalous deposition, that is, alloys were deposited much more easily than expected from the noble behaviour of Ni and Co metals. Coating compositions ranging from 0 to about 37% Ni and 20% Co were obtained. The chemical composition of the coatings depended very much on the electrolytes nature and operating conditions. The Ni content of deposits increased with increase in Ni bath concentration, temperature, pH and solution agitation but decreased considerably with increase in current density. The throwing power of the Zn-Ni solution deteriorated as Ni metal bath concentration increased.

The Co content of deposits also increased with increase in Co bath concentration and temperature, and decreased with increase in current density. However, the addition of commercial organic additives to Zn-Co plating solutions suppressed considerably the amount of Co in the coatings. The Co content of deposits plated from Zincrolyte solution was found to be more sensitive to variation in current density than in the case of deposits plated from the alkaline Canning solution.

The chromating procedures were carried out using laboratory formulated solution and commercially available ones. The deposit surface state was of great significance in influencing the formulation of conversion coatings. Bright and smooth deposits acquired an iridescent colour when treated with the laboratory formulated solution. However, the dull deposits acquired a brownish appearance.

The correlation between the electrochemical test results and the neutral salt spray in marine environment was good. Non-chromated Zn-Ni coatings containing about 11-14% Ni increased in corrosion resistance compared to pure Zn. Non-chromated Zn-Co deposits of composition 4-8% were required to show a significant improvement in corrosion resistance

Corrosion resistance was improved considerably by conversion coating. However, the type of conversion coating was very important. Samples treated in a laboratory solution performed badly compared to those treated in commercial solutions. Zn alloy coatings were superior to pure Zn, the Schloetter sample (13.8% Ni) had the lowest corrosion rate, followed by the Canning sample (1.0% Co) and then Zincrolyte (0.3% Co). Neither the chromium content of the conversion films nor the chromium state was found to have an effect on corrosion performance of the coatings.

Keywords: Electrodeposition, Zinc, Alloys (Zn-Ni and Zn-Co), Conversion coatings, Corrosion testing

DEDICATION

To my mother who brought up five children in a war time and
to all those who love(d) her.

ACKNOWLEDGEMENTS

The author is very much indebted to the Algerian Government's Ministry of Higher Education whose financial assistance is gratefully acknowledged.

I would also like to thank Dr. J.K Dennis and Dr. N.R Short, my supervisors, for the liberal use of their time and for their valuable guidance and help.

My thanks are also extended to Plated Press Work Ltd. of Dartford and I.M.F (Institute of Metal Finishing) for their financial contribution and to the staff of Mechanical & Production and Civil Engineering departments of Aston University for their much appreciated assistance.

List of Contents

	Page
Title page	1
Thesis summary	2
Dedication	3
Acknowledgements	4
List of contents	5
List of tables	10
List of figures	13
1 Introduction	20
2 Literature survey	26
2.1 Zinc plating	26
- Alkaline zinc plating	26
- Acid zinc plating	27
2.2 Zinc alloy plating	29
- Anomalous codeposition	29
2.3 Zinc-nickel alloy systems	33
2.3.1 Plating conditions	33
2.3.1.1 Acid based solutions	33
- Sulphate and/or sulphamate baths	33
- Chloride baths	37
2.3.1.2 Alkaline based solutions	40
2.3.2 Properties of Zn-Ni alloy deposits	42
- Hardness	42
- Strength and ductility	43
- Internal stress	44
- Appearance	45
- Corrosion	45
2.4 Zn-Co alloy systems	49
- General considerations	49
- Corrosion behaviour	51
2.5 Zn-Fe alloy systems	54
- General considerations	54
2.6 Conversion coatings	57
2.6.1 Introduction	57
2.6.2 Zn alloy systems	58
2.6.3 Types of chromates	60

	PAGE
2.6.4 Mechanism of film formation	61
2.6.5 Protection mechanism	63
 2.7 Corrosion and corrosion control	 66
2.7.1 Corrosion	66
2.7.1.1 Definition	66
2.7.1.2 The basic corrosion cell	
- Dissimilar metal electrode cells	67
- Concentration cells	68
- Differential temperature cells	71
2.7.2 Corrosion control	71
2.7.3 Corrosion testing	72
2.7.3.1 Salt spray tests	72
- ASTM B117 Salt spray test	72
- ASTM D2247 Humidity test	73
- ASTM B287 Acetic acid salt spray	74
- ASTM B368 CASS test	74
- ASTM 380 Corrodokote	74
- Kesternich DIN 50018 Sulphur dioxide test	75
2.7.3.2 Electrochemical tests	76
- Background and theory	77
- Polarization techniques	79
- Linear polarization	79
- Tafel plot	82
- Potentiodynamic polarization scan	83
- Pitting scan	84
- Conclusion	85
 3 Experimental procedures	 86
3.1 Laboratory prepared dull deposits	86
3.1.1 Zn-Ni electrodeposition	86
3.1.1.1 Ammonium chloride based electrolytes	86
- Preparation of the plating solution	86
- Electrodeposition	87
- Cathode Current Efficiency, (C.C.E)	89
- Effect of temperature, pH and agitation on Ni content of the deposits and C.C.E.	91
- Effect of temperature	91
- Effect of pH	92
- Effect of agitation	92
3.1.1.2 Zn-Ni Potassium chloride based electrolyte	93
3.1.2 Zn-Co electrodeposition	94
3.2 Commercial bright deposits	96
3.2.1 Zincrolyte system	96

	PAGE
- Effect of current density	97
- Effect of temperature	97
3.2.2 Canning Zn-Co system	97
- Effect of current density	98
3.3 Plating solutions and chemical analyses	99
3.3.1 Atomic Absorption Spectrophotometry (AAS)	99
3.3.1.1 Plating solutions control	100
- Determination of Ni and Co plating solutions	100
- Determination of Zn in plating solutions	101
- Analysis of Zn-Ni alloy deposits	102
- Determination of Zincrolyte K make up	103
3.4 Metallurgical examination and characteristics of coatings and plating solutions	104
3.4.1 Metallurgical examination	104
- Specimen preparation	104
- Scanning Electron Microscope (S.E.M)	104
- Electron Probe Microanalysis	105
3.4.2 Characteristics of coatings and plating solutions	105
- Deposit microhardness measurements	105
- Solution throwing power measurements	106
- Deposit distribution measurements	107
- Example of calculation	108
3.5 Conversion coatings	112
- Chromating procedures	112
- Measurements of open-circuit potentials during conversion coatings	113
- Conversion film analysis and examination	114
- XPS analysis details	115
3.6 Corrosion study	116
3.6.1 Salt spray tests	116
- Salt spray sample preparation	119
3.6.2 Beaker immersion study	120
3.6.3 Electrochemical measurements	121
- Experimental procedures	121
- Corrosion measurement equipment reliability	121
- Sample preparation	123
- Linear polarization measurement	124
- Potentiodynamic polarization	124

	PAGE
4 Results	125
4.1 Plating solutions and coating characteristics	125
4.1.1 Zn-Ni alloy systems	125
4.1.1.1 Ammonium chloride based solutions	
- Effect of current density and solution Ni concentration on deposit Ni content and C.C.E	125
- Macro throwing Power results	130
- Effect of temperature, pH and agitation on coating composition and C.C.E	134
- Zn-Ni deposits characteristics	136
A-Hardness of Zn-Ni alloy deposits	136
B-Microscopic study of Zn-Ni alloy deposits	137
4.1.1.2 Zn-Ni potassium chloride based solutions	139
- Effects of current density and solution Ni concentration on deposit composition at 25.0 and 30.0°C	139
4.1.2 Zn-Co alloy systems	143
4.1.2.1 Zn-Co dull deposits	143
- Effect of current density and Co solution concentration on Co coating composition	143
4.1.2.2 Bright deposits	147
- Zincrolyte system	147
- Canning system	149
4.2 Conversion coatings	150
- Commercial chromated sample	151
- Appearance of conversion films obtained from solution (1) for different immersion times	160
- Chromate film structure	165
- XPS study results	169
4.2.2 Schloetter chromating solution	173
4.2.3 Canning chromating solution	176
4.3 Corrosion	179
4.3.1 Non-chromated systems	179
- Electrochemical testing	179
- Salt spray testing	179
4.3.2 Chromated systems	180
A) Results of non-chromated systems	181
- Electrochemical testing	181
- Neutral salt spray testing	186

	PAGE
- Immersion testing	189
B) Results of chromated systems	193
- Electrochemical testing	193
- Neutral salt spray testing	196
- XPS study	203
- Scanning electron microscopy study of corroded chromated samples	204
5 Discussion	207
5.1 Zn Alloy electrodeposition	207
5.1.1 Generalities	207
5.1.2 Zn-Ni systems	208
5.1.2.1 Ammonium chloride based solution	208
- Macrothrowing power	211
- Deposit characteristics	213
5.1.2.2 Potassium chloride based solution	214
5.1.3 Zn-Co systems	215
- Dull deposits	215
- Bright deposits	216
5.2 Conversion coatings	219
5.2.1 Laboratory treated samples	219
5.2.2 Commercial chromating solutions	226
- Schloetter chromating solution	226
- Canning chromating solution	227
5.3 Corrosion	229
5.3.1 Non-chromated systems	229
- Electrochemical testing	229
- Neutral salt spray testing	233
- Corrosion mechanism of non-chromated systems	233
5.3.2 Chromated systems	236
- Corrosion mechanism of chromated systems	238
6 Conclusions	241
- Zn Alloy electrodeposition	241
- Conversion coatings	243
- Corrosion	244
7 Recommendations for further work	246
8 List of references	249

List of Tables

	PAGE
Table 1.1 Excelzinc Series	24
Table 2.1 Zn Alloy systems of commercial significance	30
Table 2.2 Different Zn-Ni processes reported in the literature	34
Table 2.3 Chemical composition and operating conditions of Udylite and Schloetter processes	39
Table 3.1 Ammonium chloride based Zn-Ni bath formulation	87
Table 3.2 Plating solution used to study the effect of temperature, pH and agitation	92
Table 3.3 Potassium chloride based solution	93
Table 3.4 Zn-Co plating solution	95
Table 3.5 Zn-Co Base plating solution	96
Table 3.6 Canning commercial Zn-Co plating solution	98
Table 3.7 Conversion coating solutions and treated samples identification	113
Table 3.8 List of non-chromated Zn-Ni dull deposits for corrosion study	117
Table 3.9 List of non-chromated Zn-Co dull deposits for corrosion study	118
Table 3.10 List of non-chromated commercial bright samples (as received)	118
Table 3.11 List of chromated dull and commercial bright samples for corrosion study	119
Table 3.12 Polarization parameters obtained for stainless steel in 1.0N H ₂ SO ₄	122
Table 4.13 Effect of current density on deposit Ni content and C.C.E Solution Ni content: 1.0 g l ⁻¹	125
Table 4.2 Solution Ni content: 5.0 g l ⁻¹	126
Table 4.3 Solution Ni content: 10.0 g l ⁻¹	126
Table 4.4 Solution Ni content: 15.0 g l ⁻¹	126
Table 4.5 Solution Ni content: 20.0 g l ⁻¹	127
Table 4.6 Solution Ni content: 30.0 g l ⁻¹	127

	PAGE
Table 4.7 Solution Ni content: 40.0 gl ⁻¹	127
Table 4.8 Effect of current density and Ni solution concentration (in terms of percentage weight) on coating composition	129
Table 4.9 Effect of solution composition on MTP	130
Table 4.10 Metal distribution on Hull cell panels	132
Table 4.11 Effect of temperature on coating composition and C.C.E	134
Table 4.12 Effect of solution pH on coating composition and C.C.E	134
Table 4.13 Effect of agitation on deposit Ni content and C.C.E	135
Table 4.14 Microhardness of the deposits	136
Table 4.15 Effect of current density and Ni solution concentration (KCl based) on deposit Ni content. Temperature:25.0°C	139
Table 4.16 Effect of current density and Ni solution concentration (KCl based) on deposit Ni content. Temperature:30.0°C	139
Table 4.17 Effect of current density and Ni solution concentration (in terms of percentage weight) on coating composition. Temperature:25.0°C	141
Table 4.18 Effect of current density and Ni solution concentration (in terms of percentage weight) on coating composition. Temperature:30.0°C	141
Table 4.19 Effect of current density and Co solution concentration on coating composition. Solution used at 25.0°C.	143
Table 4.20 Effect of current density and Co solution concentration on deposit Co content. Solution used: Zn-Co KCl based solution without additives at 30.0°C	143
Table 4.21 Effect of C.D and Co solution concentration (in terms of percentage weight) on deposit Co content. Solution used: Zn-Co KCl based solution without additives at 25.0°C	145
Table 4.22 Effect of C.D and Co solution concentration (in terms of percentage weight) on deposit Co content. Solution used: Zn-Co KCl based solution without additives at 30.0°C	145

	PAGE
Table 4.23 Effect of current density on deposit Co content and C.C.E. Solution used: Zincrolyte	147
Table 4.24 Effect of temperature and organic additives on deposit Co content of the deposits and C.C.E. Solution used: Zincrolyte	148
Table 4.25 Effect of C.D on coating composition and thickness. Solution used: Canning	149
Table 4.26 Potential time results for deposits treated in solution (1)	154
Table 4.27 Chromating characteristics of dull and bright deposits treated in (1)	156
Table 4.28 Chemical composition of laboratory and commercially chromated samples, (as received)	169
Table 4.29 Chromating characteristics of dull deposits treated in Schloetter chromating solution	173
Table 4.30 Chromating characteristics of dull deposits treated in Canning solution	177
Table 4.31 Variation of Corrosion rate and corrosion potential with time for dull non-chromated deposits	182
Table 4.32 Variation of Corrosion rate and corrosion potential with time for non-chromated bright deposits, (as received)	184
Table 4.33 Salt spray results for non-chromated dull deposits. After 365 hours exposure	186
Table 4.34 Corrosion rate results obtained from potentiodynamic curves	193
Table 4.35 Salt spray results of commercial chromated samples, (as received) After 580 hours exposure	196
Table 4.36 Salt spray results of commercial bright deposits treated in chromating solution (1) for 120 seconds. After 580 hours exposure	199
Table 4.37 Salt spray results of dull deposits treated in chromating solution (1) for 120 seconds. After 580 hours exposure	201
Table 4.38 Relationship between the Cr(III)/Cr(VI) ratio of the chromated samples and resistance to white rust	203

List of Figures

	PAGE
Fig. 2.1 Generalized relationship between deposit composition and C.D for anomalous deposition	30
Fig. 2.2 Relationship between the deposit Ni content having the same thickness and the corrosion resistance in the salt spray test	46
Fig. 2.3 Electrochemical corrosion cells	69
Fig. 2.4 Typical linear polarization curve	79
Fig. 2.5 Typical Tafel plot	83
Fig. 3.1 Corrosion cell	123
Fig. 4.1 Effect of C.D and Ni solution concentration on coating composition.	128
Fig. 4.2 Effect of C.D and Ni solution concentration on C.C.E	128
Fig. 4.3 Relationship between coating composition and Ni content in solution	129
Fig. 4.4 Relationship between different plating solution composition and MTP.	131
Fig. 4.5 Metal distribution on Hull cell panels	133
Fig. 4.6 Metal distribution on Hull cell panels	133
Fig. 4.7 Metal distribution on Hull cell panels	133
Fig. 4.8 Effect of temperature on Ni content of deposits	135
Fig. 4.9 Effect of pH on Ni content of deposits	135
Fig. 4.10 Relationship between hardness (Hv) and deposit Ni content	136
Fig. 4.11 Zn-Ni deposit showing elemental distribution across the coating cross section	137
Fig. 4.12 Zn-Ni deposit showing fine grained structure	138
Fig. 4.13 Zn-Ni deposit showing columnar structure	138
Fig. 4.14 Scanning micrograph showing pitted surface of Zn-Ni deposit	138

	PAGE
Fig. 4.15 Sound Zn-Ni coating obtained using agitation	138
Fig. 4.16 Effect of current density and Ni solution concentration on coating composition obtained at 25.0°C	140
Fig. 4.17 Effect of current density and Ni solution concentration on coating composition obtained at 30.0°C	140
Fig. 4.18 Relationship between coating composition and Ni content in solution. Solution used at 25.0°C	142
Fig. 4.19 Relationship between coating composition and Ni content in solution. Solution used at 30.0°C	142
Fig. 4.20 Effect of C.D and Co solution concentration on coating composition obtained at 25.0°C	144
Fig. 4.21 Effect of C.D and Co solution concentration on coating composition obtained at 30.0°C	144
Fig. 4.22 Relationship between coating composition and Co content in solution. (KCl solution at 25.0°C)	146
Fig. 4.23 Relationship between coating composition and Co content in solution. (KCl solution at 30.0°C)	146
Fig. 4.24 Effect of C.D and organic additives on coating composition. Zincrolyte solution used	148
Fig. 4.25 Effect of temperature and organic additives on Zn-Co coating composition Zincrolyte solution used	148
Fig. 4.26 Effect of C.D on coating composition for both Zincrolyte and Canning solutions	149
Fig. 4.27 Photographs of commercially chromated samples (as received)	152
a- Zincrolyte sample, (0.3%Co)	152
b- Canning sample, (0.7%Co)	152
c- Schloetter sample, (13.8% Ni)	152
Fig. 4.28 Optical micrographs of commercially chromated samples (as received)	153
a. Schloetter sample	153
b. Canning sample, (0.7% Co)	153

	PAGE
Fig. 4.29 Potential-time curves recorded for Zn and Zn-Ni dull deposits during chromating in solution (1)	155
Fig. 4.30 Potential-time curves recorded for Zn and Zn-Co dull deposits during chromating in solution (1)	155
Fig. 4.31 Potential-time curves recorded for bright commercial samples during chromating in solution (1)	155
Fig. 4.32 Chromating characteristics of dull Zn-Ni deposits treated in solution (1)	157
a- Weight of Zn dissolved	157
b- Weight of Ni dissolved	157
c- Sample weight change	157
d- Estimated 'true' film weight	157
Fig. 4.33 Chromating characteristics of dull Zn-Co deposits treated in solution (1)	158
a- Weight of Zn dissolved	158
b- Weight of Co dissolved	158
c- Sample weight change	158
d- Estimated 'true' film weight	158
Fig. 4.34 Chromating characteristics of bright deposits treated in solution (1)	159
a- 0.3%Co (Zincrolyte sample)	159
b- 0.7%Co (Canning sample)	159
c- 13.8%Ni (Schloetter sample)	159
Fig. 4.35 Photographs of dull deposits treated in solution (1) for 30 seconds	160
a- Zn	160
b- 0.3%Ni	160
c- 12.4%Ni	161
d- 21.3%Ni	161
e- 5.1%Co	162
f- 14.7%Co	162
Fig. 4.36 Photographs of Commercial bright deposits treated in solution (1) for 15 seconds	163
a- Pure Zn	163
b- 13.8%Ni, (Schloetter sample)	163
c- 0.3%Co, (Zincrolyte sample)	164
d- 0.7%Co, (Canning sample)	164
e- 1.0%Co. (Canning sample)	164

	PAGE
Fig. 4.37 Scanning micrographs of dull deposits treated in solution (1) for 120 seconds	165
a- 0.3%Ni	165
b- 12.4%Ni	165
c- 21.3%Ni	166
d & e 14.7%Co	166
Fig. 4.38 Scanning micrographs showing film growth on Canning deposit (0.7%Co) treated in solution (1)	167
a- After 15 seconds	167
b- After 120 seconds	167
Fig. 4.39 Scanning micrographs showing film growth on Schloetter deposit (13.8%Ni) treated in solution (1)	168
a- After 15 seconds	168
b- After 120 seconds	168
Fig. 4.40 XPS spectra generated from chromated samples in solution (1) for 120 seconds Sample: 12.4%Ni	170
a- High resolution	170
b- Low resolution	170
Fig. 4.41 High resolution XPS spectra generated from 0.3% Co dull deposit treated in solution (1) for 120 seconds	171
a- High resolution	171
b- Low resolution	171
Fig. 4.42 Selected XPS spectra for Cr a- With curve fitting	172
Fig. 4.43 Chromating characteristics of dull Zn-Ni deposits treated in Schloetter solution	174
Fig. 4.44 Chromating characteristics of dull Zn-Co deposits treated in Schloetter solution	174
Fig. 4.45 Photographs of dull deposits treated in Schloetter solution for 40 seconds	175
a-Pure Zn	175
b-12.4%Ni	175
c-21.3%Ni	175

	PAGE
Fig. 4.46 Chromating characteristics of dull Zn-Ni deposits treated in Canning solution	178
a- For 90 seconds	178
b- For 120 seconds	178
Fig. 4.47 Chromating characteristics of dull Zn-Co deposits treated in Canning solution	178
a- For 90 seconds	178
b- For 120 seconds	178
Fig. 4.48 Polarization curves for non-chromated dull deposits	181
a- Zn	181
b- 0.3%Co	181
c- 12.4%Ni	181
Fig. 4.49 Variation of corrosion rate with time for non-chromated dull Zn & Zn-Ni deposits	183
Fig. 4.50 Variation of corrosion potential with time for non-chromated dull Zn & Zn-Ni deposits	183
Fig. 4.51 Variation of corrosion rate with time for non-chromated dull Zn & Zn-Co deposits	183
Fig. 4.52 Variation of corrosion potential with time for non-chromated dull Zn & Zn-Co deposits	183
Fig. 4.53 Variation of corrosion rate with time for non-chromated commercial bright deposits	185
Fig. 4.54 Variation of corrosion potential with time for non-chromated commercial bright deposits	185
Fig. 4.55 Time to first red rust for non-chromated dull deposits	186
Fig. 4.56 Photographs of corroded dull deposits. After 365 hours exposure	187
a- Zn-Ni	187
b- Zn-Co	187
c- Zn-Ni & Zn-Co	188
Fig. 4.57 Scanning micrographs of systems in as deposited and corroded conditions	189
a- As deposited	189
b- As corroded: Zn-Ni deposits	191
c- As corroded: Zn-Co deposits	192

	PAGE
Fig. 4.58 Polarization curves obtained for commercially chromated systems	194
a- Schloetter sample, 13.85%Ni	194
b- Canning sample, 1%Co	194
Fig. 4.59 Corrosion rate of commercial samples (as received) Data extracted from polarization curves	195
Fig. 4.60 Corrosion rate of dull deposits treated in solution (1) Data extracted from polarization curves	195
Fig. 4.61 Photographs of corroded commercial chromated samples. After 580 hours of salt fog	197
Fig. 4.62 Resistance to white rust in salt spray test of commercial chromated sample, (as received)	197
Fig. 4.63 Resistance to red rust in salt spray test of commercial chromated sample, (as received)	197
Fig. 4.64 Photographs of bright non-chromated samples. After 365 hours of salt fog	198
Fig. 4.65 Resistance to red rust in salt spray test of bright non-chromated sample, (as received)	198
Fig. 4.66 Photographs of corroded commercial deposits treated in solution (1) for 120 seconds. After 580 hours of salt fog	200
Fig. 4.67 Resistance to white rust in salt spray test of bright samples treated in solution (1)	200
Fig. 4.68 Resistance to red rust in salt spray test of bright samples treated in solution (1)	
Fig. 4.69 Time to white and red rust for dull Zn-Ni deposits treated in solution (1)	201
Fig. 4.70 Time to white and red rust for dull Zn-Co deposits treated in solution (1)	201
Fig. 4.71 Photographs of corroded dull deposits treated in solution (1) for 120 seconds After 580 hours	202
a- Zn-Ni deposits	202
b- Zn-Co deposits	202

		PAGE
Fig. 4.72	Scanning micrographs showing a black spot on a corroded chromated 0.7% Co deposit	204
	a- After removal of black spot	205
	b- X-ray map for Fe	205
	c- X-ray map for Zn	205
Fig. 4.73	Scanning micrographs showing white rust on corroded chromated Schloetter deposit	206
	a- General micrograph	206
	b- X-Ray map for Cr	206
	c- X-ray map for Zn	206
	d- X-ray map for Cl	206

ELECTRODEPOSITION OF CORROSION RESISTANT ZINC ALLOY COATINGS.

1 INTRODUCTION

Zinc is one of the most widely used metallic coatings for steel surfaces, because of its ability to provide preferential corrosion protection of steel.

As much as 5×10^6 tons of zinc coated steel sheets⁽¹⁾ are produced annually by hot-dipping and electroplating. In Germany for instance, consumption for autocar use increased from 113,000 tons in 1982 to 227,000 tons in 1984⁽²⁾. About 45% of all the zinc used in the U.S. is for the coating industries while in Japan the figure is about 57%⁽³⁾. The total amount of zinc coated steel in the U.S. increased by 13.5% in the year 1986. Therefore, in parallel with looking for new resources, the existing ones must be conserved by reducing the weight of the zinc deposited without this leading to loss of corrosion protection.

The principal methods of applying such coatings are hot-dipping and electroplating. The former produces relatively heavy coatings, generally characterised by a spangled finish. These heavily coated materials are often not suitable for many forming and finishing operations. An electroplated coating on the other hand is relatively thin, with a smooth, bright surface which may be painted or press formed. Furthermore, the mechanical properties of the

substrate are hardly changed during electrodeposition.

However, the corrosion resistance of pure zinc coatings is not always satisfactory. In a very humid atmosphere, especially with periodic moisture condensation, the zinc surface gradually deteriorates and becomes coated with corrosion products in the form of zinc hydroxides and carbonates⁽⁴⁾.

Some studies have been conducted to improve the corrosion resistance of zinc electrodeposits by raising the corrosion potential of zinc, thus reducing its excessive galvanic protection, by alloying it with more noble metals such as iron, cobalt, nickel, molybdenum, aluminium, manganese or vanadium. In particular, the codeposition of nickel promises a considerable improvement of the corrosion resistance when compared to that of pure zinc⁽⁵⁾.

Kamitani et al⁽⁶⁾ developed a commercial process for electrolytic deposition of Zn-Ni alloy with good throwing power and good corrosion resistance. This bright Zn-Ni system has been adapted by several automobile manufacturers and parts suppliers in Japan.

According to a British patent, as reported by Domnikov⁽⁷⁾, the most corrosion resistant Zn-Ni alloys are those of the gamma phase (γ) containing 13-20% nickel. Unfortunately, the introduction of an adequate concentration of nickel into

the bath to achieve an alloy deposit in this composition range imposes a cost penalty which reduces its attraction in economic terms.

Recently, an electrogalvanized steel containing cobalt and chromium, has appeared on the market^(8,9,10) and is claimed to have excellent corrosion resistance at low cobalt content. Cobalt contents of 0.2 to 0.3% together with 0.05% of chromium have been reported. Corrosion behaviour in salt spray tests based on JIS Z 2371 was two to three times better than that obtained with pure zinc. Although, cobalt is more expensive than nickel, such small concentrations as compared with that quoted above for nickel content, produce improvements in corrosion resistance without a marked increase in costs.

For the past few years intense interest has been shown in methods for protecting automobile body panels from corrosion. This is necessary due to the need to meet extended warranty periods and the increasing use of de-icing salts on roads. The corrosion that occurs in automobiles may be broadly classified into two categories -i- corrosion from inside enclosed sections, causing perforation and -ii- corrosion under paints bringing about scab and filiform corrosion, referred to as 'cosmetic corrosion'. Therefore, coated steel sheets for autobodies should have high resistance to both these kinds of corrosion, along with good press formability, good paint adhesion and good spot

weldability.

Electrolytic Coatings,

As it is difficult for a single plated layer to meet these requirements; a variety of multi-layer combinations have been developed commercially^(11,12,13). Nippon Steel Corporation⁽¹¹⁾ developed a double layer coated steel, called 'Excelight' with a top layer composed of 80-90% iron, balance zinc and an inner layer of a zinc rich alloy, containing iron. This 6 μ m thick coat provides a combination of good corrosion resistance, due to the zinc and good weldability and paintability due to the iron. Two layer Zn-Fe/Zn-Ni alloy⁽¹²⁾ coated steels are intended to further increase corrosion resistance.

Nippon Kohan^(11,14,15), using sulphate based electrolytes, have commercially been able to plate a whole series of single-layer and double-layer systems of Zn-Ni and Zn-Fe alloys, called Excelzinc. The details are given in Table 1.1

As reported by Porter et al⁽¹⁶⁾, Kawasaki Steel developed a Zn/10-25% Fe system having an outer layer of an Fe-0.4% phosphorus. Work continues on development of the Zn-Fe alloys with small additions of Ni, Co, Cr, Mn and other metals.

Catanzano et al⁽¹³⁾ developed another type of multi-layer system for corrosion protection of car bodies. The product was given the registered trade name 'ZINCROX'. It consists

of three continuously superimposed electrolytic coatings, which are :

- a first layer of zinc
- a second layer of chromium
- a third layer of chromium oxide (as paint bonder)

The chromium and chromium oxide layers are extremely thin, 0.5 and 0.05 μm (minimum) respectively.

Table 1.1 Electrogalvanized Excelzinc Series

Code	Product Name	Coating Type	Structure
EZA	Excelzinc Type A	Zn-Fe Alloy Single layer	15-35% Fe up to 6 μm
EZB	Excelzinc Type B	Zn-Fe Alloy Double layer	up to 60% Fe, 2 μm 15-35% Fe, 4 μm
EZN	Excelzinc Type N	Zn-Ni Alloy Single layer	11-15% Ni, 6 μm
EZL	Excelzinc Type L	Zn-Ni + Zn-Fe Double Layer	up to 60% Fe, 2 μm 11-15% Ni, 4 μm
EZN-UC	Excelzinc Type N with Universal Coat	Zn-Ni Alloy + chromate film	11-15% Ni, 6 μm + chromate film (0.5-3 μm)

Zinc alloyed with 30 to 50% Mn is another possibility⁽¹⁷⁾. The product is obtained on a conventional electrogalvanizing line using sulphate based electrolytes. The corrosion resistance without painting of Zn-Mn alloy electroplated steel is particularly increased when the manganese content is above 30%. The corrosion resistance of Zn-40% Mn deposits is 40 times greater than that of pure zinc deposits

having the same thickness. Thus Zn-Mn alloys show a high performance which had not been reported previously in the literature. Whether this will be enough to justify the high cost of the alloying element remains to be seen.

The objective of the present work was first to produce Zn alloy coatings (Zn-Ni and Zn-Co) from simple base solutions under various plating conditions such as current density, temperature, pH and solution composition. Inevitably the deposits will be dull and matt and their surface morphology and structure will differ from those of bright deposits. The second aim was to chromate the obtained deposits and assess their corrosion behaviour in marine environment (both chromated and chromated deposits). Commercial bright systems will be included for comparative purposes.

2 LITERATURE SURVEY

2.1 Zinc Plating

While the name of the first person to electrodeposit zinc has long been lost, it is of interest to note that the protective value of zinc was recognised as early as 1829⁽¹⁸⁾. However, it was not until the development of bright, cyanide zinc plating in the mid 1930's that electrodeposited zinc was accepted as a true decorative finish as well as a protective coating for iron and steel.

- Alkaline Zinc Plating

The cyanide solution contains zinc in two forms: as a zincate, NaHZnO_2 , and , as the double cyanide, $\text{Na}_2\text{Zn}(\text{CN})_4$. Neither of these solutions is satisfactory for plating on its own. The zincate solution without cyanide, although quite efficient, will produce dark and spongy deposits. A zinc cyanide solution with no NaOH added will produce fine-grained smooth deposits but will have a cathode current efficiency of only about 10-15%.

The cyanide zinc baths have high throwing power, which is an important factor in plating. However, due to their toxicity and the strict regulations governing effluent treatment, extensive work has been carried out to find low or cyanide free electrolytes. Plants for destroying the cyanide add to the overall costs.

Alkaline cyanide free solutions which require only simple neutralization of the effluent have been introduced⁽¹⁹⁾ but these baths have the limitations in that the deposition rate is slow, and the operating cost high⁽²⁰⁾. Also these processes use weak complexing agents which can create chromating problems, due to iron contamination. With cyanide in the plating solution, iron forms sodium ferrocyanide and is relatively inert. but without cyanide or in the presence of such weak complexing agents, Fe in the ferrous (soluble) state will codeposit with Zn resulting in dark deposits and therefore difficulty in chromating.

- Acid Zinc Plating

Early attempts at acid zinc plating were performed with sulphate containing baths⁽²¹⁾. These were characterized by poor throwing power and production of dull coatings. However, they have found application on steel sheet strip and other tubing or mill products for which appearance and throwing power are not important factors, since low current density areas are not encountered, and the products are subjected to further treatment such as painting.

Later, a simple zinc ammonium chloride complex was introduced and formed the basis for the bright acid chloride zinc plating processes. However, a disadvantage of adding ammonium chloride is that many plating shops have a variety of metals present in their effluent and metals such

as copper or nickel can combine with the ammonium ion from the zinc solution to form stable complexes that make waste treatment more difficult. Also limitations have been placed on the amount of ammonia permitted in the effluent.

To overcome these problems, a bright acid zinc solution, containing potassium chloride and boric acid has been developed.

Most of these solutions are non-chelating and metallic impurities can be removed with relative ease. The most common contaminant is iron, which is readily removed by the addition of dilute hydrogen peroxide and filtration(22).

At the present time all of the above plating systems are being used commercially, each having its own applications and advantages. The development of zinc alloy systems, which is the main interest of the present study, will increase appreciably the possibility of satisfying a wide variety of practical requirements not met by the pure zinc deposits. In particular the codeposition of zinc with the iron-group metals such as nickel and cobalt promises a considerable improvement in corrosion resistance when compared with that of pure zinc.

2.2 Zinc Alloy Plating

Although the standard electrode potential of zinc (-0.76 V) is far less than those of iron-group metals such as nickel (-0.25 V), cobalt (-0.28 V) and iron (-0.44 V), zinc codeposits readily with these metals. In the alloy deposit the ratio of the less noble metal (Zn) to the more noble metal is larger than in the bath at certain current density range. This phenomenon has been studied by Brenner⁽²³⁾ and described as an 'anomaly' in the codeposition of metals of the ferrous group with zinc.

Most research and development has been devoted to the Zn-Ni alloy systems. However, recently, the deposition of a Zn-Fe alloy has come to the fore, especially in the motorcar industry. Relatively little has been reported of the deposition of Zn-Co alloys, although at least one commercial solution is being marketed⁽²⁴⁾. Table 2.1 gives a list of zinc alloy systems of commercial significance.

- Anomalous Codeposition

This is characterised by the peculiarity that the less noble metal deposits preferentially. This may occur only over a certain range of the plating conditions for a given bath. The most important aspect of anomalous codeposition is the unusual variation of alloy composition with current density as shown in Figure 2.1⁽²⁵⁾. The point P (see Figure 2.1) indicates the metal percentage Zn in the bath. In the low current density region (branch a-b), the codeposition

Table 2.1 Zinc alloy systems of commercial significance

Alloying element	Percent by Wt.	Application	Electrolyte	Reference
Co	0.6-0.8	Fasteners	Chloride	26
	0.5-0.8	Fasteners	Alkaline	
			Zincate	*
Co, Cr	0.2, 0.5	Strip	Sulphate	9
Fe	8-20	Strip	Sulphate	27
Mn	30-50	Strip	Sulphate	17
Ni	13	Strip	Sulphate	28
	8-15	Brackets & Fasteners	Chloride	
				6,29

* New process from W.Canning Ltd, Birmingham

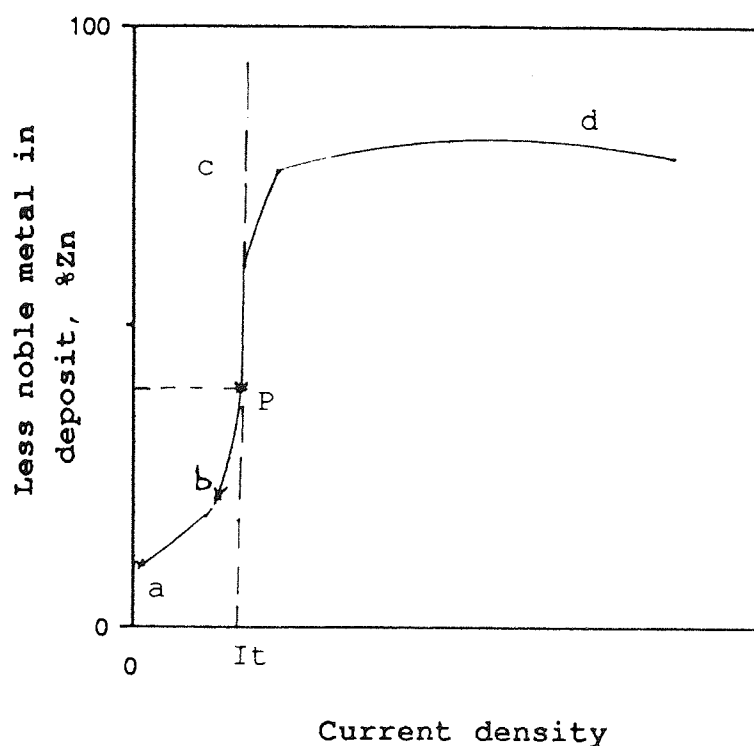


Fig. 2.1 Generalized relationship between deposit composition and current density for anomalous codeposition. After Hall(25).

appears to be of the normal type, that is, the deposit contains a smaller content of the less noble, Zn, than corresponds to the metal percentage Zn in the bath (P).

However, instead of approaching a limit of value of P with increasing current density, as would be the case with regular codeposition, the deposit rapidly increases in Zn content. Above I_t (transition current), the deposit contains more Zn than corresponds to the metal percentage Zn in the bath (P) i.e. anomalous deposition is observed.

Although various explanations have been advanced^(30,31), the hydroxide suppression mechanism^(32,33,34,35) is widely accepted. Dahms et al⁽³³⁾ investigated the dependence of the anomalous codeposition of Fe-Ni alloys on the pH at the cathode surface. They found that anomalous codeposition only occurs when the surface pH is high enough to cause the formation and precipitation of ferrous hydroxides on the cathode. As long as the surface pH stays close to that of the bulk solution there are no anomalies in the deposition rates. The authors showed that at low current densities, i.e. at low hydrogen evolution current, Ni rich deposits were obtained, resulting in the normal codeposition which reflects the nobility of each metal. Hydroxides of both Fe and Ni ions were formed when the diffusion limited current of hydrogen ions is exceeded in both cases, in the deposition of single metals as well as in codeposition. They considered that since the anomalous suppression of the

rate of Ni (more noble) deposition occurs only during codeposition, but not during deposition of Ni alone, this aspect must be attributed to the formation of ferrous hydroxides. The suppression of Ni discharge in the presence of ferrous hydroxide can be accounted for by assuming preferential adsorption of ferrous hydroxide at the cathode which blocks the deposition of Ni. Therefore deposits rich in Fe (less noble) were obtained.

Higashi et al⁽³²⁾ reached the same conclusion, by studying the electrodeposition of Zn alloys containing small amounts of Co. During anomalous codeposition of Zn with Co, the electrodeposition of Zn proceeds with the formation of Zn hydroxide on the cathode, which results from a rise in pH in the vicinity of the cathode. The concentration of Zn hydroxide resulting from the rise in pH in the vicinity of the cathode was estimated by electrochemical and spectroscopic studies. On the other hand, since the critical pH for Co hydroxide precipitation is not attained in the cathode layer, Co deposition occurs by the direct discharge of Co^{2+} ions through the Zn hydroxide film, which makes the Co deposition difficult. Consequently, the greater nobility of Co compared with Zn is cancelled out by the film resistance of Zn hydroxide, resulting in the preferential deposition of Zn in anomalous codeposition.

2.3 Zinc-Nickel Alloy Systems

A survey of the literature indicates that this alloy can be obtained from various types of baths, e.g. chloride^(36,37,38,39), sulphate^(40,41), ammoniacal^(41,42) sulphate-sulphamate⁽⁴³⁾, sulphate-chloride⁽⁴⁴⁾, cyanide⁽⁷⁾ and pyrophosphate⁽⁴⁵⁾.

Usually Zn-Ni deposits obtained from cyanide solutions have a lower nickel content (about 0.2-2% by weight) than their counterparts from cyanide free systems. Most of the studies of codeposition of Zn-Ni have been made with acid baths containing simple salts of the metals. A small amount of work has been done with baths containing complex ions. This is possibly due to the expensive effluent treatment requirements for solutions containing complexes.

Some of the baths that have been reported in the literature and their recommended operating conditions are given in Table 2.2.

2.3.1 Plating Conditions

2.3.1.1 Acid Based Solutions

- Sulphate and/or Sulphamate Baths

Most of the investigations have been carried out using sulphate solutions, due to their relatively low cost, safety features and pollution control characteristics.

Kurachi et al⁽⁴⁶⁾ used a pH 4 sulphate bath at 50°C to

Table 2.2 Zn-Ni Plating Solutions Reported in the Literature

Nickel Salt	gl ⁻¹	Zinc salt	gl ⁻¹	Other Additives	gl ⁻¹	Operating Conditions			Ref
						Adm ⁻²	pH	Temp, °C	
Nickel sulphamate Nickel (Metal)	190 34	Zinc sulphate Zn as a metal	266 60	Sodium Lauryl sulphate	0.38	-	5.0	-	43
NiCl ₂ .6H ₂ O Nickel as a metal	134.5 33.5	ZnCl ₂ Zn as a metal	139.12 66.6	Acetic acid % of bath volume	3.0	8.0	3.0	50	3
Nickel sulphate Nickel chloride	90 10	Zn sulphate	50	Boric acid Sodium gluconate	20 60 -	-	3.0	25 - 45	30
NiCl ₂ .6H ₂ O	3 - 5	ZnCl ₂	50-80	Aromatic aldehyde Ammonium ions	1.0 5.0	0.1 - 6.5	3 - 7.0	10 - 30	47
Ni as cyanide salt	0.50	Zn as complex salts	32	Sodium cyanide Sodium hydroxide	90 70	1.3	-	20 - 25	7
Nickel sulphate	65	Zn sulphate	180	Boric acid Sodium sulphate 25% NH ₄ OH (NH ₄) ₂ SO ₄	20 120 25 0.6N	4.0	10	20	41

electrodeposit a wide range of Zn-Ni alloy compositions. Zinc ion concentrations of 0.1 to 0.65 mole per litre in the bath produced silver-white gamma phase alloys at a current efficiency of more than 90%. Thus the desirable (γ) phase alloy could be deposited over a wide range of bath compositions. In the absence of H_3BO_3 and NH_4Cl , powdery grey deposits were obtained at current efficiencies below 70%. Baths containing about 0.78 to 0.88 mole per litre of zinc produced grey, semi-bright coatings containing the eta and gamma ($\eta + \gamma$) phases.

Similar results were obtained by Dini and Johnson⁽³⁴⁾ who reported a mixed sulphate-sulphamate bath at pH 5 with a Ni:Zn mole ratio of about 0.5. Increasing the bath temperature from 27 to 93°C increased significantly the nickel content of the alloy. At a constant temperature, deposits with the highest nickel contents were obtained at the lowest current densities. The cathode current efficiencies were generally 90% or higher and essentially constant for bath temperatures from about 25 to 60°C. Above 60°C, current efficiency rose to more than 100% at low current density. The solution used by these authors was different from that used by Roehl⁽³⁷⁾ in that no chlorides were present. The reason for this modification was that one potential application of the work was corrosion protection for uranium and its alloys which are susceptible to attack by chlorides. Also, Roehl recommended a small

amount of acetic acid as a buffer to promote ease of pH control for his chloride containing baths. Dini and Johnson found this to be unnecessary and furthermore discovered, as a result of Hull cell tests, that acetic acid reduced the covering power of the solution.

Repeated measurements revealed that the efficiency at 0.5 Adm^{-2} was greater than 100%, which is indicative of either material being occluded in the deposit or autocatalytic deposition. X-ray diffraction analysis on some coatings revealed the presence of zinc sulphate hydroxy hydrate, $\text{ZnSO}_4 \cdot 3\text{Zn}(\text{OH})_2 \cdot 4\text{H}_2\text{O}$; NiO and NaNiO_2 . These compounds were responsible for the grey or black unattractive appearance.

As a concluding remark in their work, Dini and Johnson stated that a brightener system would have to be developed if this deposit were to compete with cadmium.

However, these problems can be solved by the addition of suitable brighteners to the plating bath. According to Raman and his associates⁽⁴⁴⁾, an addition of piperonal at a concentration of 0.3 to 1.0 ml l^{-1} , along with 0.01 to 0.1 gl^{-1} of the sodium salt of lignin sulfonic acid was found to give bright deposits containing 10 to 20% nickel over a current density range of 2 to 7 Adm^{-2} . A higher pH of 5, tends to produce a dull deposit containing less nickel. At low pH values ($\text{pH} < 1.5$), the deposits obtained were matt and unattractive. Increasing the zinc percentage of the

alloy to more than 90% resulted in grey-black, powdery deposits.

- Chloride Baths

Rynne⁽⁴⁷⁾ published formulations for both ammoniacal and non-ammoniacal chloride baths for depositing relatively low Ni content alloys with up to 5% nickel using a current density ranging from 0.1 to 6.4 Adm^{-2} and very low nickel-zinc mole ratios (from 0.03 to 0.1). The soluble Ni salt was present in the solution in an amount which provided between approximately 3 and 5 gl^{-1} of Ni metal. The brightener and controller systems consisted of non-ionic polyoxyalkylated surfactant (phenol alcohol, ethylene oxide, or fatty acid) and aromatic aldehydes (aryl aldehyde, thiophene aldehyde) respectively.

It was found that at concentrations of ammonium ions in solution of less than 1 gl^{-1} , the addition of boric acid was required as if the bath were ammonia-free. At concentrations greater than 10 gl^{-1} , the ammonium ions caused difficulties in the removal of heavy metals from effluent with conventional waste treatment systems.

The ammonia-free bath was identical to the ammonium containing bath except that the ammonium base salt was replaced by either potassium or sodium chloride salts. Boric acid and an aromatic carbonyl compound such as benzoic or nicotinic acid were also included in this bath. Boric acid,

which acted as a buffer and a high current density grain refiner, must be added in order to keep the zinc ions in solution.

Recently, Kamitani and co-workers⁽⁶⁾ developed a suitable system for rack and barrel plating operation. It was reported that alloys in the range 15 to 25% nickel did not lend themselves to chromate post-treatment. An improved chemical additive system has been developed to avoid problems due to high nickel content and subsequent poor chromate coverage, by suppressing nickel codeposition at low current densities. The bath composition and operating conditions are given in Table 2.3.

Another chloride based electrolyte containing ammonium was developed recently in laboratories of Dr-ING Max Schloetter⁽²⁹⁾. Table 2.3 gives the bath formulation and operating conditions. The process has two organic additives in order to ensure a regular composition of the alloy, and also good covering power at low current densities. According to the manufacturer, the process has been accepted by Volkswagen and results are now being obtained under relevant production conditions.

The process uses separate Zn and Ni anodes to which a current is applied by two separate circuits with current Zn:Ni of about 5:1 i.e geometric surface ratio Zn:Ni should

Table 2.3 Chemical Composition and Operating Conditions of Udylite and Schloetter Processes.

Bath Constituent (gl ⁻¹)	Schloetter Process (29)	Udylite (OMI) Process (6)
Zn ions	28-32	80-120
Ni ions	20-28	120-160
Ammonium ions	100-110	180-220
Additive (Slotoloy 13)	20-30	30-60 ml ⁻¹ *
Additive (Slotoloy 14)	20-30	1-3 ml ⁻¹ **
Operating conditions:		
pH range	5.9-6.1	5.5-6.0
Temperature range	40-45°C	32-40
Cathode current density	0.5-3.0 Adm ⁻²	2-6
Anode current density	<1.0 Adm ⁻²	1-4
Anode Material	Zn-Ni	Zn
Current distribution Ratio:		
Zn:Ni	5:1	-
Agitation	Air	Air

* Primary Brightener A

** Secondary Brightener B

be around 5:1. The use of such a high anodic current ratio will lead to Zn build up in the plating solution and consequently to difficulty in controlling the deposit chemical contents. Investigation by Domnikov⁽⁷⁾ of current distribution on the Zn and Ni anodes with the same surface area showed that the amount of current on the Zn is approximately 5 times that on the Ni anode. As a result, there took place a preferential dissolution of Zn and its build up in the electrolyte. Therefore, for the purpose of making the rate of dissolution of Zn and Ni from the anodes approximately equal to the rate of their deposition on the cathode, the current on the anode of both metals must be distributed in relation to their relative concentrations in the cathode deposit. For example, an alloy containing about 15% Ni and 85% Zn, the current density on the Zn anode must be approximately the same as for Ni anode, i.e. Zn:Ni ratio of about 1.0 must be used.

2.3.1.2 Alkaline Based Solutions

Domnikov⁽⁷⁾ has described the codeposition of zinc and nickel from cyanide and ammoniacal solutions. The cyanide salt was prepared by dissolving Ni(OH)_2 or nickel sulphate in an excess of sodium-cyanide. The best quality coating obtained was the light coloured bright deposit containing 2% nickel. When the nickel concentration in the solution was increased to 6 gl^{-1} , the concentration of nickel in the deposit increased to 5%. However, the cathode current

efficiency dropped to 70% and below, and the coating appearance became dark and matt. With a nickel concentration of about 15 gl^{-1} , spongy deposits formed on the cathode.

While investigating the conditions of zinc and nickel codeposition from the ammoniacal solution, it was established that deposits up to 3% nickel were obtained at a temperature of about 40°C and a pH of 6.5-6.7.

For both types of solutions investigated the increase in current density led to a decrease in nickel content in the deposit and cathode current efficiency.

Another ammoniacal type solution was investigated by Marchenko and Batyuk⁽⁴¹⁾. Again, it was shown that low current density plating favours the codeposition of nickel. At 1.0 Adm^{-2} a deposit having up to 50% nickel could be obtained. The appearance of the deposits changed with the nickel contents of the coatings. Ammonia was added to the baths to form the complex and Na_2SO_4 and $(\text{NH}_4)_2\text{SO}_4$ to increase conductivity. A study was also made of the factors that might raise the output of the process, such as the use of the reversal current (periodic) and stirring of the electrolyte. The former yielded deposits that were smoother and brighter than when direct current was used. Stirring of the electrolyte was unsatisfactory since the deposit became coated with black sludge.

2.3.2 Properties of Zn-Ni Alloy Deposits

Although several investigations have reported that the relationship between the properties of the electrodeposited Zn-Ni alloy and the various deposition parameters when considered singly can be explained satisfactorily, it is very difficult to attribute the variation of any property of an electrodeposited Zn-Ni alloy unambiguously to a single operating parameter independently of the others. Acting simultaneously, these parameters determine the condition of the cathode layer and the process occurring at the cathode/solution interface, and consequently the properties of the deposits.

Usually data from different sources refers to deposits produced from solutions of different compositions operating at different conditions and observations have been made at various deposit thicknesses. Therefore, it is very difficult to compare the results of different investigators and to establish the general trends of a property or a condition of a deposit with the conditions under which it was produced.

- **Hardness**

In general the hardness of the Zn-Ni alloy deposits increase with increase in the amount of nickel in the alloy. Rajagopalan⁽⁴²⁾ measured the microhardness of Zn-Ni alloys across the entire composition range with a Vickers pyramidal indenter. Alloys containing more than about 70% Ni had an essentially constant Vickers hardness of about 600. Below

70% nickel content, hardness decreased almost linearly with decreasing nickel content to a Vickers hardness of about 65 for pure zinc.

This agrees well with the data reported by Marchenko and Batyuk⁽⁴¹⁾, who found that the hardness of the Zn-Ni deposit increased from above 60 to 520 Hv when the deposit ranged from pure zinc to about 50% nickel.

Somewhat harder deposits, i.e. 150 to 180 Hv obtained from 5 to 10% nickel alloys were reported by Tsuji and Kamitani⁽⁴⁸⁾. This greater hardness, as compared to either zinc or low carbon steel, should make them of value when sacrificial corrosion protective action of zinc is desired along with a certain amount of wear resistance.

- Strength and Ductility

To obtain good formability for automobile body fabrication, it is important to ensure that the plating process does not result in a reduction in mechanical properties of the base steel.

Noumi et al⁽⁴⁹⁾ measured the mechanical properties of several grades of steel sheet before and after Zn-Ni electroplating. They found that the coating caused essentially no deterioration in yield strength, tensile strength or elongation properties. Zn-Ni deposits did not flake even when deformation was severe enough to break the base metal.

The pH values have a marked effect on the ductility of the deposits⁽⁷⁾. By lowering the solution pH to 3 - 4, their brittleness was increased. However there was no reason to attribute this phenomenon to the inclusion of hydrogen in the coatings, because the amount of hydrogen liberated at the cathode at these pH values changed very little. Neither should the brittleness of the deposits be ascribed to inclusion of metal hydroxides, because they were not formed in the plating solutions used.

- Internal Stress

Using a rigid-strip technique, Dini and Johnson⁽⁴³⁾ measured a stress of less than 35 MNm^{-2} . The deposit stress was relatively insensitive to variations in deposition current density or temperature. Roehl and Dillon⁽³⁸⁾ found that the tensile stress of deposits containing more than 10% nickel could be reduced greatly by raising the bath pH to about 4.0. Whereas Tsuji and Kamitani⁽⁴⁸⁾ found that the internal stress of an alloy containing 5 to 10% Ni was essentially equal to that of zinc deposited from a zinc ammonium chloride bath.

Based on the degree of cathode bending during electrolysis, the internal stress measurements carried out by Domnikov⁽⁷⁾ showed that internal stresses increased with higher nickel contents. She related this to the lattice parameters changes associated with the different phase structures of the deposits. In the majority of cases these deposits were

supersaturated solid solutions of Zn in Ni, with enlarged parameters of the (beta) or (gamma) phase lattice.

- Appearance

For most applications today, it is essential to produce a bright deposit which can be passivated to give a pleasant appearance, provided the corrosion resistance of the coating system is maintained.

Pitting, can be eliminated by the use of a compatible wetting agent. Some of the wetting agents used in commercial nickel plating have been found satisfactory, as for example sulphated or sulphonated lauryl alcohol^(37,43).

Tsuda and Kurimoto⁽⁵⁰⁾ found that adding at least 0.05 g^l-1 of strontium compound (SrSO₄) to Zn-Ni plating baths produced bright deposits. Tsuji and Kamitani⁽⁴⁸⁾ developed brightener systems selected from those used for zinc deposition from chloride baths. Bright alloys having 5 to 10% nickel were obtained. A cathodic dichromate process or a leach-type chromate treatment provided a clear passivated surface.

- Corrosion Behaviour

According to Noumi et al⁽⁴⁹⁾, 12 to 14% Ni provided the best corrosion resistance, as shown in Figure 2.2. Only the gamma-phase (γ) was identified in the deposits, whereas alloys with a lower or higher nickel content also contained

the eta (η) and alpha (α) phases respectively, showing that the maximum corrosion resistance was produced by a single phase alloy. A similar conclusion was reached by several other investigators (7, 51).

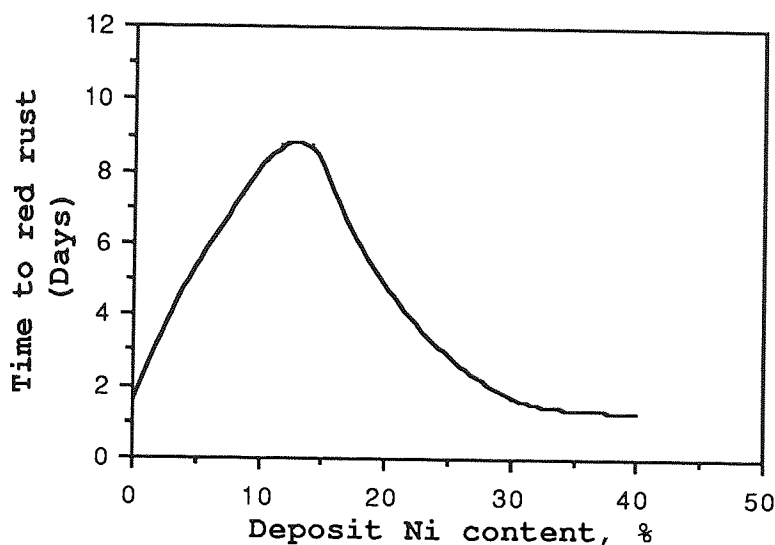


Fig. 2.2 Relationship between the Ni content in the deposits having the same thickness and corrosion resistance in salt spray test, (ASTM B117). After Noumi et al (49)

Kurachi et al (46) measured corrosion potentials (E_{corr}) over the whole range of Zn-Ni alloy compositions produced from sulphate electrolytes. They found that the corrosion potentials became more negative with increasing zinc content until the ($\gamma+\eta$) phase alloy was reached. Also Domnikov (7) reported that deposits containing more than about 20% nickel tend to have galvanic potentials more noble than those of iron and steel. Deposits having about 5 to 15% Ni had potentials that were anodic to those of iron and

steel and appeared to protect the underlying iron or steel better than an equivalent thickness of unalloyed zinc. The 2% Ni coatings which were obtained from the cyanide solution behaved in similar manner to the pure zinc.

Much of the corrosion testing of Zn-Ni deposits has been carried out following ASTM B117 specifications, in a 5% neutral salt spray environment at 35°C. Dini and Johnson⁽⁴³⁾ for example, found red rust on 12.5 μm thick zinc-plated steel panels after 72 to 168 hours, while the 12.5 μm Zn-Ni coatings on steel did not develop red rust until between 240 and 336 hours of exposure. The latter result also compared favourably with red rust development on 12.5 μm cadmium plated steel, i.e. after 192 to 360 hours. A somewhat better result for Zn-Ni was recently obtained⁽⁵²⁾, i.e. red rust development on 5 μm thick coating of an alloy containing 10.4% Ni on steel panels occurred after 240 hours.

In immersion tests of 15 μm thick coatings on steel in 3% NaCl solution, rust spots were observed after 30 hours with nickel coatings, after 80 hours with zinc and after 120 hours with zinc alloy containing 15% Ni⁽⁴²⁾. Also, Hall⁽⁵³⁾ reported that considerable rust was found on zinc plated steel after four 4 hour cycles of copper accelerated salt spray testing whereas only a few small spots appeared after six cycles when the same thickness (12 to 13 μm) of coating contained 11 to 13% Ni.

Zn-Ni alloys have also been electroplated on thin nickel underlayers to make a duplex coating in an effort to further improve corrosion resistance⁽⁵⁴⁾. Hirt and Dillon⁽⁵⁴⁾ claimed that the duplex coating provided about twice the corrosion protection of the Zn-Ni alloy deposited directly onto steel. For example, a 0.5 μm nickel 'strike' deposited under a 2.5 μm Zn-Ni coating reduced its corrosion rate from 0.045 to 0.02 $\mu\text{m}/\text{hour}$ in the ASTM B117 neutral salt spray test. Thus the use of a nickel underlayer, one-fifth as thick as an overlying zinc coating with about 15% nickel may provide an economic advantage.

There is no definite theory concerning the corrosion control mechanism of the zinc alloy coatings. Only a protective action mechanism of nickel enriched surface layer formed by dezincification was proposed for Zn-Ni alloy coatings⁽⁵⁵⁾. The same proposition was also put forward by Shibuya and his associates⁽⁵¹⁾. They found using X-ray photoelectron spectroscopy that the corrosion products on Zn-Ni alloy plated steel sheet consisted of zinc compounds such as zinc hydroxides and zinc carbonates. As corrosion proceeded zinc had dissolved preferentially. Therefore, the corroded surface was covered with a nickel rich layer containing corrosion products of zinc. Because of the protection afforded by this layer, Zn-Ni alloy plated steel sheet was considered to show much better corrosion resistance than pure zinc coated.

2.4 Zinc-Cobalt Alloy Systems

- General Considerations

Information concerning the possible codeposition of Zn-Co alloys was given by Kochergin⁽⁵⁶⁾. He used radioactive isotopes as an analytical method to study the composition of the deposit, but his work contained no data on physical and chemical properties of the alloys, or on the field of application and operating conditions of the electrolyte.

The Zn-Co alloy systems from pyrophosphate⁽⁵⁷⁾ and sulphate baths⁽⁵⁸⁾ were investigated by Rama Char and his associates. White grey deposits in the composition range 0-90% Co were obtained by variation of the current density from 0.5 to 15 Adm^{-2} , and other plating parameters. The sulphate bath was found to be more satisfactory than the pyrophosphate based electrolyte. The efficiency values were quite high (69-90%), unlike the low values of 6 to 71% for the pyrophosphate bath. Again no details about the physical or chemical properties of the coatings were given.

It was not until recently that much interest has been shown towards the electrodeposition of Zn-Co alloys on a commercial scale^(10,24,26).

Leidheiser⁽⁵⁹⁾ studied the chemical state of Co in an electrodeposited Zn-Co alloy, using a Mossbauer Spectroscopy technique. He reported deposits having 0.03 to 0.2% Co from a sulphate bath containing Co and a very small amount of

Cr. He found that Co was present in the zinc deposits as isolated atoms at substitutional sites in the zinc matrix.

All the work carried out by Adaniya et al^(9,10,60) was based on sulphate baths, and concerned continuous coating of strip, that is the use of high current densities and high temperatures. Although it was stated that zinc chloride could be used, all examples given were of sulphate baths which contained a very small amount of chromium⁽⁹⁾. It was shown that the flow rate of the electrolyte was the most important factor in controlling the Co content in the deposit. For example, when the flow rate was 0.5 m per second and the Co content in the bath varied from about 5 to 35 g l⁻¹ then the Co content in the deposit varied from 0.05 to about 0.98%; whereas when the flow rate was only about 0.1 m per second, the Co content of the deposit was between 0.5 to about 5.2%.

However, the sulphate baths exhibit poor throwing power⁽²⁶⁾, and therefore are unsuitable for components whose geometry result in wide variations in current density over their profile.

It has been found that Zn-Co deposits on individual components could be plated by the use of an acid chloride Zn-Co plating bath. The process called 'Zincrolyte'^(24,61) has been commercialised for use for both rack and barrel plating. The bath formulation includes zinc chloride, a

source of Co ions, boric acid, sodium chloride and an additive system which controls the Co content as well as the appearance of the deposits.

The composition of the deposited alloy depended on various plating parameters. The Co content of the deposit increased with an increase in concentration of Co ions in the electrolyte and the operating temperature. Increasing the Co ions in the bath up to 15 gl^{-1} leads to an increase in Co deposited to about 1.7%. Also the increase of temperature from 20 to 35°C resulted in an increase in Co content from about 0.4 to about 0.85%.

It has been found that the brightener systems, commonly employed for acid zinc plating were unsuitable for Zn-Co plating. A new additive system has been developed which has resulted in a uniform alloy composition and bright deposits.

- Corrosion Behaviour

The corrosion resistance of the 'Zincrolyte' deposits⁽²⁴⁾ was greatly improved at concentrations up to 1.0% Co. During accelerated corrosion test in neutral salt spray in accordance with DIN 50021 SS specification, the corrosion resistance of non chromate passivated Zincrolyte coatings with Co concentrations between 0.5 to 1.0% improved by a factor of 4 when compared with pure zinc deposits. It has also been shown that the rate of spreading of red rust over a steel surface was greatly reduced as a result of the

codeposition of Co with zinc. French and German car manufacturers have carried out cyclic humidity and cyclic road tests using assembled components. In these tests a 50 to 100% improvement over conventional zinc has been reported.

Adaniya et al⁽⁶⁰⁾ studied the effect of various elements on corrosion resistance of Zn electroplated coatings and it was found that Co was the most effective in improving the corrosion resistance. When a 0.2% Co deposit was salt sprayed in accordance with JIS Z 2371, the corrosion resistance was twice as high as that of pure zinc coatings. When the Zn-Co deposit contained a small amount of chromium, the corrosion resistance increased by a factor of 2.5.

The reasons why such alloys have superior resistance to corrosion are not yet clear. However, examination of the Zn, Co and Cr remaining on the specimens undergoing salt spray corrosion testing, indicated that the loss of Co and Cr was extremely small⁽¹⁰⁾. Based on this fact, it was considered that during the progress of corrosion, zinc in the coating dissolved but Co and Cr remained and formed a bright barrier which improved resistance to corrosion.

As mentioned earlier, Leidheiser^(59,62) found that Co was present in the zinc deposits as isolated atoms in the zinc matrix. As a result of this chemical state of Co in the Zn-Co alloys, Leidheiser suggested that Co entered the oxide

film on zinc during the corrosion process as an isolated atom or ion, and acted as a cathodic corrosion inhibitor.

2.5 Zinc-Iron Alloy Systems

- General Considerations

Zn-Fe is an excellent paint base (as is Zn-Ni), protects welding tips (as Zn-Ni does) but Zn-Fe plating baths are much more difficult to control. However, Zn-Ni is more expensive from a compositional standpoint. Moreover, Nickel is classified as a potentially carcinogenic metal, especially when welding nickel containing alloys.

Iron has been codeposited with Zinc from different types of base solutions: sulphates^(14,15,27,63), chlorides^(64,65), pyrophosphate⁽⁶⁶⁾, sulphamate⁽⁶⁷⁾ and alkaline zincates⁽⁶⁸⁾.

The process is considered ultra-sensitive to bath chemistry and variables such as bath temperature, agitation, pH, and current density. For example, as reported by Jepson et al⁽⁶⁵⁾, the iron content of the alloy decreases by 3% per 0.1 decrease pH in bath. The presence of iron in the electrolyte as two states, ferrous (II) and ferric (III), makes the process very difficult to control and unattractive. Some Fe(III) ions are precipitated in the form of $\text{Fe}(\text{OH})_3$ by an amount depending on the bath pH. This decreases drastically the efficiency^(63,66) and incorporation of $\text{Fe}(\text{OH})_3$ in the deposit causes poor coating adherence on steel⁽⁶³⁾.

However, the Zn-Fe system normally gives very good paint adhesion, press workability, good weldability and an

improved corrosion resistance. Considerable attention is being given towards the Zn-Fe systems by the automobile industry.

Nippon Kokan⁽⁶³⁾, using a bath based on ferrous and zinc sulphates have been able to plate commercially either a 15-20% Fe alloy for corrosion resistance or a 50% Fe alloy on top of a 15-20% Fe layer to enhance paintability. However, problems arose regarding oxidation of iron at the insoluble anodes, contamination of the bath by lead from the anodes, and comparatively low conductivity of the bath.

Kawasaki steel⁽¹⁴⁾ developed a chloride based bath using ferrous Zn and ammonium chlorides and slightly higher operating temperatures (50°C) to produce 10-25% Fe deposits. They incorporated about 0.4% phosphorous in these deposits and found that the corrosion resistance of the Zn-Fe alloy electroplated steel was improved remarkably.

These systems, however, like most of their counterparts e.g. Zn-Ni discussed previously, relate to steel strips or sheets produced by continuous plating. Zn-Fe systems are mainly used to provide primers for phosphating or painting. Nippon Hyomen Kagaki Co. Research Laboratory⁽⁶⁸⁾ have developed a Zn-Fe alloy suitable for the production of electroplated articles for various applications. The system 'Jasco Stronzinc' as it is called is obtained from an electrolyte consisting of sodium hydroxide, chelating agents and

proprietary brighteners. It is claimed to possess a better corrosion resistance than pure zinc. Samples containing 0.3 to 0.7% Fe have given About 800 hours to white rust appearance. Details regarding associated problems concerning bath control or chromating procedures were not given. Without doubt an improved corrosion resistance, at relatively low cost, (0.3-0.7% Fe), is a very attractive bonus indeed.

2.6 Conversion Coatings

2.6.1 Introduction

Zn or Zn alloy coatings are normally conversion coated to reduce the rapid formation of white rust. Chromates also make an excellent base for paint and other organic finishes. Recently, considerable work has been done to improve the corrosion resistance of zinc electroplated substrates by the substitution of Zn alloy coatings for pure Zn deposits. It has been stated, however that the formation of coloured or visible chromate films having high corrosion resistance on such Zn alloys is much more difficult than on pure Zn coatings^(69,70). For instance, black spotting occurred on components which were stored after Zn plating and passivation. It was discovered that the spots were due to Ni impurities which had been introduced to the plating bath by the use of stainless steel supports for the zinc anodes⁽⁷¹⁾. Additions of 0.09 mg l^{-1} of Ni metal to a zinc cyanide plating solution, prepared from reagent grade chemicals, resulted in deposits which, when chromated, were susceptible to the formation of dark spots when immersed in water. Incidentally, the spots were not produced by the salt spray.

Little information on the chromating of Zn alloy coatings and properties of the conversion films formed is available. No work at all was reported in literature concerning the mechanism of formation of the conversion coatings on these deposits nor about their chemical composition.

2.6.2 Zinc Alloy Systems

Recently, a work described in an U.S. patent No. 4 591 416 listed several chromating solutions which could be applied to Zn-Ni systems containing up to 15% Ni by weight. The solutions are acidic having a pH of 1.3 to 2.7 and comprising a weight ratio of $\text{SO}_4^{2-}:\text{Cr(VI)}$ of about 0.025-1.5:1.0 and operating at temperatures of about 25 to 35°C. The deposits are immersed in the solutions for a period of time sufficient to form the desired coloured films. It has been found that the surface of the Zn-Ni alloy electrodeposit may become inactive or inert if it is exposed to the atmosphere for any significant period of time before being subjected to the chromating treatment. In such cases, it has been found desirable to use higher temperatures, up to 55°C. In some instances, a flash of electrodeposited Zn having a thickness of about 1 μm , obtained at a current density of 0.1 to 3 Adm^{-2} for 5 seconds may be applied to Zn-Ni coats before immersion. Alternatively, the activation of these deposit surfaces may be accomplished by making them the anode and electrolysing for 5 seconds at low current densities, 0.1 Adm^{-2} ; after which the electrolysis is discontinued and Zn-Ni alloy surface is maintained in the chromating solution until the desired coloured film formed.

More recently Nikolova et al⁽⁶⁹⁾ investigated the properties of chromate films on pure Zn, Zn-0.5% Co and Zn-0.25% Ni. They observed the following peculiarities during chromatization of these deposits: when solutions for

colourless passivation of pure zinc were used, containing 0.5 gl^{-1} chromium anhydride, $30-45 \text{ gl}^{-1}$ sulphate ions and $1-1.5 \text{ gl}^{-1}$ fluoride ions, the films formed displayed poor quality i.e. bad adhesion to substrate and discontinuous film structure. However, when the samples were treated for iridescent yellow and green passivation of zinc, sound chromate films were formed on these deposit alloys. The chromate film colour was somewhat darker than that of pure zinc. This may be as a result of the inclusion of Co or Ni from the substrate. The surface structures of chromate films, formed upon Zn and Zn alloy coatings showed no substantial differences. The details about the formulations and operating conditions of these conversion solutions were referred to in Bulgarian patents No. 29959 and 33228 for iridescent yellow and green passivating solutions respectively. Studies concerning the chromating mechanism of these coatings and their chemical composition were not investigated.

Adaniya et al⁽⁶⁰⁾ investigated the effect of additive elements on the chromating characteristics of Zn electroplated steel strip. A chromating solution, consisting of CrO_3 and H_3PO_4 was sprayed onto the strip surface. The solution temperature was 45°C and the standard spraying time was 4 seconds. The reactivity of the surface with the chromating solution was evaluated by determining the amount of chromium deposited.

It was found that among the various elements added singly, Co was the one which reduced considerably the reactivity of the deposit in the chromate solution. However, it has been shown that the incorporation of small amounts of chromium (0.02 to 0.06%) in the Zn-Co deposit improved the reactivity with chromate by about 50%.

The Zincrolyte system has been claimed to accept a passivation treatment (24,61). It has been reported that passivation can be achieved in a similar way to that possible with conventional zinc coatings. However, the colour was somewhat darker, depending upon the Co content in the deposits. A good chromate passivation was obtained using hexavalent chromium free passivating solutions. It has also been suggested that a thin layer of pure Zn be deposited on the Zn-Co coat and this zinc flash to be then converted to a zinc passivate. The thin coat was pure zinc 99.95% having a thickness of less than 0.5 μm and was produced by electrolysis for 20 to 30 seconds (26). Undoubtedly, the use of such a flash deposit of Zn will increase the cost of treatment. For black passivation, two different passivates have been used, one for rack and one for barrel application. No details about the passivation solutions and treatment were given.

2.6.3 Types of Chromates

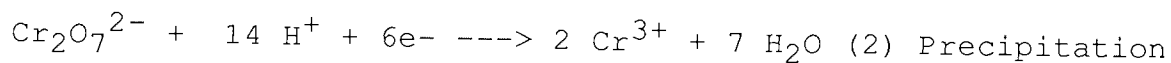
Chromate conversion coatings are classified by colour, which in turn identifies the film thickness and chromate content.

Colours vary from clear, light blue, yellow, olive drab to black. Slight variation in thickness of light weight film coatings create colour interferences giving an iridescence typical of the coatings. Generally the heavier the coating the darker the colour.

The colour selection and type of chromate used is based on the application, either decorative purposes, identification requirements, or corrosion resistance specification. Colour is related not only to film thickness but also to composition. The ratio of Cr(VI) to Cr(III) and the presence of other metals such as silver influence the colour of the deposit. Generally a chromating solution with a low Cr(VI) content and a low pH will generate light coloured films. Olive drab coatings on Zn owe their colour to Cr(III) compounds (72).

2.6.4 Mechanism of Film Formation

The formation of chromate conversion coatings on pure Zn is considered as a dissolution-precipitation mechanism (71,73):



First, zinc dissolves according to equation (1) and hexavalent chromium is reduced to Cr^{3+} , equation (2). The pH increase at the zinc surface causes precipitation of the chromate probably in some form of hydrated oxides. These

reactions, however, are dependant on anions such as chlorides, sulphates, or fluorides known as 'activators' (74). For example, in pure CrO_3 solution, zinc does not dissolve to any appreciable extent (55,74).

The mechanism of the chromating of zinc has been studied in CrO_3 solution containing sulphates (Na_2SO_4), chlorides (NaCl) and nitrates (NaNO_3) (75). Potential-time profiles and film weight measurements have shown that activation of the reaction is by sulphate and chloride only. In pure CrO_3 solution, the potential is shown to increase with time indicating that the surface had passivated. There is no indication of zinc dissolution. Similar observations were made when nitrates were added to the solutions. However, on the addition of sulphates or chlorides, the potential decreased some 700 mV and the decay curves showed a decreasing potential with time, suggesting a very active surface. Correspondingly, Zn dissolution was observed and an iridescent film was formed on zinc surfaces.

It is well known that chromium conversion coatings are very hydrous and gel like when fresh and still wet. A sufficient thickness of zinc must be available in order to produce an even satisfactory coating. The thickness of the chromate film is diffusion controlled during its formation. Therefore, agitation is recommended in order to maintain good transfer of reactants and reaction products across the

film when it is forming.

contrary. They argued

Despite widespread use of these treatments on zinc deposits, little is known about their composition. Furthermore, there has been marked disagreement between analyses that have been carried out (76,77,78,79,80). Chromium conversion coatings have been variously described to be composed of chromium chromate (73,78), chromium ferricyanide (73,80), chromic chromate: $\text{Cr}_2\text{O}_3 \cdot \text{CrO}_3 \cdot x\text{H}_2\text{O}$ and soluble chromates: $\text{Cr}(\text{OH})_3 \cdot \text{Cr}(\text{OH}) \cdot \text{CrO}_4$ (73,74,81). According to some workers (73,81), Zn is only found in the film in trace quantities and normally accumulates in the chromating solutions. Others showed that the yellow conversion films consisted mainly of Zn chromate represented by ZnCrO_4 and ZnO (82,83,84).

Much confusion has resulted from the very wide range of treatments commercially available, which produce coatings of differing character and composition as pointed out by Barnes et al (76). Films produced from one particular treatment may be very variable depending on the conditions of preparation and drying.

2.6.5 Protection Mechanism

According to Anderson (85) the major factor that determines corrosion resistance is the amount of Cr(VI) in the chromate conversion film. The insoluble compounds of Cr(III) in the film have only a small effect. However, Pocock (72) and

other authors have suggested to the contrary. They argued that some coatings containing little or no soluble chromates, Cr(VI), showed excellent protective value. After all, olive drab films show the best corrosion resistance and they are composed mainly of Cr(III) compounds.

In any case, the comparative corrosion protection of the film depends to a large extent on the type of environment in which they are exposed⁽⁷²⁾ and other factors such as ageing⁽⁸⁶⁾ and the nature of the zinc deposits^(85,87).

When panels were subjected to excessive heat i.e., Cr(VI) converted to Cr(III), the chromate was not leached from the film during salt spray testing and there was accompanying loss in corrosion resistance. However, when the same panels were subjected to an outdoor exposure test, the corrosion resistance of the panels heated to even 80°C for two hours gave similar performance to air dried panels⁽⁸¹⁾.

It has been shown that zinc chromated samples, when, dried at room temperature showed no sign of corrosion after 96 hours of salt spray. However, after drying at 50°C, trace of corrosion appeared on the samples after the same number of hours of exposure⁽⁸⁶⁾. The reason for this is that ageing affects the extraction of the chromate from the films.

Some work^(85,87) showed that for zinc plate prepared under the same conditions, there was a correlation between time to

failure in the salt spray and chromate content. When zinc samples were obtained from a number of different sources and then chromated under the same conditions, the chromate content did not correlate with the time to failure in the salt spray test. These results illustrate the importance of the nature of the zinc deposits. Moreover, when the panels were exposed outdoors, it was not possible to make any correlation between chromate content and corrosion resistance, even with panels plated and chromated under identical conditions.

Therefore, although the chromate content enhances the protective value of chromate conversion films, it is not a good measure of the corrosion resistance.

2.7 Corrosion and Corrosion Control

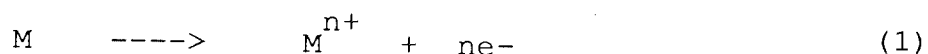
2.7.1 Corrosion

2.7.1.1 Definition

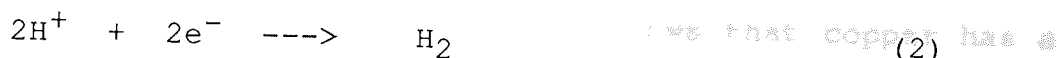
There are two general classes of corrosion reactions : those in which there is a direct combination of metals with non-metallic elements, and those in which the metal first dissolves, usually in an aqueous environment, later to combine with non-metallic constituents in the environment to form corrosion products. The former is referred to as ' Dry Corrosion' and the latter as 'Wet Corrosion'. Both types of corrosion are electrolytic in character and depend upon the operation of electrochemical cells at the metal surface, i.e. a chemical effect which induces the passage of an electric current.

2.7.1.2 The Basic Corrosion Cell

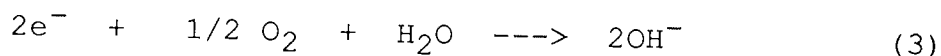
The dissolution of a metal in a liquid environment may be the oxidation reaction :



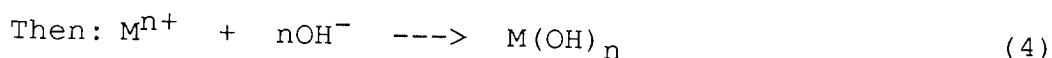
Reaction (1) represents the formation of the ion, M^{n+} , in the solution from the metal, (M), leaving n free electrons in the vicinity of the metal surface. To maintain electrical neutrality in the metal, there must be a simultaneous cathodic reaction in which electrons are consumed. This may be achieved in a number of ways depending on the environment. In acid solutions the cathodic reaction is likely to be :



In near neutral solutions, commonly found in natural environments the cathodic reaction is of the type :



Reaction (3) illustrates the combination of oxygen dissolved in the electrolyte with water and the electrons from the anodic reaction (1) to form hydroxyl ions (OH^-) in the electrolyte.



The basic electrochemical cell is shown in Figure 2.3a. In practice, anodes and cathodes are not shown as in Figure 2.3a, except in bimetallic contact. More usually, corrosion cells are very small and numerous and occur at different points on the same metal surface. They arise from local differences in metal structure and environment. Frequent examples are breaks in metal coatings, the presence of impurities or different alloy phases at the surface and local differences in oxygen concentration in the electrolyte. There are considered to be three types of electrochemical corrosion cells: (i) dissimilar metal electrodes (galvanic cell); (ii) concentration cells; and (iii) differential temperature cells.

- Dissimilar Metal Electrode Cells

An example of this type of cell is that of a copper pipe connected to an iron pipe. Consideration of the



electrochemical series (Appendix 1) shows that copper has a more positive redox potential and therefore becomes cathodic to the iron which dissolves. Advantage is taken of this effect in the cathodic protection of iron by zinc. Zinc is anodic to iron and, therefore dissolves in preference to iron which is protected. This situation is shown schematically in Figure 2.3b. Other example of this type of cell is the galvanic corrosion cell set up at surface of steel due to the presence of different phases (ferrite and cementite), as illustrated in Figure 2.3c.

- **Concentration Cells**

These are cells having two identical electrodes each in contact with a solution of differing composition . There are two types of concentration cells, namely salt concentration (metal ion) cell and differential aeration oxygen cell. The latter, which in practice is the more important, accounts for pronounced damage at crevices such as are formed at the interface of two coupled pipes or at threaded connections. It also accounts for pitting damage under rust as shown in Figure 2.3d. The amount of oxygen reaching the metal that is covered by rust or other insoluble reaction products is less than the amount that contacts other portions. Thus at the centre where the concentration of available oxygen is least, the anodic reaction predominates, i.e.



At the peripheral region the oxygen supply from the

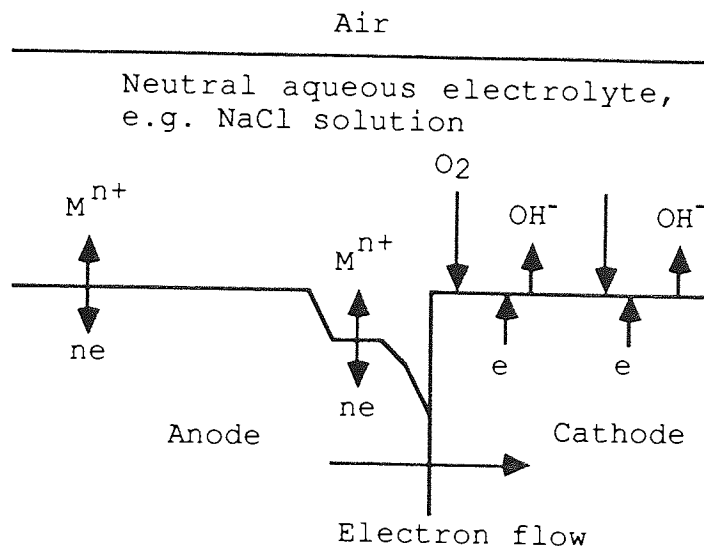


Fig.2.3a Principle of electrochemical corrosion cell existing between two different metals in contact with each other.

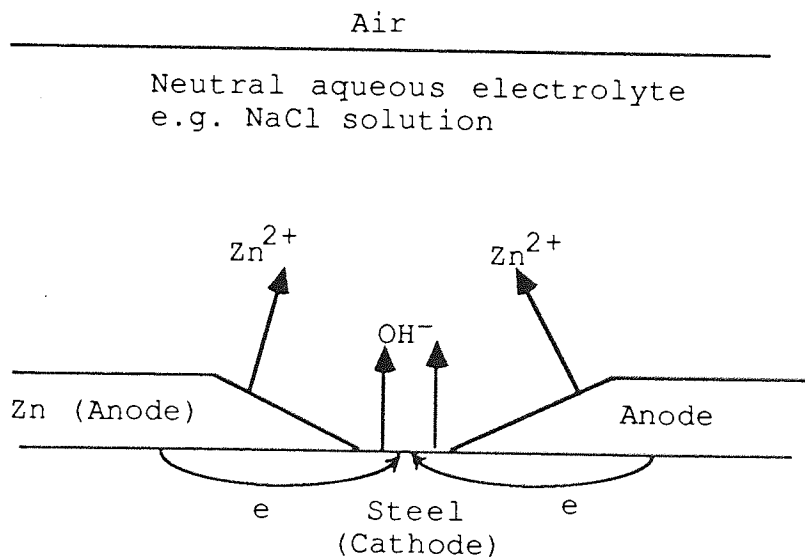


Fig.2.3b Anodic coating corrodes preferentially to protect the metal beneath, e.g. Zn on steel as shown.

($\text{Zn}(\text{OH})_2$ may precipitate to give further protection)

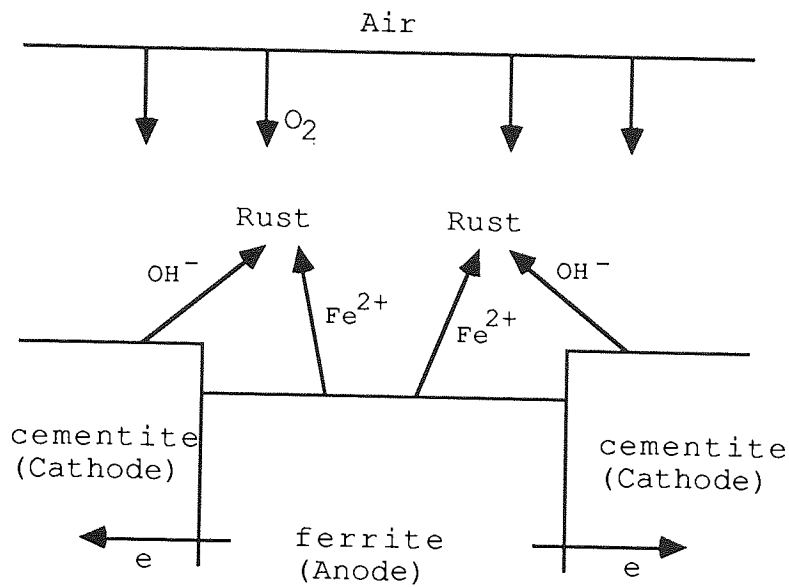
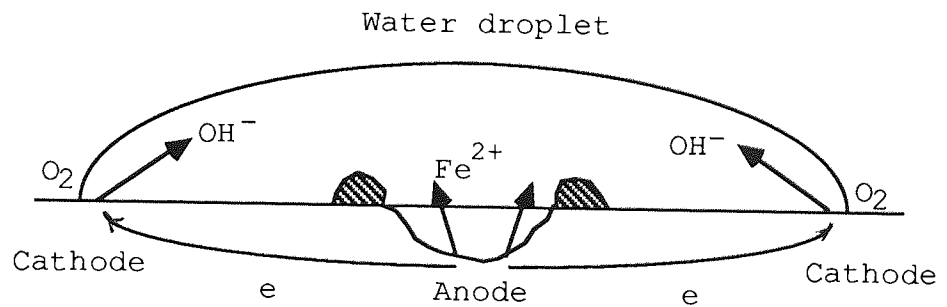


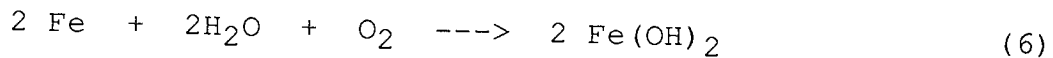
Fig.2.3c Preferential corrosion of ferrite in pearlite.



Rust formed around
the anode

Fig.2.3d Differential aeration cell on iron giving rise to corrosion.

atmosphere maintains the cathodic reaction of reaction (3). These two equations may be combined:



- **Differential Temperature Cells**

Components of these cells are electrodes of the same metal, each of which is at a different temperature, immersed in an electrolyte of the same composition. These are found in heat exchangers, boilers, etc.

2.7.2 Corrosion Control

For corrosion to occur, four elements are required as illustrated in Figure 2.3. These elements are : a cathode, an anode, an electrolyte and a flow of electrons. Therefore, by eliminating one of these elements, reduction of corrosion could be achieved. A few practical examples are:

- Protective coatings
- Cathodic protection
- Addition of inhibitors

The primary purpose of a metallic coating is to isolate the substrate metal from the corrosive environment by means of a thin coating. Metallic coatings fall into two general classes. Those in which the coating metal is anodic to the substrate, as in the case of zinc coatings on iron and steel, and those in which the coating metal is cathodic,

i.e. nickel on a ferrous substrate.

2.7.3 Corrosion Testing

As well as service trials of plated specimens in the actual environment in which they will be exposed, two types of tests are used to evaluate the corrosion resistance of coatings, namely accelerated and outdoor exposure corrosion tests. In this work, only the accelerated corrosion tests are used, mainly the salt spray and electrochemical corrosion techniques.

2.7.3.1 Salt Spray Tests

Real life exposures are complicated events, that involve several factors such as temperature and humidity variation, soiling, etc. Therefore it is essential that the accelerated test chosen should simulate 'real life' corrosion mechanisms as closely as possible. The most widely used accelerated test for Zn and Zn alloy coating systems^(43,52) is the ASTM B117 neutral salt spray.

- ASTM B117 Salt Spray Test

The salt solution utilized simulates the corrosive effects of outdoor exposure on automobile hardware (except some decorative nickel and chromium applications). The corrosion mechanisms involved are oxygen concentration cell and galvanic effects accelerated by :

- Use of an electrolyte with a sodium chloride content of 5% by weight.

- Elevated temperature (about 38°C). salt slows down the
- Inclination of test specimen. By inclining the specimen, the corrosion cell is continuously formed and replenished with fresh electrolyte; therefore the reaction is never slowed by the accumulation of metal ions and hydroxides.
- Utilization of a fine-fog mist. This results in the formation of a large number of corrosion cells which are set up and continuously replenished during the exposure period.

Results of salt spray testing are very sensitive to operating conditions. Variables that must be controlled carefully include uniformity of the environment throughout the cabinet, angle of the panels with respect to the vertical, atomization pressure, humidity of the air used for atomization, pH, purity of salt solution and collection rate.

The object of the salt spray test is to compare the relative resistance of several specimens or to evaluate the differences between a test sample and a part that has been previously tested and shown to provide satisfactory service. The test cannot be used to predict service life on a part that has had no previous salt spray-service correlation. Other commonly used corrosion tests are :

- ASTM D 2247 Humidity Test

The corrosion mechanism is the same as that for salt fog

testing, except that the absence of salt slows down the reaction. This test evaluates the corrosion resistance of coated metal products for indoor usage.

- **ASTM B 287 Acetic Acid Salt Spray Test**

This test is more accelerated than the salt fog test, due to acid attack (pH: 3.0-3.3). It is generally used for plated and painted coatings over steel substrates.

- **ASTM B 368 CASS Test**

The copper accelerated salt spray (CASS) test was developed to rapidly test copper-nickel-chromium or nickel-chromium on steel and zinc die castings for exterior automobile service. The corrosion mechanism is the same as that for the salt spray test except that the presence of copper adds galvanic potential and the lower pH (3.0-3.3) provides some acid attack. This test is too severe to be used for Zn deposits.

- **ASTM B 380 Corrodkote Test**

This test was also developed for specific use on copper-nickel-chromium coatings on ferrous and non-ferrous substrates. The corrosion mechanisms employed are oxygen concentration cells and galvanic effects produced by copper, iron, chloride and ammonium ions. This corrosive medium is applied as a slurry, i.e. a paste, forming numerous corrosion cells held in place much like dirt on an automobile.

- Kesternich DIN 50018 Sulphur Dioxide Test

The Kesternich test uses an atmosphere containing either 0.07 or 0.7% sulphur dioxide, combined with cyclic condensation. It is very common with German car manufacturers. Verberne⁽⁶¹⁾ used this test for Zn-Co coating systems and showed that the cycles to red rust increased linearly with the cobalt content of deposits.

However, the validity of the salt spray test as screens for actual conditions is not yet clear, as conflicting results and conclusions depending on the nature of the coating and the test cycle used, are reported in the literature^(29,88,89). One of the most obvious complicating factors in this method of corrosion evaluation is the use of different types of tests wherein different failure mechanisms are operative as explained previously.

Results on non-chromated pure Zn and Zn-Ni systems⁽²⁹⁾ obtained from a Schloetter process, showed that there is no discernible difference between the two deposits after the condensation-alternating humidity test according to DIN 50017. However, the Kesternich test DIN 50018 showed a lower resistance for Zn-Ni than pure Zn, especially on chromated samples. The Zn-Ni chromate does not offer an extra barrier against the chemical attack of sulphur dioxide in the test atmosphere. The pure Zn chromate proves more resistant in this case through its voluminous corrosion growth. In the neutral salt spray test (DIN 50021), the Zn-Ni alloy proved

superior to plated Zn.

50 to 100% improvement in corrosion resistance compared with conventional Zn is obtained with Zn-Co finishes containing 0.6 to 0.8% Co deposited from Zincrolyte solution(88). These results are based on cyclic humidity and road tests using assembled components of black passivated parts with commercially plated deposits 7.5 to 10 μm in thickness. These findings are consistent with results from standard tests such as neutral salt spray and the Kesternich test DIN 50018. However, contrary results have been observed in static tests, (i.e. roof exposure in an industrial atmosphere).

Results reported by Townsend et al(89) indicate that Zn-4%Al and 7%Al hot dip coated steel showed superior salt spray resistance over Zn coated steel, whereas, all the coatings performed similarly in industrial, mild marine and rural environment.

Clearly, any decision such as coating material selection based solely on salt spray testing methods should not be taken. In this present work, neutral salt spray and electrochemical techniques are employed.

2.7.3.2 Electrochemical Tests

Since corrosion is an electrochemical phenomenon, various techniques have been developed whereby the

electrical properties of interface metal-solution (electrical double layer) can be measured as a means of expressing corrosion rates. Unlike the salt spray or gravimetric methods, the electrochemical techniques provide means of determining an instantaneous corrosion rate and also one can follow electrochemically how the rate varies with time. They are automated easily⁽⁹⁰⁾. In some cases the techniques are fast enough to be used for routine quality control⁽⁹¹⁾, or even as the basis for on-line corrosion monitoring^(92,93).

- Background and Theory

In a corroding system, oxidation of the metal (reaction 1 page 66) and reduction of some species in solution (reaction 2, page 67)) are taking place at the same rate, and the net measurable current is zero. The corroding metal will assume a potential that is dependant upon the metal itself and the nature of the solution. This 'open circuit' i.e. no external potential is applied to the cell, is referred to as the corrosion potential, E_{corr} . A specimen at E_{corr} has both anodic and cathodic currents present on its surface (oxidation, I_{ox} and reduction, I_{red} currents) equal and non zero.

$$I_{meas} = I_{ox} - I_{red} = 0 \quad , \text{ at } E_{corr} \quad (7)$$

$$\text{and } I_{corr} = I_{ox} = I_{red}$$

If the current flowing through the specimen were measured at E_{corr} , only the total current (zero) would be obtained. This is unfortunate because a direct measurement of I_{ox} is the same as I_{corr} (corrosion rate), i.e. the rate of conversion of M to M^{n+} .

It is possible to impose potentials (E_{app}) other than E_{corr} from an external voltage source such as a potentiostat. This is referred to as polarizing the specimen - solution interface. The total current (I_{meas}) is now finite and measurable according to the following equation:

$$I_{\text{meas}} = I_{\text{ox}} - I_{\text{red}} \quad (8)$$

Stern and Geary (94) have shown that by applying a controlled potential scan ($\pm 20\text{mV}$) with respect to E_{corr} , the resulting total current (I_{meas}) varies linearly with the applied voltage (E) as illustrated in Figure 2.4.

The slope of the potential-current graph at E_{corr} , (R_p), is used together with the Tafel constants (b_a and b_c) to determine I_{corr} . The slope $R_p = E / I_{\text{meas}}$ has units of resistance, hence linear polarization resistance.

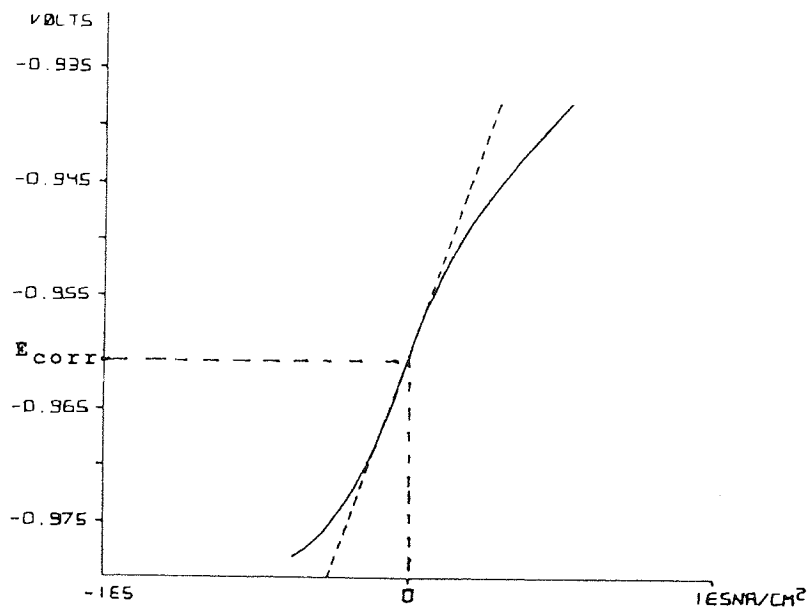


Fig. 2.4 Typical Linear Polarization curve.

Polarization Techniques

The most commonly used techniques are:

- Linear Polarization
- Tafel Plot
- Potentiodynamic scan
- pitting

In the present work, only the first three techniques were used.

- Linear Polarization

This is an extremely rapid procedure for determining corrosion rates. At a scan rate of 0.1 mV per second, a potential range of 40 mV is scanned in less than 4 minutes. Since the applied potential is never far removed from the

corrosion potential (E_{corr}), the surface of the test sample is not materially affected by the experiment. Therefore, the same specimen can be used for other studies or for on-line monitoring procedures.

An estimate of the corrosion current (I_{corr}) can be obtained by assuming values for the Tafel constants (b_a and b_c) or inferring them from the literature for similar chemical systems. The most accurate results are obtained when the constants are determined experimentally for the metal-solution interface.

In recent years, however, several authors⁽⁹⁵⁻⁹⁷⁾ have noted that even within 5 to 20 mV of the rest potential, polarization graphs have considerable curvature and serious errors in determining corrosion rates from those graphs are introduced as a result.

Le Roy⁽⁹⁸⁾ reviewed different approaches towards calculating corrosion rates from linear polarization measurements. The experimental polarization data consist of a series of measurements of the current which flows when the sample is polarized by a potential with respect to E_{corr} . Le Roy pointed out that the errors are mainly due to the assignment of anodic and cathodic Tafel constants. It is well known that the b values may vary with time, composition of material and the electrolyte⁽⁹⁸⁾.

Mansfeld⁽⁹⁹⁾ suggested a graphical method to evaluate the I_{corr} from the E Vs I_{meas} curves without the need to know or estimate the Tafel constants; eliminating therefore the source of errors.

However, correlation with weight loss data has been very successful in a number of systems⁽¹⁰⁰⁻¹⁰³⁾. Corrosion monitoring in alkaline sulphide pulping liquors has been performed by means of linear polarization resistance and electrical resistance methods. The linear polarization technique has been shown to be an acceptable method for measuring corrosion rates when approximate corrections are applied, consistent with the measured Tafel constants⁽¹⁰⁰⁾.

Dattilo⁽¹⁰¹⁾ has shown that the correlation between the weight loss determined by solution analysis and the linear polarization resistance is excellent for Zn plated steel wire.

Electrochemical tests were conducted on several Zn-Al coated steels whose long term atmospheric corrosion performance is known in order to evaluate such tests as a screening technique. LPR measurements were made in an aerated 1.0 N NaCl and 0.5 N Na₂SO₄ both at pH 4 to simulate marine and industrial environments. The results obtained from both environments were in good general agreement with the data from atmospheric exposures⁽¹⁰²⁾.

- **Tafel Plot**

The Tafel technique focuses on the problem of accurately determining the corrosion rate of a material. In this technique, a controlled potential scan is typically applied to a sample of the material, starting at E_{corr} (corrosion potential) and extending in either the anodic or the cathodic direction for a few hundred millivolts, typically 300 mV. When the resultant potential current function is plotted on semi-log paper, it characteristically exhibits a linear region, see Figure 2.5. The plot itself is known as the Tafel plot. Extrapolation of these linear regions yields straight lines with the slopes known as Tafel constants (b_a and b_c). Tafel constants are expressed in terms of volts per decade of current. As indicated in the Figure 2.5, if the straight line fitted to the anodic or cathodic Tafel plot is extended to E_{corr} , then I_{corr} can be determined.

The Tafel plot technique provides an extremely rapid means of determining the corrosion rate when compared with the conventional weight change method. The technique can be very advantageous for such studies as inhibitor evaluations, oxidizer effects and alloy comparisons. In this work, the technique was used for determining Tafel constants (b_a and b_c) for further use in linear polarization measurements.

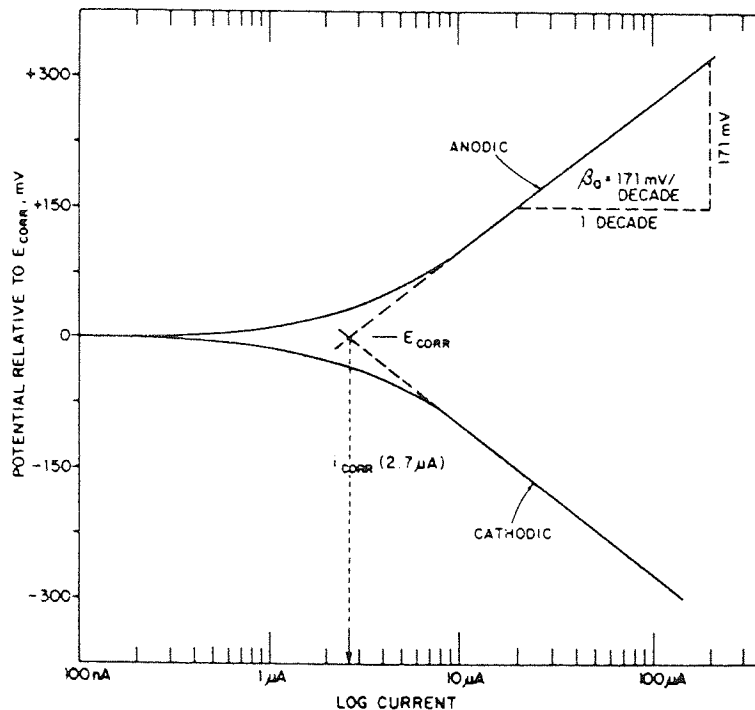


Fig. 5.2 Typical Tafel plot

- Potentiodynamic Polarization Scan

The technique is suited for giving an overall view of the corrosion behaviour of a material. Potentiodynamic polarization is the characterisation of a metal specimen by its current-potential relationship. In the case of potentiodynamic anodic polarization, the specimen is scanned slowly in the anodic direction i.e. the specimen is forced to act as an anode such that it corrodes or forms an oxide coating. The measurements are used to determine corrosion characteristics of metal specimens in the environment of interest. A complete current potential plot of a specimen can be measured in a few hours, or in some

cases in a few minutes. Investigations such as passivation tendencies and effects of inhibitors or oxidizers of specimens can be performed with this technique.

Siitari et al (104) conducted anodic polarization in nitrogen saturated 5% NaCl solution on Zn-Ni alloy coatings in order to determine the effect of Ni composition on their electrochemical behaviour. Some correlation between the structures of the corroded surfaces and the polarization behaviour was made. For the 11% and 25% Ni samples, a change in the slope of the polarization curves at more noble potentials (approximately -950 and -650 mV respectively) was observed. This was attributed to the localised corrosion which was then taking place. The polarization curve for 25% Ni specimen showed a drastic decrease in slope i.e. the surface after polarization showed both large cracks and coating loss. Correspondingly, the red rust resistance in a salt spray test (SST) was poor. However the 14% Ni sample which showed the best SST performance, the slope of the polarization curve did not decrease, but in fact increased slightly near -800 mV.

- Pitting Scan

Unlike Tafel and polarization resistance measurements, which are primarily the technique for determining the corrosion rate of a material; the pitting technique is directed towards determining the tendency of a material to undergo pitting or crevicing when placed in a specific corrosion

environment. This technique is very useful in the development of alloys required to be 'pit' resistant. this technique was not used in this present work.

- Conclusion

Although, an understanding of the mechanism, and proper interpretation of accelerated test results are essential for obtaining reproducible and accurate information, it must however be emphasised that it is not possible to predict the exact life to be expected under service conditions. It is therefore usual to confirm the results from accelerated tests by the longer term outdoor exposure and service trials.

3 EXPERIMENTAL PROCEDURES

3.1 Laboratory Prepared Dull Deposits

3.1.1 Zinc-Nickel Electrodeposition

3.1.1.1 Ammonium Based Electrolytes

- *Preparation of the plating solutions*

A base solution having the composition shown in Table 3.1 was prepared by adding the appropriate amounts of zinc and nickel chloride to cold distilled water in a 5 l glass beaker and stirring well. The conducting salt (NH_4Cl) was dissolved in a separate glass beaker with heating ($60-70^\circ\text{C}$) and stirring. When all the salts were dissolved the solutions were allowed to cool and then mixed together. The resulting solution was diluted with cold distilled water to the volume desired (10 l) in order to give the correct concentrations and then the pH adjusted. A Buchner funnel was used to filter the solution which was then stored in a large plastic container. The plating solution of the composition listed in Table 3.1 was used initially.

The pH of the solution was adjusted by the addition of either hydrochloric acid(50%) or ammonia (25%). The resulting change in concentration is insignificant. A Phillips digital pH meter was used for the pH measurements and calibration was carried out by using two buffer solutions of pH = 4.0 and 7.0.

Table 3.1. Ammonium Chloride based Zn-Ni Bath formulation.

Constituent Salt	Conc. gl^{-1}	Metal Conc. gl^{-1}	
ZnCl ₂	62.5	30.0	Base solution
NH ₄ Cl	200.0	-	
NiCl ₂ .6H ₂ O	4.1	1.0	

Temperature 30.0 \pm 0.5°C

pH 5.5 \pm 0.2

Anode Pure zinc

Agitation Air

- **Electrodeposition**

Seven different nickel concentrations were investigated: 1.0, 5.0, 10.0, 15.0, 20.0, 30.0, and 40.0 gl^{-1} of nickel metal in the plating solutions. The zinc metal and the conducting salt, ammonium chloride (NH₄Cl), contents were kept constant at 30.0 and 200.0 gl^{-1} respectively throughout the work.

For each individual nickel concentration, electrodeposition was carried out at five current densities (0.5, 1.0, 2.0, 3.0, and 4.0 Adm^{-2}) using a glass beaker of 3 l capacity. For each test about 1.5 l of fresh solution was electrolysed for the appropriate time. The used electrolyte was stored and a new one used for each current density.

The results are given in Tables 4.1 - 4.7 and illustrated graphically in Figures 4.1.

The beaker containing the plating solution was partially immersed in a water bath fitted with an immersion heater and thermostat. Heat and evaporation losses from the water bath and the plating beaker were reduced by using layers of small polypropylene croffles which floated on the liquid surface.

A pure zinc anode approximately 7 x 14 cm was used. This was cast in the foundry, degreased with acetone, pickled with a concentrated solution of 1:1 $\text{HNO}_3:\text{HCl}$ for 30 seconds, swilled in distilled water and put in a terylene bag. A rectifier with an output of (12 V and 10 A) was employed for the electrodeposition, connections being made via crocodile clips. The power supply was used in the constant current mode throughout the work.

Mild steel panels, about 4 x 5 cm were used as test-pieces. These were cut and drilled in the workshop, rinsed with acetone, dried and lacquered on one face and the edges. They were left to dry overnight, then weighed individually using a balance with a capacity of 100 g and an accuracy of 0.01 mg. Prior to plating, the specimens were subjected to the following pretreatment :

- Anodic treatment in a hot, commercial alkaline solution at 4 Adm^{-2} and 60°C for 60 seconds.

- Rinse in cold distilled water.
- Dip in hydrochloric acid (50% V/V acid).
- Anodic treatment in a cold, commercial cyanide cleaning solution at 4 Adm^{-2} for 60 seconds
- Rinse in cold distilled water.
- Dip in sulphuric acid (20% V/V acid).
- Rinse in cold distilled water.
- Electroplate.

Adequate pretreatment is essential to remove any contaminants such as dirt, grease and rust so as to ensure activation of the surface and good adhesion of the coating.

After cleaning, each test specimen was transferred immediately to the plating cell and plated at the chosen conditions. The samples were suspended in plating solution using copper wire which was masked off with PVC tape. After plating, the test panel was rinsed, dried in a warm air stream and weighed immediately. After weighing, the samples were stored in a desiccator for later use for corrosion and chromating studies, although whenever possible they were analysed immediately after preparation. The coating weights were used to evaluate the cathode current efficiencies under the conditions employed.

- Cathode Current Efficiency

The following assumptions were made when calculating the efficiency :

- The total current was used to deposit or liberate the three relevant elements Zn, Ni (or Co) and H₂; that being used to liberate hydrogen representing the wasted energy.
- A Faraday (F) deposits the gramme-equivalent weight (g.equiv.wt.) of each element which is :

$$\text{For Zn, } \frac{65.38}{2} = 32.69$$

$$\text{For Ni, } \frac{58.69}{2} = 29.34$$

$$\text{For Co, } \frac{58.64}{2} = 29.32$$

The cathode current efficiency was calculated on the basis of comparing the theoretical number of g.equiv.wt. deposited with the actual number (19).

For example, a deposit having 16.1% Ni and 83.9% Zn, (weight %), weighing 0.23858 g was obtained after passing 0.1 A for 120 minutes. The cathode current efficiency is calculated as follows:

One Faraday (96500 C) deposits 1g.equiv.wt.

$$0.1 \times 120 \times 60 = 720 \text{ C deposit } \frac{720}{96500} = 0.00746 \text{ g.equiv.wt.}$$

The weight of Ni in the deposit :

$$\frac{0.23858 \times 16.1}{100} = 0.03841 \text{ g}$$

used to study the effect of

$$\text{The weight of Zn in the deposit} = \frac{0.23858 \times 83.9}{100} = 0.20017 \text{ g}$$

$$\text{No. of g.equiv.wt. of Ni} = 0.03841/29.34 = 0.00131$$

$$\text{No. of g.equiv.wt. of Zn} = 0.20017/32.69 = 0.00612$$

$$\text{Total} \quad \quad \quad 0.00743$$

$$\% \text{ C.C.E} = \frac{\text{g.equiv.wt.deposited}}{\text{theoretical g.equiv.wt.}} \times 100$$

$$= \frac{0.00743}{0.00746} \times 100 = 99.6\%$$

- Effect of Temperature, pH and Agitation on Ni Content of the Deposits and Cathode current efficiency

The effects of temperature, pH, and agitation on deposit Ni content and cathode current efficiency were studied, using a Zn-Ni bath having the composition shown in Table 3.2.

Effect of Temperature

Four different temperatures were studied: 25.0, 30.0, 35.0 and 40.0°C, using the following conditions:

pH 5.5 ± 0.2

C.D 3.0 Adm⁻²

Air Agitation

The plating solution, specimen preparation and the analyses were carried out in the same way as described previously. For each test panel a fresh aliquot of electrolyte was used.

Table 3.2 Plating solution used to study the Effect of Temperature, pH and Agitation.

Constituent Salt	Conc. gl^{-1}	Metal Conc. gl^{-1}
ZnCl_2	62.5	30.0
$\text{NiCl}_2 \cdot 6\text{H}_2\text{O}$	60.7	15.0
NH_4Cl	200.0	-
Ammonia (25%)	50.0	-

Effect of pH

The pH values studied were: 3.5, 4.5 and 5.8; and the plating conditions were :

Temperature $30.0 \pm 0.5^\circ\text{C}$

C.D 3.0 Adm^{-2}

Agitation Air

At and above pH 6.4, a white crystalline precipitation was observed.

Effect of Agitation

Two test panels were plated to study the effect of agitation. The first was plated using agitation and the second without it. A temperature of 30.0°C , pH of 5.5 and current density of 3.0 Adm^{-2} were used in both cases.

Tables 4.11, 4.12 and 4.13 and Figures 4.8 and 4.9 illustrate the effect of the temperature and pH on Ni

content of the deposits.

3.1.1.2 Zn-Ni Potassium Chloride Based Electrolyte

Potassium chloride based solutions were used for comparison with Zn-Co systems and for plating large panels (about 10 x 15 cm in size) for salt spray corrosion testing. A large plastic container of 10 l capacity and two large pure Zn anodes (15 x 20 cm in size) were used. Five different Ni concentrations electrolytes were prepared. These were: 1.0, 5.0, 10.0, 20.0, and 40.0 gl^{-1} . For each individual nickel concentration, the electrodeposition was carried out at four current densities (1.0, 2.0, 3.0 and 4.0 Adm^{-2}), and two different temperatures (25.0 and 30.0°C). The solution preparation was exactly the same as for the ammonium based one described previously. The plating solution having composition listed in Table 3.3 was used initially.

Table 3.3 Potassium Chloride Based Solution

Constituent Salt	Conc. gl^{-1}	Metal Conc. gl^{-1}	
ZnCl ₂	83.3	40.0	Base solution
KCl	210.0	-	
H ₃ BO ₃	25.0	-	
NiCl ₂ .6H ₂ O	4.1	1.0	

Temperatures: 25.0 and 30.0 \pm 0.5°C

pH: 5.5 ± 0.2

Agitation Air

Note that the solution contained 40.0 gl^{-1} zinc metal, unlike the ammonium based solution which contained 30.0 gl^{-1} , (see Table 3.1). This was because the Zn-Co plating solution contained this same amount of Zn.

The effect of Ni solution concentration, current density and temperature on deposit Ni content are given in Tables 4.15 and 4.16 and Figures 4.16 and 4.17.

3.1.2 Zinc-Cobalt Electrodeposition

Only a potassium chloride based solution was used for the Zn-Co systems. Several Co concentrations were used: 1.0, 5.0, 7.0, 10.0, 15.0, 20.0, and 25.0 gl^{-1} . The reason for taking a 7.0 gl^{-1} Co electrolyte was for comparison purposes; since the commercial Zn-Co solution (Zincrolyte*) which will be described later, contained this amount of Co. For each individual Co concentration plating solution, five different current densities and two different temperatures were used in order to study their effect on the Co content of the deposits. Again large samples $10 \times 15 \text{ cm}$ in size, a container of 10 l capacity and two anodes ($15 \times 20 \text{ cm}$ in size) system were used. The solution preparation and analyses were exactly the same as for Zn-Ni systems. The solution given in Table 3.4 was used initially.

* Trade name for Zn-Co plating solution developed by OMI International.

Table 3.4 Zinc-Cobalt Plating Solution

Constituent Salt	Conc. gl^{-1}	Metal Conc. gl^{-1}	
ZnCl ₂	80.3	40.0	Base Solution
KCl	210.0	-	
H ₃ BO ₃	25.0	-	
CoCl ₂ ·6H ₂ O	4.07	1.0	

Temperature 25.0 and 30.0 \pm 0.5°C

pH 5.3 \pm 0.2

Agitation Air

The Co solution concentration, current density and temperature effects on deposit Co content are shown in Tables 4.19 and 4.20 and Figures 4.20 and 4.21.

The 7.0 gl^{-1} Co electrolyte was used for further investigation. Four different temperatures (25.0, 30.0, 35.0, and 40.0°C) were studied keeping the following plating conditions constant:

Current Density 2.0 Adm^{-2}

pH 5.3

Plating Time 30 minutes

Agitation Air

Table 4.24 and Figure 4.25 illustrate the effect of temperature on deposit Co content.

3.2 Commercial Bright Deposits

Two commercial Zn-Co plating solutions were used for this part of the work: acidic having a pH of 5.3 (Zincrolyte) and alkaline (Canning).

3.2.1 Zincrolyte System

Table 3.5 gives the system base solution which was prepared in exactly the same way as were the previous electrolytes.

Table 3.5 Zn-Co base Plating solution

Constituent Salt	Conc. gl ⁻¹
ZnCl ₂	83.3
KCl	210.0
H ₃ BO ₃	25.0

After solution preparation, the following additions were then made as recommended by the supplier :

Zincrolyte	K Make up*	25.0 ml ⁻¹
Zincrolyte	ACA *	40.0 "
Brightener		0.5 "

The pH was adjusted using hydrochloric acid or potassium hydroxide. Panels of size 4 x 5 cm sized panels were used as test-pieces. The same preplating, specimen preparation and analysis procedures used previously were applied for this

* Trade name for Zn-Co plating solution additives developed by OMI International.

system. For each test panel, a fresh solution was used.

- Effect of Current Density

Four different current densities were investigated (1.0, 2.0, 3.0 and 4.0 Adm^{-2}) under the following conditions:

Temperature 30.0 \pm 0.5°C

pH 5.3 \pm 0.2

Agitation Air

Anode Pure zinc

Table 4.23 and Figure 4.24 illustrate the effect of the current density on deposit Co content and cathode current efficiency.

- Effect of Temperature

The current density was kept constant at 2.0 Adm^{-2} and pH was maintained at 5.3. Using air agitation, the plating solution was electrolysed at four different temperatures (25.0, 30.0, 35.0 and 40.0°C).

Table 4.24 and Figure 4.25 illustrate the effect of the temperature on deposit Co content and cathode current efficiency.

3.2.2 Canning Zn-Co System

Large mild steel samples about 10 x 15 cm in size were plated from a large tank of capacity of 280 l at Canning Research Laboratory (Birmingham). An alkaline zincate based

solution was used. The bath formulation and operating conditions are given in Table 3.6 below.

Table 3.6 Canning Commercial Zn-Co System Plating solution.

Bath Constituent	gl ⁻¹
Zn metal	10.0
Co metal	0.8
NaOH	100.0
Complexant	25.0
+ Brightener additives	-
Temperature	22-23°C
Agitation	None
Anodes	Combination of Zn and Mild Steel anodes

- Effect of Current Density

Five different current densities were investigated: 1.0, 2.0, 3.0, 4.0 and 5.0 Adm⁻². Prior to plating, the panels were pretreated as follows:

- Anodic clean in a hot alkaline solution at 3.0 Adm⁻² and 80°C for 2 minutes.
 - Dip in HCl solution (10% V/V) containing an inhibitor.
 - Rinse and periodic reverse clean in an alkaline solution.
- Three cycles procedure was used: cathodic for 20 seconds - anodic for 10 seconds - and cathodic for 20 seconds.
- Rinse and dip in H₂SO₄ solution
 - Rinse and electroplate.

The results are given in Table 4.25 and Figure 4.26

illustrate the effect of the current density on Co content of the deposits.

3.3 Plating Solutions Control and Chemical Analyses

3.3.1 Atomic Absorption Spectrophotometry (AAS)

The basic principle of atomic absorption spectrophotometry is as follows: atoms where all the electrons are in their ground state will absorb radiation of specific wavelengths, characteristic of the element, and the intensity of this absorption is a function of their concentration. The wavelengths absorbed are the same as those that would be emitted in exciting the element.

The essential requirements for an atomic absorption spectrophotometer include:

- 1- a light source of radiation to emit the spectrum of the element to be determined, under conditions which ensure the production of extremely sharp lines.
- 2- a means of atomizing the sample solution
- 3- a wavelength selector to isolate the desired resonance line and,
- 4- a radiation detector and some means of measuring the amount of absorbed radiation.

In the first step of an analysis, the elements under study must be atomized by spraying solution into a flame where the solvent in the solution evaporates. Then the resulting solid particles thermally decompose to give molecules in the gaseous phase, and finally, the molecules dissociate into

free atoms. The flame is placed between two lenses so that the radiation from a source is focussed at the centre of the flame and then refocussed on to the wavelength selector which separates the desired resonance line from all other lines emitted by the sharp-line source. A resonance line is a spectral line due to a transition between the excited state and the ground state.

A 'Perkin Elmer' atomic absorption spectrophotometer model No. 560 was used to determine the composition of the plating solutions and some deposits.

3.3.1.1 Plating Solution Control

- Determination of Ni and Co in Plating Solutions

The linear range for detecting Ni (or Co) is between 0 and 5 ppm using an air/acetylene flame. Test solutions were diluted sufficiently so that the concentration of Ni or Co fell within this range. To maintain maximum accuracy a systematic procedure was adapted whereby all glassware was rinsed in dilute nitric acid (20 %) and then distilled water. This was found to be time consuming but essential if reliable results were to be produced.

A standard solution (5 ppm) was produced by pipetting 1 ml of nickel (or Co) nitrate (1000 ppm) into a 200 ml flask and making up to the mark with distilled water. For a blank solution (0 ppm), distilled water was used. At first problems were encountered due to considerable baseline drift and lack of accuracy and repeatability. These problems

were overcome by adopting the following procedures:

- The use of combined standards, each containing all the elements (different metals and salt ions) that are present in the plating solution to be analysed. Any inter-element effects were cancelled out by this method
- The base salt ions such as K^+ , Cl^- or NH_4^+ present in the plating solutions were also added to the blank solution.
- The pH of the standards, blanks and sample solutions were adjusted to about the same value.
- The use of two standards method ($S_1 = 1$ ppm and $S_2 = 5$ ppm); and the test solutions were diluted to fall within S_1 and S_2 .

- Determination of Zn in Plating solutions

The same procedures as above were used for zinc determination, except that the linear range for detecting zinc is between 0 and 1 ppm, so the zinc test solution and standards were more dilute.

In both cases, the analytical procedure was as follows:

The appropriate lamp was installed, the lamp current was set, the gain increased, the absorption wavelength adjusted, the diffraction grating slit width set and the burner height was adjusted. The acetylene/air mixture was then ignited. Maximum absorbance was found by adjusting the burner head position (in relation to the beam from the lamp) and the fuel/oxidant settings, while aspirating the standards. The

sampling time was set for 2 seconds and average of readings set to 5. The instrument was then ready for use. A blank solution was introduced to the nebulizer and the zero level set. This was followed by aspirating the standards, then finally by aspirating the sample solution and noting the concentration of the element analysed. Distilled water was passed through the nebulizer between each setting. Each reading was repeated three times and the mean value taken. The standard and zero had to be reset between every reading because of the background drift.

- Analysis of Zn-Ni Alloy Deposits

To determine the percentage composition of the alloy, a small piece of the test panel was cut and stripped in 20 ml of stripping solution, which consisted of:

- HCl (concentrated) 600 ml⁻¹
- Antimony trioxide 3 g^l⁻¹

The concentrated HCl was diluted to the appropriate volume and the indicated amount of antimony trioxide added. The 20 ml of solution containing the dissolved alloy was diluted with distilled water. Further dilution was made to bring the amount of metal to the appropriate range for analysis.

The main purpose of this exercise was to cross-check some of the results obtained by analysis in the Scanning Electron Microscope (S.E.M.) which was used for coating analysis throughout the work.

- **Determination of 'Zincrolyte' K Make up**
(Method used by the supplier firm)

A 'Beckman' U.V. spectrophotometer, Model 24 was used to determine the amount (ml^{-1}) of the 'Zincrolyte' K Make up in the Zn-Co commercial plating solution. The technique is based on the principle that organic compounds in solution absorb ultra-violet light (200-400 nm). The absorbance at a given frequency is given by $\log I_0/I$; where I_0 is the intensity of the incident light and I is the intensity of the transmitted light. Furthermore, the absorbance is directly proportional to the concentration of the solution to be analysed.

A portion of the plating solution to be analysed was filtered to remove any suspended solids. 2 ml of the filtered sample was pipetted in a 100 ml volumetric flask. 10 ml of 1.0 N sulphuric acid was added and the solution made up to 100 ml with distilled water. The sample was mixed thoroughly and analysed.

Distilled water was used as a reference liquid. The absorbances at wavelengths of 350, 300, and 270 nm were measured and the quantity of the additive was calculated as follows:

ml^{-1} Zincrolyte K Make up =

$$(A_{270} - A_{350}) - 0.89 (A_{300} - A_{350}) \times 98.$$

where,

A_{270} = Absorbance measured at 270 nanometers

A_{300} = Absorbance measured at 300 nanometers

A_{350} = Absorbance measured at 350 nanometers

3.4 Metallurgical Examination and Characteristics of Coating and Plating Solutions

3.4.1 Metallurgical Examination

- Specimen Preparation

Samples were cut from the central area of each individual plated panel, using a manual guillotine, and prepared for microscopical study. The specimens were mounted in conducting thermosetting resin and ground by hand on successively finer silicon carbide papers and diamond pads. They were then cleaned ultrasonically in a detergent solution for five minutes, rinsed in water and dried. Finally, they were analysed using a Scanning Electron Microscope.

Some samples were etched using 1% HCl in alcohol (50% V/V alcohol) solution, washed thoroughly and dried. They were examined under an optical microscope and appropriate photomicrographs were taken. Some other samples (in the unetched conditions) were further polished for the electron probe microanalysis.

- Scanning Electron Microscope, (SEM)

All the deposits were analysed using a Cambridge Instrument Model 150 SEM and analysed with an energy dispersive X-ray analysis (EDXA) attachment, and corrections carried out

using a Z.A.F programme. All the values are quoted in weight percent.

Considerable time was saved by mounting a large number of specimens side by side on a single mount, so that a batch of analyses could be completed at one time, without the need to 'pump down' the vacuum system for each individual analysis.

Non-conducting samples such as corroded and chromated films were electrically connected to the SEM with colloidal silver and also a thin conducting layer of carbon was deposited onto their surfaces. This avoids charging of the samples in the SEM and improves the resolution.

- Electron Probe Microanalysis

A Cambridge MK5 Electron probe microanalyser was used to determine the distribution of alloy constituents in the deposits. The analysis was performed at a scan rate of 7.5 μm per minute.

3.4.2 Characteristics of Coating and Plating Solutions

- Deposits Microhardness Measurements

Hardness was determined using a Leitz microhardness tester and the average values of measurements made in five different areas were taken. Table 4.14 and Figure 4.10 illustrate the effect of Ni content on the deposit hardness.

- Solutions Throwing Power Measurements

For evaluation of microthrowing power, a 267 ml Hull-Cell was employed using copper cathodes 7.5 x 10 cm and a pure zinc anode of about 6 x 7 x 0.5 cm. The anode was fitted at the rectangular end of the cell and the cathode along the sloping side.

The cathode was stopped off, except on the working face, with a protective lacquer. Prior to plating, each cathode was scribed with vertical lines at measured intervals, so that a deposit thickness determination at specific positions on the cathode panel could be made. Finally, the cathodes were cleaned as follows :

- Anodic treatment in a hot alkaline solution at 4.0 Adm^{-2} for 60 seconds
- Rinse in cold water
- Cathodic treatment in a cold alkaline (at room temperature) solution at 4.0 Adm^{-2} for 60 seconds
- Rinse in cold water
- Dip in sulphuric acid solution (10% V/V concentrated acid)
- Rinse in cold water
- Plate

The cell was immersed in a water bath to maintain the temperature of the plating solution at the chosen value.

Zn-Ni plating solutions of four different nickel

concentrations were evaluated. These were 10.0, 15.0, 30.0 and 40.0 gl^{-1} nickel metal. For comparison, pure zinc and Zincrolyte commercial Zn-Co plating solutions were tested. The pure zinc plating solution consisted of :

NH_4Cl 200.0 gl^{-1}

ZnCl_2 62.5 gl^{-1} (30.0 gl^{-1} zinc metal)

The following plating conditions were used for each of the plating solutions :

Temperature $30.0 \pm 0.5^\circ\text{C}$

pH 5.5 ± 0.2

Cell Current 1.0 Ampere

Plating Time 60 minutes for Zn-Ni solutions
 45 minutes for pure Zn solution
 30 minutes for Zn-Co solution.

Agitation Air was used in all cases.

- Deposit Distribution Measurements

After plating, the cathodes were cleaned and dried. Each cathode was cut into strips and cross-sections mounted in bakelite so that they could be polished metallographically. Thickness of deposit was measured using the optical system of the microhardness (Vickers Photoplan) tester, as close as possible to the vertical scribe lines. In order to identify the current densities at specific positions on the cathode panel, the following formula was employed :

$i = I (4.08 - 3.96 \log x)$, where

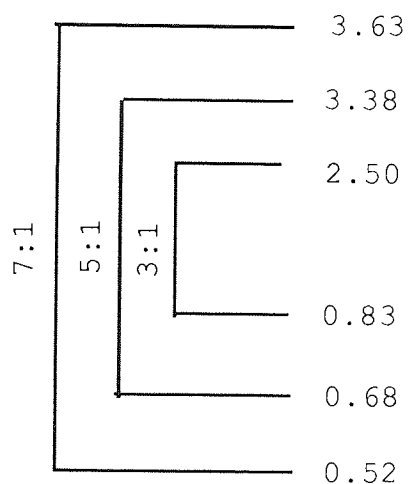
i = primary current density, Adm^{-2}

I = total current used, A

and x = distance (cm) from the high current density end of panel, between 0.6 and 8.2 cm.

Primary current densities were chosen according to the method published by Watson⁽¹⁰⁵⁾, to give current density ratios of 3:1, 5:1 and 7:1 as shown below.

Primary Current density (Adm^{-2})



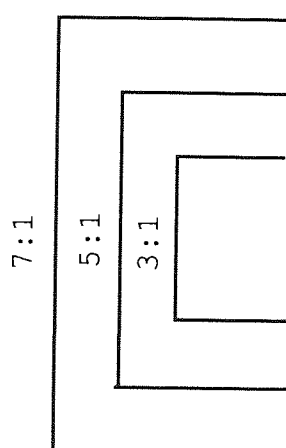
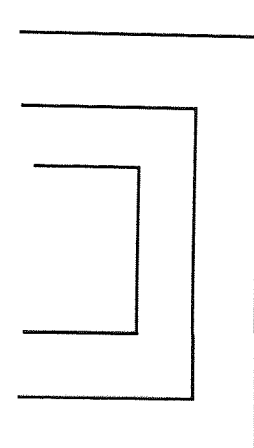
The thicknesses corresponding to current densities chosen were read from the graphs, and hence the metal distribution (M) was obtained.

- Example of Calculation

The positions on the Hull Cell cathode corresponding to primary current density at ratios of 3:1, 5:1, and 7:1 were

chosen arbitrarily since it has been shown by Watson (105) that the effect of using other positions is small. Two methods of calculation were used based on different current ratios. The calculation of throwing power for the pure zinc solution is given as an example :

- **Method I**

Primary C.D. Adm ⁻²		Distance from H.C.D. end, cm		Thickness (read from graph), μm	
	3.63	1.3	48		
	3.38	1.5	44		
	2.50	2.5	33.2		
	0.83	6.6	12		
	0.68	7.2	10		
	0.52	7.9	7.7		

The following primary current ratios (**P**) correspond to the following metal distribution ratios (**M**) :

P	M
3:1	2.77
5:1	4.40
7:1	6.23

The macrothrowing power (M.T.P) value according to Field's equation as quoted by Luke⁽¹⁰⁸⁾ is given by the expression:

$$M.T.P = \frac{100 (P-M)}{P+M-2} \quad \%$$

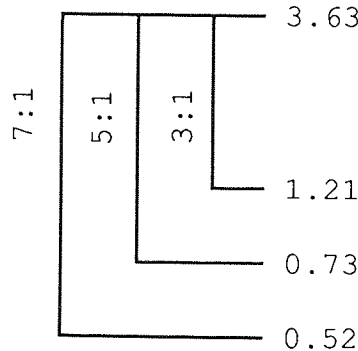
$$M.T.P (3) = \frac{100 (3-2.77)}{3+2.77-2} = +6.1\%$$

$$M.T.P (5) = \frac{100 (5-4.4)}{5+4.4-2} = +8.11\%$$

$$M.T.P (7) = \frac{100 (7-6.23)}{7+6.23-2} = +6.86\%$$

Method II

Throwing power was recalculated from the same panels by obtaining the primary current ratios by the following method

Primary C.D. Adm^{-2}	Distance from H.C.D end, cm	Thickness (read from graph), μm
	1.3 	48.0
	5.3	17.5
	7.0	10.5
	7.9	7.7

The following primary current ratios correspond to the following metal distribution ratios :

P	M
3:1	2.74
5:1	4.57
7:1	6.23

$$\text{M.T.P (3)} = \frac{100 (3-2.74)}{3+2.74-2} = +6.95\%$$

$$\text{M.T.P (5)} = \frac{100 (5-4.57)}{5+4.57-2} = +5.68\%$$

$$\text{M.T.P (7)} = \frac{100 (7-6.23)}{7+6.23-2} = +6.86\%$$

Both methods were used to calculate all the results which are shown in Table 4.9 and Figure 4.4.

3.5 Conversion Coatings

Two different types of electrodeposits were studied for this part of the work: dull deposits obtained previously from additive free solutions and smooth bright commercial deposits. The different types of chromating solutions, operating conditions used and coating systems treated are listed in Table 3.7.

It was decided to establish the effect of chromating solution type and the immersion time on conversion film colour, chemical composition and corrosion resistance. Five different immersion times were investigated: 15, 30, 60, 90 and 120 seconds. The details of conversion coating solutions and samples treated are given in Table 3.7.

- *Chromating Procedures*

Prior to passivation, samples about 3.0 cm² in size were carefully prepared by degreasing in acetone followed by rinsing with distilled water and hot air drying. For each sample about 100 ml of fresh conversion solution was used for the appropriate time. After treatment, the samples were rinsed in hot distilled water (at about 60°C) and dried in a hot air stream. The solution was then analysed for metal dissolution using the AAS. The change in weight was determined by weighing the dried samples before and after treatment. An estimate of the true coating weight was obtained by adding the sample weight change to the weight of the deposit constituents dissolved during chromating.

Table 3.7 Conversion coating Solutions and Treated Samples Identification.

Conversion coating solutions	Samples treated
Solution (1):	
CrO ₃ 12.0 gl ⁻¹	Dull deposits: Pure Zn
NaCl 17.0 gl ⁻¹	0.3, 7.6, 12.4 and 21.3% Ni
pH = 1.0	0.3, 5.1 and 14.7% Co
Temperature = 22.0°C	Bright deposits: 0.3, 0.7
	1.0% Co and 13.8% Ni
Time = 15, 30, 60, 90 and 120 seconds	
Agitation : Movement of the test piece	
Solution (2):	
Canning Solution	Dull deposits only
Temperature = 20.0°C	
Time = 90 and 120 seconds	
Agitation : Movement of the test piece	
Solution (3):	
Schloetter Solution	Dull deposits only
Temperature = 40.0°C	
Time = 40 seconds	
Agitation : Air	

- Measurement of Open circuit Potentials during Conversion coating

The conversion film formation on samples treated in solutions (1) was also followed by potential-time variations. These were recorded continuously on a 'Teckman'

chart recorder Model TE 200, with variable speed and full scale deflection settings. The full scale deflection was usually set at 2.0 volts and the speed at 300 mm/min. In all cases, the potentials have been quoted with respect to a saturated Calomel electrode. The recorder was calibrated frequently against a 'Farnell' stabilised power supply (Model L10-3C).

- Conversion film Analysis and Examination

Surface colouring and appearance were assessed visually and appropriate photographs taken. Conversion film morphologies were examined and chemical compositions determined. The result of film analyses determined by EDXA are presented in Tables 4.29 and 4.30. These results should be treated with caution due to the limitation of the technique when examining thin cracked coatings. Substrate elements will be included in the analysis due to exposure of the substrate at cracks and beam penetration of very thin coatings. EDXA analyses a volume of material (about 1 μm in depth) rather than just the atoms at the surface.

An X-ray photo-electron spectroscopy (XPS) study was also carried out as a complementary method of studying the chemical composition of the surface film. XPS was chosen to exploit its ability to analyse the outermost surface layer and to assess the chemical state of the elements as well as indicating their presence. This technique permits examination up to a depth of 10 nm.

- XPS Analysis Details

Specimens 15 x 7 mm in size were cut from chromated panels and subjected to XPS analysis. This was performed in a Kratos X SAM 800 ESCA-Auger instrument, with both Mg and Al K_{α} -X radiation. An ultrahigh vacuum of about 10^{-9} Torr was maintained inside the sample analysis chamber while measurements were taken. The use of double source, Al and Mg was very important in eliminating the problem of interference of the elements, in the cases of very thin chromate films. The spectra of the elements of interest such as Cr, Zn, Ni, Co, Cl and O were recorded, (see Figures 4.40-4.42). The peak positions in the spectra were referred to C 1s at a binding energy of 285.0 eV. The C 1s spectra are due to hydrocarbons on the specimen surfaces and they are often used as a reference value in XPS analysis.

Data was collected and recorded with an Apple IIe microcomputer system linked with the spectrometer. Software was available for data analysis purposes, such as non-linear background subtraction and curve fitting. An example of curve fitting is illustrated in Figure 4.42. The XPS study results are summarized in Table 4.28.

3.6 Corrosion Study

To investigate the various claims of the superior ability of Zn-Ni and Zn-Co alloy deposits to withstand corrosion, a number of test programme have been set up. Various coating systems were studied:

- Non-chromated dull pure Zn, Zn-Ni, (Table 3.8) and Zn-Co deposits, (Table 3.9) obtained from potassium chloride based solutions.
- Non-chromated (as received) commercial bright pure Zn, Zn-Ni and Zn-Co deposits, (Table 3.10).
- Laboratory chromated dull and commercially treated (as received) systems of pure Zn, Zn-Ni and Zn-Co, (Table 3.11).

The details of the above samples are given in Tables 3.8 to 3.11. Their corrosion behaviour was observed in 5% (by weight) NaCl solution. Different methods were used to evaluate corrosion resistance: salt spray, beaker immersion and electrochemical techniques.

The nature of the corrosion products formed on Zn and Zn alloy coatings as well as their chemical composition have been investigated using electron probe micro-analysis (EPMA), X-ray diffraction (XRD) and scanning electron microscopy (with X-ray analytical attachment).

3.6.1 Salt Spray Tests

A standard salt spray corrosion cabinet was employed for both chromated and non-chromated systems. The test solution

was prepared and placed in the salt spray cabinet reservoir. In order to ensure a collection rate of 1 - 2 ml/hour as specified by B.S. 5466 (1977). The collection rate was determined using two measuring cylinders each having a funnel of diameter of 100 mm ; one was placed near the fog tower and the other as far away as possible. The collected solution was analysed for chloride content using a U.V spectrophotometer Model 24. The pH and the chloride content of the collected solution were found to be within the limits specified in BS 5466.

Table 3.8 List of Non-Chromated Zn-Ni Dull Deposits (Obtained from KCl based solutions and about 15 μ m thick) for Corrosion Study

Material	Plating Conditions				Used for
	gl ⁻¹ Ni in Bath	Temp °C	C.D Adm ⁻²		
Pure Zn	-	25.0	4.0		S.S
0.3	1.0	25.0	3.0		S.S
1.3	1.0	30.0	3.0		S.S
4.1	5.0	25.0	4.0		
6.3	10.0	30.0	4.0		S.S
7.6	10.0	30.0	3.0		
8.4	20.0	25.0	4.0		S.S
10.8	20.0	30.0	4.0		S.S
12.4	20.0	30.0	2.0		S.S
13.9	40.0	25.0	4.0		S.S
15.9	20.0	35.0	2.0		S.S
18.8	40.0	30.0	4.0		S.S
21.3	40.0	30.0	2.0		S.S - P - L.P

S.S = Salt Spray testing
P = Potentiodynamic scan
L.P = Linear Polarization

Table 3.9 List of Non-Chromated Zn-Co Dull Deposits (about 15 μ m thick) for Corrosion Study

Material	Plating Conditions			Used for
	gl ⁻¹ Co in Bath	Temp °C	C.D Adm ⁻²	
Pure Zn	—	25.0	4.0	S.S
0.3	1.0	25.0	4.0	S.S
1.5	5.0	25.0	4.0	S.S
5.1	5.0	30.0	2.0	S.S
8.2	15.0	25.0	4.0	S.S
10.6	10.0	30.0	3.0	
11.2	10.0	30.0	2.0	S.S
13.5	10.0	30.0	1.0	S.S
14.7	20.0	25.0	4.0	S.S
15.7	20.0	25.0	3.0	
16.9	25.0	22.0	2.0	S.S
19.9	20.0	25.0	2.0	S.S - P - L.P

Table 3.10 List of Non-Chromated Commercial Bright Deposits, (As received), for Corrosion Study

Material	Thickness μ m	Used for
Pure Zinc	9.2	S.S - P - L.P
Zincrolyte (0.3% Co)	12.0	S.S - P - L.P
Canning (0.7% Co)	5.5	S.S
Canning (1.0% Co)	12.0	S.S - P - L.P
Schloetter (13.8% Ni)	9.5	S.S - P - L.P

Table 3.11 List of Chromated Dull and Commercial Bright Samples for Corrosion Study

Material	Used for
Dull Deposits*:	
Pure Zn	S.S - P
0.3 %Co	S.S - P
1.5 "	S.S
5.1 "	S.S
8.2 "	S.S - P
14.7 "	S.S
0.3 %Ni	S.S - P
1.3 "	S.S
7.6 "	S.S
12.4 "	S.S - P
13.9 "	S.S
21.3 "	S.S
Bright Commercial Deposits*:	
Pure Zn, 9.2 μ m	S.S
Zincrolyte (0.3% Co, 12.0 μ m	S.S
Canning (0.7% Co), 5.5 μ m	S.S
Canning (1.0% Co), 12.0 μ m	S.S
Schloetter (13.8% Ni), 9.5 μ m	S.S
Chromated Bright Commercial Deposits**:	
Zn L7C (Yellow passivate), 9.2 μ m	S.S - P
Zn CR31 (Clear passivate), 9.2 μ m	S.S
Zincrolyte (0.3% Co), 12.0 μ m	S.S - P
Canning (0.7% Co), 5.5 μ m	S.S
Canning (1.0% Co), 12.0 μ m	S.S - P
Schloetter (13.8% Ni), 9.5 μ m	S.S - P

* Treated in solution (1) for 120 seconds

** Used as received

- Sample Preparation for Salt spray Testing

The edges of the plated panels were stopped off with lacquer and PTFE tape to expose areas of about 9 x 12 cm. The specimens were ultrasonically degreased, wiped gently

with cotton wool using distilled water to remove any film formed during degreasing; then placed on plastic racks. Spacing between each panel was carefully adjusted so that they did not touch each other. The position of each individual panel was noted. In this test, failure is considered to be the time to appearance of red rust for non-chromated samples and white rust for chromated samples. The time for black rust was also noted. The test was run with short breaks in order to ensure the spray jet did not become blocked and also to inspect the samples for failure. At the end of the test, the panels were removed, cleaned with distilled water to remove all loose debris from their surface and left to dry. Photographs were then taken for visual documentation.

3.6.2 Beaker Immersion Study

Information regarding corrosion mechanisms was obtained by immersing specimens in an aerated 5% NaCl solution for various times. The observations were made after 60 minutes, 48 hours and one week immersion.

Chemical analysis of the deposits on a microscale was made using an S.E.M with EDXA. Samples were examined as deposited and after various times of exposure to the corroding solution. The appropriate micrographs were taken using scanning electron microscope. These are illustrated in Figure 4.57. The test was carried out for dull non-chromated deposits only.

3.6.3 Electrochemical Measurements

A Princeton Applied Research Model 350 corrosion measurement console was used. In all electrochemical tests, potentials were measured with respect to a saturated Calomel electrode. A scan rate of 0.166 mV per second was used throughout the work. Both chromated and non-chromated systems were studied.

- Experimental Procedures

The samples were suspended in a beaker containing the test solution (5% NaCl) and linked to the corrosion measurement console as shown in Figure 3.1. The ionic contact between the test solution and the reference electrode was made through a salt bridge, the tip of which was adjusted so it was 2 to 3 mm from the test electrode surface. The salt bridge solution consisted of :

- Agar 6%
- Potassium nitrate 3%
- Distilled water 91%

- Corrosion Measurement Equipment Reliability

The reliability of the corrosion measurement console was assessed as depicted by ASTM G 59-78 code of practice. A sample of the standard ferritic Type 430 stainless steel whose composition is given in Table 3.12 was used in 1.0 N H_2SO_4 solution at 30°C. The solution was de-aerated before testing by bubbling H_2 through it. The sample preparation

involved a final wet polish using 600 grit SiC paper prior to the experiment with a delay time of about 30 minutes. The polarization resistance R_p was determined graphically as the tangent of the curve E Vs I at $\Delta E = 0$. To evaluate I_{corr} (corrosion rate) from the linear polarization curve, the Stern-Geary (94) equation was used:

$$I_{corr} = \frac{b_a \times b_c}{2.3 (b_a + b_c) R_p} \quad (9)$$

Where, b_a and b_c represent the Tafel constants obtained from a separate experiment. Table 3.12 shows the values of b_a , b_c and I_{corr} reported by 8 different laboratories.

Table 3.12 Polarization Parameters obtained for Stainless Steel Type 430 in 1.0 N H_2SO_4 , H_2 , 30°C (From ASTM G 59-78)

Laboratory	R_p $\Omega.cm^2$	b_a mV	b_c mV	I_{corr} mA/cm ²
1	7.53	79	108	2.63
2	7.93	90	105	2.65
3	8.96	106	122	2.75
4	12.00	120	150	2.40
5	8.85	83	97	2.19
6	11.00	120	130	2.50
7	8.90	79	116	2.30
8	8.33	82	118	2.52
Present work	12.06	113	125	2.12

- Sample Preparation

An insulated copper wire was soldered on to one face of each sample. The samples were then cleaned with microcleaner to remove the flux residues. The soldered face, the edges of the samples and any exposed copper wire were lacquered to expose a net area of 2 to 4 cm² and left to dry. The exposed area was measured, using a Linear Traverse Measurescope, and noted. The samples were then degreased with acetone and distilled water. Care was taken not to dissolve the lacquer when degreasing with acetone. After ultrasonic cleaning, the samples were suspended in a beaker containing the test solution and linked to the console as shown in Figure 3.1. Prior to taking the measurements, each panel was left in the solution for 60 minutes in order to stabilize. A scan rate of 0.166 mV per second was used.

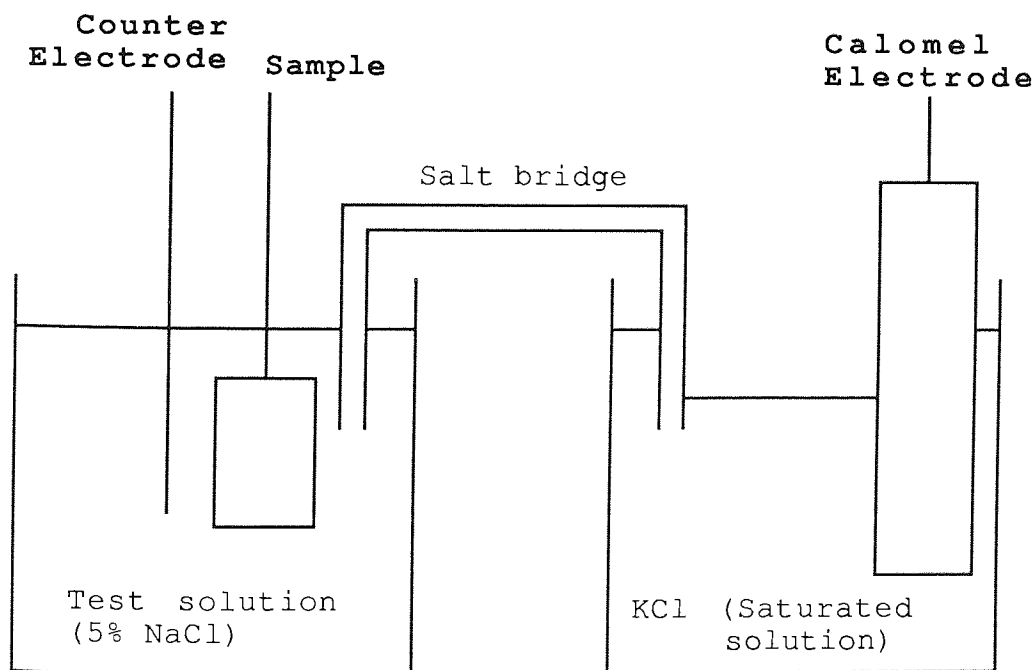


Fig. 3.1 Corrosion Cell

- Linear Polarization Measurements

These were performed as a function of time for non-chromated samples only. The corrosion rate and the corrosion potential of each individual sample was monitored at weekly intervals. When taking individual measurement, the scan range was ± 10 mV relative to E_{corr} . Visual observations for any sign of failure were also made.

In the presence of oxygen, as in this case, the cathodic reaction of O_2 was considered to be diffusion controlled and the equation (9) was modified as follows⁽¹⁰⁷⁾:

$$I_{\text{corr}} = \frac{b_a}{2.3 (R_p)} \quad (10)$$

- Potentiodynamic Polarization Study

Potentiodynamic polarization scans were run for several systems, both chromated and non-chromated, in order to determine both their anodic and cathodic behaviour as well as their corrosion rates. The potential scans were started at -500 mV and ended at +800 mV at a scan rate of 0.166 mV per second. The curves obtained were also used to determine the Tafel constants b_a and b_c for linear polarization measurements.

4 RESULTS

4.1 Plating Solutions and Coating Characteristics

4.1.1 Zinc-Nickel Alloy Systems

4.1.1.1 Ammonium Chloride Based Solutions

- Effect of Current Density and Solutions Nickel Concentration on Coating Composition and Cathode Current Efficiency, (C.C.E)

The Zn metal content of the solution was kept constant to 30 gl^{-1} , and the Ni content was varied. The plating solutions were operated at a temperature of 30.0°C and a pH of 5.5. The results are given in Tables 4.1-4.7 and displayed graphically in Figures 4.1 and 4.2.

Table 4.1 Solution Ni content : 1.0 gl^{-1}

Current density Adm^{-2}	Ni %	Zn %	C.C.E %
0.5	9.9	90.1	99.6
1.0	9.1	90.9	99.0
2.0	9.2	90.8	98.5
3.0	8.7	91.3	97.0
4.0	7.9	92.1	94.4

Table 4.2 Solution Ni content: 5.0 gl⁻¹

Current Density Adm ⁻²	Ni %	Zn %	C.C.E %
0.5	14.5	85.5	99.7
1.0	13.6	86.4	99.0
2.0	11.8	88.2	98.2
3.0	11.3	88.7	96.5
4.0	10.3	89.7	93.4

Table 4.3 Solution Ni content: 10.0 gl⁻¹

Current Density Adm ⁻²	Ni %	Zn %	C.C.E %
0.5	16.1	83.9	99.6
1.0	15.0	85.0	96.0
2.0	13.8	86.2	90.4
3.0	12.2	87.8	89.2
4.0	11.8	88.2	87.4

Table 4.4 Solution Ni content: 15.0 gl⁻¹

Current Density Adm ⁻²	Ni %	Zn %	C.C.E %
0.5	20.6	79.4	97.3
1.0	19.6	80.4	94.4
2.0	17.4	82.6	96.5
3.0	16.6	83.4	92.0
4.0	16.0	84.0	90.5

Table 4.5 Solution Ni content: 20.0 gl^{-1}

Current Density Adm^{-2}	Ni %	Zn %	C.C.E %
0.5	21.6	78.4	97.4
1.0	18.7	81.3	97.0
2.0	17.3	82.7	94.1
3.0	16.5	83.5	93.9
4.0	15.7	84.3	90.0

Table 4.6 Solution Ni content: 30.0 gl^{-1}

Current density Adm^{-2}	Ni %	Zn %	C.C.E %
0.5	26.3	73.7	98.0
1.0	23.7	76.3	96.0
2.0	21.3	78.7	94.4
3.0	19.3	80.7	96.9
4.0	16.3	83.7	91.0

Table 4.7 Solution Ni content: 40.0 gl^{-1}

Current Density Adm^{-2}	Ni %	Zn %	C.C.E %
0.5	36.6	63.4	102.0
1.0	28.9	71.1	98.0
2.0	26.0	74.0	96.2
3.0	23.5	76.5	97.1
4.0	20.2	79.8	96.4

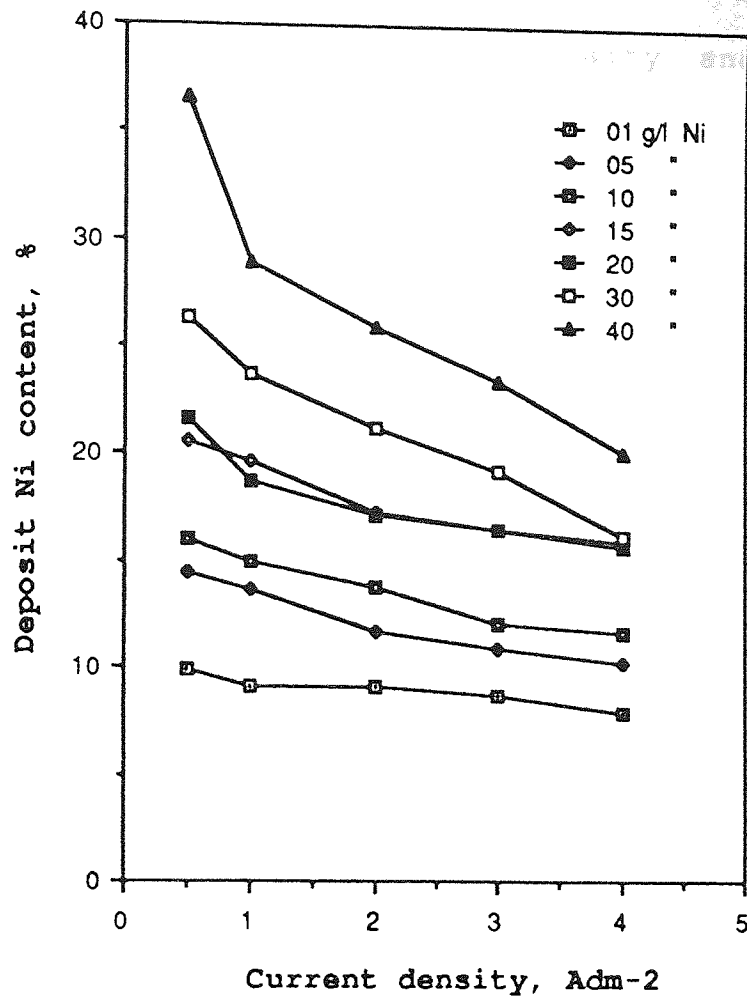


Fig. 4.1 Effect of Current density and Ni Solution concentration on Coating composition

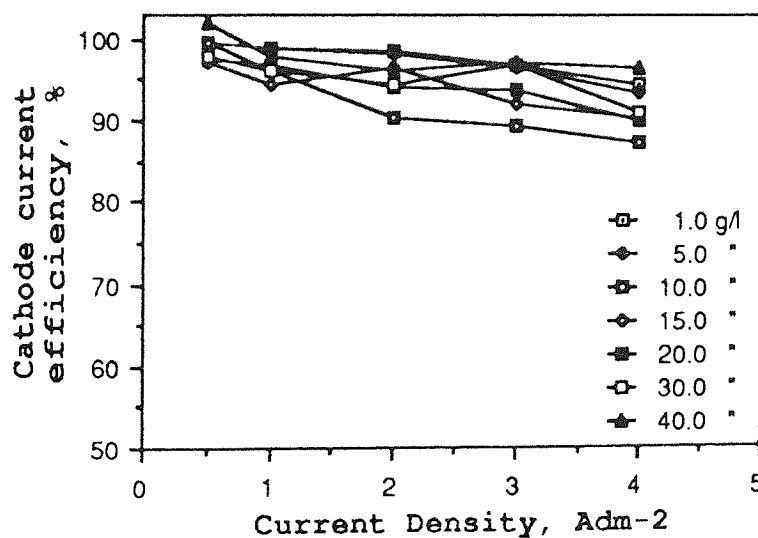


Fig 4.2 Effect of Current density and Ni Solution concentration on Cathode current efficiency

The effects of the current density and Ni solution concentration on coating composition results shown in Tables 4.1-4.7 are displayed again in Table 4.8 below. The concentration of Ni in the solutions is given in terms of percentage weight as well as in gl^{-1} .

Table 4.8 Effect of Current density and Ni Solution Concentration on Coating Compositions.

Ni content in bath		Current density, Adm^{-2}				
gl^{-1}	Wt, %	0.5	1.0	2.0	3.0	4.0
1.0	3.2	9.9	9.1	9.2	8.7	7.9
5.0	14.3	14.5	13.6	11.8	11.3	10.3
10.0	25.0	16.1	15.0	13.8	12.2	11.8
15.0	33.3	20.6	19.6	17.4	16.6	16.0
20.0	40.0	21.6	18.7	17.3	16.5	15.7
30.0	50.0	26.3	23.7	21.3	19.3	16.3
40.0	57.0	36.6	28.9	26.0	23.5	20.2

The above results are shown graphically in Figure 4.3 below.

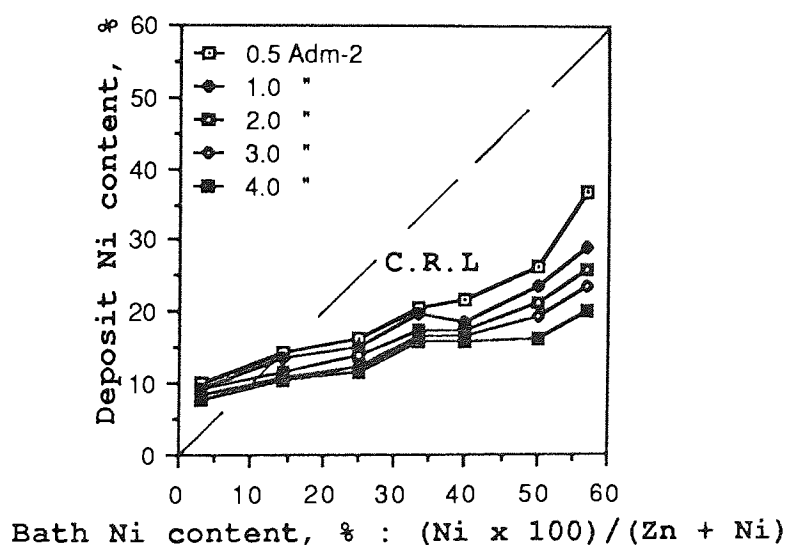


Fig. 4.3 Relationship between Coating composition and Ni Content in Solution.

(C.R.L stands for Composition Reference Line)

- Macro Throwing Power (M.T.P) Results

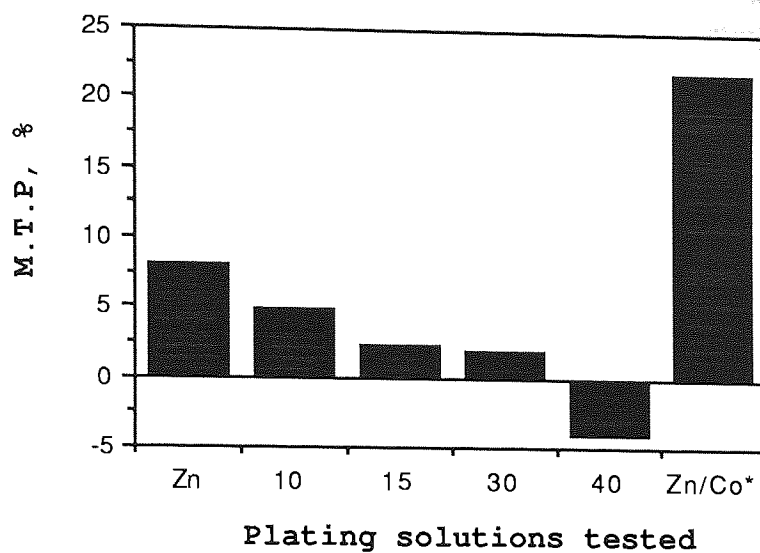
The two methods described earlier (page 107-111) were used to calculate the macrothrowing power of the different nickel content plating solutions. Table 4.9 illustrates the effect of the solution composition on macro throwing power.

Table 4.9 Effect of Solution Composition on Macro Throwing Power.

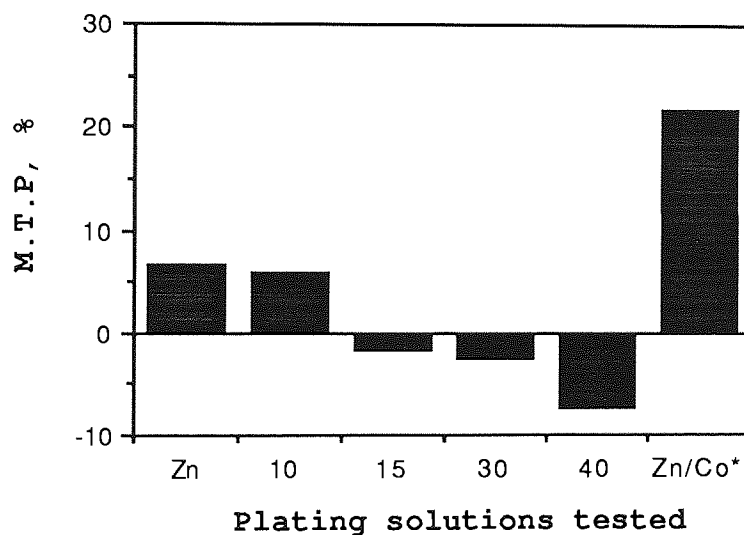
Plating solutions	METHOD I			METHOD II		
	MTP (3)	MTP (5)	MTP (7)	MTP (3)	MTP (5)	MTP (7)
Pure Zinc	+6.10	+8.11	+6.86	+6.95	+6.81	+6.86
10 gl^{-1} Ni	+3.09	+4.85	+6.29	+5.82	+5.68	+6.29
15 "	+3.09	+2.30	+2.04	-6.76	-1.60	+2.04
30 "	-0.99	+2.04	+5.45	-9.09	-2.44	+5.45
40 "	-5.66	-3.85	-2.44	-13.04	-7.19	-2.44
Zincrolyte solution	+14.90	+22.14	+25.00	+14.29	+21.77	+25.50

The results of M.T.P(5) for both methode I and II are illustrated in Figure 4.4.

Metal distribution on Hull cell panels plated in electrolytes of varying composition is reported in Table 4.10 and Figures 4.5-4.7.



(a)



(b)

Fig. 4.4 Relationship between different plating solution composition and M.T.P (5).

(a) Method I

(b) Method II

* Commercial solution (Zincrolyte), 0.3 %Co
The figures 10, 15, 30 and 40 represent the Ni content of the Zn-Ni solutions.

Table 4.10 Metal distribution on Hull cell panels.

Distance from H.C.D end, cm	Deposit thickness, μm					
	Zn	10 gl^{-1}	15 gl^{-1}	30 gl^{-1}	40 gl^{-1}	Zn-Co
1.0	58.5	70.0	66.9	65.1	70.0	43.9
1.5	44.0	62.5	50.0	46.1	50.4	38.9
2.0	37.1	55.9	42.3	38.1	42.5	36.1
2.5	33.2	47.5	35.8	32.3	36.2	30.7
3.0	30.0	41.4	32.2	27.8	31.1	27.8
3.5	26.9	37.1	27.8	24.9	27.1	24.6
4.0	23.9	31.8	24.8	22.2	22.8	22.3
5.0	18.6	25.8	18.6	15.7	17.1	17.1
6.0	13.9	19.6	14.3	12.1	12.8	13.6
7.0	10.5	14.3	10.7	9.6	9.6	10.9
7.9	7.7	9.6	7.8	7.8	7.1	8.9

The above results are illustrated in graphs 4.5 - 4.7.

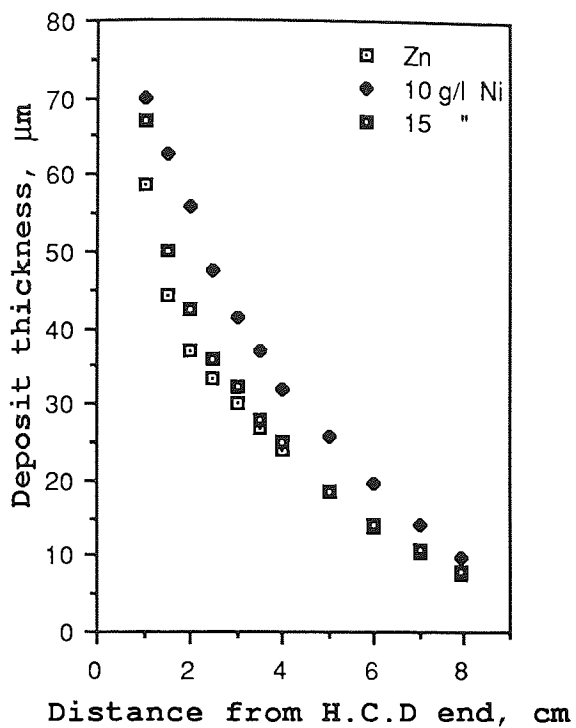


Fig 4.5 Metal distribution on Hull cell panels.

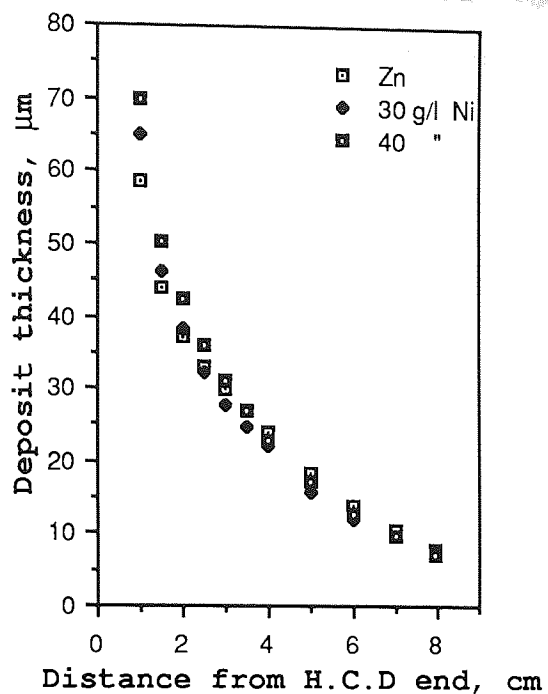


Fig 4.6 Metal distribution on Hull cell panels.

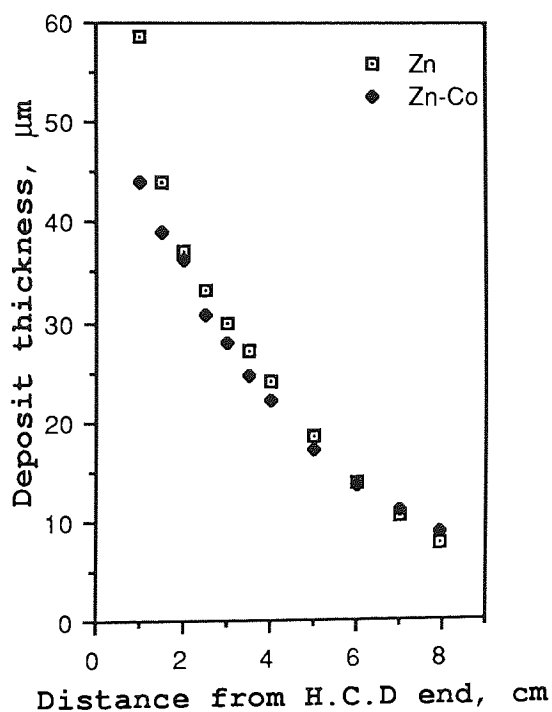


Fig 4.7 Metal distribution on Hull cell panels.

- Effect of Temperature, pH and Agitation on Coating composition and Cathode current efficiency.

The Zn-Ni plating solution listed in Table 3.2 (page 92) was used for this purpose, and the results are listed in Tables 4.11-4.13 and illustrated graphically in Figures 4.8 and 4.9.

Table 4.11 Effect of Temperature
(Plating conditions: C.D = 3.0 Adm^{-2} , pH = 5.5 and using Air Agitation)

Temperature °C	Ni %	Zn %	C.C.E. %
25.0	12.5	87.5	95.9
30.0	17.0	83.0	97.0
35.0	20.5	79.5	97.9
40.0	28.8	76.2	98.8

Table 4.12 Effect of Solution pH
(Plating conditions: C.D = 3.0 Adm^{-2}
Temperature = 30°C and using Air Agitation)

pH	Ni %	Zn %	C.C.E. %
3.5	9.8	90.2	98.7
4.5	13.0	87.0	96.8
5.5	15.8	84.2	94.8

Table 4.13 Effect of Agitation
(Plating conditions: C.D = 3.0 Adm⁻², pH = 5.5 and
Temperature = 30.0°C)

	Ni %	Zn %	C.C.E. %
Air Agitation	17.0	83.0	97.5
No Agitation	13.0	87.0	90.5

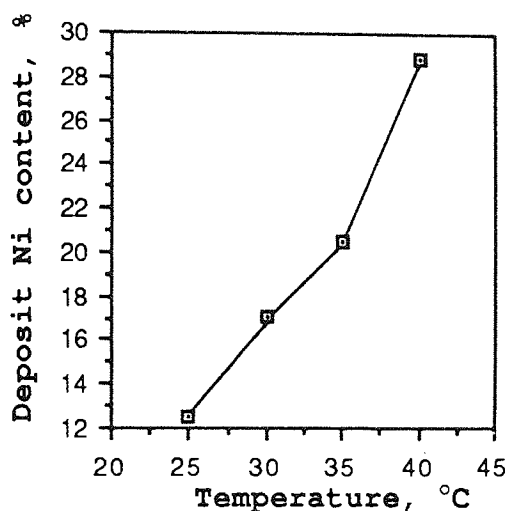


Fig. 4.8 Effect of Temperature on
Ni content of deposits.

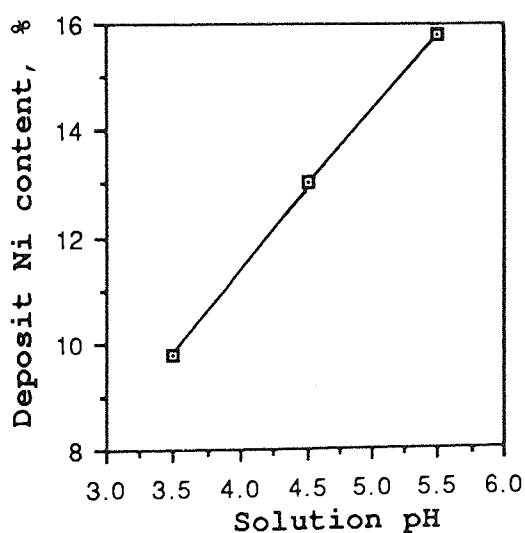


Fig. 4.9 Effect of pH on Ni content
of the deposits.

- Zn-Ni Deposits Characteristics

A- Hardness of Zn-Ni Deposits

Microhardness values of Zn-Ni alloy coatings were obtained using a Vickers pyramidal indenter and a load of 25 g. The results are shown in Table 4.14 and Figure 4.10 below.

Table 4.14 Microhardness of the deposits, Hv.

Deposit Ni content, %	Hardness Hv
Pure Zn	61.9
9.2	201.3
11.3	244.5
12.5	277.6
13.6	307.1
17.0	385.8

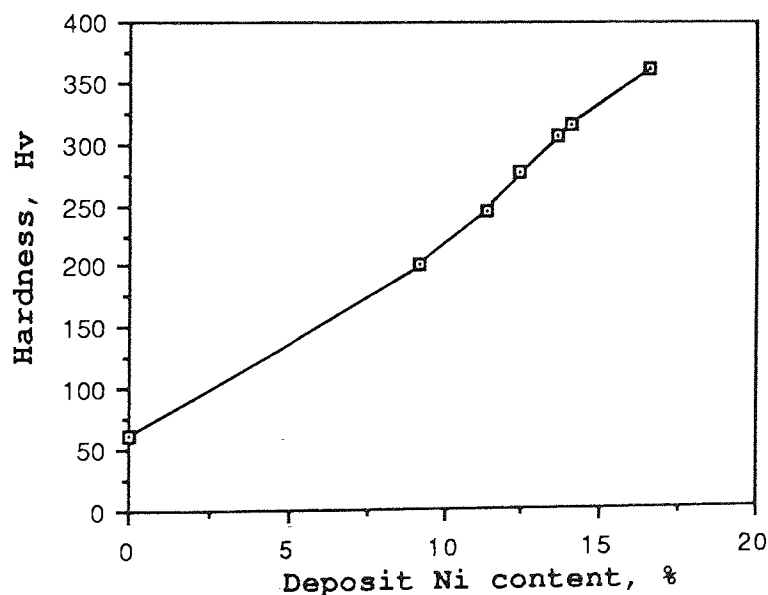


Fig. 4.10 Relationship between Hardness and deposit Ni content.

B- Microscopic Study of Zn-Ni Deposits

Figure 4.11 shows the elemental distribution across a Zn-Ni deposit cross-section obtained using an electron probe microanalyser. Figures 4.12-4.15 illustrate the effect of plating conditions on coating appearance and structure. It can be seen clearly that the absence of solution agitation resulted in pitted deposit, see Figures 4.12 and 4.13. The use of low current density favoured fine grained structure deposit as illustrated in Figure 4.14 whereas the use of high current density resulted in columnar structured coating.

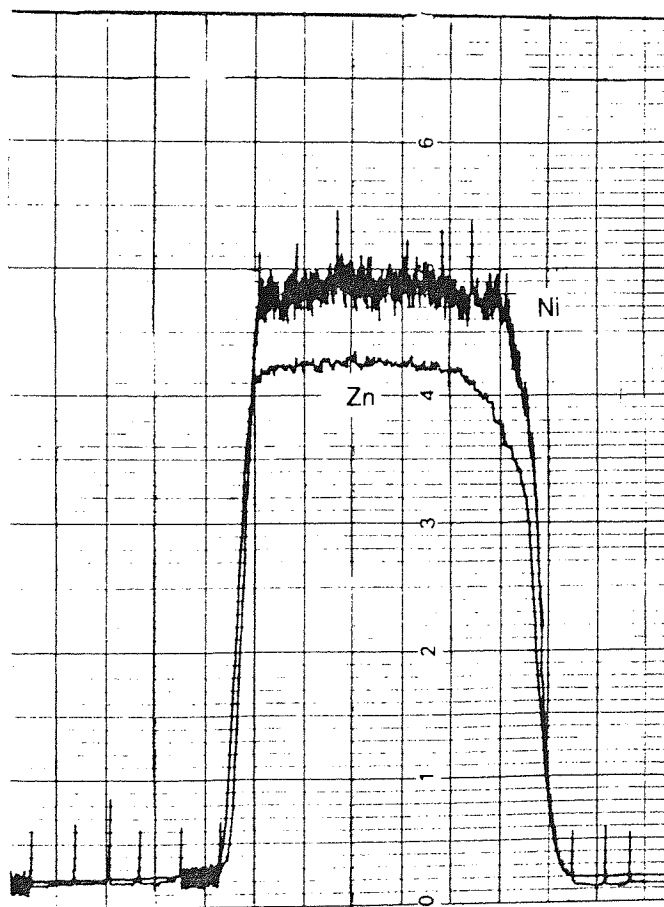


Fig. 4.11 Zn-Ni deposit (12.5% Ni) showing elemental distribution across the coating cross-section.

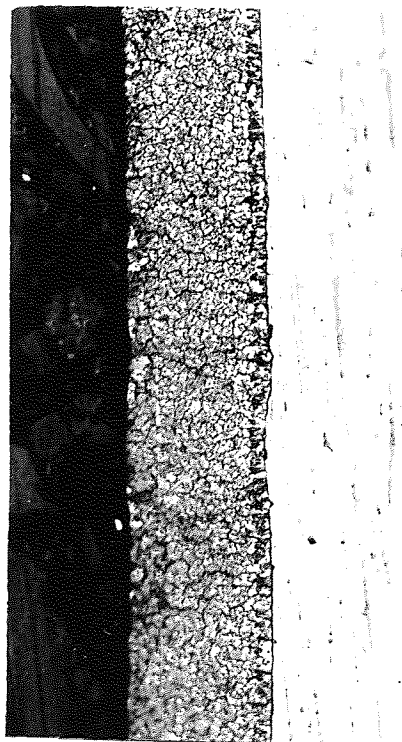


Fig. 4.12 Zn-Ni deposit (16.1% Ni) showing Fine Grained structure obtained at 0.5Adm-2. x980

Etchant: 1% Sodium metabisulfite.

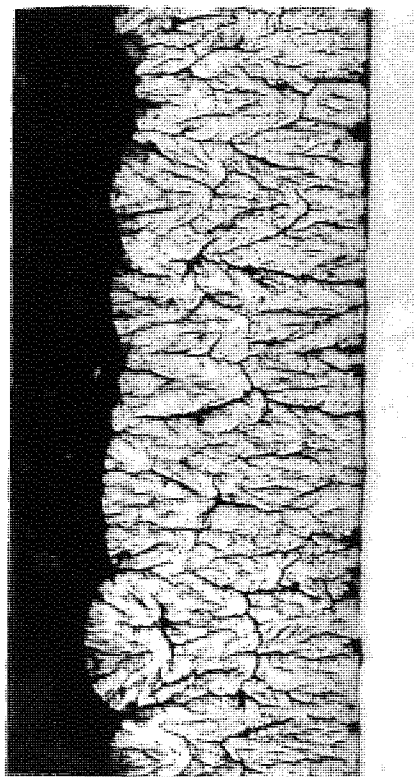


Fig. 4.13 Zn-Ni deposit (16.0% Ni) showing Columnar structure obtained at 4.0Adm-2. x1900

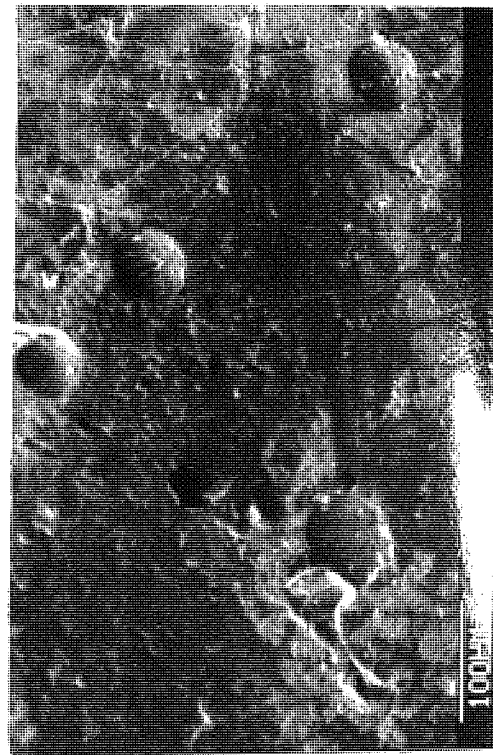


Fig. 4.14 Pitted Surface resulted from a non-agitated solution

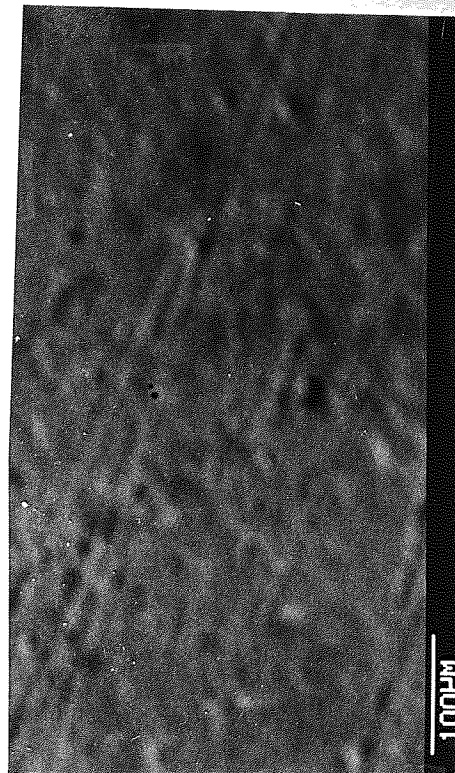


Fig. 4.15 Zn-Ni coating obtained using Agitation

Scanning micrographs showing the Effect of C.D and Agitation on Zn-Ni coating Structure and Surface state.

4.1.1.2 Zn-Ni Potassium Chloride Based Solutions

- Effects of Current Density and Solution Ni Concentration on Deposit Composition at 25.0°C and 30.0°C.

Table 4.15 Effect of Current density and Ni solution concentration on Ni content of deposits. (Plating Conditions: pH = 5.5, Temperature = 25.0°C and using Air Agitation).

	gl ⁻¹ Ni				
C.D Adm ⁻²	1.0	5.0	10.0	20.0	40.0
1.0	0.6	4.2	6.0	12.4	18.9
2.0	0.4	4.0	5.0	10.3	15.4
3.0	0.4	3.7	4.3	8.7	12.0
4.0	0.4	3.7	4.5	8.0	12.2

Table 4.16 Effect of Current density and Ni solution concentration on Ni content of deposits. (Plating Conditions: pH = 5.5, Temperature = 30.0°C and using Air Agitation).

	gl ⁻¹ Ni				
C.D Adm ⁻²	1.0	5.0	10.0	20.0	40.0
1.0	1.8	4.6	8.1	15.0	23.8
2.0	1.2	4.3	7.4	11.5	20.0
3.0	1.0	4.0	6.9	10.9	19.0
4.0	1.1	3.6	6.2	10.5	18.1

The results shown in Tables 4.15 and 4.16 above are illustrated graphically in Figures 4.16 and 4.17.

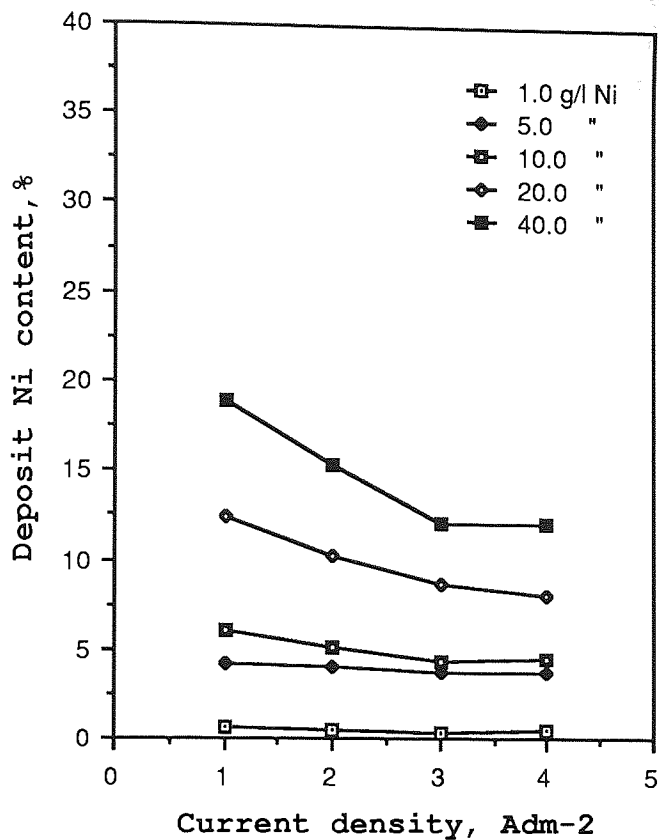


Fig. 4.16 Effect of Current density and Ni Solution concentration on Coating composition
(Deposits obtained at 25.0°C)

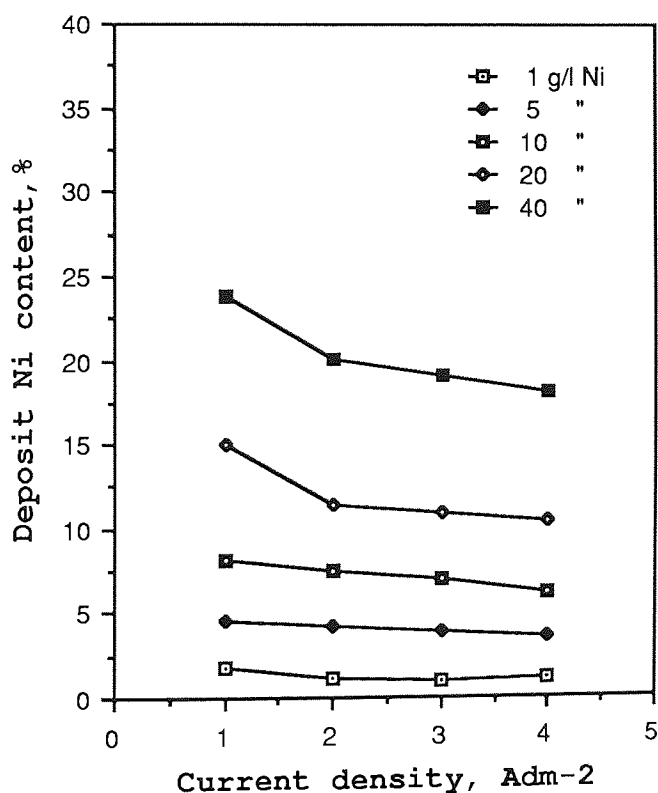


Fig. 4.17 Effect of Current density and Ni Solution concentration on Coating composition
(Deposits obtained at 30.0°C)

The results shown in Table 4.15 and 4.16 are retabulated below in terms of weight percentage of the solution concentrations and displayed in Figures 4.18 and 4.19.

Table 4.17 Effect of Current density and Ni solution concentration on Ni content of deposits. (Plating Conditions: pH = 5.5, Temperature = 25.0°C and using Air agitation).

Ni content in bath		Current density, Adm^{-2}			
gl^{-1}	Wt, %	1.0	2.0	3.0	4.0
1.0	2.4	0.6	0.4	0.4	0.4
5.0	11.1	4.2	4.0	3.7	3.7
10.0	20.0	6.0	5.0	4.3	4.5
20.0	33.3	12.4	10.3	8.7	8.0
40.0	50.0	18.9	15.4	12.0	12.2

Table 4.18 Effect of Current density and Ni solution concentration on Ni content of deposits. (Plating Conditions: pH = 5.5, Temperature = 30.0°C and using Air agitation).

Ni content in bath		Current density, Adm^{-2}			
gl^{-1}	Wt, %	1.0	2.0	3.0	4.0
1.0	2.4	1.8	1.2	1.0	1.1
5.0	11.1	4.6	4.3	3.9	3.7
10.0	20.0	8.1	7.4	6.9	6.2
20.0	33.3	15.0	11.5	10.9	10.5
40.0	50.0	23.8	20.0	19.0	18.1

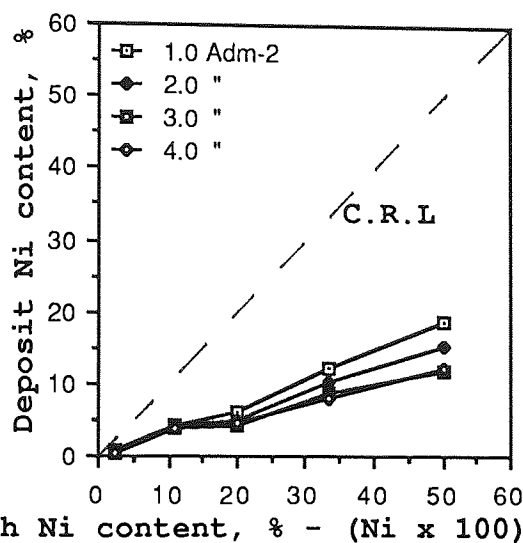


Fig. 4.18 Relationship between Coating composition and Ni content in Solutions.
(KCl based solutions used at 25.0 °C)

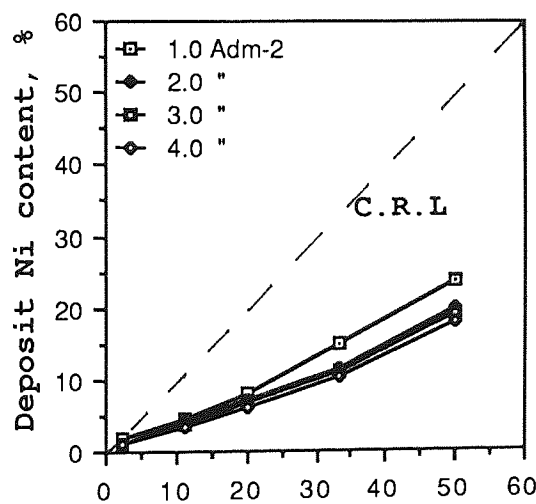


Fig. 4.19 Relationship between Coating composition and Ni content in Solutions.
(KCl based solutions used at 30.0 °C)

4.1.2 Zinc-Cobalt Alloy Systems

4.1.2.1 Zn-Co Dull Deposits

- Effect of Current density and Co Solution concentration on Coating composition.

Table 4.19 Effect of Current density and Co Solution concentration on Coating composition. (Plating conditions: Temperature = 25.0°C, pH = 5.3 and using Air Agitation).

	g l ⁻¹				
Adm ⁻²	1.0	5.0	7.0	10.0	20.0
1.0	0.8	6.4	10.8	12.0	20.3
2.0	0.5	5.0	8.7	10.0	18.0
3.0	0.4	3.2	6.9	9.2	15.0
4.0	0.4	1.2	6.2	5.7	14.1

Table 4.20 Effect of Current density and Co Solution concentration on Coating composition. Plating conditions: Temperature = 30.0°C, pH= 5.3 and using Air Agitation).

	g l ⁻¹ Co				
Adm ⁻²	1.0	5.0	7.0	10.0	15.0
1.0	1.0	7.5	11.2	13.3	15.1
2.0	0.6	4.6	10.0	11.0	13.8
3.0	0.6	4.6	8.7	9.8	12.6
4.0	0.5	3.1	4.7	7.8	10.7
5.0	-	-	3.6	-	-

The above results are also shown in graphical form in Figures 4.20 and 4.21.

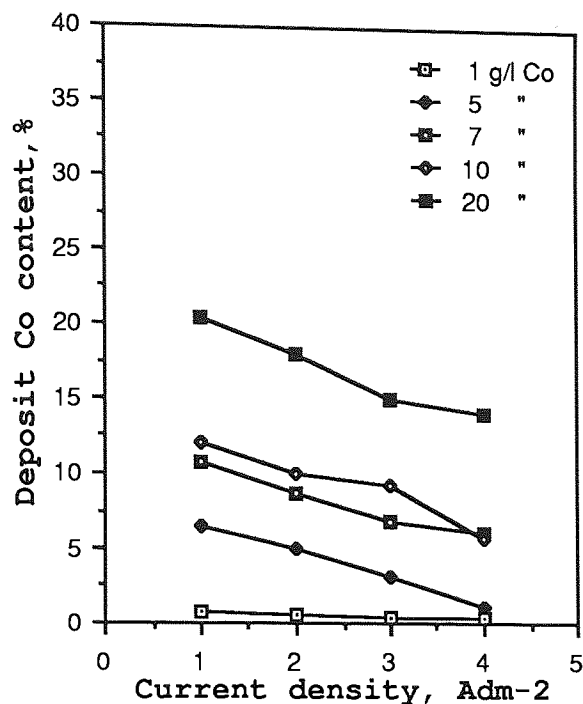


Fig. 4.20 Effect of Current density and Co Solution concentration on Coating composition
(Deposits obtained at 25.0°C)

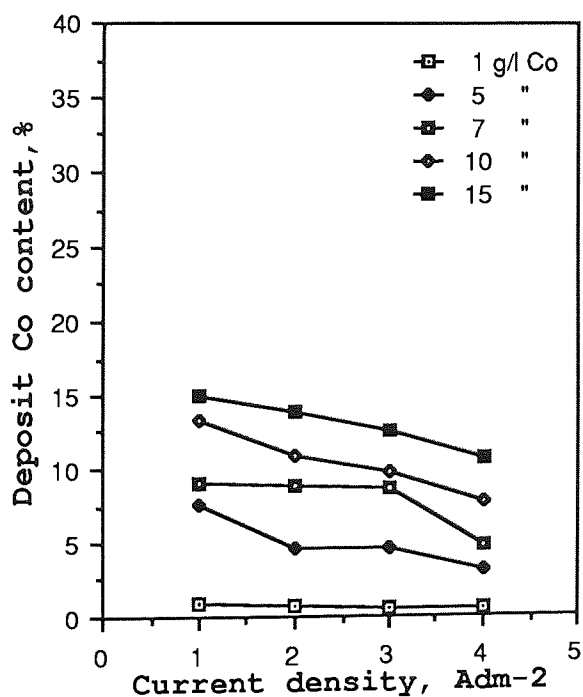


Fig. 4.21 Effect of Current density and Co Solution concentration on Coating composition
(Deposits obtained at 30.0°C)

The effects of the current density and Co solution concentration on coating composition results shown in Tables 4.19 and 4.20 are displayed again in Tables 4.21 and 4.22 below. The concentration of Co in the plating solutions is given in terms of percentage weight as well as in gl^{-1} . The results are also presented in Figures 4.22 and 4.23.

Table 4.21 Effect of Current density and Co solution concentration on Co content of deposits. (Plating Conditions: pH = 5.3, Temperature = 25.0°C and using Air agitation).

Co content in bath		Current density, Adm^{-2}			
gl^{-1}	Wt, %	1.0	2.0	3.0	4.0
1.0	2.4	0.8	0.5	0.4	0.4
5.0	11.1	6.4	5.0	3.2	1.2
7.0	14.9	10.8	8.7	6.9	6.2
10.0	20.0	12.0	10.0	9.2	5.7
20.0	33.3	20.3	18.0	15.0	14.1

Table 4.22 Effect of Current density and Co solution concentration on Co content of deposits. (Plating Conditions: pH = 5.3, Temperature = 30.0°C and using Air agitation).

Co content in bath		Current density, Adm^{-2}			
gl^{-1}	Wt, %	1.0	2.0	3.0	4.0
1.0	2.4	1.0	0.6	0.6	0.5
5.0	11.1	7.5	4.6	4.6	3.1
7.0	14.9	11.2	10.0	8.7	4.7
10.0	20.0	13.3	11.0	9.8	7.8
15.0	27.3	15.1	13.8	12.6	10.7

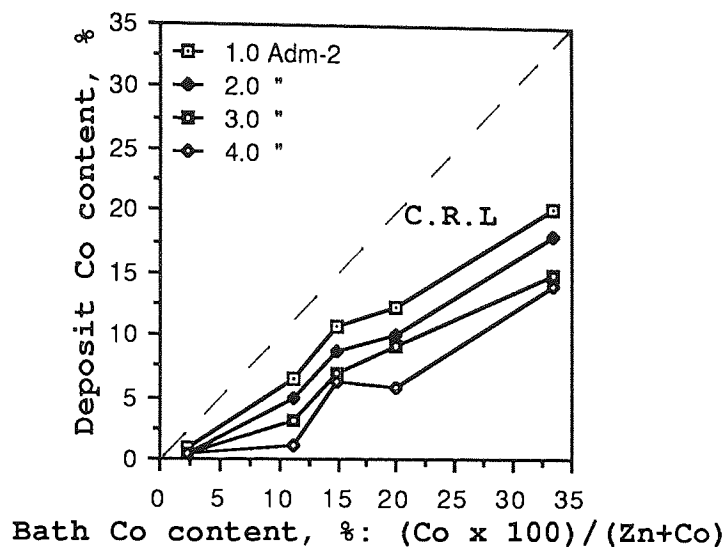


Fig. 4.22 Relationship between Coating composition and Co content in Solutions.

(Plating solutions used at 25.0 °C)

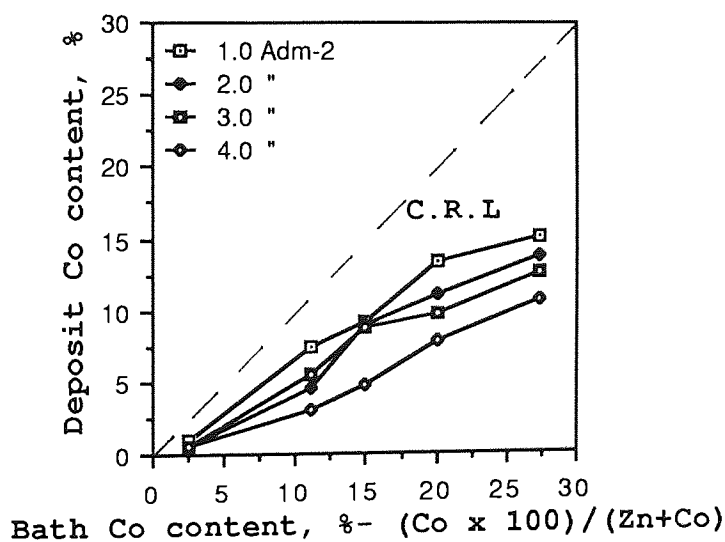


Fig. 4.23 Relationship between Coating composition and Co content in Solutions.

(Plating solutions used at 30.0 °C)

4.1.2.2 Bright Deposits

Two different commercial plating solutions were used: an acidic (Zincrolyte) and an alkaline (Canning) zincate based electrolyte. The Zincrolyte system is based on potassium chloride salt and have a pH of about 5.3.

- Zincrolyte System

The effects of current density and temperature on coating composition and cathode current efficiency are shown in Tables 4.23 and 4.24 and in Figures 4.24 and 4.25. For comparison, the results obtained from Zn-Co plating solutions containing no organic additives reported earlier in Tables 4.20 are included in Table 4.23. The suppression of Co deposition by the organic addition is very obvious as shown in Figures 4.24 and 4.25).

Table 4.23. Effect of Current Density on Co content of the deposits and Cathode Current Efficiency, C.C.E. (Plating Conditions: $7.0 \text{ gl}^{-1} \text{ Co}$ pH = 5.3 Temperature = 30°C and using Air Agitation).

Current Density Adm^{-2}	Co %	Zn %	C.C.E. %	Co* %
1.0	0.8	99.2	99.9	11.2
2.0	0.9	99.1	98.0	10.0
3.0	1.2	98.8	98.3	8.7
4.0	2.7	97.3	97.4	4.7

* Taken from Table 4.20

Table 4.24. Effect of Temperature and Organic additives on Co content of the deposits and C.C.E. (Plating conditions: $7.0 \text{ g l}^{-1} \text{ Co}$, $\text{C.D.} = 2.0 \text{ Adm}^{-2}$ $\text{pH} = 5.3$ and using Air Agitation).

Temperature $^{\circ}\text{C}$	Co %	Zn %	C.C.E. %	Co* %
25.0	0.7	99.3	96.4	7.9
30.0	0.9	99.1	97.9	10.4
35.0	1.1	98.9	97.7	14.4
40.0	1.6	98.4	98.9	15.7

* Results obtained from Zn-Co plating solution containing no organic additives.

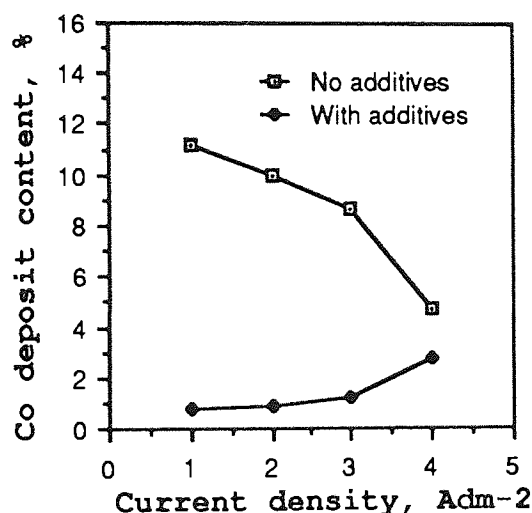


Fig. 4.24 Effect of Current density and organic additives on Coating composition

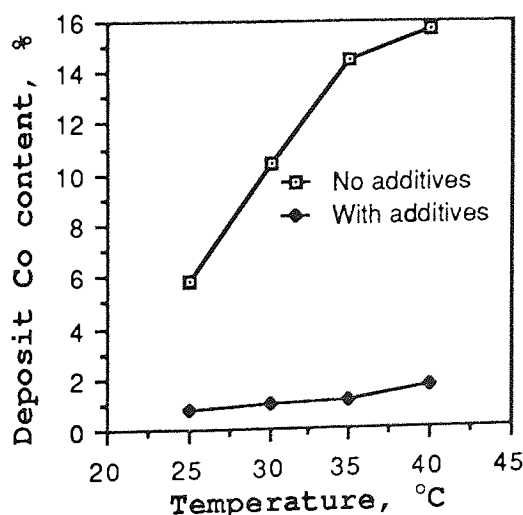


Fig. 4.25 Effect of Temperature and organic additives on Coating composition

- Canning System

For this work large samples about 10 x 15 cm in size were plated from a tank of capacity of 280 l at Canning research Laboratory. The details of the solution used are given in Table 3.6 page 98. The effects of current density on deposit Co content and thickness results are given in Table 4.25 below. The deposit Co content results are also displayed in Figure 4.26 together with those of Zincrolyte for comparison. It is apparent that the cobalt content of the deposits plated from the latter solution is more sensitive to variation in current density than in the case of deposits plated from the alkaline Canning solution.

Table 4.25 Effect of Current density on Coating composition and Thickness (Plating conditions: Temperature = 22-23°C using still solution).

Current density Adm^{-2}	Co %	Thickness μm
1.0	1.0	12.0
2.0	0.9	7.5
3.0	0.8	7.0
4.0	0.7	6.3
5.0	0.7	5.5

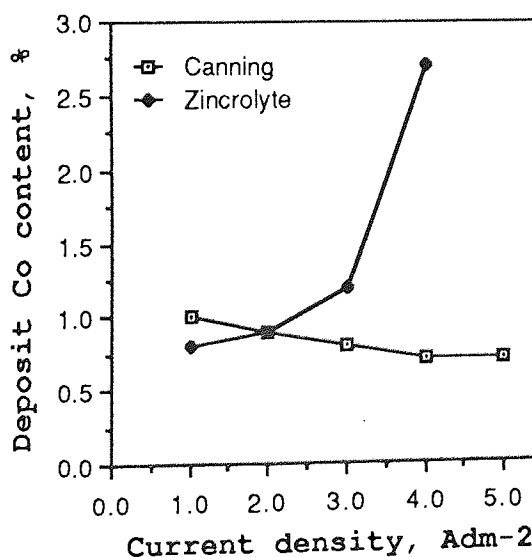


Fig.4.26 Effect of Current density on deposit composition of both Canning and Zincrolyte Systems

4.2 Conversion Coatings

Three different types of conversion solutions were used for this part of the work, (see Table 3.7 page 113 for details):

1- Laboratory formulated solution based on chromic acid and sodium chloride referred to as solution (1) and used for chromating both dull and bright deposits.

2- Commercial Schloetter and Canning processes used for dull deposits only. However the commercially chromated samples in as received conditions are also included in this section. Their photographs and optical micrographs are given in Figures 4.27 and 4.28.

The chromating characteristics at various immersion (treatment) times of the above solutions were evaluated in terms of:

1- The amount of chromate film formed referred to as 'True estimate'; the sample change in weight which was determined by weighing the dried samples before and after treatment and also the amount of metal (Zn and Ni or Co) dissolved during the chromating process.

2- The conversion film appearance (colour) which was assessed visually and their chemical composition determined by XPS.

The conversion film formation on samples treated in solution (1) was also followed by potential-time variation. The results are given in Table 4.26 and shown in graphical form in Figures 4.29-4.31. All the systems seemed to show the same general behaviour i.e. the potential decreased rapidly

from an instantaneous value on immersion to a minimum where it remained constant until the end of the test. Table 4.27 and Figures 4.32-4.34 illustrate the chromating characteristics of the solution (1) at various immersion times. The photographs and scanning electron micrographs of some treated samples are also presented in Figures 4.35-4.39. The XPS results are given in Figures 4.40-4.42 and summarised in Table 4.28. The XPS study was carried only on samples treated in solution (1) for 120 seconds and on some of the commercial chromated samples destined for corrosion resistance evaluation.

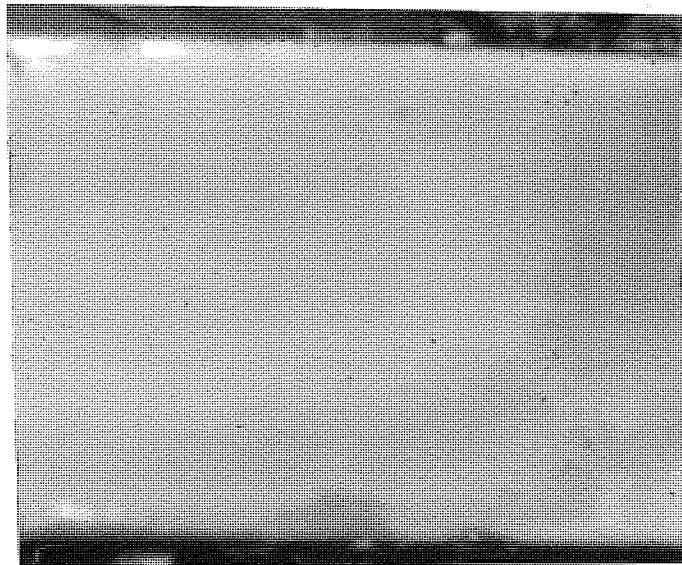
The chromating characteristics results of the Schloetter solution are given in Table 4.29 and Figures 4.43-4.45 and those of Canning commercial solution in Table 4.30 and Figures 4.46 and 4.47. For both chromating solutions no Ni or Co metal dissolution took place during the immersion times studied. Only the Zn metal dissolution values were reported. In the case of Canning solution at immersion times of less than 90 seconds, even the Zn metal dissolution did not take place and consequently no change in samples appearance was observed.

- Commercial Chromated Samples (as received)

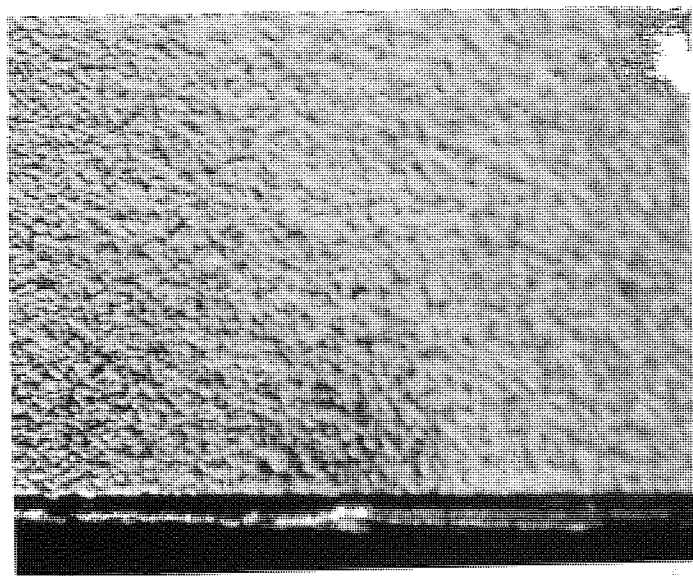
The photographs shown in Figure 4.27a-c illustrate the appearance of chromated commercial samples of both Zn-Ni (a) and Zn-Co systems (b and c) in as received conditions.

Fig.4.27 Photographs of Commercially chromated
Samples (as received). Magnification: x6.

a- Schloetter
(13.8% Ni)



b- Zincrolyte
(0.3% Co)



c- Canning
(0.7% Co)

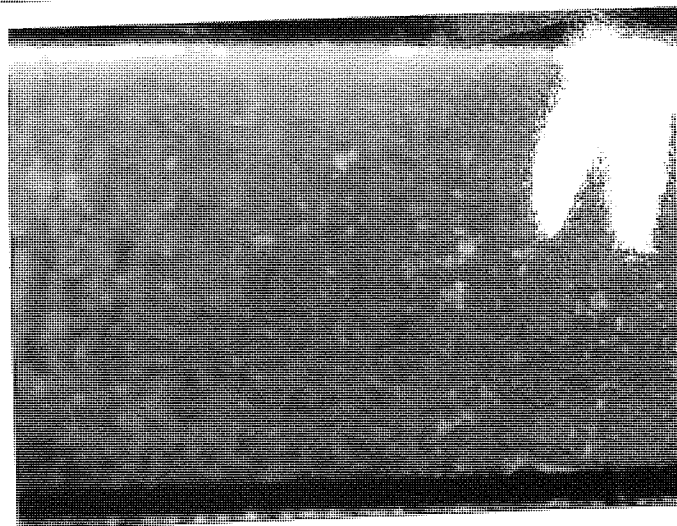
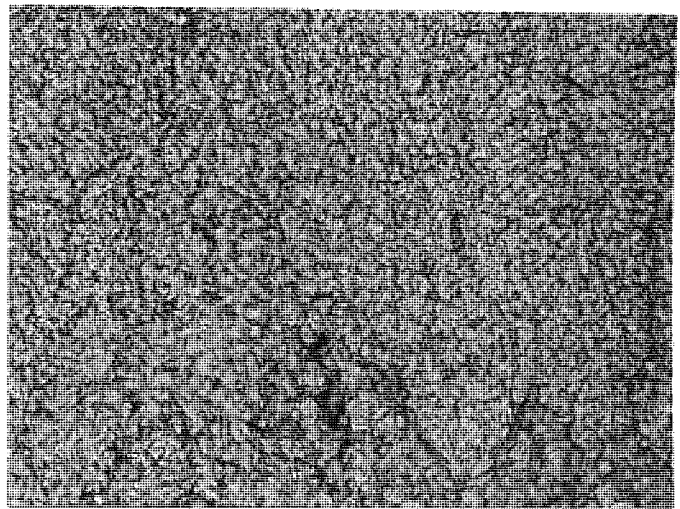


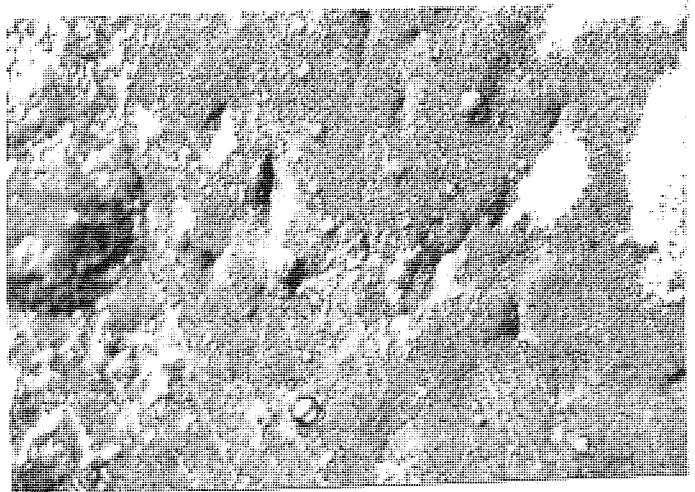
Fig.4.28 Optical Micrographs of Commercial Chromated Samples, (as received).

The micrographs shown below were taken using an optical microscope fitted with polarized light filter. The micrograph for the Zincrolyte sample could not be taken due to its very shiny surface.

a- Schloetter Sample
(13.8% Ni)



b- Canning Sample
(0.7% Co)



Magnification: x490

Table 4.26 Potential-Time Results Obtained for Deposits Treated in Solution (1).

Time Seconds	Zn-Ni dull deposits				Zn-Co dull deposits			Bright deposits		
	Zn	0.3	12.4	21.3	0.3	5.1	14.7	0.7% Co*	13.8 % Ni*	
0.0	-0.443	-0.400	0.000	0.000	0.00	0.015	-0.375	-0.575	-0.300	
0.2	-	-	-	0.165	-	0.000	-0.325	-0.545	-	
0.3	-	-	0.080	-	-	-	-	-	-	
0.4	-	-0.500	-	-	-	-	-	-	-	
0.6	-	-	-	-	-0.295	-	-	-	-0.305	
0.8	-0.543	-0.509	-	-	-0.395	-	-0.380	-0.670	-	
1.2	-	-	-	0.010	-0.458	-0.320	-	-	-0.280	
1.3	-	-	-0.050	-	-	-	-	-	-	
1.4	-0.530	-	-	-	-	-	-	-	-	
1.5	-	-0.485	-	-	-	-	-	-	-	
2.0	-	-	-	0.095	-	-0.325	-	-	-0.380	
3.6	-	-	-	-	-	-	-0.349	-	-	
6.0	-	-0.650	-0.200	-	-0.510	-0.390	-0.380	-0.690	-	
8.0	-0.640	-	-0.370	-0.010	-	-	-	-0.700	-	
14.0	-	-	-	-	-	-	-0.400	-	-	
16.0	-	-	-	-	-	-	-	-	-	
26.0	-	-	-0.405	-	-	-	-	-	-	
28.0	-	-	-	-	-0.540	-	-	-	-	
32.0	-	-	-	-	-	-	-0.410	-0.720	-	
40.0	-0.850	-	-0.408	-0.120	-	-0.520	-	-0.720	-	
42.0	-	-0.750	-	-	-	-	-	-	-0.400	
60.0	-	-0.780	-0.409	-0.230	-0.580	-	-0.420	-	-	
68.0	-	-0.780	-	-	-	-	-	-	-	
70.0	-	-0.780	-	-	-0.670	-0.540	-	-	-	
76.0	-0.858	-0.780	-	-	-	-	-	-0.722	-	
80.0	-0.858	-0.780	-0.406	-0.360	-0.701	-0.540	-0.419	-0.721	-	
90.0	-0.860	-0.780	-0.405	-0.400	-	-0.542	-0.418	-	-0.410	
100.0	-0.858	-0.781	-0.404	-0.410	-0.705	-0.539	-	-	-0.410	
110.0	-0.859	-0.780	-0.408	-0.411	-	-	-	-0.720	-	
120.0	-0.861	-0.788	-0.410	-0.407	-0.702	-0.539	-0.421	-0.719	-0.411	

* Canning sample, ** Schloetter sample
The results above are also illustrated in Figures 4.29-4.31.
The units of the results are in V with respect to S.C.E

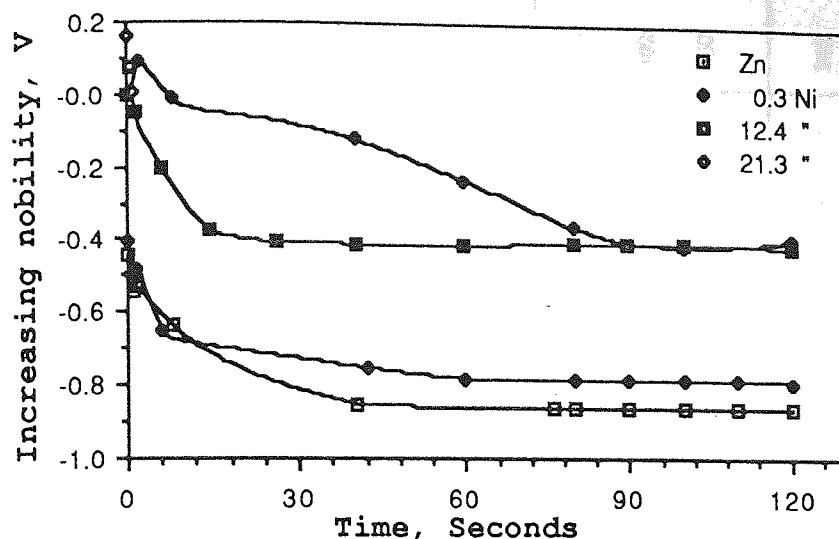


Fig. 4.29 Potential-time curves recorded for Zn and Zn-Ni dull deposits during chromating in solution (1).

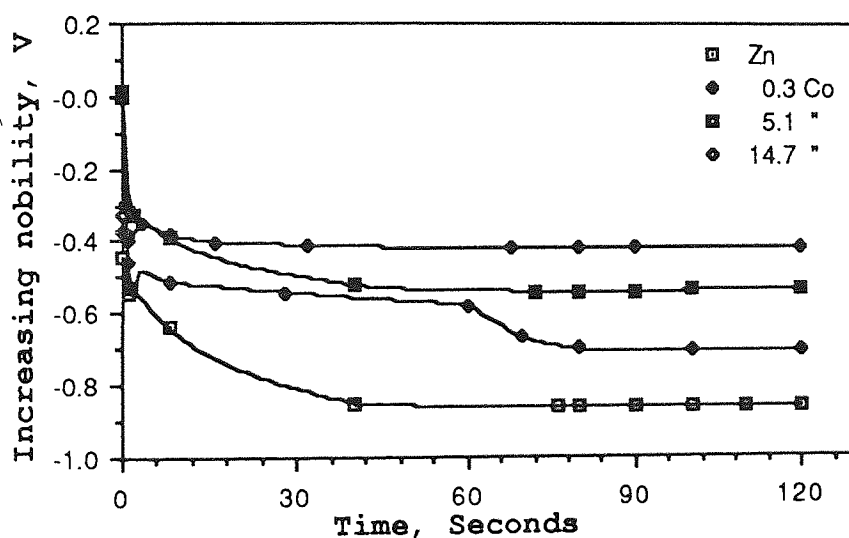


Fig. 4.30 Potential-time curves recorded for Zn and Zn-Co dull deposits during chromating in solution (1).

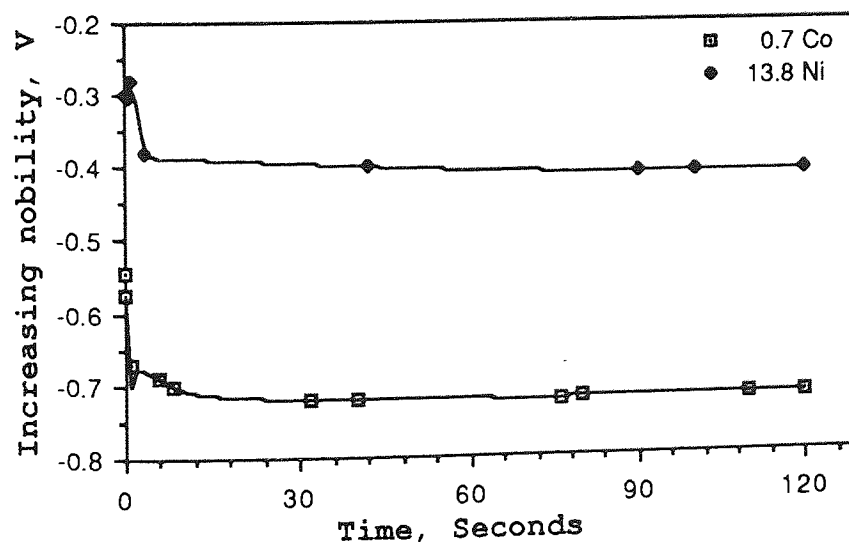


Fig. 4.31 Potential-time curves recorded for bright deposits during chromating in solution (1).

Table 4.27 Chromating Characteristics of Dull* and Bright Deposits Treated in Solution (1)**

Samples	15 seconds					30 seconds				60 seconds				90 seconds				120 seconds			
	Ni / Co	Zn	Weight change	True estimate	Ni / Co	Zn	Weight change	True estimate	Ni / Co	Zn	Weight change	True estimate	Ni / Co	Zn	Weight change	True estimate	Ni / Co	Zn	Weight change	True estimate	
Zn *	-	306	- 50	256	-	491	- 100	391	-	646	- 150	496	-	714	- 200	541	-	764	- 220	544	
0.3 Ni	0	272	- 50	222	0	406	- 90	361	4	529	- 150	383	5	580	- 180	405	5	641	- 220	426	
7.6 "	3	190	- 40	153	7	280	- 70	217	8	350	- 100	258	7	421	- 140	288	9	467	- 180	296	
12.4 "	5	174	- 40	139	9	270	- 70	209	11	344	- 90	265	12	400	- 130	282	12	424	- 150	286	
21.3 "	9	158	- 30	137	14	228	- 60	182	12	305	- 90	227	14	380	- 130	264	13	416	- 160	269	
0.3 Co *	0	257	- 40	217	0	381	- 80	301	3	508	- 140	368	5	580	- 180	405	4	623	- 200	427	
5.1 "	0	167	- 30	137	4	284	- 60	228	6	389	- 100	295	6	445	- 150	301	7	465	- 170	302	
14.7 "	8	140	- 20	128	15	214	- 60	169	17	283	- 80	220	19	355	- 130	244	18	382	- 150	250	
0.3 Co **	0	196	- 20	176	0	310	- 60	250	0	420	- 110	310	4	495	- 150	349	4	512	- 170	346	
0.7 "	0	210	- 40	170	0	286	- 50	236	3	374	- 100	277	5	476	- 160	321	7	490	- 180	317	
13.8 Ni	3	94	0	97	7	200	- 40	167	9	288	- 90	207	10	330	- 110	230	12	356	- 140	228	

The units above are in 10^{-3} mg/cm²
The above data are also presented in Figures 4.32-4.34

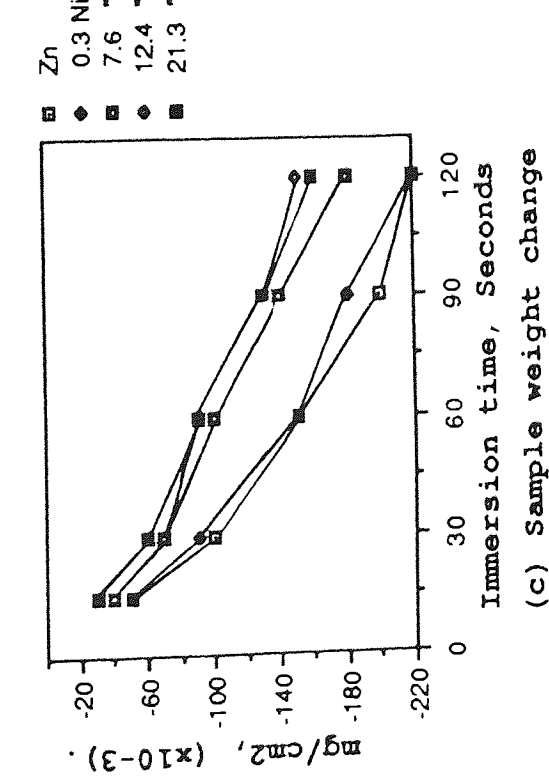
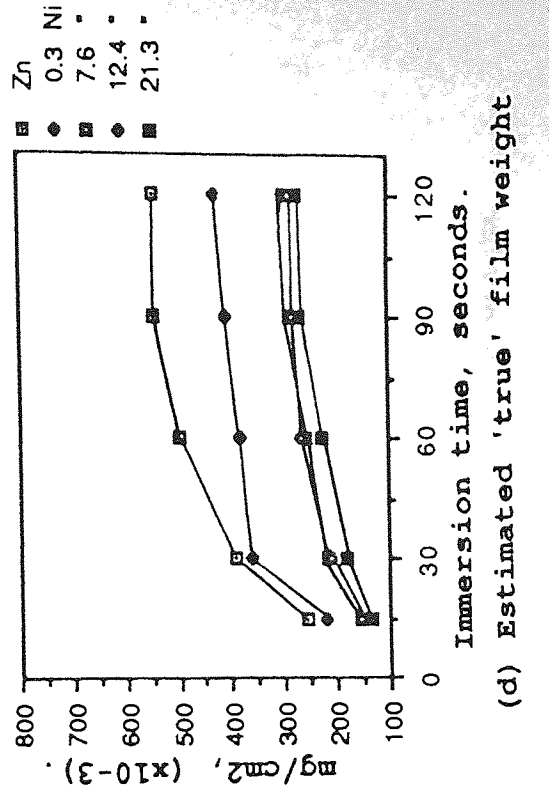
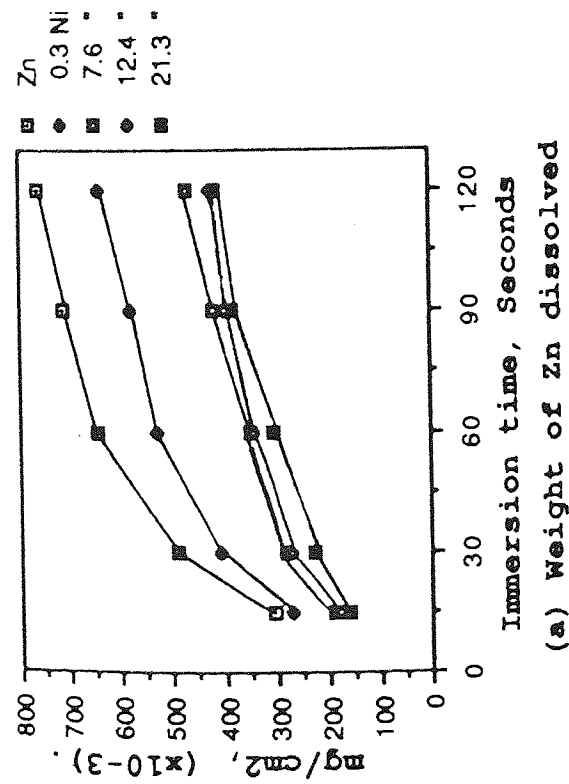
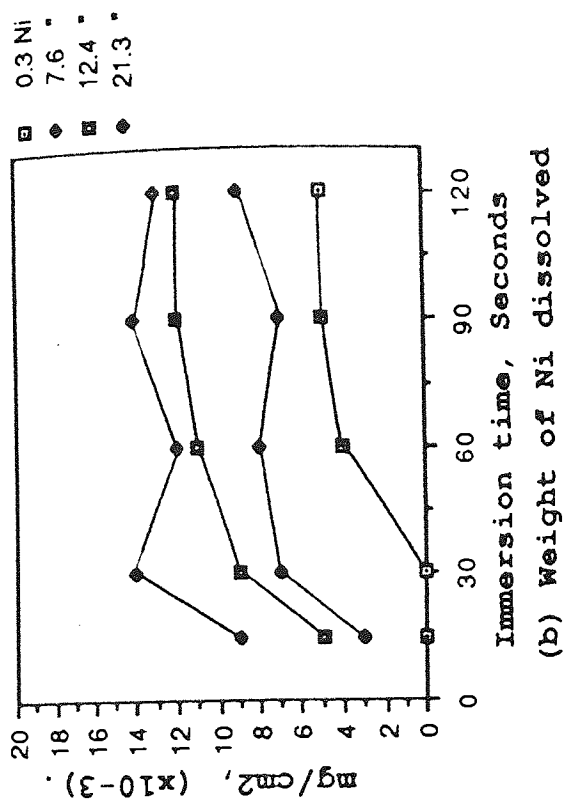


Fig.4.32 Chromating Characteristics of Dull Zn-Ni Deposits Treated in Solution (1).

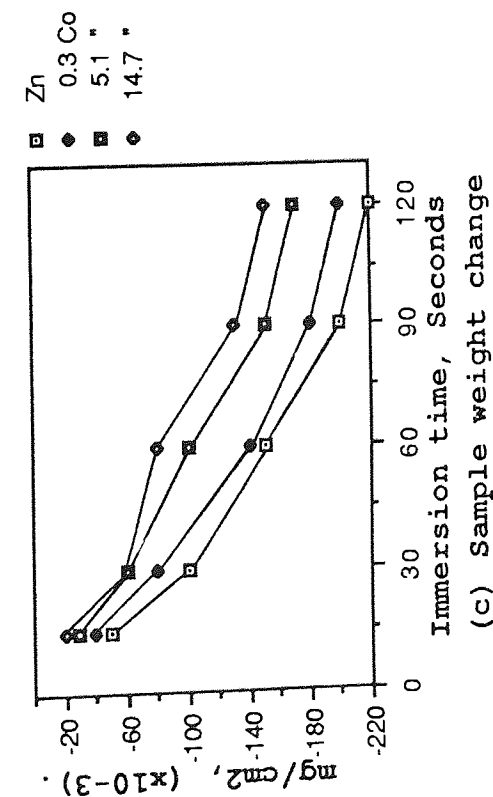
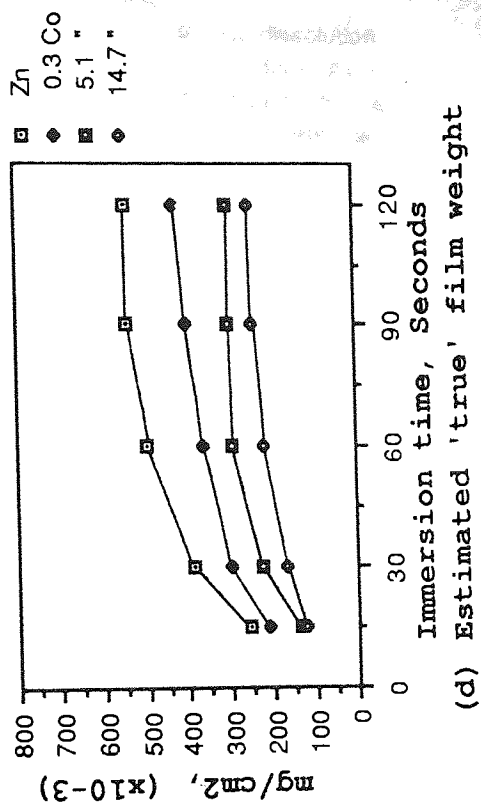
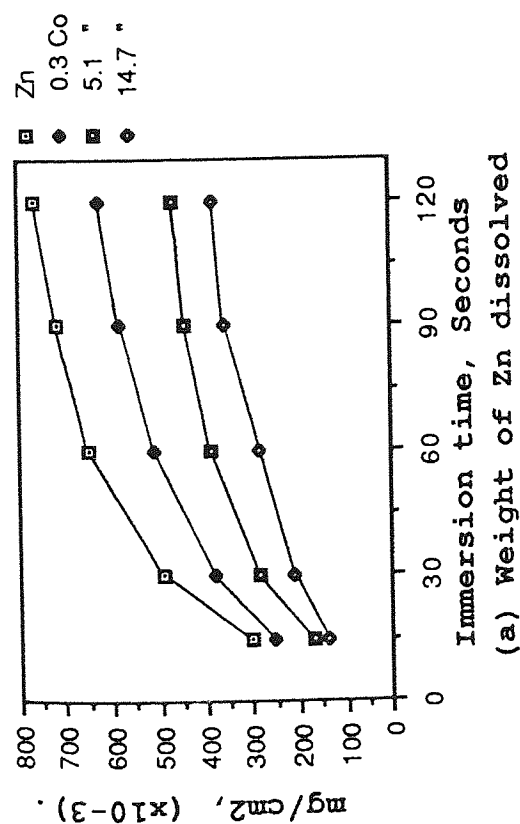
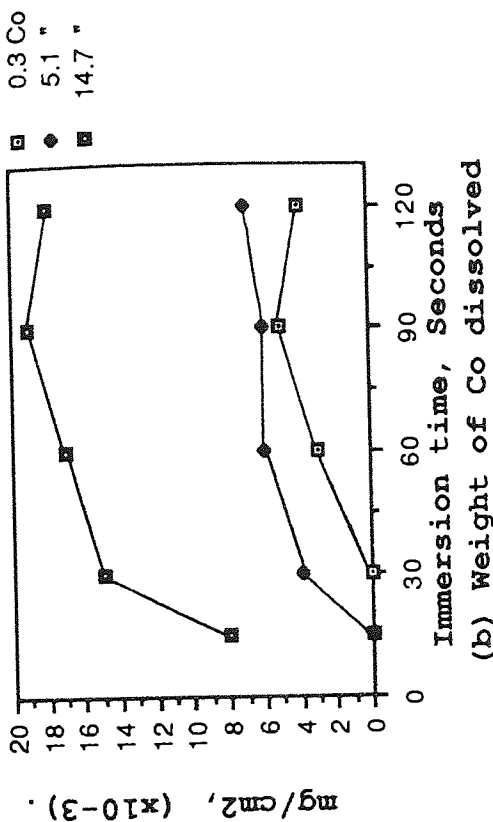
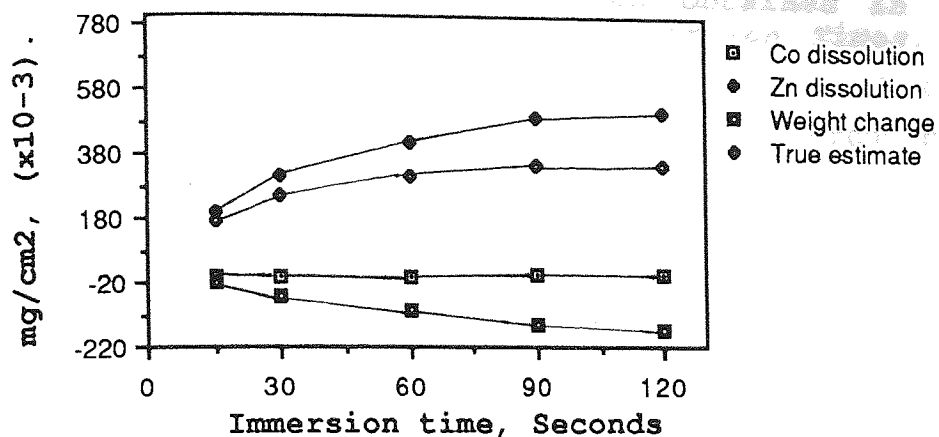
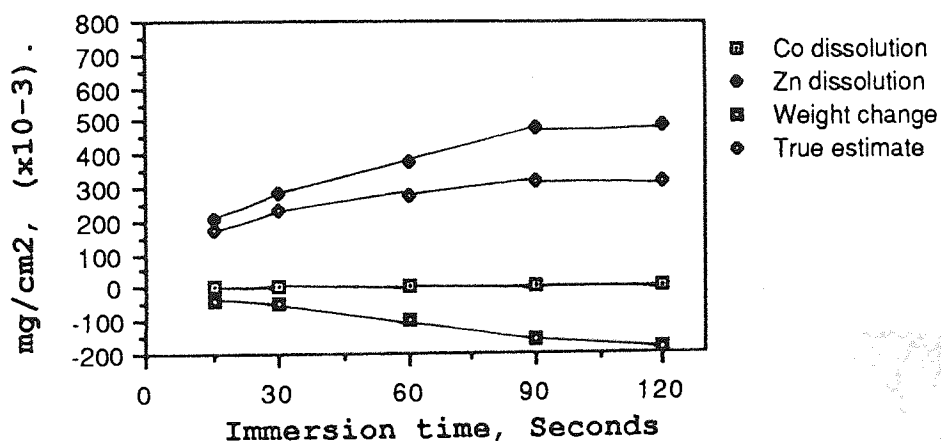


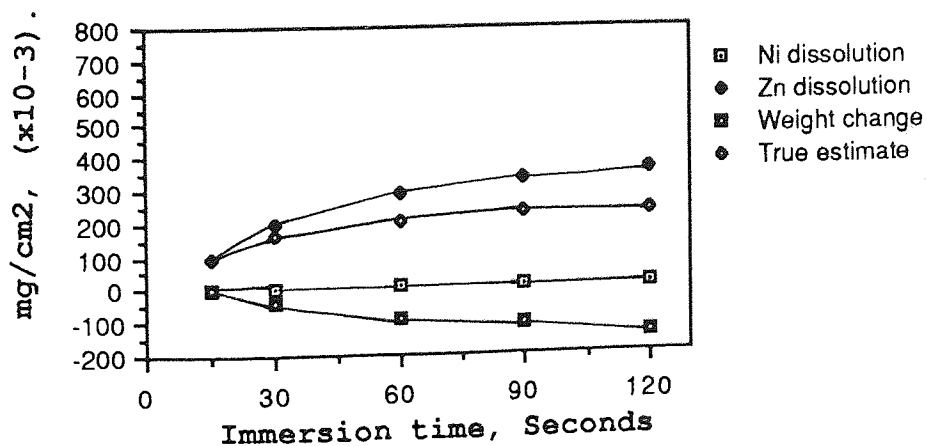
Fig.4.33 Chromating Characteristics of Dull Zn-Co Deposits Treated in Solution (1).



(a) 0.3% Co (Zincrolyte)



(b) 0.7% Co (Canning)



(c) 13.8% Ni (Schloetter)

Fig.4.34 Chromating Characteristics of Bright Samples Treated in Solution (1).

- Appearance of Conversion Films Obtained in Solution (1) for Different Immersion Times.

The following photographs show the effects of substrate nature (pure Zn, and Zn-Ni / Zn-Co with different Ni and Co contents) and its surface conditions (in terms of dullness, roughness and brightness) on the appearance of the chromated films formed in solution (1). Figure 4.35 represents dull deposits and Figure 4.36 bright and smooth deposits.

**Fig.4.35 Dull Deposits treated for 30 seconds.
Magnification: x6.**

a- Pure Zn



b- 0.3% Ni



c- 12.4% Ni



d- 21.3% Ni



e- 5.1% Co



f- 14.7% Co



Fig.4.36 Commercial bright deposits treated in
solution (1) for 15 seconds.
Magnification: x6.

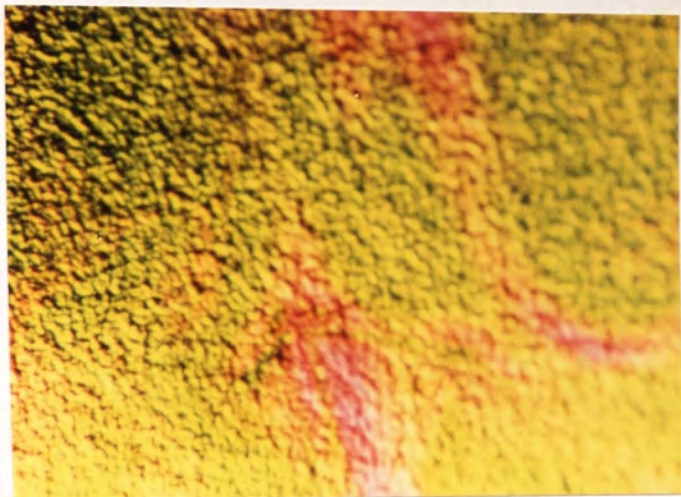
a- Pure Zn



b- Schloetter
(13.8% Ni)



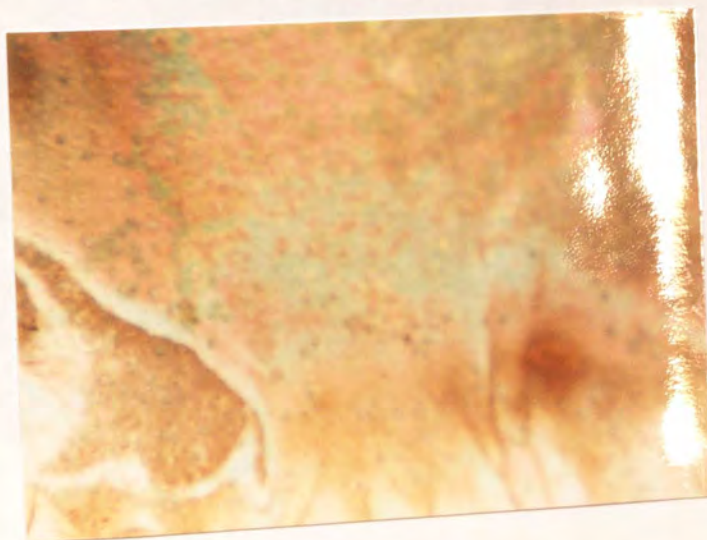
c- Zincrolyte
(0.3% Co)



d- Canning
(0.7% Co)



e- Canning
(1.0% Co)

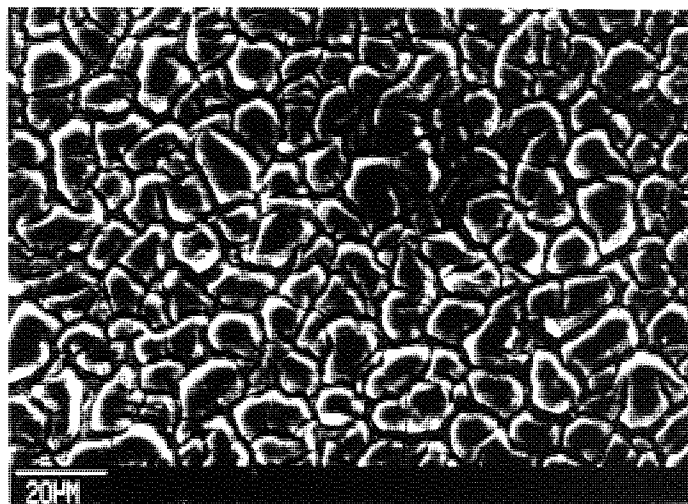


- Chromate Films Structures

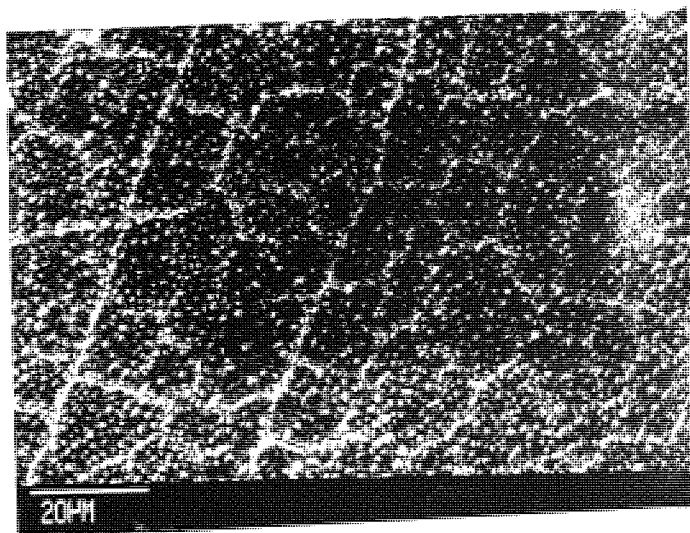
the following micrographs show clearly the variability in the film structures suggesting different reactivity rates depending on deposit Ni (or Co) content as in Figure 4.37) or immersion time as illustrated in Figures 4.38 and 4.39 for bright deposits.

Fig.4.37 Scanning electron micrographs of dull deposits treated in solution (1) for 120 seconds.

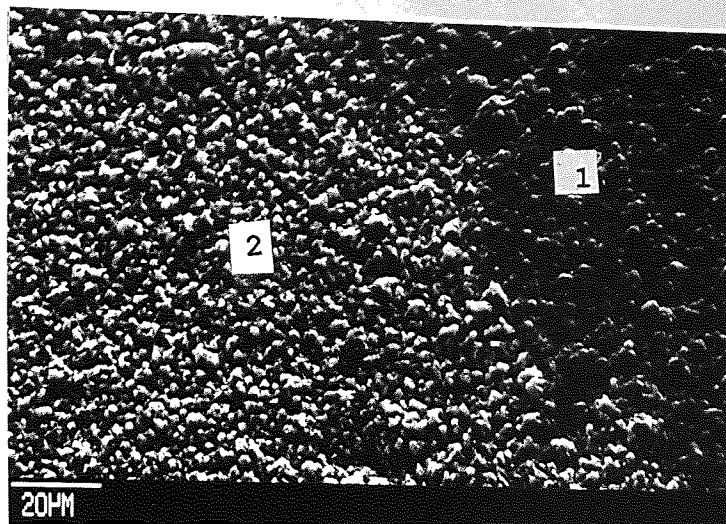
a- 0.3% Ni



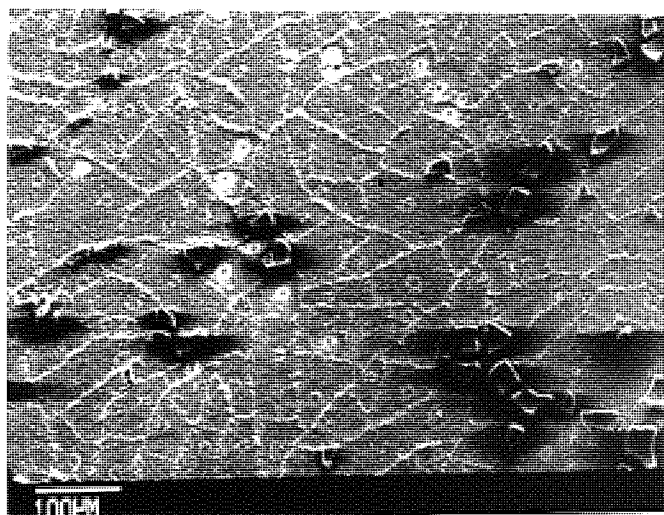
b- 12.4% Ni



c- 21.3% Ni
(1):As deposited
(2):Chromated



d- 14.7% Co



e- Same as (d)

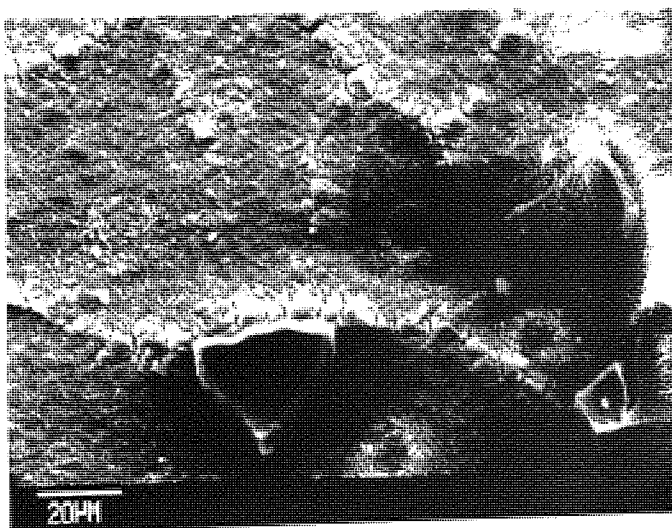
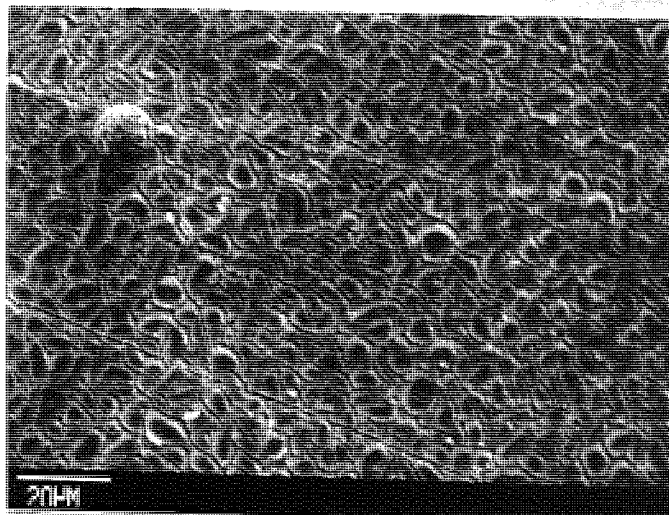


Fig.4.38 Scanning electron micrographs showing chromate film growth on Canning bright deposit (0.7% Co) treated in solution (1).

a- After 15 seconds



b- After 120 seconds

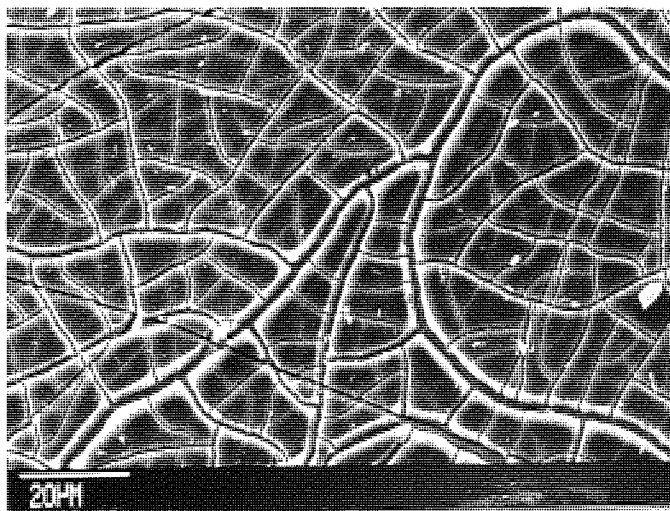
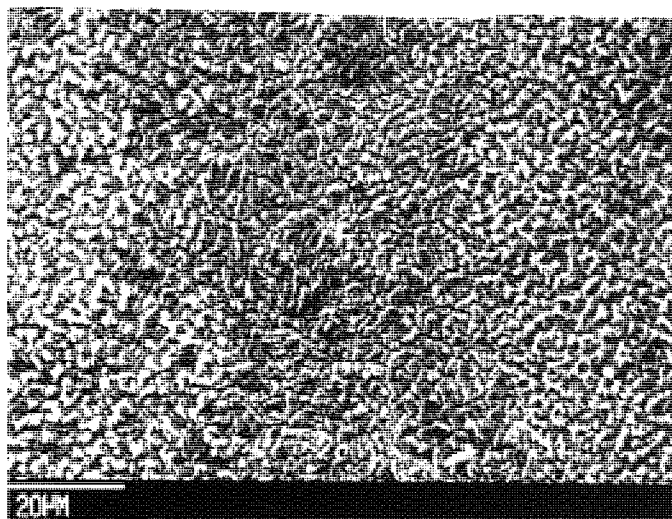
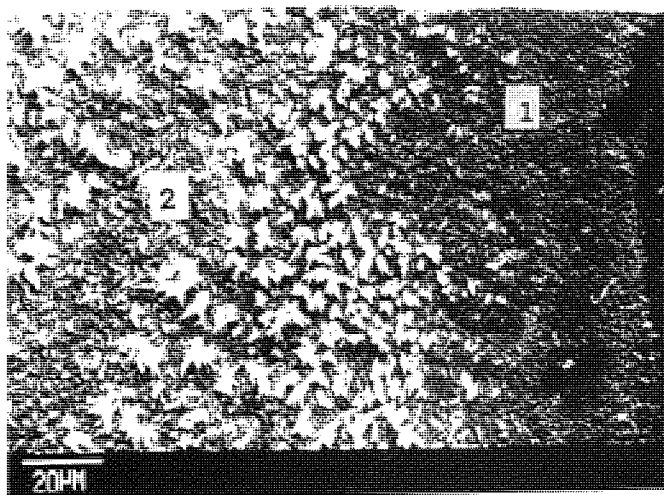


Fig.4.39 Scanning electron micrographs showing chromate film growth on Schloetter bright deposit (13.8% Ni) treated in solution (1).

a- After 15 seconds



b- After 120 seconds
(1):As deposited
(2):Chromated



- XPS Study Results

The XPS technique was used to study the chemical compositions on some of the samples destined for salt spray testing. The results are summarized in Table 4.28 below and in Figures 4.40-4.42. Selected peaks from Cr were measured at high resolution for a detailed study of their valence states, see Figure 4.42.

Table 4.28 Chemical Composition of Laboratory* and Commercially, (as received), chromated Samples.**

Samples	Binding Energy B.E, (eV)	Intensity (eV)	F.W.H.M (eV)	Area	Cr (III) Cr (VI)	Elements	
						Zn	Ni/Co
Zn *	Cr 574.6	1.4	1.7	0.7	6.0	X	-
	Cr (III) 576.4	92.6	3.0	85.3			
	Cr (VI) 578.7	15.2	3.0	14.2			
0.3 Ni	Cr 574.6	12.9	1.7	6.6	6.4	-	-
	Cr (III) 576.3	95.3	2.8	81.5			
	Cr (VI) 578.6	15.2	2.8	12.8			
12.4 "	Cr 574.6	37.7	1.8	21.8	19.5	X	-
	Cr (III) 576.1	82.4	2.8	74.2			
	Cr (VI) 578.6	4.4	2.8	3.8			
0.3 Co	Cr 574.6	9.7	1.8	3.9	1.1	-	-
	Cr (III) 578.4	75.0	2.8	49.7			
	Cr (VI) 580.7	62.6	3.0	46.6			
5.1 "	Cr 574.5	0.0	1.6	0.0	4.0	X	-
	Cr (III) 576.6	85.9	2.9	79.2			
	Cr (VI) 578.1	21.0	2.9	19.7			
14.7 "	Cr 574.6	2.1	1.7	1.0	3.6	X	-
	Cr (III) 576.7	91.3	2.8	77.7			
	Cr (VI) 578.9	24.8	2.9	21.3			
**							
Zn (L7C)	Cr 574.6	21.7	1.9	11.9	6.8	X	-
	Cr (III) 576.3	93.8	2.8	76.1			
	Cr (VI) 578.7	13.9	2.8	11.2			
13.8 Ni	Cr 574.6	25.4	1.9	14.7	10.6	X	-
	Cr (III) 576.1	86.8	2.9	75.4			
	Cr (VI) 578.2	8.4	2.8	7.1			
0.7 Co	Cr 574.6	4.1	1.9	2.3	5.6	X	-
	Cr (III) 576.4	97.4	2.8	82.7			
	Cr (VI) 578.6	17.4	2.8	14.6			

x Element present in the chromate film

- Element not present

F.W.H.M stands for Full Width at Half Maximum height

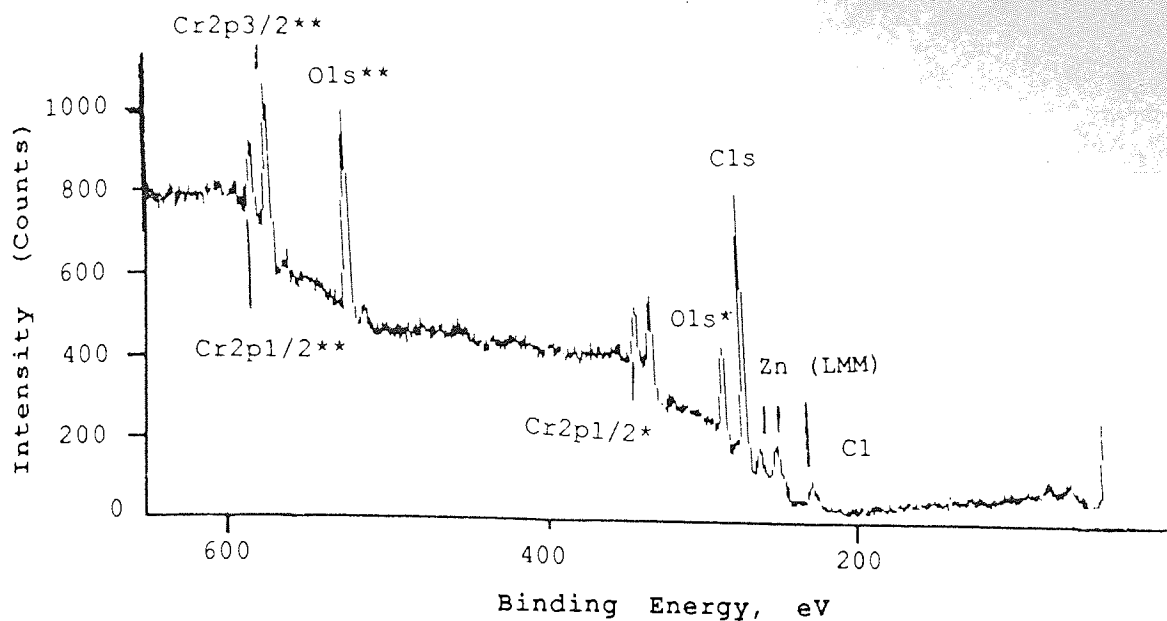


Fig. 4.40a- Low resolution XPS spectra generated by Mg and Al X-ray sources from dull 12.4% Ni sample treated in solution (1) for 120 seconds.

* Generated by Mg X-ray source
 ** Generated by Al X-ray source

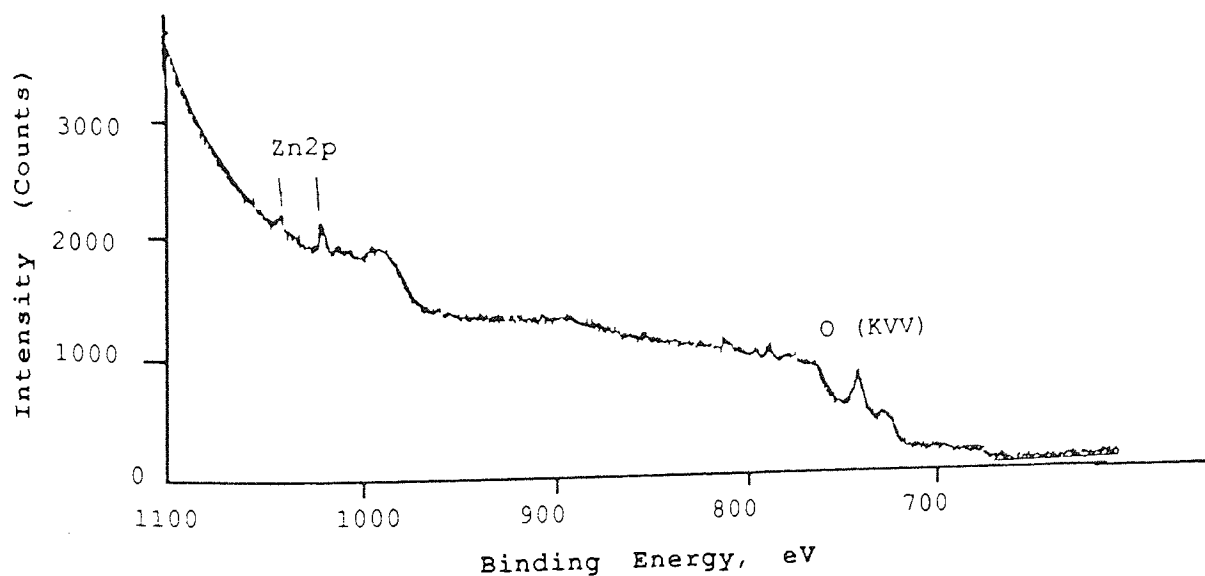


Fig. 4.40 b- Same as above

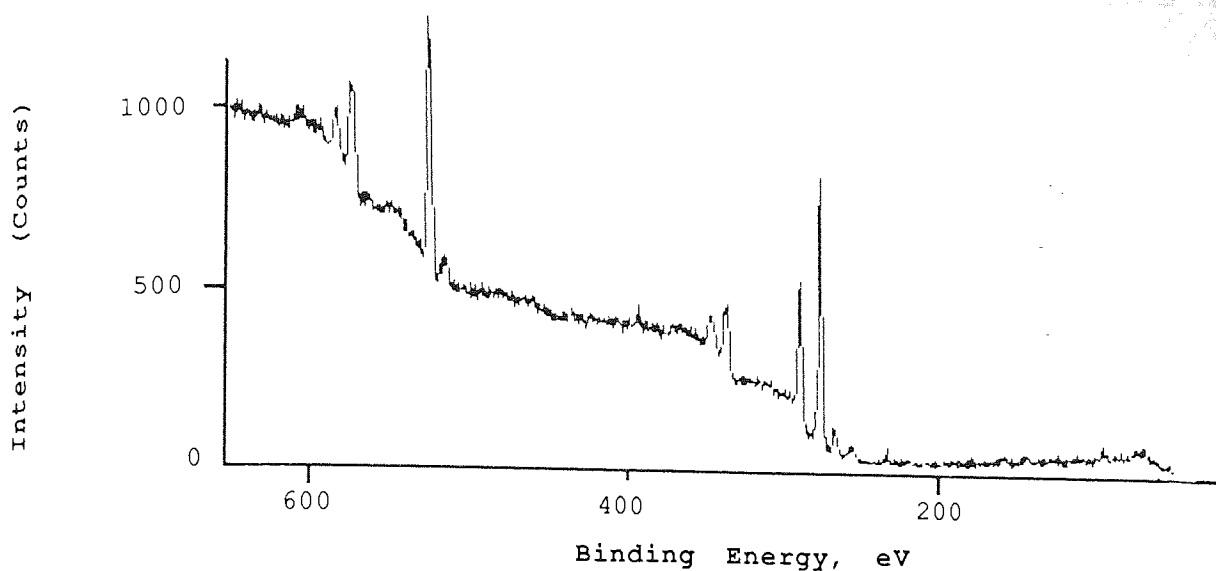


Fig. 4.41a- Low resolution XPS spectra generated by Mg and Al X-ray sources from dull 0.3% Co sample treated in solution (1) for 120 seconds.

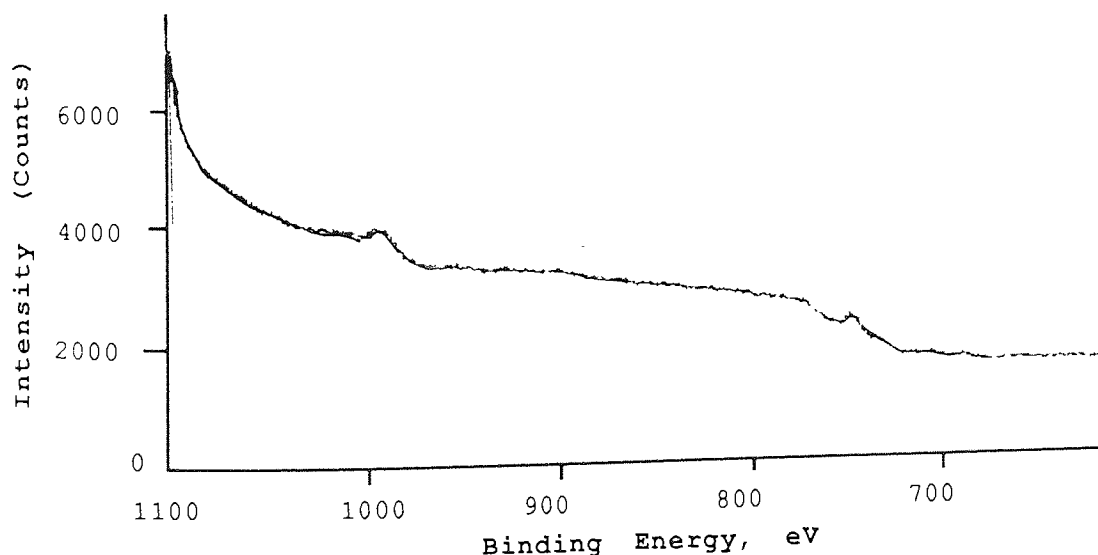


Fig. 4.41 b- Same as above

(Note the absence of Zn peaks at 1021.4 and 1044.5 eV)

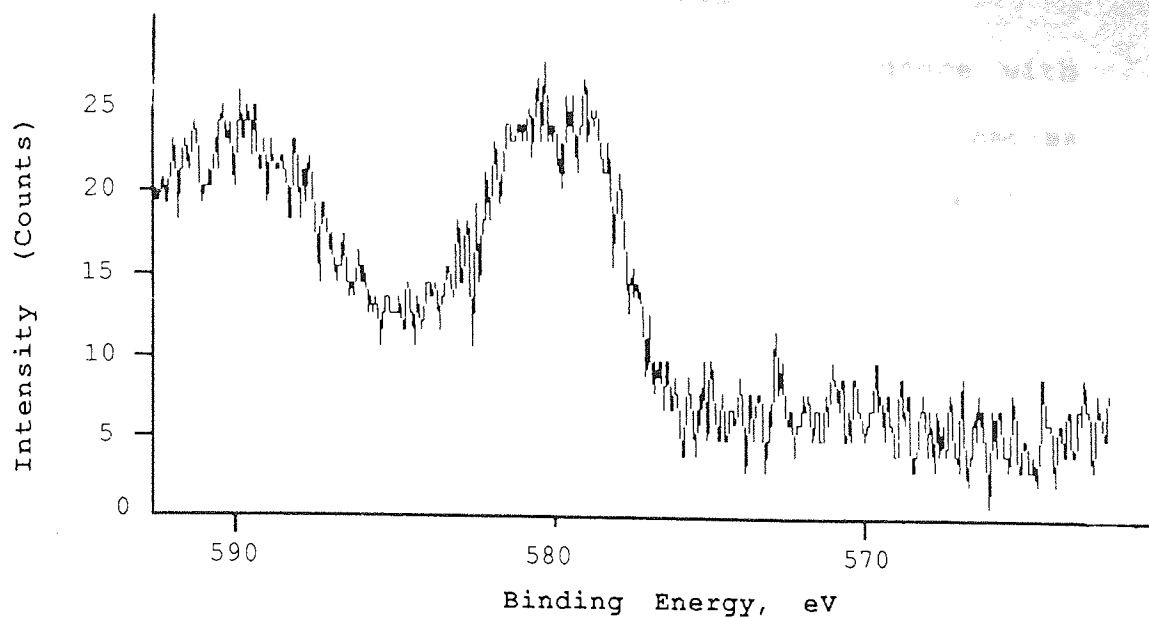


Fig. 4.42a- High resolution XPS spectra of Cr₂p
(Extracted from Fig. 4.41)

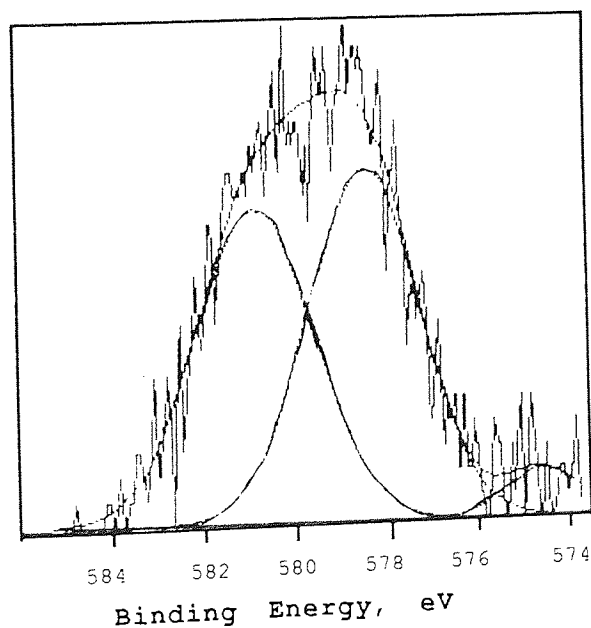


Fig. 4.42 b- Same as above
(with curves fittings)

4.2.2 Schloetter Chromating Solution

The chromating solution was used in accordance with conditions specified for commercial use, that is the samples were treated at a temperature of 40°C for 40 seconds. This solution was developed for Zn-Ni systems having high Ni contents of about 14% Ni. However, in this present work it has also been used for dull pure Zn and Zn-Co alloy coatings. The chromating characteristics of the deposits are summarized in Table 4.29 below and also given in Figures 4.43 - 4.45.

Table 4.29 Chromating Characteristics of Dull Samples treated in Schloetter Solution.

Samples	Zinc dissolved	Weight change	True estimate	Weight %, Cr	Appearance
Zn	60	-30	30	1.7	Very light yellowish
0.3 Ni	39	-20	19	2.2	"
12.4 "	99	-10	89	5.9	Iridescent (Colourful)
21.3 "	98	0	98	7.8	Brownish
0.3 Co	50	-20	30	1.2	Very light yellowish
5.1 "	52	-10	42	3.5	"
14.7 "	41	-20	21	2.1	No change

The results above are also illustrated in Figures 4.43-4.45. The units are in 10^{-3} mg/cm².

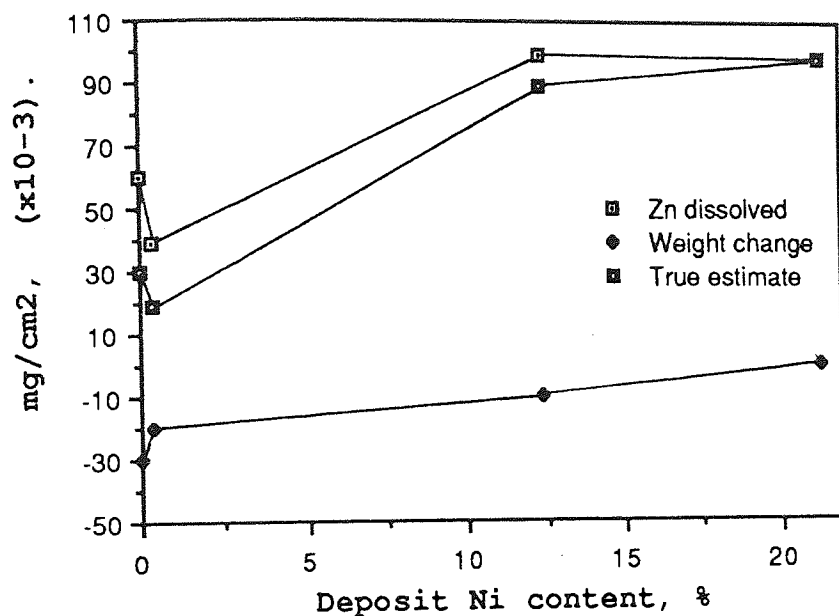


Fig. 4.43 Chromating characteristics of Zn-Ni dull deposits treated in Schloetter Chromating solution

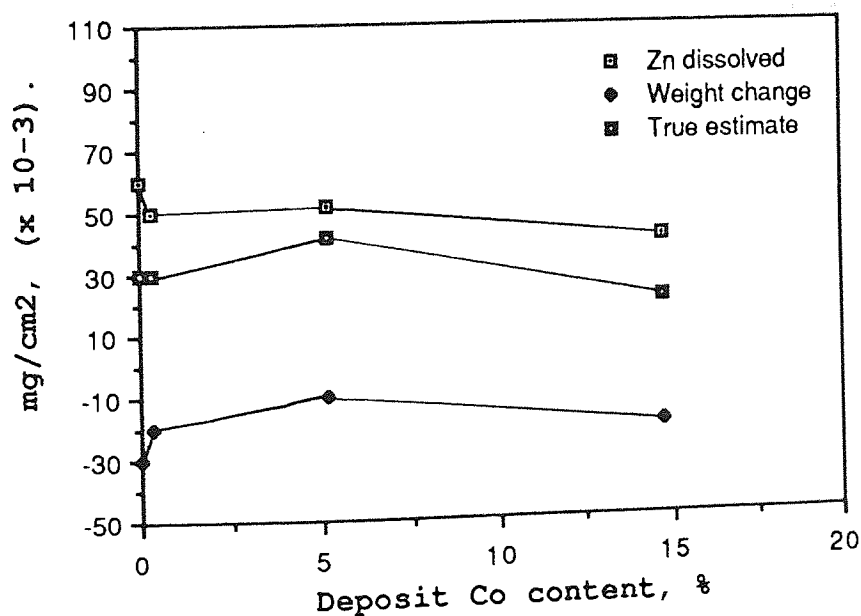


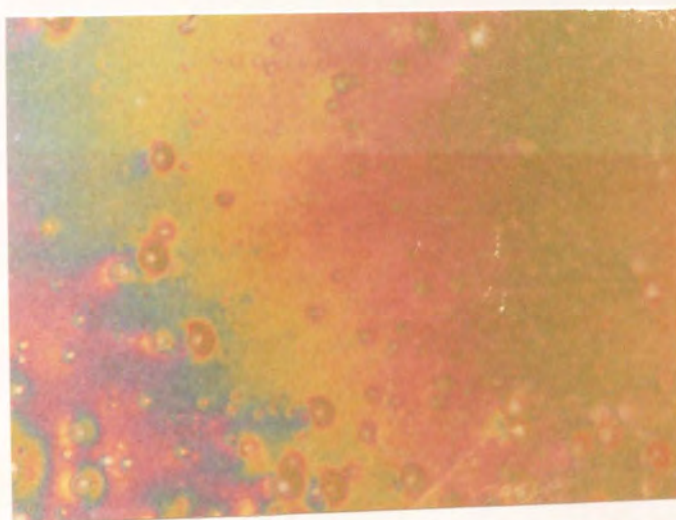
Fig. 4.44 Chromating characteristics of Zn-Co dull deposits treated in Schloetter Chromating solution

Fig.4.45 Photographs of Dull deposits treated in
Schloetter solution for 40 seconds.

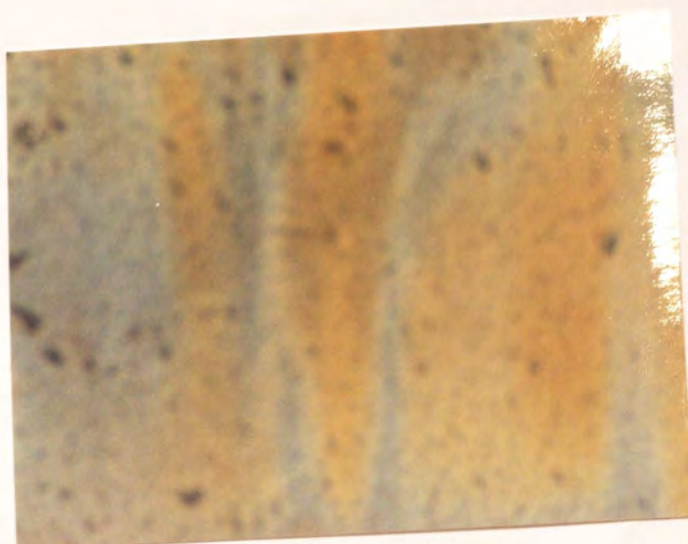
a- Pure Zn



b- 12.4% Ni



c- 21.3% Ni



4.2.3 Canning Chromating Solution

Initially five immersion times were envisaged as in the case of the solution (1) but it was found that only the long times 90 seconds and above gave reasonable change in appearance, as shown in Table 4.30. Treating for times less than 90 seconds gave no colour changes. Even for an immersion period as long as 120 seconds, only pure Zn, 0.3% Ni and 0.3% Co showed slight changes in colour. This solution was developed for bright and smooth Zn-Co systems having Co contents up to about 1.0%.

Table. 4.30 Chromating Characteristics of Dull Deposits Treated in Canning Chromating Solution.

Samples	90 seconds					120 seconds				
	Zn dissolution	Weight change	True estimate	Weight %, Cr	Zn dissolution	Weight change	True estimate	Weight %, Cr	Appearance	
Zn	56	- 10	4 6	2.3	6 8	- 20	4 8	2.6	Yellow	
0.3 Ni	49	- 20	2 9	3.2	6 2	- 30	3 2	2.9	Light yellow	
7.6 "	42	- 20	2 2	1.8	6 0	- 20	4 0	1.2	No change	
12.4 "	42	- 10	3 2	1.9	6 1	- 40	2 1	1.0	No change	
21.3 "	44	- 10	3 4	0.6	5 4	- 30	2 4	0.6	No change	
0.3 Co	49	- 30	1 9	1.2	6 3	- 30	3 3	1.8	Light yellow	
5.1 "	44	- 20	2 4	1.4	5 5	- 30	2 5	1.2	No change	
14.7 "	52	- 30	2 2	1.2	6 0	- 40	2 0	0.9	No change	

The results above are displayed graphically in Figures 4.46 and 4.47.

The units above are in 10^{-3} mg/cm²

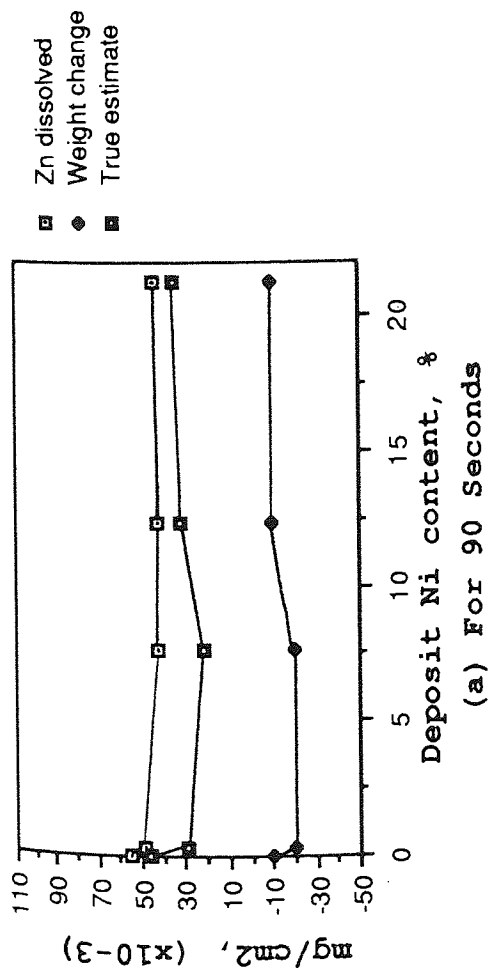
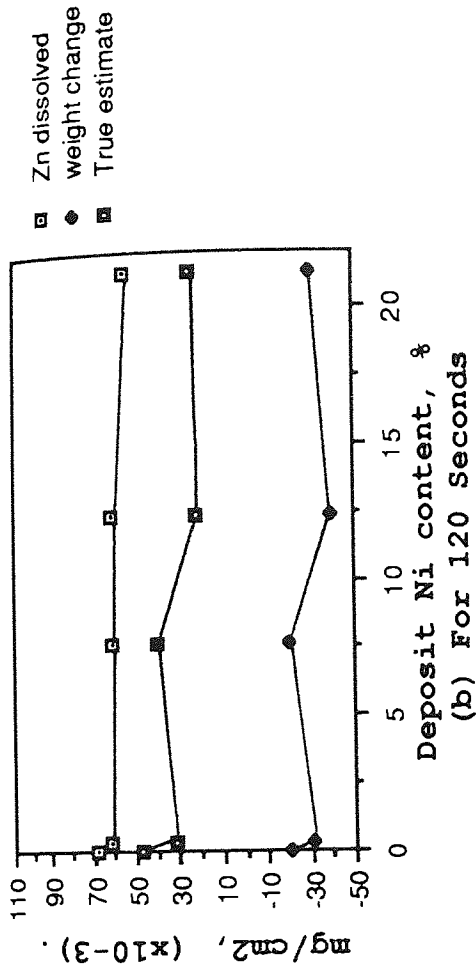


Fig. 4.46 Chromating Characteristics of Dull Zn-Ni Deposits Treated in Canning solution for 90 and 120 Seconds

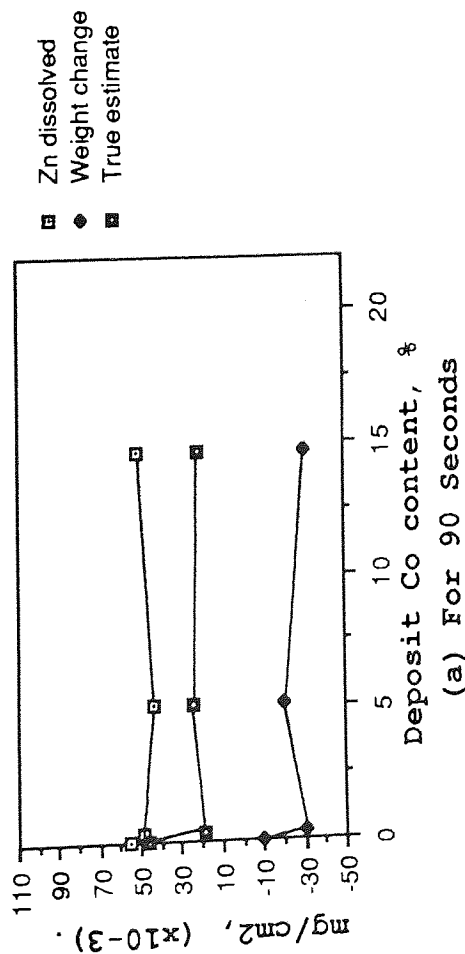
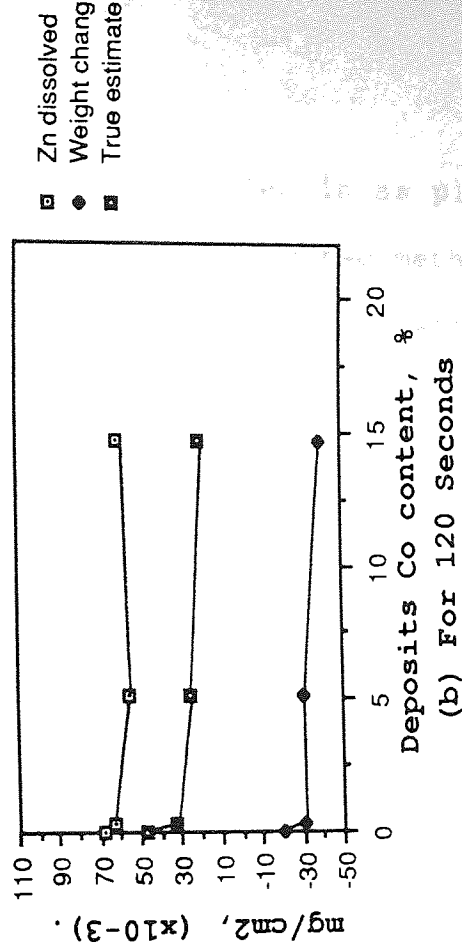


Fig. 4.47 Chromating Characteristics of Dull Zn-Co Deposits Treated in Canning Solution for 90 and 120 Seconds

4.3 Corrosion

Both commercial and laboratory prepared samples in as plated and in as chromated conditions were tested using two methods: neutral salt spray and electrochemical tests. 5% (by weight) NaCl solution was used as testing solution throughout.

4.3.1 Non-Chromated Systems

- *Electrochemical Testing*

In order to determine the corrosion rates from linear polarization curves, potentiodynamic scans were run first so that the Tafel constants could be obtained. Figure 4.48 shows potentiodynamic graphs for some of the dull samples tested. Tafel constants, corrosion rates and corrosion potentials results obtained for dull deposits by periodical measurements using linear polarization technique are listed in Table 4.31 and subsequent Figures 4.49 - 4.52. Table 4.32 and Figures 4.53 and 4.54 illustrate the results for bright commercial non-chromated samples.

- *Neutral Salt Spray Testing*

All the salt spray test results are reported in terms of times to first red or white rust. Table 4.33 and subsequent Figures 4.55 and 4.56 show the relationships between Ni or Co content in the deposits and times to first red rust for dull deposits. It can be seen clearly that low Ni and Co content deposits offer little advantage over pure Zn. 12.4% Ni and 5.1% Co deposits gave the maximum corrosion resistance in the case of Zn-Ni and Zn-Co systems respectively as illustrated

in Figure 4.56c.

4.3.2 Chromated Systems

The corrosion rate results given in Table 4.34 were obtained from potentiodynamic curves by back extrapolation method, (for more details refer to section under the heading of 'Tafel plot' page 82). Corrosion resistance was improved by conversion coating as shown in Table 4.34 which includes also the results of non-chromated samples for comparative purposes. However, the type of conversion coating is very important. It can be seen from the Table 4.34 that the corrosion resistance is greatly improved for commercially chromated deposits as opposed to the laboratory chromated samples.

The same general observations can be made from salt spray test results shown in Tables 4.35-4.37 and subsequent Figures 4.61-4.71.

A- Results of Non-Chromated Systems

- Electrochemical Testing

Fig.4.48 Polarization curves for non-chromated dull deposits.

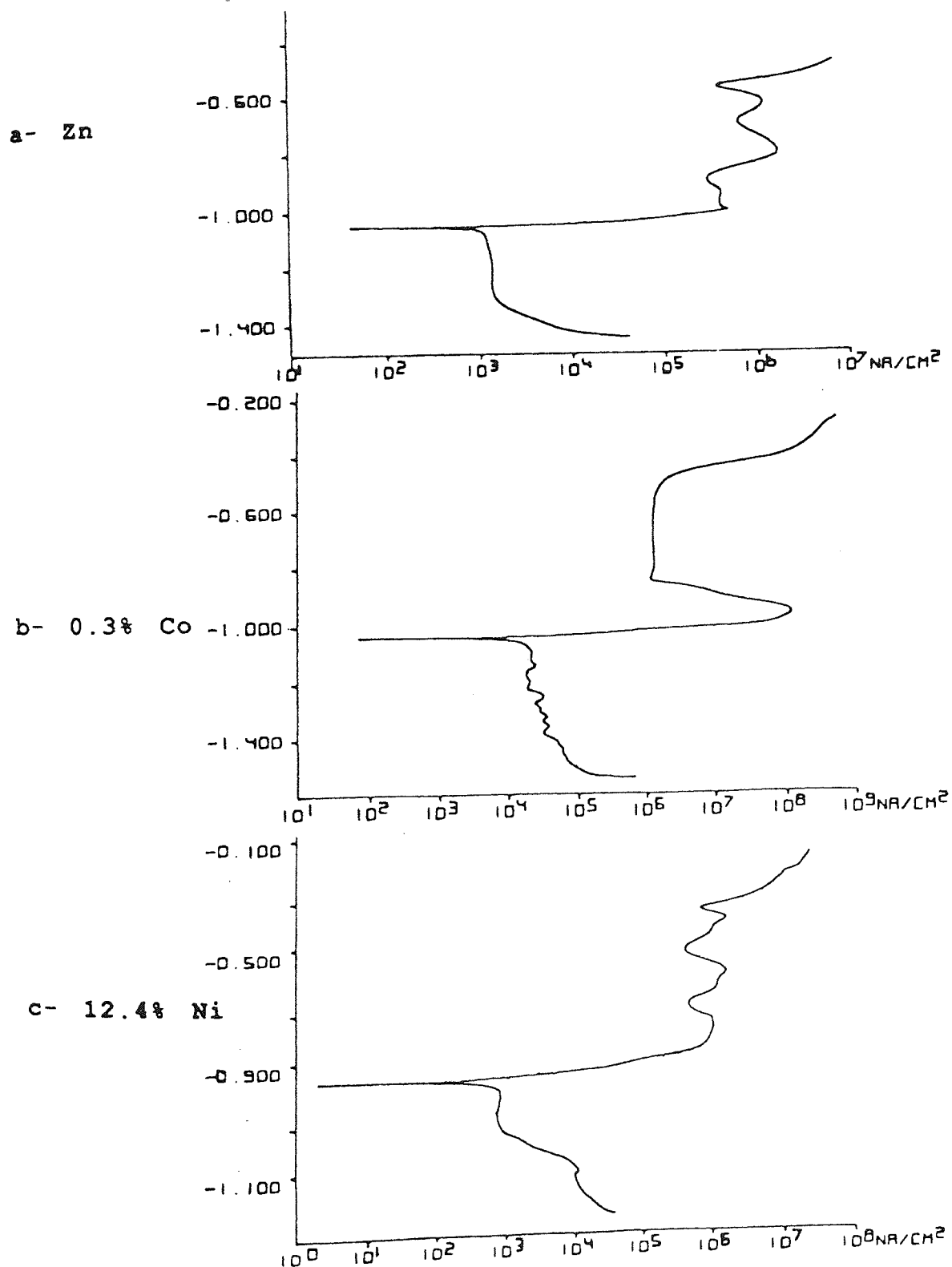


Table 4.31 Variation of Corrosion Rate and Potential with Time for Dull Non-Chromated Deposits

Samples	b _a mV/dec	Immersion time, Days					
		60 mins	7	14	21	28	35
Pure Zn	12.9	- 1050 26.5	- 1053 19.9	- 1033 17.6	- 1020 14.3	- 1000 13.0	- 980 12.0
0.4 Ni	23.5	- 1035 18.9	- 1033 11.5	- 1034 8.9	- 1029 9.0	- 1027 11.9	- 1019 18.0
4.6 "	"	- 1033 25.0	- 1036 12.6	- 1022 19.0	- 959 16.0	- 886 6.1	- 858 8.1
12.4 "	34.0	- 965 25.0	- 940 12.9	- 879 7.3	- 765 4.6	- 744 3.1	- 750 2.8
21.3 " *	36.0	- 840 28.1	- 795 20.4	- 637 14.3	- 630 10.0	- 620 8.3	- 631 9.4
0.4 Co	17.6	- 1035 22.9	- 1042 19.3	- 1026 16.2	- 1014 15.81	- 990 10.4	- 981 9.0
4.6 "	"	- 1107 10.5	- 1015 9.1	- 1008 7.4	- 1001 2.0	- 987 4.5	- 924 8.1
7.5 "	27.0	- 1021 22.3	- 1017 12.1	- 1019 9.5	- 1016 8.4	- 1009 9.1	- 994 6.8
19.9 " *	35.3	- 1070 24.2	- 796 18.1	- 713 8.6	- 728 10.0	- 739 9.0	- 709 7.7

The negative values represent the values of Corrosion potentials in mV.
 The Corrosion rates are expressed in $\mu\text{A}/\text{cm}^2$
 The results are also illustrated in Figures 4.49-4.52
 * Obtained from large container (10 l capacity)

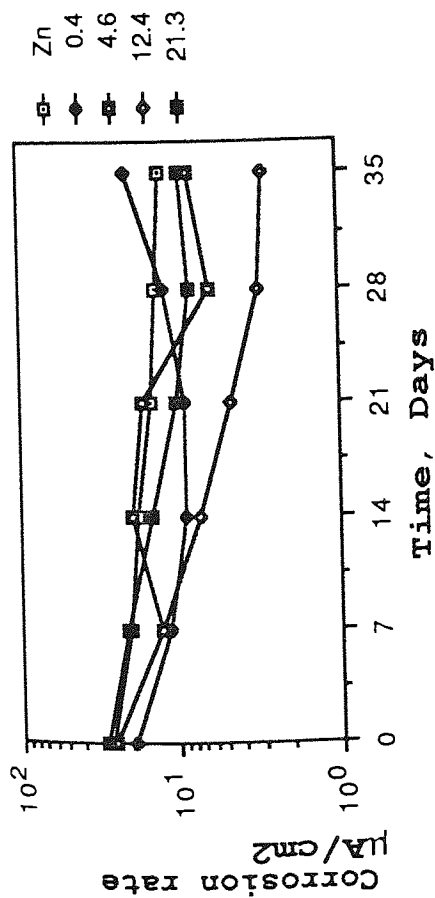


Fig. 4.49 Corrosion rate-Time Relationship

Variation of Corrosion Rate and Potential with Time for non-Chromated Dull Zn-Ni Deposits.

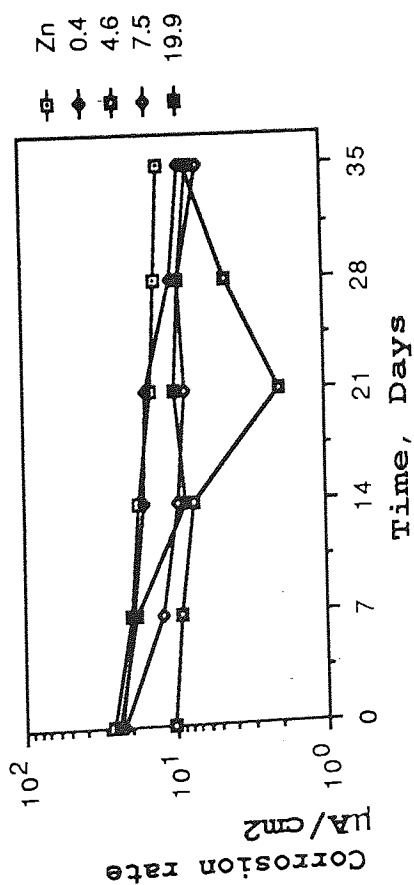


Fig. 4.51 Corrosion rate-Time Relationship

Variation of Corrosion Rate and Potential with Time for non-Chromated Dull Zn-Co Deposits.

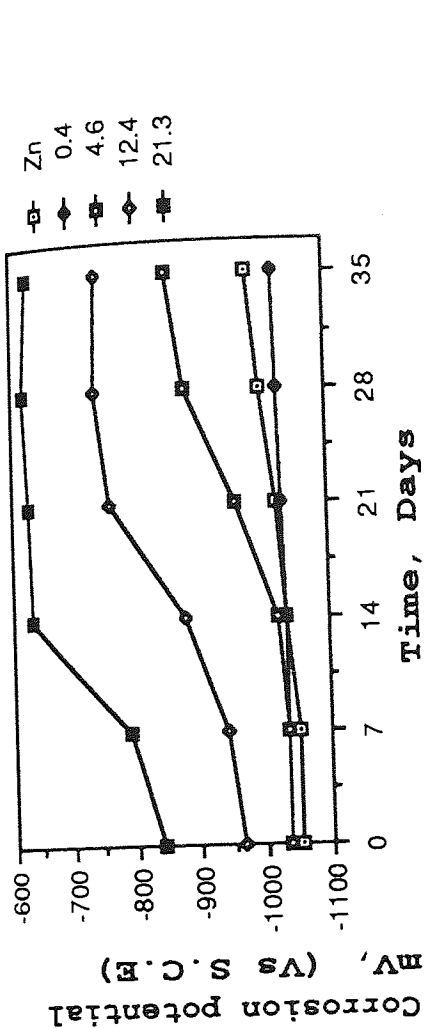


Fig. 4.50 Corrosion potential-Time Relationship

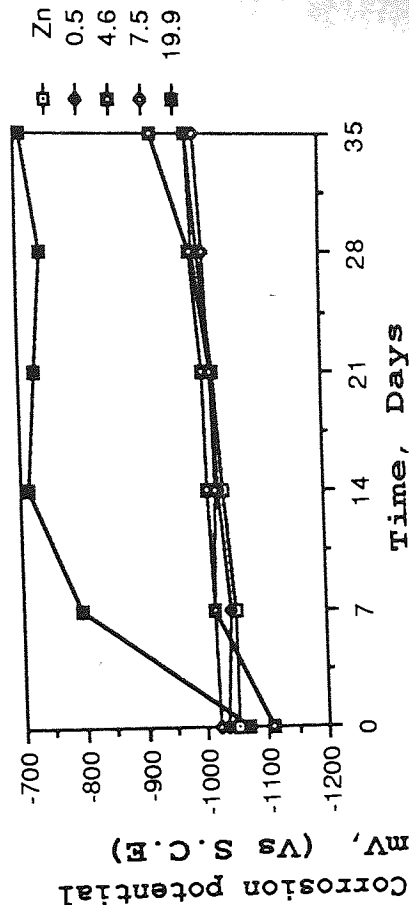


Fig. 4.52 Corrosion potential-Time Relationship

Table 4.32 Variation of Corrosion Rate and Potential with Time for Non-Chromated Bright Deposits (as received).

Samples	b _a mV/dec	Immersion time, Days						
		60 mins	2	7	14	21	28	35
Pure Zn	40	-1059 29.1	-1048 25.4	-1046 18.0	-1030 16.5	-1026 13.6	-1010 12.0	-1010 11.4
0.3 Co	33	-1012 28.7	-992 25.6	-987 18.6	-980 14.4	-974 11.2	-970 12.9	-958 11.6
1.0 "	58.3	-1026 25.5	-994 14.8	-979 10.1	-970 11.2	-962 7.4	-965 6.5	-
13.8 Ni	29.2	-912 18.7	-904 12.0	-902 11.2	-896 9.8	-894 7.0	-850 5.4	-810 3.1

The above results are also illustrated in Figures 4.53 and 4.54.

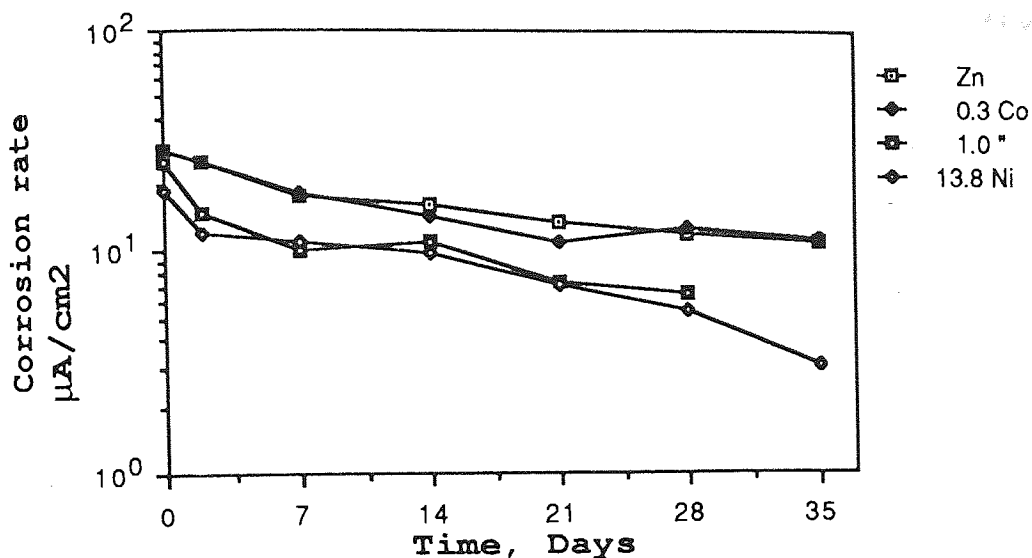


Fig. 4.53 Variation of corrosion rate with time for non-chromated commercial bright deposits
(As received)

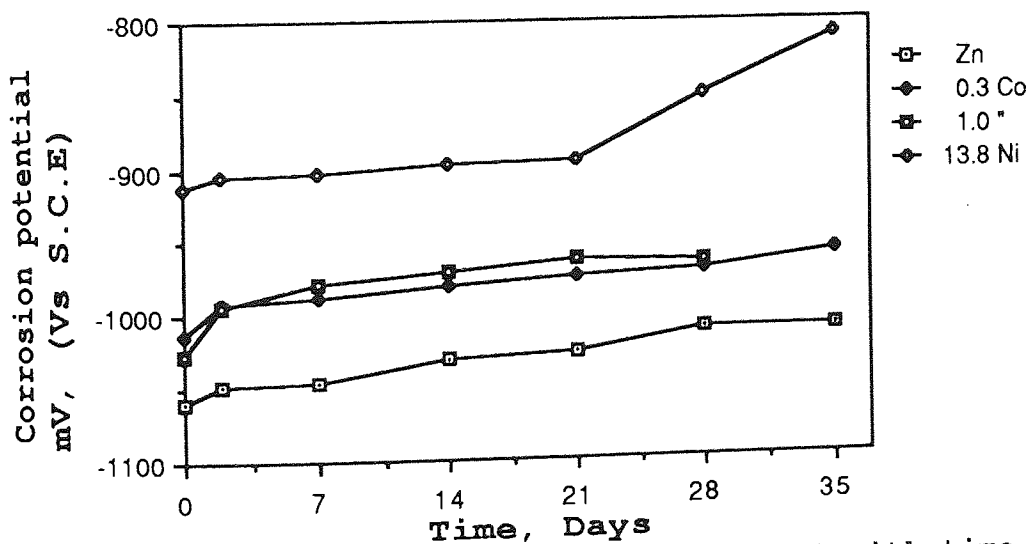


Fig. 4.54 Variation of corrosion potential with time for non-chromated commercial bright deposits
(As received)

- Neutral Salt Spray

Table 4.33 Salt spray results for non-chromated dull deposits having thicknesses of about 15 μm . after 365 hours exposure.

Zn-Ni System		Zn-Co System	
Samples (% Ni)	Hours to first Red rust	Samples (%Co)	Hours to first Red rust
Zn	95		
0.3	117	0.3	117
1.3	117	1.5	105
6.3	150	5.1	290
8.4	140	8.2	283
10.8	240	11.2	120
12.4	365	13.5	130
13.9	290	14.7	130
15.9	180	16.9	120
18.8	260	19.9	130
21.3	270		

The above results are shown in Figures 4.55-4.57.

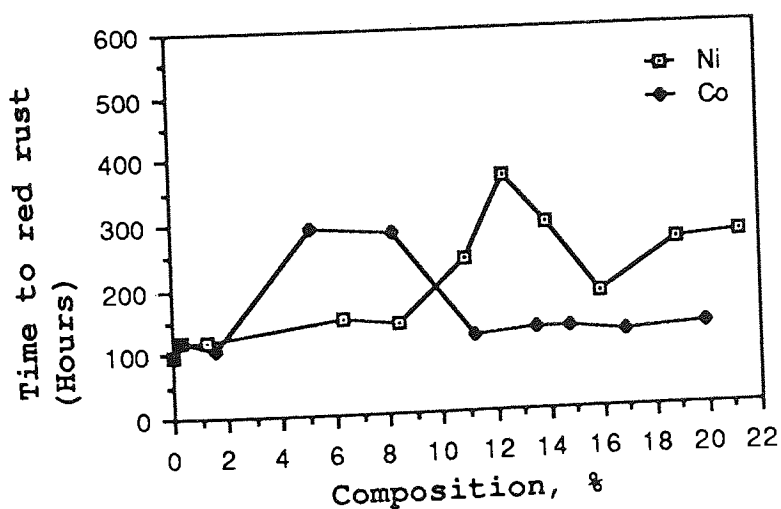
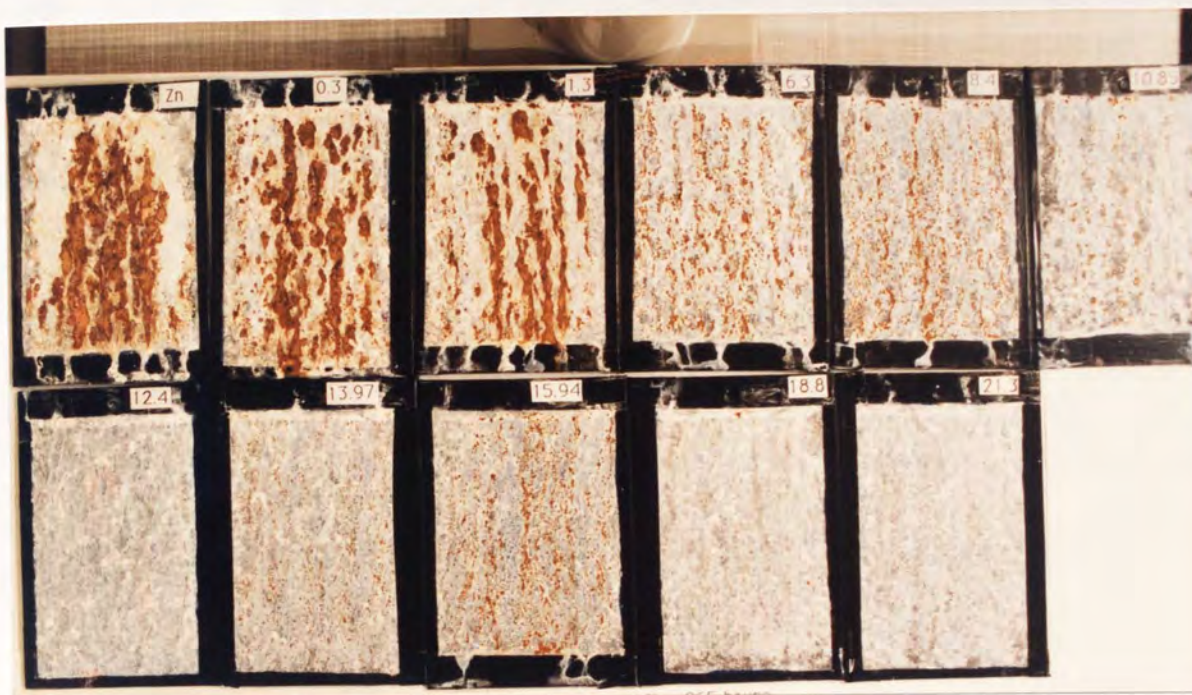
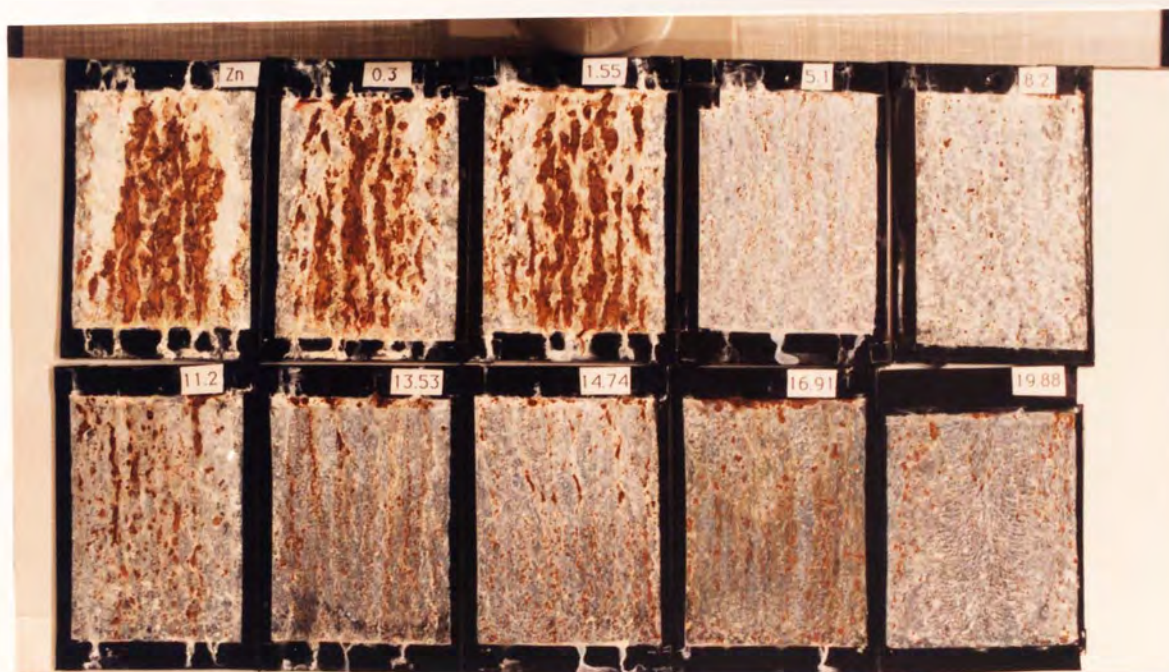


Fig. 4.55 Time to first red rust for non-chromated dull deposits

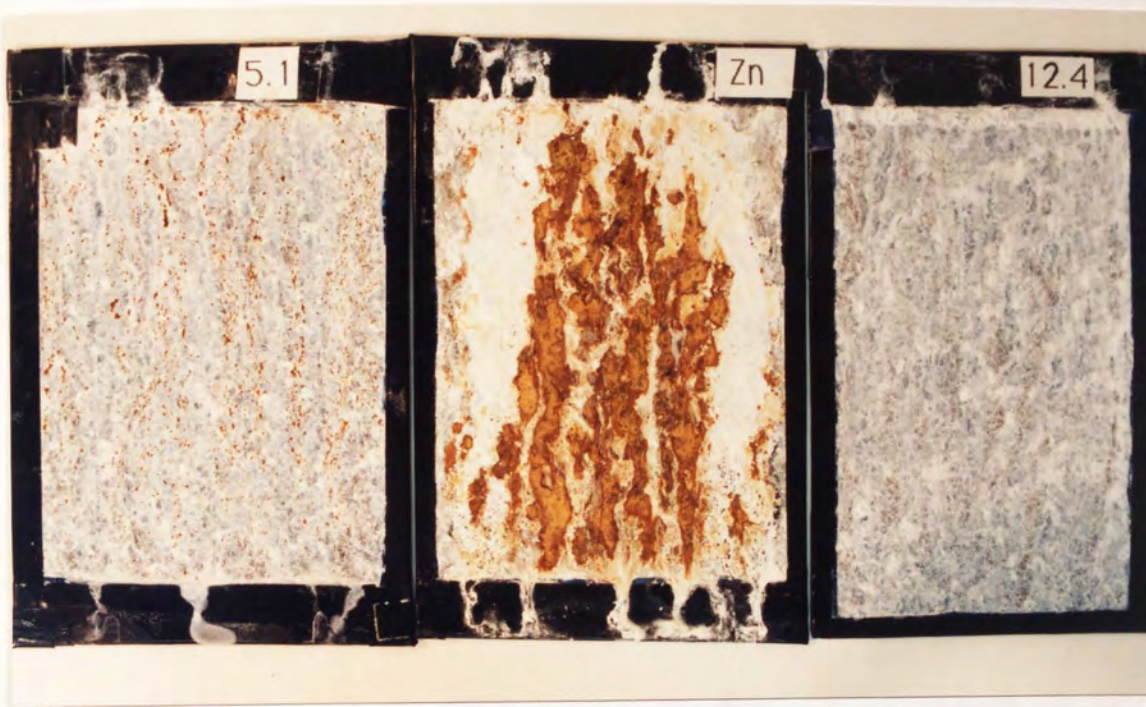
Fig.4.56 Photographs of corroded dull deposits.
After 365 hours of salt fog.



a- Zn-Ni Coatings



b- Zn-Co Coatings



(1)

(2)

(3)

c- Selected panels shown in larger format.

- (1) 5.1% Co
- (2) Pure Zn
- (3) 12.4% Ni

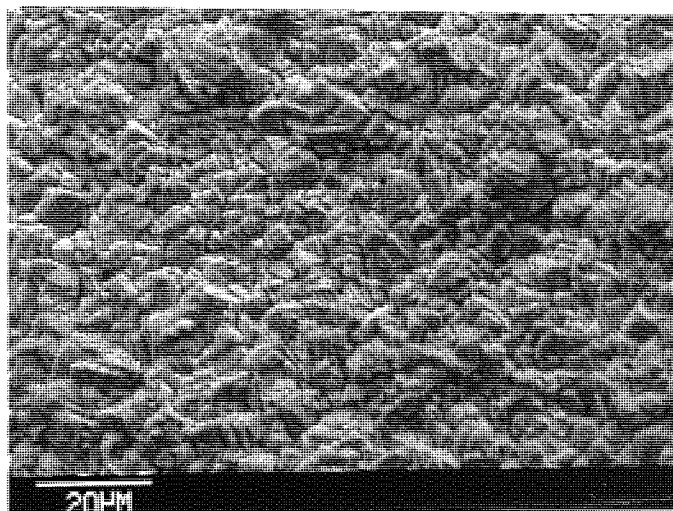
- *Immersion Testing*

The following micrographs shown in Figure 4.57 illustrate the morphology of dull non-chromated deposits in as deposited and corroded conditions.

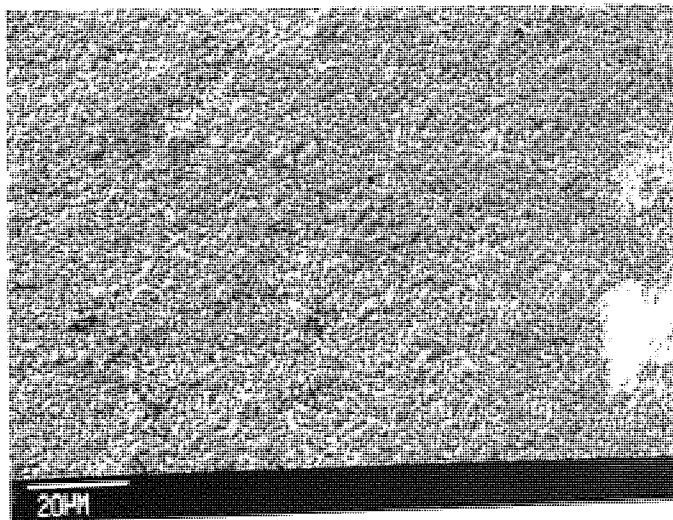
Fig.4.57 Scanning micrographs showing systems in as deposited and corroded conditions

a-As deposited

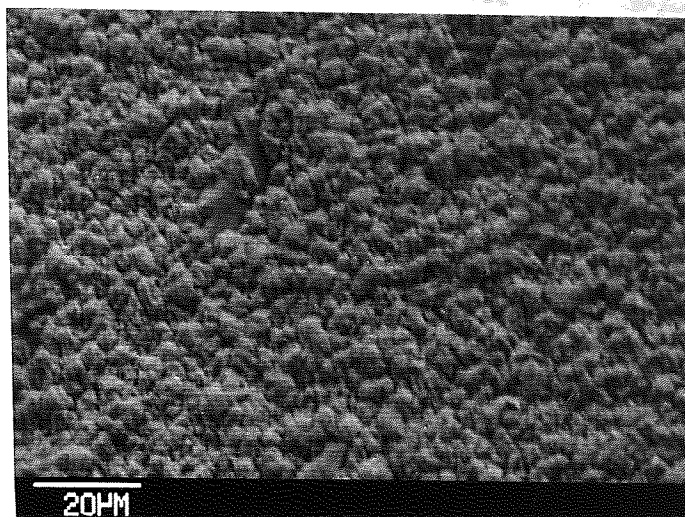
0.3% Ni



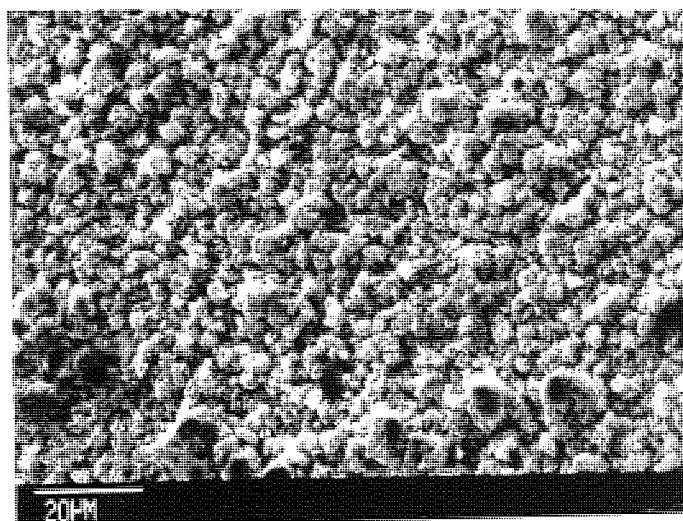
12.4% Ni



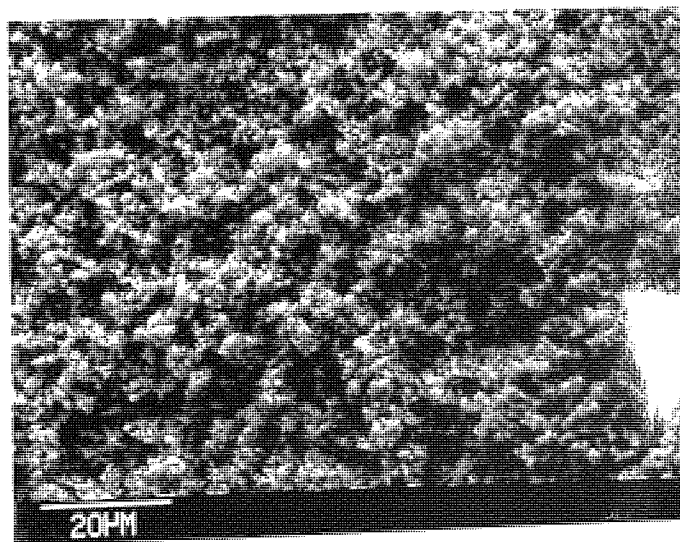
0.3% Co



5.1% Co

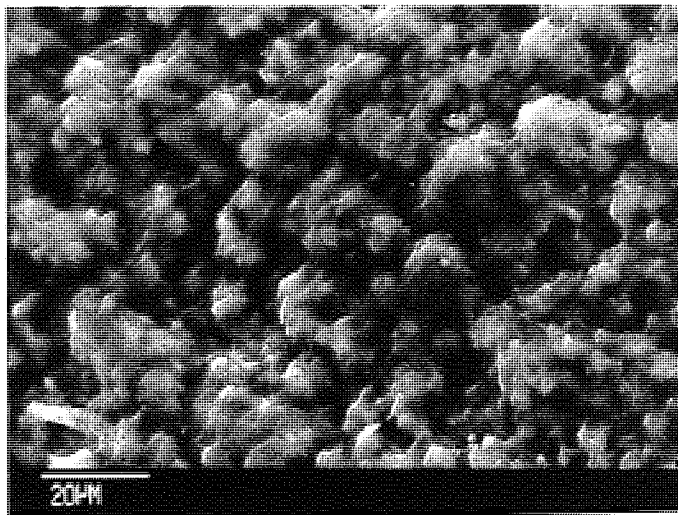


19.9% Co

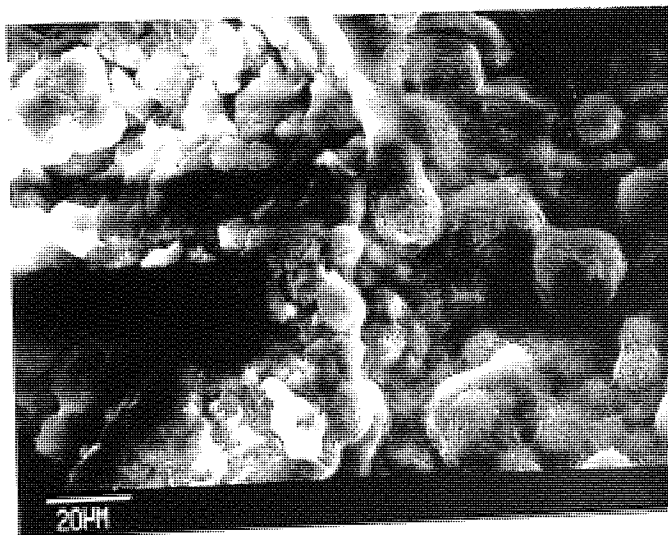


b- Corroded Zn-Ni coating, (0.3% Ni)

After 2 days
immersion



After 7 days
immersion

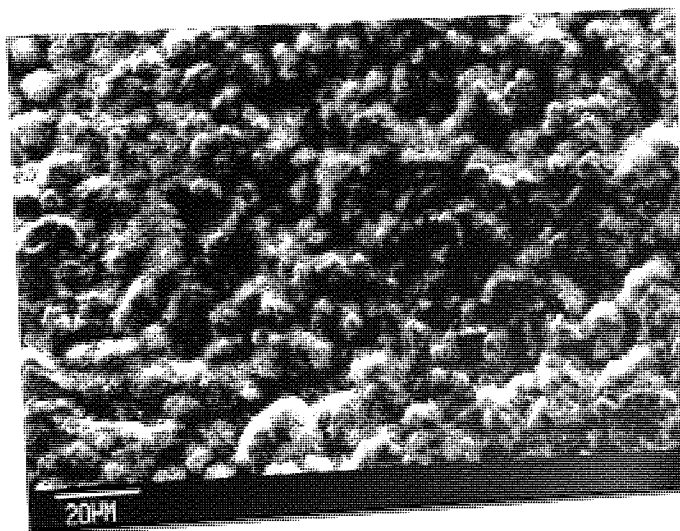


c- Corroded Zn-Co coating, (0.3% Co)

After 2 days
immersion



After 7 days
immersion



B- Results of Chromated Systems

- Electrochemical Testing

Table 4.34 below gives the corrosion rates results obtained from potentiodynamic curves of chromated deposits (Both laboratory and commercially treated samples). For comparison those of non-chromated deposits are also included. Although for each individual sample a potentiodynamic scan was run, Figure 4.58 represents those of Schloetter and Canning systems only for sake of clarity.

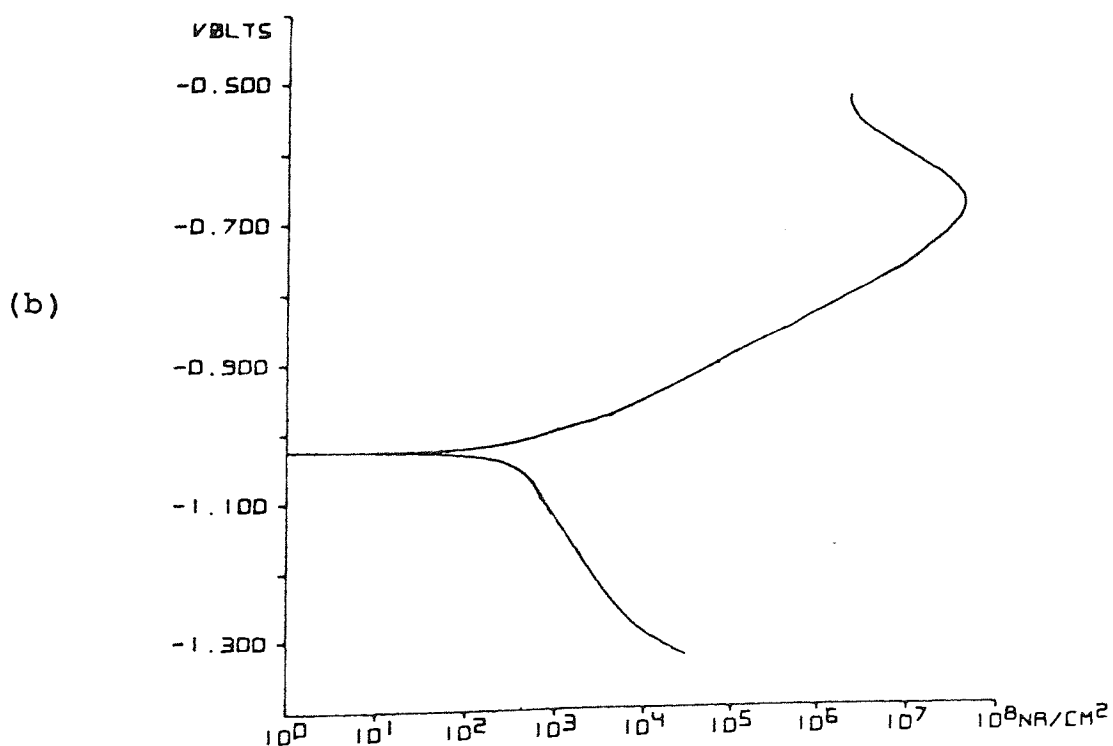
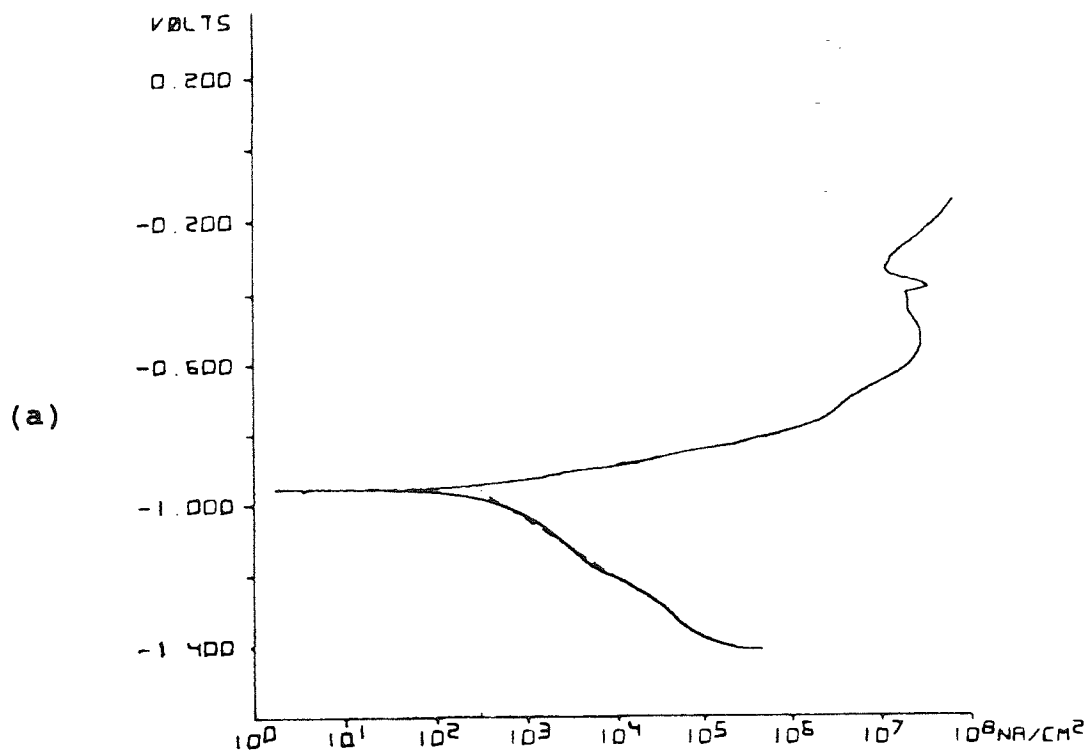
Table 4.34 Corrosion rate results obtained from potentiodynamic curves.

Samples	Code	I_{corr} μAcm^{-2}
Chromated commercial samples (as received):		
Pure Zn (L7C)	Zn	4.6
Zincrolyte (0.3% Co)	Znct	1.4
Canning (0.7% Co)	cann 1	-
Canning (1.0% Co)	cann 2	0.4
Schloetter (13.8% Ni)	Sch	0.3
Non-chromated commercial samples (as received):		
Pure Zn	Zn*	10.0
Zincrolyte	Znct*	7.3
Schloetter	Sch*	4.5
Dull deposits treated in solution (1) for 120 seconds:		
Pure Zn		8.7
0.3 Ni		8.1
12.4 "		2.9
0.3 Co		6.1
8.2 "		5.3

The codes assigned to samples are arbitrary.

The results are illustrated graphically in Figures 4.59 and 4.60.

Fig.4.58 Polarization curves for Commercially Chromated Systems: (a) Schloetter (13.8% Ni) and (b) Canning (1.0% Co) samples.



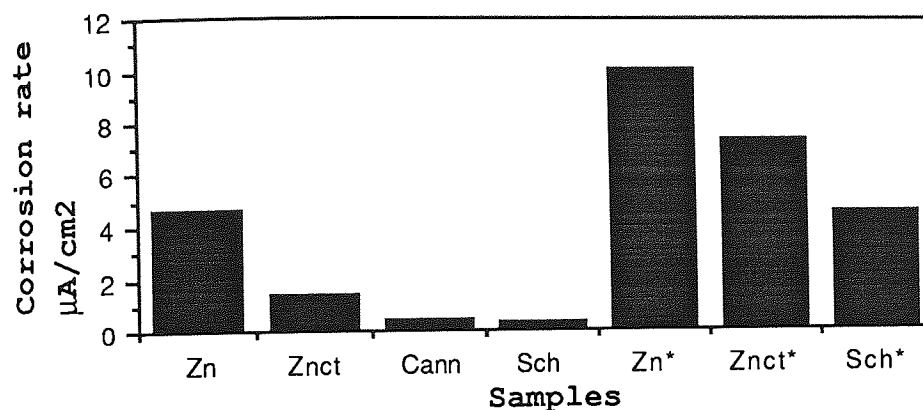


Fig. 4.59 Corrosion rate of Commercial samples, (as received)
* Non-chromated samples.

(Data extracted from potentiodynamic curves)

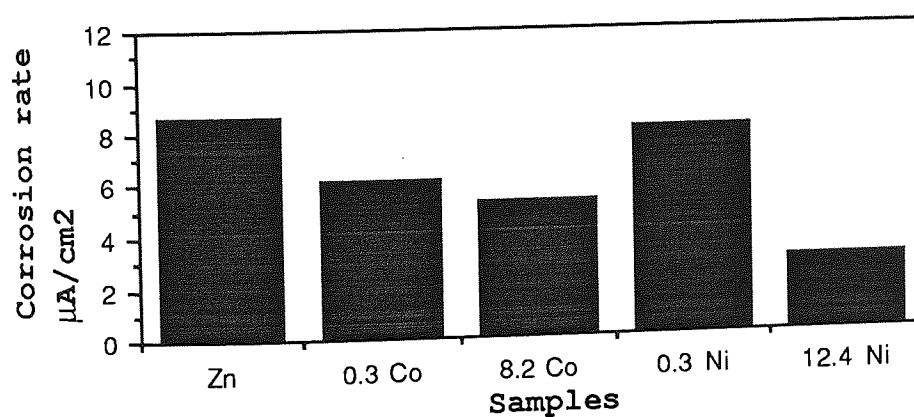


Fig. 4.60 Corrosion rate of Dull deposits Treated
in solution (1).

(Data extracted from potentiodynamic curves)

- Neutral Salt Spray Testing

Tables 4.35-4.37 and Figures 4.61-4.68 show the results obtained in neutral salt spray testing for chromated deposits, (both commercially and laboratory treated samples). Again the results of some non-treated deposits are also given for comparison. The results are reported as time (hours) to first black, white and red rust.

Table 4.35 Salt spray results of commercial chromated samples, (as received). After 580 hours of salt fog.

Samples	Thickness μm	Hours to Black rust	Hours to White rust	Hours to Red rust
Zn (CR31)	9.2	-	30	96
Zn (L7C)	9.2	102	148	201, 122*
Zincrolyte (0.3% Co)	12.0	148	201	480, 201*
Canning (0.7% Co)	5.5	201	226	302, 110*
Canning (1.0% Co)	12.0	-	360	>580, 302*
Schloetter (13.8% Ni)	9.5	417	480	>580, 360*

*Non-chromated samples after 365 hours of salt fog.

The above results are also displayed in Figures 4.61-4.63.

Fig.4.61 Photographs of corroded commercial chromated samples. After 580 hours of salt fog.

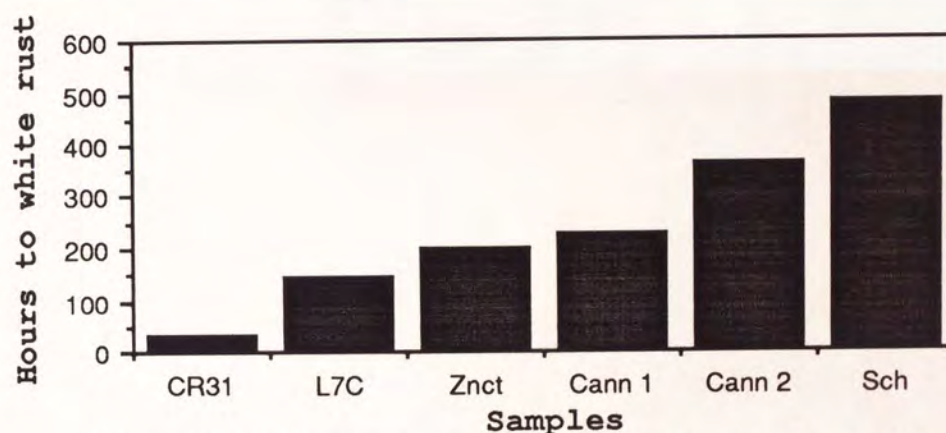
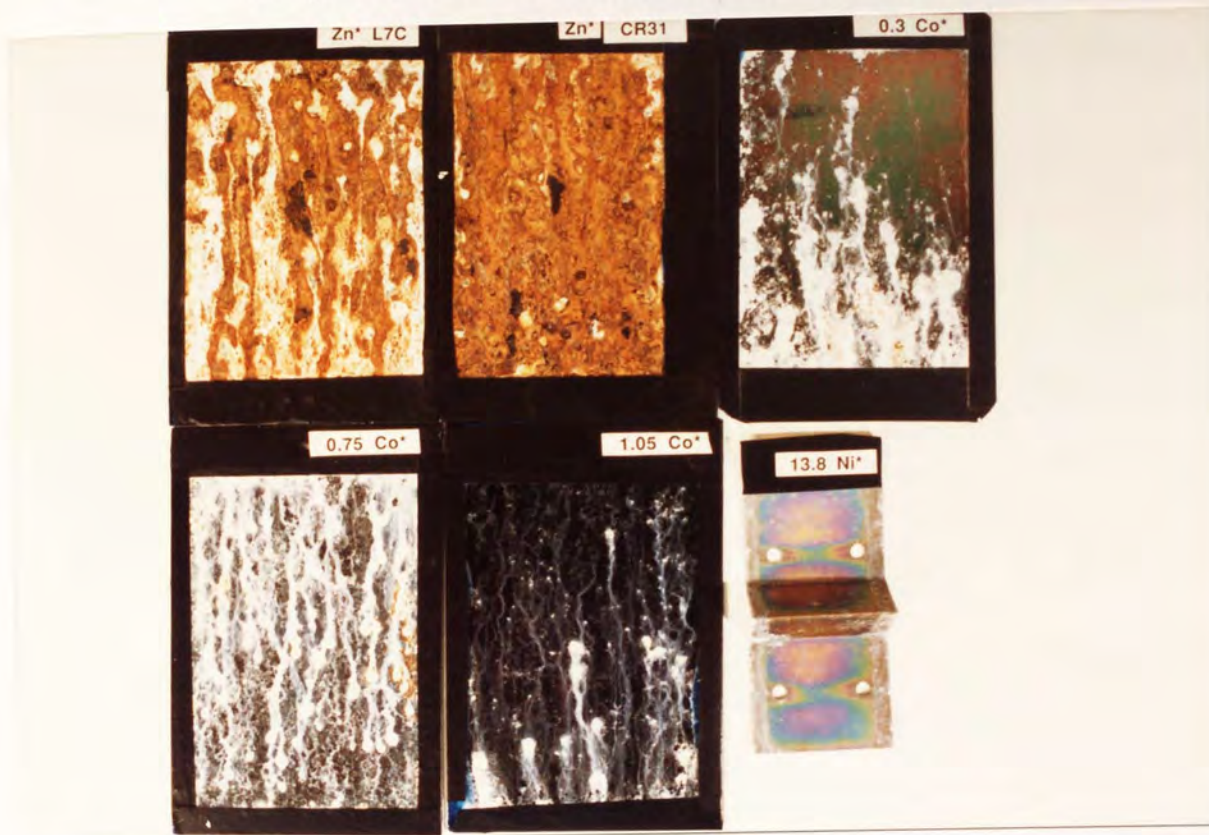


Fig. 4.62 Resistance to White rust in Salt spray test of Commercial Chromated samples, (as received).

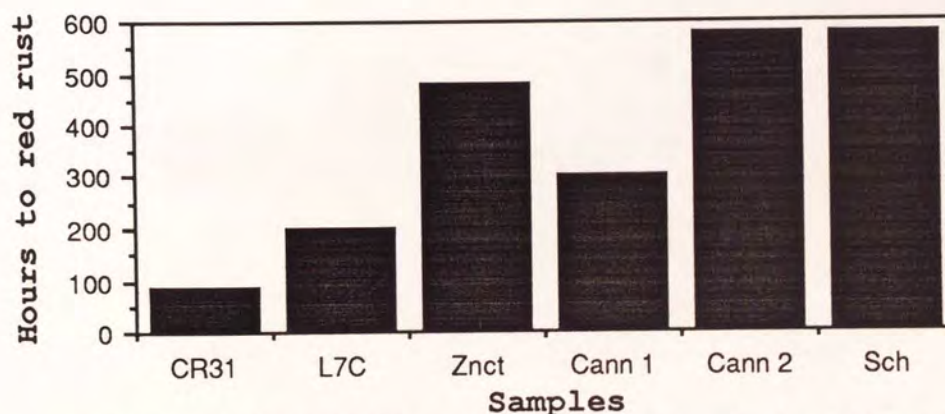


Fig. 4.63 Resistance to Red rust in Salt spray test of Commercial Chromated samples, (as received).

Fig 4.64 Photographs of bright non-chromated samples.
After 365 hours of salt fog.

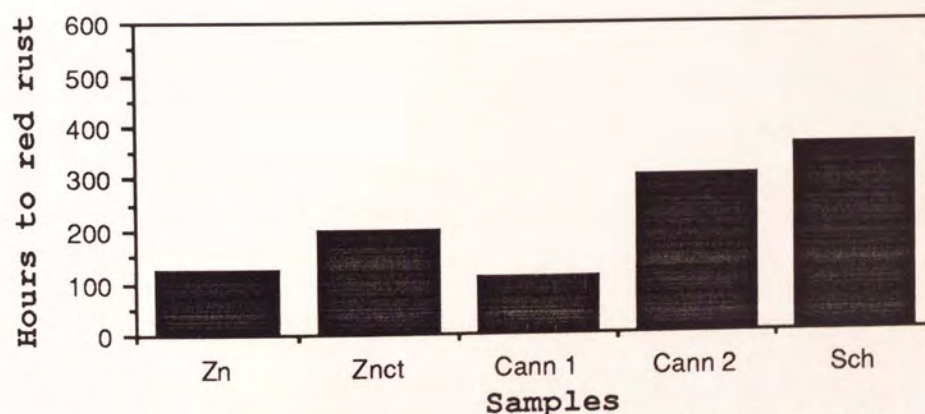
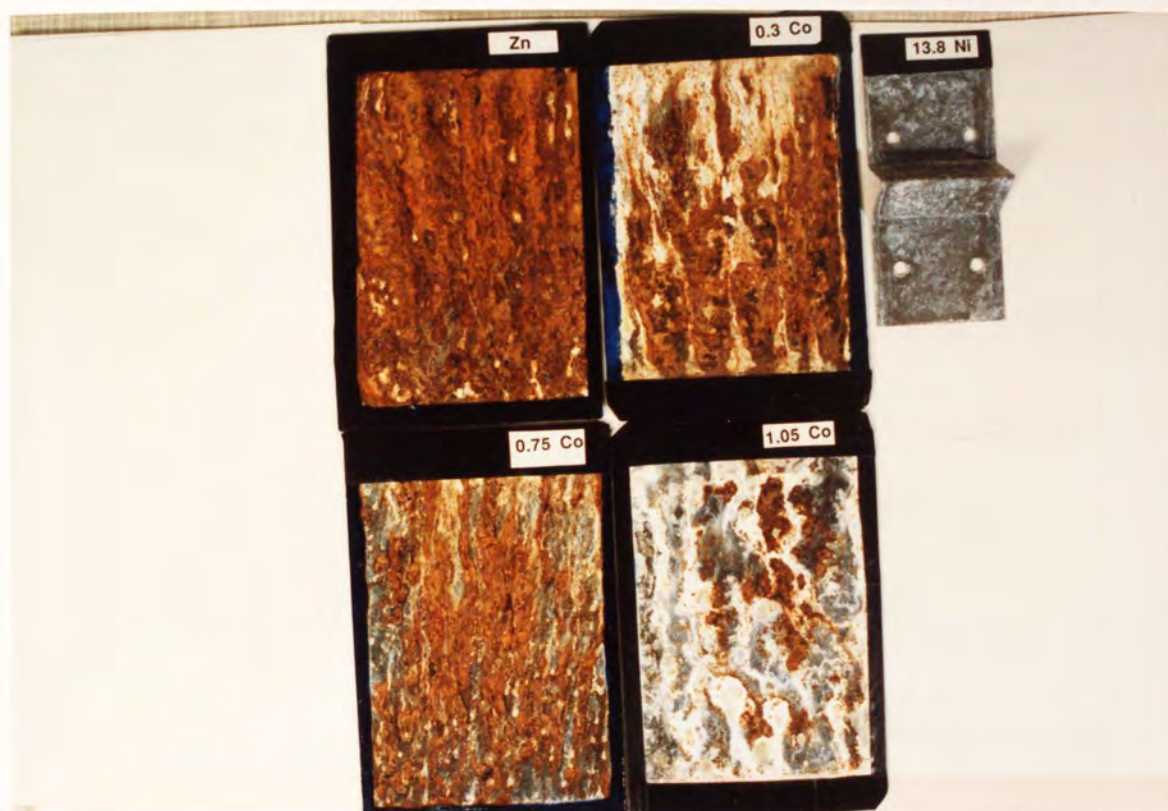


Fig. 4.65 Resistance to Red rust in Salt spray test of
Bright Non-Chromated samples, (as received).

Table 4.36 Salt spray results of commercial bright samples {treated in solution (1) for 120 seconds, after 580 hours of salt fog.

Samples	Hours to White rust	Hours to Red rust
Zn	102	148
Zincrolyte	102	360
Canning (0.7% Co)	60	226
Canning (1.0% Co)	70	450
Schloetter	110	480

The above results are also illustrated in Figures 4.66-4.68.

Fig. 4.66 Photographs of corroded commercial deposits treated in solution (1) for 120 seconds. After 580 hours of salt fog.

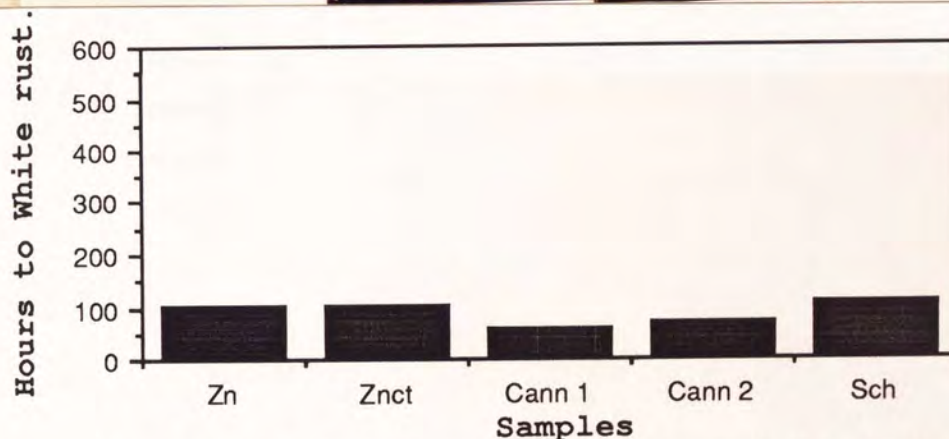
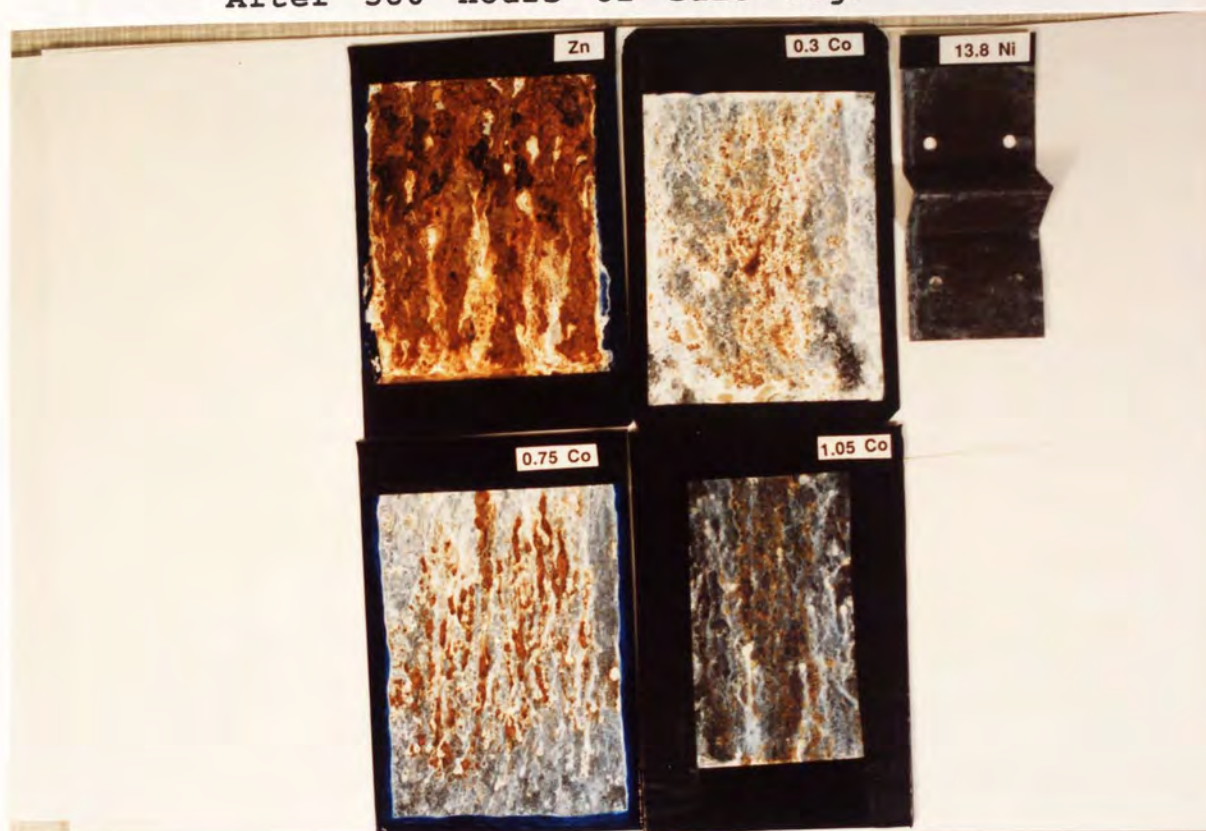


Fig. 4.67 Resistance to White rust in Salt spray test of Bright samples Treated in Solution (1).

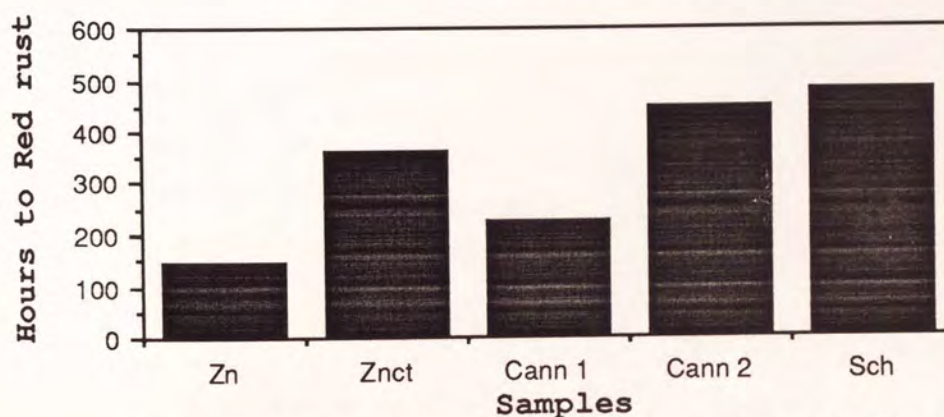


Fig. 4.68 Resistance to Red rust in Salt spray test of Bright samples Treated in Solution (1).

Table 4.37 Salt spray results of dull deposits {treated in solution (1) for 120 seconds}. After 580 hours of salt fog.

Zn-Ni Systems			Zn-Co Systems		
% Ni	Hours to White rust	Hours to Red rust	% Co	Hours to White rust	Hours to Red rust
Zn	102	190	0.3	102	210
0.3	102	201	1.5	102	292
1.3	102	201	5.1	110	360
7.6	201	> 580	8.2	70	360
12.4	60	490	14.7	60	500
13.9	70	490			
21.3	70	360			

The above results are also illustrated in Figures 4.69-4.71.

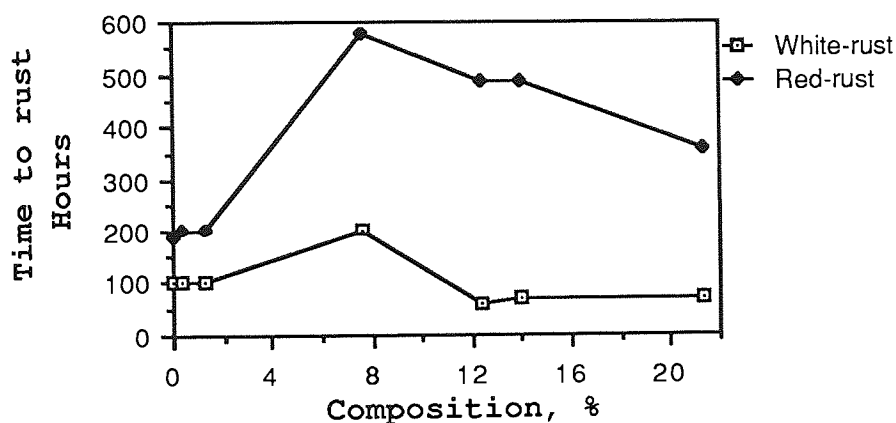


Fig.4.69 Time to White and Red rust for Dull Zn-Ni deposits Treated in Solution (1).

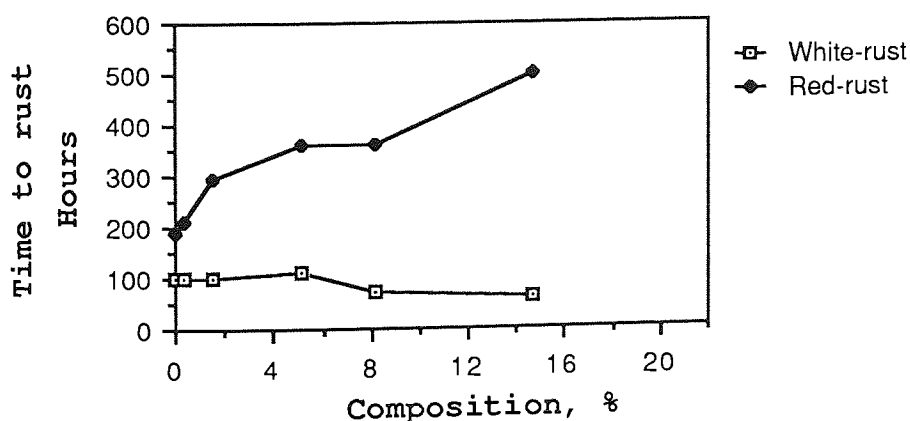
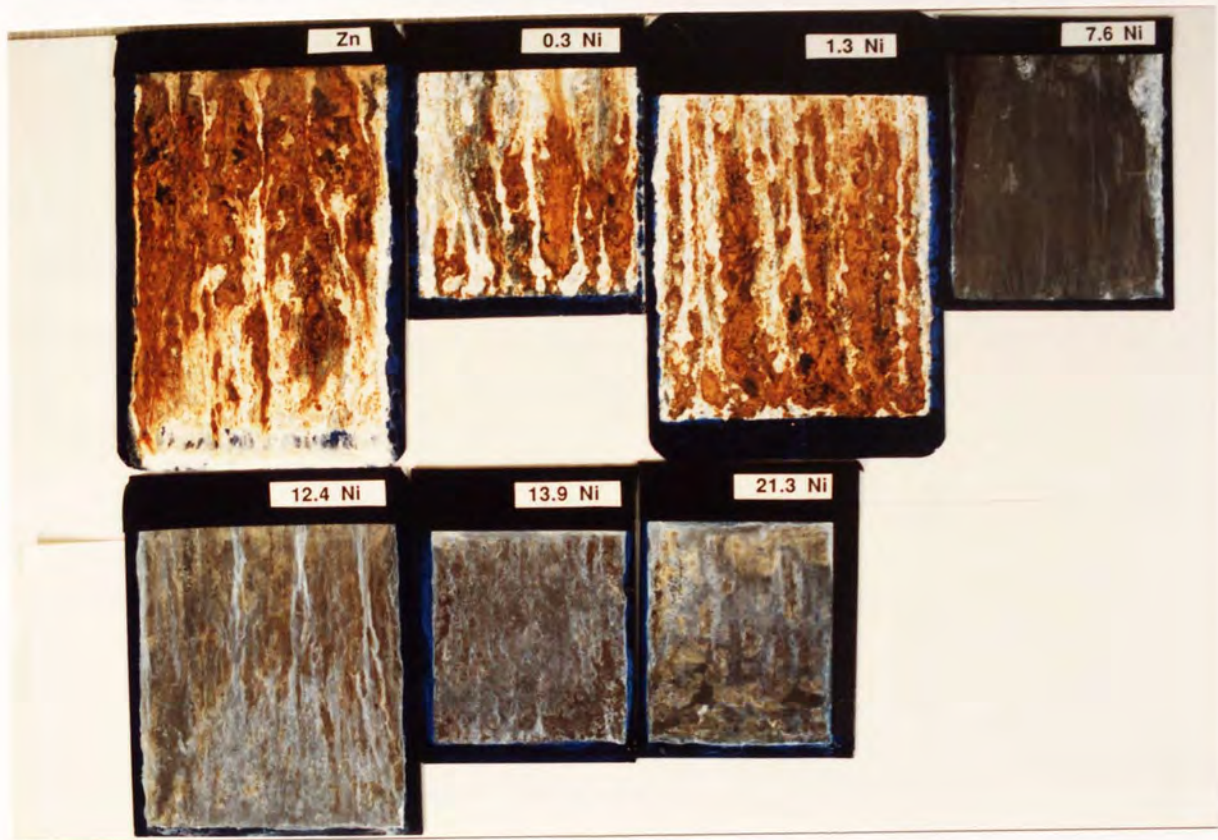


Fig.4.70 Time to White and Red rust for Dull Zn-Co deposits treated in Solution (1).

Fig.4.71 Photographs of corroded chromated dull deposits treated in solution (1) for 120 seconds. After 580 hours of salt fog.



a- Zn-Ni Coatings



b- Zn-Co Coatings

- XPS Study

Several workers (85,72) relate the resistance to white rust of chromated samples to the amount of Cr and to the ratio of Cr(III) to Cr(VI) in the chromate film.. However as shown in Table 4.38 below this is not the case. Neither of these factors had an effect on the white corrosion resistance of the systems studied in this work.

Table 4.38 Relationship between the Cr(III)/Cr(VI) ratio, %Cr in the film and the resistance to white rust.

Samples	Cr(III)** Cr(VI)	%Cr	Hours to White rust
Zn	6.0	39	102+
0.3% Ni	6.4	35	102+
12.4 "	19.5	21	60+
0.3 Co	1.0	33	102+
5.1 "	4.0	29	110+
14.7 "	3.6	26	60+
<hr/>			
Zn * (L7C)	6.8	6	148++
0.7% Co*	5.6	3	226++
1.0% Co*	5.6	-	360++
13.8% Ni*	10.6	9	480++

* Commercial chromated samples (as received)

** Taken from Table 4.28

+ Taken from Table 4.37

++ Taken from Table 4.35

- Scanning Electron Microscopy Study of Corroded Chromate Samples

The following micrographs illustrate the probable mechanisms of failure of some of commercially chromated samples.

Figure 4.72 shows the presence of a black spot on the surface of 0.7% Co plate 5.5 μm thick. When the spot was removed (Figures 4.72a-c), it can be seen clearly that corrosion had occurred through to the steel substrate.

Figure 4.73 shows white rust on a 13.8 % Ni sample (9.5 μm thick). The subsequent X-ray maps for Cr, Zn and Cl indicated that as corrosion proceeded, the depletion of Cr took place (Figure 4.72b) exposing therefore the underlayer coat of Zn-Ni.

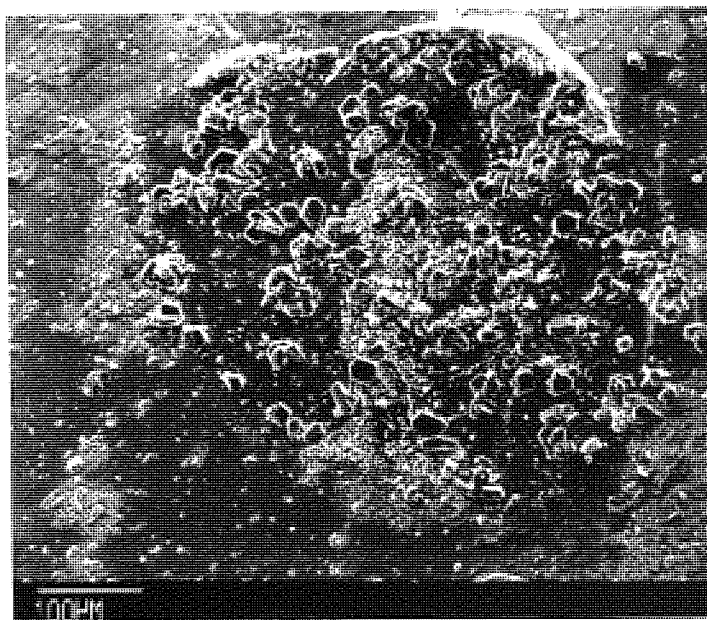
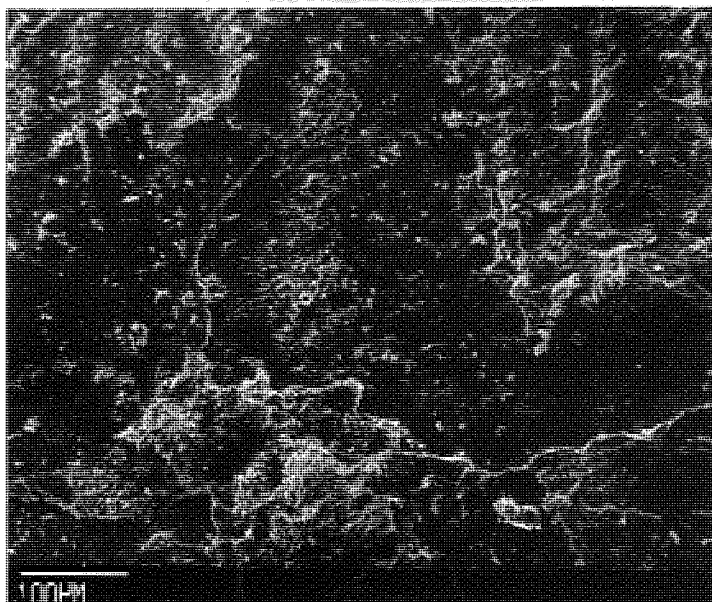
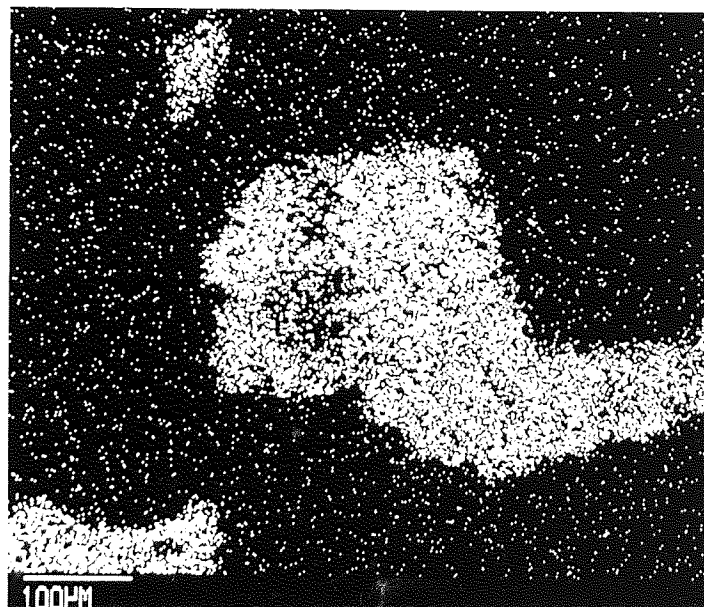


Fig.4.72 Scanning electron micrograph showing a black spot on a corroded chromated 0.7% Co deposit. After 580 hours of salt fog.

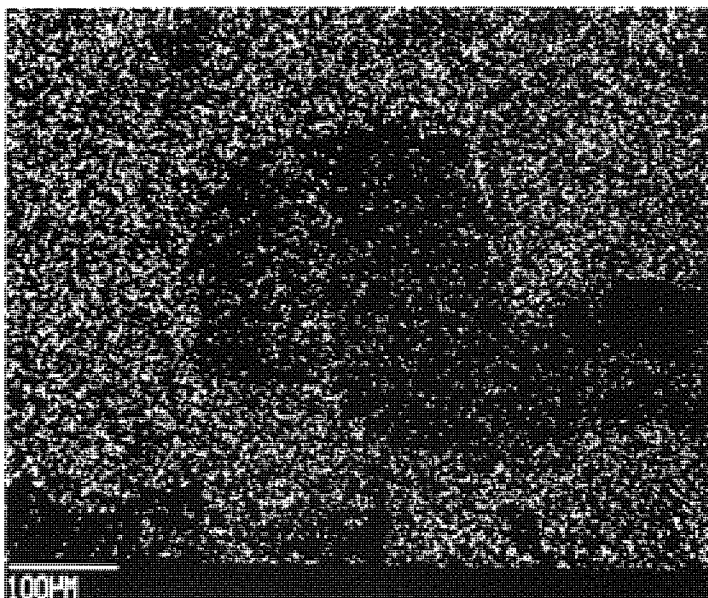
a- After removal
of black spot

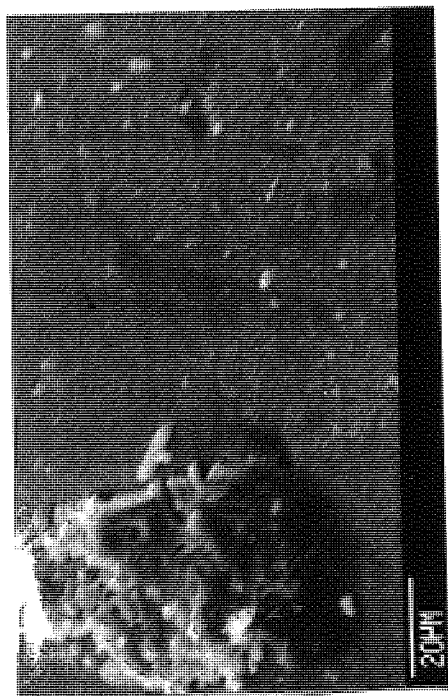


b- X-ray map
for Fe

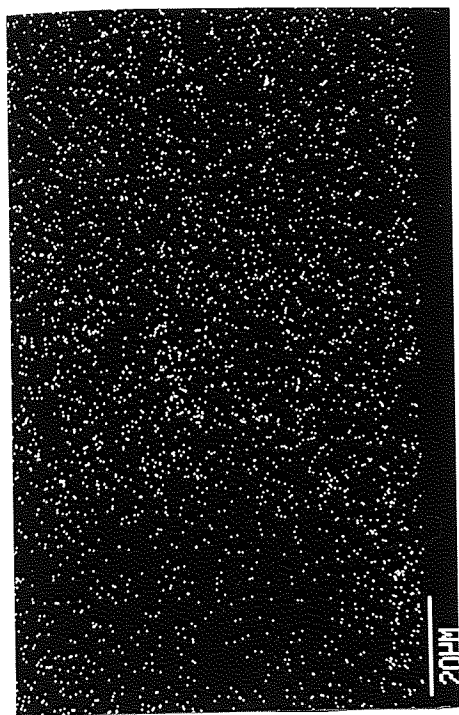


c- X-ray map
for Zn

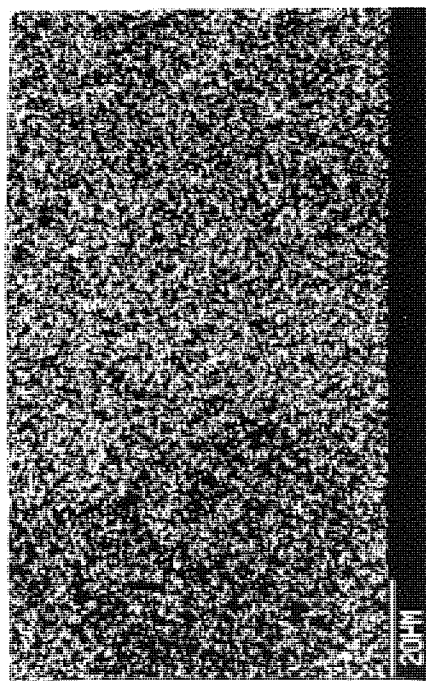




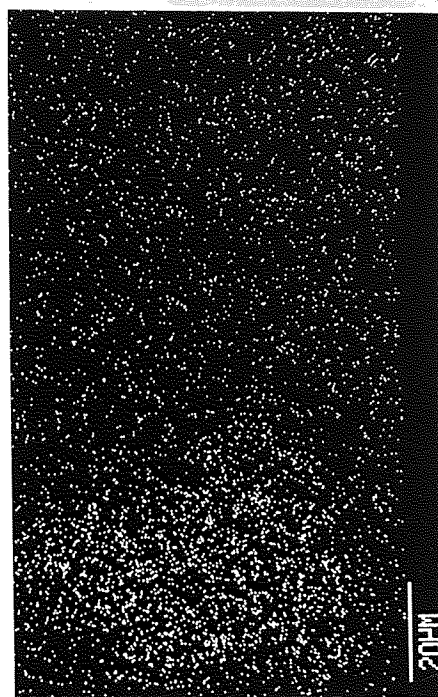
(a) General micrograph



(b) X-ray map for Cr



(c) X-ray map for Zn



(d) X-ray map for Cl

Fig. 4.73 Scanning electron micrographs showing white rust on corroded chromated Schloetter deposit (13.8% Ni). After 580 hours of salt fog.

5 DISCUSSION OF RESULTS

5.1 Zn Alloy Electrodeposition

5.1.1 Generalities

It is well known that for two metals to codeposit, the conditions must be such that the more negative potential of the less noble metal (Zn in this case) must be attained by the more noble (Ni or Co) without using an excessive current density^(23,109); the potentials of the two metals must be brought close together. The importance of this condition follows from the fact that the more noble metal deposits preferentially in a two metal system. An electrode can only have one potential at a time; therefore for the two reactions to take place simultaneously at an electrode, they must take place at the same potential.

The static electrode potential of Zn is -0.76 V, that of Ni -0.25 V Ni and that of Co -0.28 V, (on the hydrogen scale), with a separation of 0.51 V for Zn-Ni system and 0.48 v for Zn-Co system. Therefore it would appear to be impractical to codeposit them from simple salt solutions. In fact, as shown in this work, the codeposition was not only possible but the Zn deposited in higher concentrations in the alloy in most cases, (e.g., Figure 4.1). This is referred to as "Anomalous codeposition" and is characterised by the anomaly that the less noble metal deposits preferentially. The broken line in Figure 4.3 (page 129) labelled C.R.L indicates the Composition Reference Line which shows that the weight

percentage composition of the alloy just equals the metal percentage of the bath.

The metal percentage of a metal in the bath is defined by Brenner⁽²³⁾ as $(Ax100)/(A+B)$, where A and B are, respectively, the concentrations by weight of each metal in the alloy plating bath. In the case in which the content of Ni or Co metal in the alloy lies above the CRL, the electrodeposition of normal type occurs, because the alloy contains a larger ratio of Ni or Co to Zn than in the bath, and hence the electrochemically more noble Fe-group (Ni or Co) metal deposits preferentially. On the other hand, the points below the CRL represent the anomalous codeposition in which the preferential deposition of less noble Zn occurs.

5.1.2 Zn-Ni Systems

5.1.2.1 Ammonium Chloride Based Solutions

As shown in Figures 4.1 and 4.3, the deposit Ni content increased gradually with increasing Ni concentrations in the electrolytes and decreased with increasing current density. The effect of the latter was more pronounced at higher Ni bath concentrations (see Figure 4.1). At low Ni bath content (1.0 gl^{-1}), more uniform deposit composition was achieved over the current density range studied ($0.5\text{--}4.0 \text{ Adm}^{-2}$). In the case of the deposits obtained from 1.0 gl^{-1} Ni solution, the deposit Ni content varied from 9.9 to 7.9 over the current density range studied, whereas in the case of the deposit obtained from 40.0 gl^{-1} Ni solution, the deposit Ni

content varied from 36.6 to 20.2% Ni over the same current density range. Thus the production of Zn-Ni alloy of consistent composition from high Ni plating solutions would require much closer control than would be the case for low Ni content baths. For solutions containing 5.0, 10.0, 15.0 and 20.0 gl^{-1} Ni, the effect was more pronounced at low current density range ($0.5\text{--}1.0 \text{ Adm}^{-2}$). At and above 2.0 Adm^{-2} , there was a relatively small change in alloy composition.

In all cases, the cathode current efficiency for alloy deposition decreased with increasing current density, i.e., at high current densities the formation of hydrogen lowered the current efficiency. However there seemed to be no effect of Ni concentration in the plating solutions on the cathode current efficiency.

As illustrated in Figure 4.3, the anomalous behaviour was affected by current density as well as by the Ni solution concentrations. For each individual plating current density studied, there existed a limiting bath composition, (point at which the curve and CRL intercept) and this increased with decreasing current density. At 0.5 adm^{-2} the bath composition limit was about 15% Ni whereas at 4.0 Adm^{-2} it was about 10 %. Therefore for the plating solution having Ni concentration less than 10% by weight (1.0 gl^{-1}), the codeposition is normal for the current density range investigated whereas for those having more than 15% by

weight (5.0 g l^{-1}) the reverse is true.

Several attempts have been made by other workers to explain the mechanism of anomalous codeposition. It is widely accepted that the most plausible mechanism is explained by the hydroxide suppression mechanism. This concept is based on the postulation that Ni deposition is retarded by the formation of a Zn hydroxide film on the cathode surface due to an increase of pH adjacent to the cathode. It follows therefore that plating conditions which promote formation of this film decrease the Ni content of the deposit and vice versa.

As shown in Table 4.13 (page 135) the deposit obtained using air agitation contains 17.0% Ni and the deposit obtained under the same plating conditions but without agitation consisted of 13.0% Ni. Undoubtedly, the effect of turbulence due to agitation disturbed and influenced the growth of the Zn hydroxide layer, permitting therefore high Ni contents in the deposits. During air agitation, a certain amount of carbon dioxide is available to react with the Zn hydroxide forming basic carbonates. These are less protective than the hydroxides⁽¹¹⁰⁾ and hence allow Ni ions to diffuse through onto the cathode resulting in higher Ni content in the coatings.

Figure 4.8 shows the effect of temperature on deposit Ni content. As the temperature varied from 25.0 to 40.0°C, the

Ni content in the deposits increased from 12.5 to 28.8 % respectively. The increase in temperature has also resulted in increase in cathode current efficiency (Table 4.11), therefore the level of hydrogen evolution was expected to decrease. Probably this latter was preventing the rise in pH in the vicinity of the cathode and subsequent formation of a Zn hydroxide layer on the cathode surface.

That a high pH produced a high Ni content in the coatings (Figure 4.9) seemed to be inconsistent with the hydroxide suppression mechanism.

- Macro Throwing Power, (M.T.P)

One of the most important properties of an electrolyte is its throwing power. In electroplating, throwing power is a measure of the extent to which a plating bath deposits a coating of uniform thickness on different parts of a cathode surface. According to Bandes⁽¹¹¹⁾, two main factors affecting the throwing power: 1- polarization and 2- variation in current efficiency with current density. As we have seen previously (Figure 4.2 page 128)), as the current density increased, the cathode current efficiency decreased, therefore there would be less tendency for thick deposits to be plated in high current density regions, i.e., the metal distribution would be more uniform over the cathode surface.

Polarization itself is a very complex phenomenon and depends on several factors such as solution agitation, temperature,

conductivity, cathode position, etc. As shown in Figure 4.4, the increase in Ni concentration of the plating solutions resulted in a gradual decrease in macro throwing power. As the Ni metal ions were added to the solutions in a form of metal chloride, the concentration of chloride ions also increased. These are known to increase conductivity. Therefore the effect of increasing the metal concentration was twofold: it increased the solution conductivity and it reduced the concentration polarization. It should be noted that the increase in conductivity favoured better throwing power⁽¹¹²⁾ whereas the increase in bath concentration reduced the throwing power⁽¹¹³⁾. It seems that the overall effect was to decrease the throwing power.

The two methods used to assess current distribution on Hull cell panels showed the same effect of Ni concentration on macro throwing power. The macro throwing power results for the commercial 'Zincrolyte' Zn-Co plating solution were also included in Figures 4.4a and 4.4b. This solution was based on potassium chloride salt, low Co content (7.0 gl^{-1}) and commercial additives whose chemical nature is not known to the present author. The bath showed high macro throwing power values. The reason for this was probably due to the addition agents since many of these are known to have a significant beneficial effect on macro throwing power^(109,114). Good throwing power was achieved although the potassium chloride based solutions have poor throwing power compared to ammonium based solutions

- Deposit Characteristics

Visual observations were made to characterise deposit appearance. Deposits plated from baths at the low and high Ni concentration ends of the range (1.0 and 40.0 gl^{-1} Ni respectively) gave dark deposits over the current density range studied. However the deposits obtained from the 40.0 gl^{-1} Ni solution appeared to be much smoother. The deposits obtained from solutions containing 5.0 to 30.0 gl^{-1} were grey in appearance, although as the Ni concentrations increased, the deposits became dark-grey mainly at the low current density range (0.5-1.0 Adm^{-2}).

Photomicrographs of cross-sections in Figures 4.12 and 4.13 which compare deposits of about the same Ni content show dissimilar structures, emphasising the effect of the current density. High current densities resulted in columnar structure deposits whereas the low current density favoured a fine grained texture.

Heavy pitting was evident in the deposit obtained from a non-agitated solution (Figure 4.14). No pitting was observed when the solution was air agitated (Figure 4.15).

The Zn-Ni alloy coating systems exhibited a greater hardness than pure Zn. The hardness of the deposits increased with increase in the amount of Ni in the alloy, Figure 4.10. This should result in better wear resistance and therefore a longer service life of the plated components in some

applications.

5.1.2.2 Potassium Chloride Based Solutions

The effect of current density and solution Ni concentrations on deposit Ni contents observed for ammonium chloride based solutions discussed previously is the same for potassium chloride based solutions. The increase in current density resulted in the decrease in Ni content in deposits and increase in Ni concentration in solutions had the opposite effect (Figures 4.16 and 4.17). Again the increase in temperature resulted in the increase in Ni content in the coatings (Tables 4.15 and 4.16).

There was however a major difference between the Ni content in deposits obtained from the two solutions. Under the same plating conditions, ammonium based solutions yielded higher Ni contents in deposits. For example using the 40.0 gl^{-1} Ni solution, at 30.0°C , pH: 5.5 and current density: 1.0 Adm^{-2} , the deposit contained 28.9 %Ni (Table 4.7 page 127); whereas the sample plated from the KCl based solution contained only 23.8 %Ni (Table 4.16). The difference was even greater with low Ni concentration solutions. Again under the same plating conditions given above, but taking the 1.0 gl^{-1} Ni solution as an example; the specimen plated from the NH_4Cl bath contained 9.1 %Ni (Table 4.1) whereas from the KCl bath the deposit contained only 1.8 %Ni (Table 4.16); the difference ratio was about 5 to 1.

This difference in deposit Ni contents given by the two solutions was the result of the normal-anomalous codeposition phenomenon. As shown in Figures 4.18 and 4.19, the anomalous behaviour for KCl solutions was observed under all the plating conditions studied including the low Ni concentration electrolytes which showed normal deposition in the case of NH_4Cl solutions (Figure 4.3 page 129).

The deposits obtained from KCl solutions were somewhat less dark than their counterparts from NH_4Cl deposited under the same conditions.

5.1.3 Zn-Co Systems

- *Dull Deposits*

Only KCl based solutions were used to produce these deposits. The effect of the metal percentage of Co in the bath on the Co content of the deposits is shown in Figures 4.22 and 4.23 for both temperatures investigated 25.0 and 30.0°C respectively. Under all the plating conditions studied (temperature, current density and Co solution concentrations), the Co content in the deposits lied below C.R.L, indicating the preferential deposition of Zn. In this respect it is similar to its counterpart Zn-Ni systems obtained from KCl based solutions.

Figures 4.20 and 4.21 show also the relationship between the Co content in the deposits and the current density for

different Co solution concentrations. The Co content of the deposits obtained from high Co concentration baths showed a big dependence on current density, mainly at and above 5.0 gl^{-1} Co. As the current density increased the Co content in the deposits decreased. The deposits obtained from 1.0 gl^{-1} baths showed little variation in Co content with current density. Again increasing the temperature resulted in deposits richer in Co content (Tables 4.19 and 4.20), as in the case of Zn-Ni systems.

The deposit appearance was similar to that of Zn-Ni which were plated from KCl baths. However the deposits obtained from the 1.0 gl^{-1} Co solution were somewhat rough.

- Bright Deposits

Two different commercial Zn-Co systems were studied under this heading: 1- Zincrolyte system using a KCl based solution operating at pH of about 5.3 and 2- 'Canning' system consisting of an alkaline cyanide-free solution (pH:14.0).

An alkaline zincate solution consists, in its simplest form, of Zn oxide dissolved in concentrated NaOH solution. Several workers^(115,116) have listed many additives applicable to alkaline non-cyanide pure Zn baths. These include mixtures such as aromatic and heterocyclic aldehydes. To avoid the precipitation of insoluble Zn compounds Hajdu et al⁽¹¹⁷⁾ suggested a minimum Zn to NaOH ratio of 1:10. However in

contrast Darken⁽¹¹⁶⁾ indicated that the most efficient solution of those that he examined was 15 gl^{-1} Zn and 100 gl^{-1} NaOH which produced efficiencies similar to those of high cyanide solutions.

Assessed visually, both deposits obtained from the two electrolytes were very similar in brightness and smoothness and both having low Co contents, as compared to dull deposits discussed previously.

When compared with Zincrolyte, the 'Canning' system was much less efficient at high current density. The efficiency varied from 99.9 to 97.4% over a current density range of 1.0 - 4.0 Adm^{-2} (Table 4.23), whereas the efficiency of the 'Canning' solution, based on thickness measurements, decreased by about 50% over the same current density range (Table 4.25). The 'Canning' system was only efficient at a low current density of 1.0 Adm^{-2} .

A drawback of the alkaline cyanide-free solution, therefore, is the reduced efficiency. However, the fact that the efficiency dropped off sharply with an increase in current density is actually an advantage in that it would contribute to good throwing power on rack plated parts of intricate shape.

A second major difference between the two systems was the effect of current density on deposit Co contents obtained

from them. As illustrated in Figure 4.26, increasing the current density resulted in a slight decrease in the Co content in the case of the 'Canning' bath, whereas the opposite effect was observed for the other bath. This was probably due to the different mechanisms of metal deposition under the effect of the different addition agents present in these solutions. Since the nature of these chemicals is not known, it is very difficult to comment on the probable deposition mechanism of these alloys. However, it is well known that electrolytes in which the metals exist as complexes (as in the case of the 'Canning' system), the metal deposition is affected under conditions of high polarization⁽¹¹⁴⁾.

When compared with Zincrolyte, the KCl Zn-Co plating solutions containing no additives yielded deposits of high Co contents under the same plating conditions, (Figures 4.24 and 4.25), illustrating the effect of the additives in suppressing the Co deposition.

5.2 Conversion Coating

5.2.1 Laboratory Treated Samples

It is common practice to use post-plate treatments to improve corrosion resistance or appearance of Zn plated parts regardless of the type of the solutions used for plating. It has been stated however by some workers^(6,118), but not shown, that the formation of coloured chromate films having high corrosion resistance of Zn alloy electrodeposits is much more difficult than on pure Zn. Scanning electron microscopy and electron spectroscopy for chemical analysis were used in this work in order to elucidate the possible differences in surface composition and morphology that would account for this difference in reactivity to chromating.

Reported literature on the Zn-Ni and Zn-Co alloy systems is very scarce with perhaps only the work of Nikolova et al⁽⁶⁹⁾ attempting to approach the process in detail. They studied low Ni (up to 0.35% Ni) and low Co (up to 1.8% Co) deposits using the chromating solutions for treating pure Zn.

The chromating solution (1) given in Table 3.7 (page 113) was used to chromate both dull and bright deposits. The results are listed in Table 4.27 (page 156). It is very clear from the results that the film weight of the samples, termed 'true estimate', was very much dependent on immersion

time; it increased with increase of the latter. However the chromate coatings formed on bright smooth commercial deposits for an immersion time of 120 seconds, seemed to be poorly adhered to the substrate as noticed during treatment. Brownish sludge was observed to drip from the samples upon their removal from the beaker at the end of chromating process. Increasing the dip time from 60 to 90 seconds for 0.7% Co deposit resulted in a film weight increase from 277 to $321 \times 10^{-3} \text{ mgcm}^{-2}$; whereas on increasing the dip time to 120 seconds, the film weight decreased to $317 \times 10^{-3} \text{ mgcm}^{-2}$ (Table 4.27). This was not observed however for dull deposits which may be due to the increased bond strength for chemical conversion coating afforded by the roughness of the dull deposits.

For all the samples treated, the metal dissolution proceeded at very high rate and non-uniformly as illustrated in Table 4.27 and Figures 4.32-4.34. This may not be acceptable in practice since high and non-uniform dissolution of the metal may result in chemical composition change of the deposits. Also this will lead to rapid contamination of the chromating solutions.

The potential-time profiles in Figures 4.29-4.31 show the effect of Ni and Co on the potential of Zn when immersed in solution (1) for 120 seconds. All the systems seemed to show the same general behaviour i.e., the potential decreased rapidly from an instantaneous value on immersion to a

minimum where it stayed constant untill the end of the test. The main difference between the various samples was their positions in terms of nobility. As illustrated in Figures 4.29-4.31 for example, the chromating film formed on Zn deposits showed more negative potentials than the rest of the other systems, indicating that the surface was active and the chromating film was forming. This agreed well with the results of the film weight listed in Table 4.27. The 21.3% Ni deposit showed some resistance to chromating upon immersion as illustrated in Figure 4.29. The potential increased sharply from an instantaneous value on immersion of about 0.0 V on the hydrogen scale to a maximum value of about +0.1 V , then decreased at a relatively slow rate to a steady value.

The surface appearance of the treated samples as, would be expected, depended on immersion times and on the nature of the substrate as illustrated in Figures 4.35 and 4.36. Dull pure Zn and low Ni and Co deposits acquired a light brown colour when immersed for 15 seconds and as the immersion time increased to 120 seconds the colour of the films formed became dark brownish. High Ni and Co deposits were much lighter in colour, as illustrated.

Chromate films formed on dull and bright deposits had a different appearance. The Zincrolyte and Canning samples (0.3 and 0.7% Co respectively) treated in solution (1) for 15 seconds acquired an iridescent colour (see Figures 4.36c

and d) competing with commercially chromated samples (Figure 4.27 page 152). However when the Co content in the deposits is higher as in the case of the Canning sample containing about 1.0% Co, the colour degraded to brownish green patchy appearance, as illustrated in Figure 4.36e. Initial thoughts were that this was due to the probable inclusion of Co into the films. This is not the case however since the XPS study (as will be discussed later) showed no presence of Co in these systems. However Co may still be the cause in that it contaminated the chromating solutions as a result of its dissolution during treatment. Adaniya et al⁽⁶⁰⁾ showed that among the various elements added singly to the chromating bath, Co was the one which reduced considerably the reactivity of the deposit in the chromating solutions.

However under the scanning electron microscope these differences in surface colour were not extended to the structures. For dull deposits, the usual cracked pattern of chromate film was observed only for long immersion times i.e., 90 seconds and above. In fact, for immersion times of 60 seconds and less, the film structures under the scanning electron microscope looked exactly the same as non-chromated samples despite the evidence of film formation given by the film weight results as shown in Table 4.27.

Figure 4.37 shows clearly the variability in the film structures depending on the substrate from which it was grown. The film formed on the 14.7% Co sample for 120

seconds was not uniform as illustrated in Figure 4.37d. It is apparent from the figures that the film was less coherent and of variable thickness as compared with that formed on low Co content deposits.

This is not the case however for bright smooth samples. Figures 4.38 and 4.39 show the chromating film growth on bright smooth 1.0% Co and 13.8% Ni containing deposits respectively. Unlike previously, immersing for a short period of 15 seconds produced a cracked film and as the dip time increased the coating became thicker (see the chromate weight results in Table 4.27). However the cracks were not that evident for 13.8% Ni deposit. According to William⁽⁸¹⁾, the chromating film cracks occur as a result of heating. He showed that when the films formed on pure Zn were air dried, the cracks were not observed for all the samples investigated.

The nature of the chromating process is best explained as a chemical reaction and by considering the overall chemical reaction resulting from separate anodic and cathodic reactions. Although these reactions have not been examined in any details, it is nevertheless possible to make some reasonable conjectures about the nature of the anodic and cathodic reaction processes in the light of the results on film formation such as metal dissolution and weight change (see Table 4.27 page 156) and also by considering the results of the XPS study on films reported in Table 4.28.

Since the chromating solution is strongly acidic (pH of about 1.0), oxidizing in character (presence of chloride ions) and the coating dissolves in it i.e., both metals Zn, Ni/or Co as shown in Table 4.27; it must be therefore assumed that the anodic reaction is as follows:



Where M represent Zn, Ni or Co and M^{n+} their corresponding ions. This dissolution of metal is accompanied by a corresponding reduction of Cr (VI), introduced in the solution as CrO_3 to Cr (III). The total amount of the dissolved metal M is a measure of the dissolution reaction. The amount of precipitation, (see Table 4.27) termed 'true estimate' is a measure for the growth of the chromating film. The presence of chloride ions is vital as several workers^(55,74) have shown that in pure CrO_3 solution Zn did not dissolve to any appreciable extent.

The surface layer composition of some selected samples, (those treated for 120 seconds and destined for salt spray testing), was investigated by the use of the XPS technique so that all the elements present in the surface of the film could be identified, (see Figures 4.40-4.42). The results are summarized in Table 4.28. These show that all kinds of the chromate layers regardless of their substrate (pure Zn, Zn-Ni or Zn-Co) consisted mainly of oxygen, zinc, chromium (in the metallic state as well as in trivalent and hexavalent states) and chlorine. In all cases the

Cr(III)/Cr(VI) ratio was equal to or above 1.0. However, it has been reported that the reduction of Cr(VI) to Cr(III) can take place during electron spectroscopy⁽⁷⁵⁾.

Some exceptions to these observations are concerned with the 0.3% Ni and 0.3% Co samples for which there was no Zn detected at all in the spectra generated by both Al and Mg sources as shown in Figure 4.41b. Cl was only detected in very small quantity for all the samples studied. In fact, unless it was specifically sought in the spectrum, the spectrum would normally have been regarded as perhaps having a slight background variation in the regions corresponding to this element, (see Figures 4.40a and 4.41a). Both Ni and Co peaks (at binding energies of 852.3 and 777.9 eV respectively) were not detected on all the surfaces of the samples studied.

Unfortunately the XPS spectroscopy techniques do not reveal the presence of hydrogen as which is known to be an important constituent in these films^(73,76,81). Using accelerated positive ions and Auger analyses, Barnes et al⁽⁷⁶⁾ have shown that a range of chromate conversion coatings on Zn deposits contained H as one of the major constituents.

Although the spectrometer used in this work was equipped with an Argon ion gun, depth profiling on specimens in order to see any change in chemical composition with the film

growth was not attempted because of the large number of different samples investigated and the consequent high costs.

The absence of Zn from the structures of certain samples such as 0.3% Ni and 0.3% Co suggests that the film is probably a hydrated basic chromium chromate of the following chemical composition: $\text{Cr}_2\text{O}_3 \cdot \text{CrO}_2 \cdot \text{H}_2\text{O}$ or $\text{Cr}(\text{OH})_3 \cdot \text{Cr}(\text{OH})\text{CrO}_4$.

The absence of Ni or Co peaks in the XPS spectra suggest that the films formed would have the same chemical composition as those formed on pure Zn. Therefore the chromate films containing Zn, Cr(III) and Cr(VI), O_2 , and assuming the presence of hydrogen, suggest from their chemical composition that the formula $\text{ZnCrO}_4 \cdot 4\text{Zn}(\text{OH})_2 \cdot \text{H}_2\text{O}$ is realistic.

5.2.2 Commercial Chromating Solutions

The main reason for using these solutions was for comparative purposes. The chemical formulations of these solutions were not known and therefore the assessment of the processes was rendered more difficult. The samples treated in the laboratory with these solutions were not analysed chemically using XPS technique. However, the technique was used to analyse the samples treated commercially, (see Table 4.28).

- *Schloetter Chromating Solution*

This solution was developed for Zn-Ni systems having high Ni contents of about 14% Ni. However, in this present work it has also been used for pure Zn and Zn-Co alloy coatings, (see Table 4.29). The surface appearance after chromating depended very much on the substrate. 0.3% Ni, 0.3% Co and pure Zn acquired the same very light clear yellowish colour. High Co content deposits (14.7% Co) did not change at all from as plated appearance i.e., it stayed dark. However an interesting feature was observed for the high Ni content deposits, e.g., 12.4% Ni sample. It acquired a colourful appearance as shown in Figure 4.45b but the appearance degraded to a brownish colour in the case of the 21.3% Ni deposit (Figure 4.45c). However, these differences in appearance were not obvious under the scanning electron microscope. The film structures resembled exactly those of non-chromated samples. This was due probably to the rough surfaces of the samples treated.

Table 4.29 and Figures 4.43 and 4.44 show the changes in sample weight, Zn dissolution, film weight termed 'True estimate' and surface appearance after treatment. It should be noted that the Ni and Co dissolution results are not given since the Ni and Co were not detected in the chromating solutions analyses by the atomic absorption spectrophotometry. As illustrated in Figures 4.43 and 4.44, the reactivity to chromating of Zn-Ni and Zn-Co systems was very different. Zn-Ni systems seemed to accept chromating

more readily as Ni content increased whereas a decrease in film true estimate for 14.7% Co was observed.

- *Canning Chromating Solution*

The ability to form chromating films on dull deposits was very much dependent on the immersion times in the case of Canning chromating solution. Treating for times less than 90 seconds gave no colour changes. Even for an immersion period as long as 120 seconds, only pure Zn, 0.3% Ni and 0.3% Co showed slight changes in colour as indicated in Table 4.30. Again under the scanning electron microscope there was no evidence of film formation at all i.e., the films structure resembled those of non-treated deposits.

5.3 Corrosion

5.3.1 Non-Chromated Systems

- Electrochemical Testing

The potential-pH equilibrium diagram⁽¹¹⁹⁾ of the Zn-Water system shows extensive corrosion zones at both low and high pH values, see Figure 5.1 below. The limitations of such equilibrium diagrams, however, are considerable, for instance practical corrosion problems more often involve significant departures from equilibrium. These diagrams refer only to pure metal and not to alloys (as in this present work) corroding in pure water with no chloride ions present.

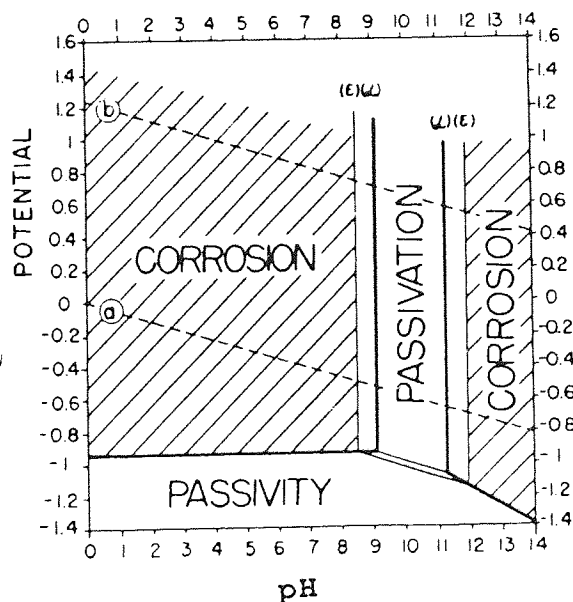


Fig.5.1 Conditions of corrosion and passivity of Zn as determined from the potential-pH diagram. Potential, in V, referred to the normal hydrogen electrode.

However, when a metal component undergoes corrosion in an aqueous environment, it cannot be treated as a single

electrode having a thermodynamically significant potential as indicated in the diagram. Instead, it will acquire a mixed potential at which the rate of release of electrons by dissolution of the sample as ions, the anodic reaction, is equal to the rate of their consumption by cathodic reactions. It is this exchange current, I_{corr} as termed throughout this work, between the anode and the cathode reactions which determine the corrosion rate of the system. For more details see section 2.7 (page 66).

The corrosion rates of both dull and bright non-chromated deposits were evaluated using the linear polarization technique. The results are given in Tables 4.31 and 4.32 (pages 182 and 184) which also include the corrosion potentials of the samples as a function of immersion time as well as b_a values, anodic Tafel constants. As it is shown clearly in Figures 4.48, potentiodynamic curves, that the Tafel slopes of the cathodic parts of the curves approached infinity. This was related to the presence of oxygen in the test solutions used as these were aerated. In the presence of oxygen the cathodic reduction (reaction 3, page 67) rate is dependent on the rate of diffusion of O_2 to the corroding sample surface. Under these circumstances, the cathodic polarization curves would typically show very steep slopes^(106,120), as illustrated in Figure 4.48.

As indicated in Tables 4.31 and 4.32 and subsequently in

Figures 4.49-4.54, Zn and low Ni and Co (<0.4%) content deposits corroded more rapidly than did the high Ni and Co deposits. This agreed well with the neutral salt spray results (as will be discussed later). Figures 4.51 and 4.52 show the variation in corrosion rate and corrosion potential with time for deposits containing up to 19.9% Co. Values of corrosion rate for alloys containing 0.4, 7.5 and 19.9% Co were very similar to those of pure Zn. Only the alloy containing 4.6% Co showed any real reduction. The corrosion potential for pure Zn and alloys containing up to 7.5% Co all showed very similar values whilst the alloy containing 19.9% Co was significantly more noble. Upon immersion, all the systems showed high corrosion rates, very active surfaces (see corrosion potentials values after 60 minutes immersion). As the immersion time increased there was a gradual significant decrease in corrosion rates. This can be related to the corrosion products formed on the samples surfaces acting as a barrier and protecting the samples.

As indicated in Table 4.31, when the Ni content of the deposits increased from 0.4 to 21.3% Ni the corrosion potential changed from -1035 to -840 mV respectively, becoming more noble. The increase in nobility of the samples with immersion time was also observed, (see Figures 4.50, 4.52 and 4.54) for all the Zn alloy systems and this was more pronounced with high alloying content deposits, mainly 12.4, 21.3 %Ni and 19.9% Co deposits. However the corrosion potentials of the samples were still lower than that of

steel (-0.570mV), therefore the galvanic protection of this latter metal may be assured.

Even though linear polarization is a very useful technique in corrosion rate determination, it has a major disadvantage in that it requires additional knowledge regarding the magnitude of the Tafel slopes of the partial anodic and cathodic reactions which are not always easy to determine. As shown in Figure 4.48, the cathodic Tafel region approached infinity due to the O_2 diffusion control and the anodic part of the curve was less than a decade. Moreover the Tafel slope values given in Table 4.31 were used throughout the tests, whereas it is well known that they vary^(94,97,98) with different reactions predominating at different corrosion potentials of the deposits, as illustrated in Figures 4.50 and 4.52. As it can be seen from Figure 4.48c, the straight line portion did not extend more than half of decade and the curvature of the anodic part of the graph made it very difficult to draw a convincing Tafel slope. Probably this was the reason for the scatter in the results obtained from linear polarization measurements, see Figures 4.49 and 4.51.

Figures 4.53 and 4.54 show the variation in corrosion rate and corrosion potential with time for the commercially (bright and smooth) produced deposits. The corrosion rate for pure Zn and the alloy containing 0.3% Co were very similar whilst those for 1.0% Co and 13.8% Ni were smaller

and very similar to each other. The corrosion potentials were very similar to those obtained when using laboratory prepared alloys of corresponding composition. Low Co content deposits did not perform as well as claimed by the supplier.

- Neutral Salt Spray Testing

Following neutral salt spray testing of non-chromated dull deposits about 15 μm in thickness, pure Zn and low Ni and Co content systems exhibited heavier corrosion than did the rest of the samples, see Figures 4.55 and 4.56, The resistance to red corrosion was superior for Zn-Ni alloys for which there was a peak in resistance at about 11-14% Ni. This agrees well with the results found by several other workers^(28,55). In the case of Co the peak was at 4-8% Co. These results are in good agreement with those obtained by the linear polarization method.

However, no work has been found in the literature on corrosion performance of Zn-Co systems having high Co contents, >1.0% Co.

- Corrosion Mechanism of Non-Chromated Systems

Attempts have been made by several workers^(55,121) to explain the superior corrosion resistance of Zn alloy coatings. The most popular theory for Zn-Ni systems is the barrier protection mechanism provided by the layer enriched with Ni remaining subsequent to dezincification⁽¹²¹⁾, i.e., during corrosion of Zn-Ni deposits Zn dissolves

preferentially leaving a top layer enriched with Ni, this would then act as a mechanical barrier towards further attack. However, this theory as it stands does not explain why 12.4% Ni performs far better than 21.3% Ni and much lower Ni contents for instance, as shown by this present work and also by the results of the workers who put forward the theory⁽⁵⁵⁾.

Certainly, the depletion of Zn and subsequent surface Ni enrichment during corrosion did take place as confirmed in this work. Suitable areas covered with white rust were cut from two non-chromated dull samples after neutral salt spray testing: 12.4 and 21.3% Ni. The corrosion products were removed in 20% CrO_3 solution at 80°C and then the samples were analysed. The EDXA results showed that the 12.4% Ni sample surface was increased to about 32% Ni and the second deposit to about 43% Ni. However it has been reported in the literature that these high Ni content deposits performed in less satisfactory manner than pure Zn coatings (55,111). This Ni enrichment phenomenon was also supported by the results of the corrosion potentials, see Figures 4.50 and 4.54 which show the increase in nobility as corrosion proceeded as a result of Ni increase on the deposits.

It is likely that the crystal structure and surface morphology will affect the corrosion performance of alloys. As illustrated in Figure 4.57, the samples in as deposited state have a rough matt surface. Even though XRD study of

the structures of the deposits in as the deposited state was not attempted in this work, it is well established that the structure of Zn-Ni coatings depends on their Ni contents. According to⁽¹²¹⁾, their structure is as follows:

<u>Percent Ni</u>	<u>Phase present</u>
Up to 11%	$(\gamma + \eta)$
11-14%	γ
Above 14%	$(\gamma + \alpha)$

Probably the best corrosion performance is given by the γ phase (12.4% Ni) due to the absence of local cells between different phases as would be the case for the systems $(\gamma + \eta)$ and $(\gamma + \alpha)$, as a result of one phase being more noble than the other.

Several investigators^(51,55) relate the superior corrosion behavior of Zn alloy coatings compared with pure Zn to the different corrosion products formed on the two systems. They showed by using the XRD technique that the corrosion products on Zn alloy (both Zn-Ni and Zn-Co) consisted of mostly Zn hydroxy chloride and some Zn hydroxy carbonate. Corrosion products on the pure Zn also contained these compounds, plus a minor fraction of Zn oxide (ZnO). Some have suggested that the Zn hydroxy chloride corrosion product is less conductive than Zn oxide, and that the lower conductivity accounts for the better corrosion performance of the Zn alloy coatings compared with pure Zn. Even when

ZnO is formed it is argued that the elements such as Ni or Co act to lower the electrical conductivity of ZnO by a doping effect as ZnO is an n-type semi-conductor.

The XRD study in this present work revealed that in the case of all samples studied, pure Zn, Zn-Ni and Zn-Co the corrosion products consisted of Zn hydroxy chloride in the form of $\text{Zn}_5(\text{OH})_8\text{Cl}_2$; moreover pure Zn and low Ni and Co contents (0.3% Ni and 0.3% Co) also contained ZnO and that is probably the reason why they gave poor corrosion performance.

5.3.2 Chromated systems

The linear polarization technique was not attempted for chromated samples since it is based on the assumption that uniform corrosion takes place over the whole specimen surface⁽¹⁰⁶⁾; a condition that would not have been obtained for the chromated samples due to their cracked structure morphology. Instead potentiodynamic polarization scans were carried out. The corrosion rates, I_{corr} , were calculated from these potentiodynamic graphs by simple back extrapolation to the corrosion potentials.

As in Table 4.34 (page 193) and subsequently Figures 4.58-4.60, chromated samples showed low corrosion rates as compared with the non-treated ones. It can be seen clearly that Zn alloy coatings are superior to pure Zn, the

Schloetter sample (13.8%Ni) had the lowest corrosion rate, followed by the Canning sample (1.0%Co) and then Zincrolyte (0.3%Co), (Figure 4.59). It should be noted, however, that not all chromate treatments are very beneficial and values for the laboratory chromated samples were only just less than the non-conversion coated ones, (Figure 4.60).

The results of the neutral salt spray tests also indicated the importance of the chromated films. Figures 4.69-4.71 show the time to white and red rust for laboratory prepared Zn-Ni and Zn-Co deposits plus a conversion coating produced using the laboratory chromate solution. In the case of Ni deposits the effect of chromating was twofold in that there was an increase in time to red rust at all compositions and the range of compositions for peak resistance was widened. Whilst in the case of Co deposits there was an increase in time to red rust for all compositions and this time increased as the percentage Co increased.

The good correlation obtained between the results from neutral salt spray and those from electrochemical tests was probably because the same corrosion mechanism was involved since the same test solution was used for both methods of corrosion evaluation, (5% by weight NaCl solution).

As reported by Verberne et al⁽⁶¹⁾, the test environment was of paramount importance. In their neutral salt spray testing (ASTM B117) they found that Zn-Ni systems performed better

than Zn-Co (0.5% Co) and pure Zn, as confirmed in this present work. However, the Kesternich test DIN 50018 results showed the reverse, i.e., Zn-Ni systems showed poor performance as compared with pure Zn and Zn-Co, this latter being the best. Their mobile testing results on the other hand showed another different trend in corrosion behaviour i.e., after 1 and 1/2 months the Zn deposits exhibited severe damage to the passivate film (black spots) whereas the Zn alloys were still perfect. After 5 months all the passivate films on Zn and Zn-Ni were completely destroyed whilst in contrast the passivate was intact on 90% of the surface of Zn-Co. Mobile testing simulate the service conditions in which the samples were attached to the underside of a vehicle on an area where water and dirt are projected during driving.

- Corrosion mechanism of chromated systems

As already shown, the corrosion resistance was improved considerably by conversion coatings and the type of the conversion coating was very important. The corrosion protection afforded by the conversion coatings depends on several factors. As reported by Darken (122), it depends on the substrate on which it forms and the composition of the chromating solution. He showed that the Zn deposits obtained from acid plating solutions corroded at a much faster rate than the alkaline deposits. Anderson (85), on the other hand indicated that the major factor that determines corrosion resistance is the amount of Cr(VI) in the chromate

conversion films, whereas Pocock et al (72) have suggested to the contrary, i.e., Cr(III) is important. This is not what has been found in the present work. As shown in Table 4.38 (page 203), the ratio of Cr(III) to Cr(VI) in the chromate films had no effect on the white corrosion resistance of the systems. For instance, the Schloetter deposit which showed the maximum corrosion resistance had a high ratio of about 10.6 and the dull Zn-Ni (12.4%) treated in the laboratory prepared conversion coating solution, which showed the least corrosion resistance, contained the highest proportion of Cr(III). On the other hand, the 14.7% Co deposit containing a relatively high proportion of Cr(VI) showed poor corrosion resistance.

Certainly the protection mechanism by these conversion films is a complex Phenomenon where several factors such as the substrate, conversion solution or Cr valence may inter-relate with one another. The systems studied in this work were totally different from one another ranging from pure Zn to different compositions of Ni and Co alloy coatings obtained from different plating solutions and treated differently. Therefore, it would be impossible to pin point the general cause or protection mechanism afforded by these systems. However some comments are worth making on the light of the present results.

The first visible sign of corrosion during neutral salt spray testing was the appearance of black spots on most

samples, as illustrated in Figure 4.72. The initial step seemed to be the breakdown of the chromate film followed by corrosion of the Zn alloy plate right to the steel substrate, as evidenced by X-ray mapping in Figure 4.72a-c. The initiation of these spots was probably due to bad chromating.

Figure 4.73 shows white rust on the Schloetter sample (13.8 % Ni) 9.5 μ m thick. Subsequent Cr X-ray mapping, (Figure 4.73b) illustrates clearly the depletion of chromium from the corroded areas of the sample, exposing therefore the Zn-Ni deposit which would result eventually in corrosion.

6 CONCLUSIONS

- Zn Alloy Electrodeposition

In the electrodeposition of alloys, difficulties are often encountered in obtaining an alloy with a consistent chemical composition. It has been found that composition depends on many plating parameters such as, solution concentration, current density, temperature, agitation and pH. The Zn alloy systems are not an exception to this as shown in this work. The plating solutions of these alloys (Ni and Co) used gave anomalous codeposition. The major conclusions found during the present work can be summarized as follows:

From the work on an ammonium chloride based solutions it was found that the following Zn-Ni plating solution and operating conditions gave the optimum results.

Constituent salt	gl ⁻¹	Metal Conc. gl ⁻¹
ZnCl ₂	-	30.0
NiCl ₂ .6H ₂ O	-	15.0
NH ₄ Cl	200	-
Ammonia (25%)	50ml ⁻¹	-

pH : 5.5
C.D : 3.0 Adm⁻²
Temp : 25.0°C
Agitation Air

The above plating solution and operating conditions yielded deposits of grey colour which were smooth and have a Ni content of about 12.5 %, the optimum composition for maximum corrosion resistance. The Zn and Ni distribution in the coating was uniform.

The deposit Ni content increased with increase in Ni bath concentration, temperature, pH and solution agitation, but decreased considerably with increase in current density. However, at a low Ni bath content of 1.0 gl^{-1} (Ni metal) the effect of current density was much less pronounced, resulting in much easier control of Ni content in the deposits.

- In all cases the cathode current efficiency decreased with increase in current density.
- As Ni metal concentration in the electrolyte was raised, the throwing power deteriorated.

- The major difference between the ammonium Zn-Ni based solution and the potassium one was that under the same plating conditions the latter yielded a lower Ni content in deposits.

- The same remarks for Zn-Ni coatings obtained from potassium based solutions can be made for their counter parts Zn-Co. i.e., under the same plating conditions the Co content in deposits obtained from potassium chloride Zn-Co solution was lower than the Ni content in the deposits obtained from the ammonium chloride based Zn-Ni solution.

- The alkaline Canning solution had a lower cathode current efficiency than the acid 'Zincrolyte' bath at high current densities. However this would contribute to good throwing power.

- Increasing the current density resulted in slight decrease in the deposit Co content in the case of 'Canning' solution, whereas the opposite effect was observed for the 'Zincrolyte' bath.

- When selecting a process for a new installation or to replace an existing bath, the plater should consider exactly which properties/characteristics are most important for the job in hand. There is no single answer for all applications. However, there are some features which make one process superior to another, for instance, as shown in this present work, the cobalt content of deposits plated from Zincrolyte solution was more sensitive to variation in current density than in the case of deposits plated from the alkaline Canning solution. Although the Zincrolyte plating solution was more efficient than the Canning process at high current density, this would, however, result in poor throwing power when plating irregular shaped articles.

- *Conversion Coatings*

The surface state (in terms of roughness/smoothness and brightness) is of great significance in influencing the formulation of conversion coatings. For instance when

'Zincrolyte' and 'Canning' bright and smooth deposits were treated with the laboratory formulated solution, they acquired an iridescent colour competing with commercially treated deposits. However, the dull deposits acquired a brownish appearance as might be expected.

- The chromating mechanism appeared to include removal of both Zn and Ni (or Co) from the sample surface in the case of laboratory formulated solution. This was not the case for the Schloetter and Canning chromating solutions, only the dissolution of Zn took place.

- The metal dissolution proceeded at a fast rate in the case of the laboratory formulated solution due to its very acidic nature. This may not be acceptable in practice since it would lead to rapid bath contamination and also to the deposits chemical composition change.

- All the films consisted of Zn, Cr(Cr⁰, Cr(III) and Cr(VI)) and chlorine. In all cases the Cr(III)/Cr(VI) ratio equal to or above 1.0.

- **Corrosion**

All the experiments reported were carried out in 5% NaCl solution (pH of about 6.2) and it must be born in mind that the following conclusions apply to this electrolyte only.

- The correlation between the electrochemical test results and the neutral salt spray was good for both chromated and non-chromated systems.

- Non-chromated Zn-Ni electrodeposits containing about

11-14% Ni increased in corrosion resistance compared to pure Zn. Non-chromated Zn-Co deposits of composition $\leq 0.4\%$ Co offered little advantage over pure Zn and compositions of 4.0 to 8.0% Co were required to show any real effect. One commercial process was claimed to provide a significant improvement in corrosion resistance over Zn at a Co content of less than 1.0%.

- Corrosion resistance was improved considerably by conversion coating and for Zn-Ni deposits the beneficial range of compositions was widened to 6-16% Ni. When chromated the 0.3% Co alloy showed some improved corrosion resistance over chromated Zn. The percentage of Co needed to be $\geq 1.0\%$ Co to be equivalent to the optimum Zn-Ni alloy, even when both were chromated.

- The type of conversion coating was very important. Samples treated in laboratory solution performed badly compared to those treated in commercial solutions.

- Zn alloy coatings were superior to pure Zn, the Schloetter sample (13.8% Ni) had the lowest corrosion rate, followed by the Canning sample (1.0% Co) and then Zincrolyte (0.3% Co). Although the price of Ni metal is less than that of Co, the incorporation of such large amount of Ni in deposits (13.8% Ni) would certainly make it uneconomical especially when nearly the same corrosion resistance can be obtained with a much smaller amount of Co in deposits as shown in this work (e.g., 1.0% Co). However, it should be born in mind that the metal cost is not the total cost of providing the metallic coating system.

7 RECOMMENDATIONS FOR FURTHER WORK

1 Development of brightener and additive systems to suppress the Ni codeposition at low current density regions are necessary. Addition of complexing agents to improve the throwing power of the solution is also desirable.

- The use of pulse plating might be an alternative for improving deposit appearance, deposit chemical composition control and solution throwing power. Although a limited amount of work on pulse plating was carried out in this project, the results were not included in thesis.

2 Anode systems need further study to determine the most suitable and economic means of operation (pure Zn with occasional addition of Ni or Zn-Ni alloy anodes or separate Zn and Ni anodes systems).

3 Adequate chromating procedures

- Depth profiling should be carried out in order to study changes in composition throughout the film thickness. This could assist in studying the mechanism of formation.

- Factors such as chromate film thickness, its structure, its content (Cr valence) and the substrate nature should be studied separately in order to determine their effect on corrosion resistance.

4 Different corrosion testing environments need to be used. An in-depth study of the corrosion products produced in each

environment should be studied by XPS. The coatings are of particular interest to car manufacturers but components are exposed to different environments, for instance parts under the bonnet undergo temperature cycling effects whereas those under the vehicle are bombarded with a great deal of dirt and mud. Therefore an understanding of behaviours in a variety of environmental conditions and tests is essential. The use of a single standardized corrosion test as suggested by some car manufacturers can lead to the type of contradictory results reported in the literature.

The interest in Zn alloy plating is illustrated by the fact that in October 1988 a one day symposium on the subject was held at Aston University and attracted a significant number of overseas delegates as well as those from the U.K. As its conclusion the need was expressed for a large scale corrosion evaluation programme to determine the most appropriate coating system for specific environment and thus to eliminate the controversy over some existing information.

APPENDIX (123)

Electrode potentials* of several metals with respect to S.H.E.

Metal	Potential (v)
<hr/>	
Mg	-2.37
Al	-1.69
Zn	-0.76
Cr	-0.56
Fe	-0.44
Cd	-0.40
Co	-0.27
Ni	-0.25
Pd	-0.13
H ₂	Arbitrary Zero
Cu	+0.34
Pt	+1.20

* Electrode potential at 25°C with the base metal in contact with its divalent ions at normal activity and taking the corresponding hydrogen electrode potential as zero.

7 LIST OF REFERENCES

- 1 J.Oka, K.Saito, H.Asano and M.Takasugi. "Process for producing a highly corrosion resistant electroplated steel sheet". 1981, U.S.Pat.4 251 329.
- 2 R.Clark. "Europe's auto-galva-boom". Metal Bulletin Monthly, 1985, (6), 21.
- 3 S.W.Morgan, "Zinc and its Alloys and Compounds", Ellis Harwood Ltd, (1985).
- 4 H.Leidheiser, Jr. and I.Suzuki. "Towards a more corrosion resistant a galvanized steel". Corrosion, 1980, **36**(12), 701.
- 5 A.Shibuya, T.Kurimoto and K.Noji. "Corrosion resistance of Zn-Ni alloy plated steel sheet". Proceedings of Interfinish 80, 128 (1980).
- 6 M.Kamitani, T.Koga and H.Tsuji. "Electrodeposition of bright Zn-Ni alloys". Annu. Tech. Conf. Proc. am. electrop. Soc., 1985 paper D2 (1-23).
- 7 L.Domnikov. "Zn-Ni alloy coatings". Metal.Finishing, 1965, **63**(3), 63.
- 8 K.Matsudou, T.Adaniya, M.Ohmura and M.Kabasawa. " The development of NKFZ high corrosion resistant, composite Zn-coated steel sheet". Nippon Kokan Technical Report Overseas, 1979, No.26, pp. 10-16.
- 9 T.Adaniya and M.Ohmura. "Process for manufacturing Electrogalvanized Steel strip". U.K.Pat. GB 2070 063A (03.03.1981).
- 10 T.Adaniya. "The Development of Corrosion resistant

composite Zn-Coated Steel Sheet". Sheet Metal industries International, 1978, **55**(12), 73.

- 11 E.J.Kubel. "New technology in Sheet Steel". Materials Engineering, 1984, **99**(3), 24.
- 12 S.Nomura, H.Sabia, H.Nishimoto, I.Kokube and M.Iwai. "Newly developed Zn-Fe/Zn-Ni double layer Electroplated Steel Sheet". SAE Technical Paper No. 830518, Detroit (Feb 1983)p.75.
- 13 A.Catanzano, G.Arrigoni, M.Palladino and M.Sarracino. "Multilayer electrogalvanized (Zn-Cr-CrOX) steel sheet for optimum corrosion protection for car bodies". SAE International Congress & Exposition, Paper No. 830583. Detroit, (28 Feb - 4 March. 1983).
- 14 T.Adaniya, T.Homa, and Y.Ohkubo. "Electrodeposition of Fe-Zn Alloy Steel sheet". Nippon Kokan Technical Report Overseas, 1982, No.34, pp.41.
- 15 T.Adaniya, T.Hara, M.Sagiyama and T.Watanabe. "Fe-Zn Alloy Electrogalvanized Steel Sheet having a plurality of Fe-Zn alloy Coatings". UK Patent Application GB No. 2140035 A (21 Nov 1984).
- 16 F.C.Porter, A.M.Stoneman and R.G. Thilthorpe. "The range of Zn Coatings". Trans.Inst.Met.Fin, 1988, **66**, 28.
- 17 M.Sagiyama, T.Adaniya, T.Hara, and T.Urakawa. "Zn-Mn Alloy Electrodeposition for Automotive Body". SAE Paper 860268, Detroit (Feb 1986) pp.107.
- 18 E.W.Horvick. "Zn in the world of electroplating". Plating, 1959, **46**, (6), 639.
- 19 H.Geduld. "Alkaline - Non-cyanide Zn plating". Metal Finishing, 1973, **71**(8), 45.

- 20 H.G.Todt. " The current state of Zn deposition from alkaline and acid electrolytes". Trans.Inst.Met.Fin, 1973, **51**, 91.
- 21 R.R.Blair. "Quality cyanide Zn plating". Plating, 1970, **57**(4), 349.
- 22 J.A. Zehnder."Trouble shooting chloride Zn plating solutions". Plating & Surface Finishing, 1978, **65**(9), 14.
- 23 A.Brenner, "Electrodeposition of Alloys", Vol 1, New York. Academic Press. 1963.
- 24 H.Kohler, E.Knaab and I.Hadley. "Improvement of the corrosion resistance of Zn by codeposition of metals of 8th of sub-group". Metall.Oberflache, 1985, **39**(4), 139.
- 25 D.E.Hall. "Electrodeposited Zn-Ni alloy coatings - A review". Plating & Surface Finishing, 1983, **70**(11), 59.
- 26 J.Hadley and J.C.Verberne. "Electroplated Zn-Co alloy". U.K.Pat. G.B. 2116588 A, Sept. 1983.
- 27 T.Watanabe, M.Ohmura, T.Honma and T.Adaniya. "Zn-Fe alloy electroplated steel for automotive body panels". SAE Paper 820424 Detroit (Feb 1982), pp.1-8.
- 28 R.Noumi, H.Nagasaki, Y.Foboh and A.Shibuya. "Newly Developed Zn-Ni Alloy plated Steel Sheet 'SZ' and its Application to Automotive Usages". SAE Tech.Paper No.820332 (1982) Presented in Detroit MI, Feb 22-26 , 1982.
- 29 Laboratories of Dr,Ing Max Schloetter. "Electroplating Motor Vehicle parts with Slotoloy 10 Zn-Ni Alloy". Finishing, 1987, (12), 35.

- 30 J.Nicol & I.Philip. "Underpotential deposition and its relation to the anomalous deposition of metals and alloys". J.Electroanal.Chem., 1976 **70**(2), 233.
- 31 D.M Kolb and H.Gerischer. "Further aspects concerning the correlation between underpotential deposition and work function differences". Surface Science, 1975, **51**, 323.
- 32 K.Higashi, T.Adaniya & K.Matsudo."Mechanism of the electrodeposition of Zn Alloys containing a small amount of Co". J.Electrochem.Soc., 1981, **128**, 2081.
- 33 H.Dahms and I.M.Croll. "Anomalous codeposition of Fe-Ni alloy". J.Electrochem.Soc., 1965 **112**, 771.
- 34 Z.Kovac. "The effect of superimposed AC on DC in electrodeposition of Ni-Fe alloys". Ibid, 1971, **118**, 51.
- 35 E.Raub. "Theoretical and practical aspect of alloy plating". Plating and Surface Finishing, 1976, **63** (2), 29.
- 36 G.F.Hsu. "Zn-Ni alloy plating: An alternative to Cd". Plating & Surface Finishing, 1984 **71**(4), 52.
- 37 E.J.Roehl. "Electroplating a ductile Zn-Ni onto strip steel". U.S.Pat.3 420 754. (12.3.1969).
- 38 E.J.Roehl & R.H.Dillon. "Electroplating a ductile Zn-Ni onto strip steel". U.S.Pat.3 558 442, (26.1.1971).
- 39 B.Lustman. "Study of the deposition potentials and microstructures of electrodeposited Zn-Ni alloys". J.Electrochem.Soc., 1943, **84**, 363.
- 40 G.Baker. "Zn-Ni alloy electrodeposits: Rack plating".

- 41 A.Marchenko & V.Batyuk. "Electrolytic deposition of Zn-Ni alloys". J.Appl.Chem.USSR, 1964, **37**, 599.
- 42 S.R.Rajagapalan. "Electrodeposition of Zn-Ni alloys" Metal Finishing, 1972, **70**(12), 52.
- 43 J.W.Dini & H.R.Johnson. "Electrodeposition of Zn-Ni alloys coatings". Metal Finishing, 1979, **77**(8), 31.
- 44 V.Raman, M.Pushpavanam and B.A.Shenoi. "A bath for the deposition of bright Zn-Ni alloys". Metal Finishing, 1983, **81**(5), 85.
- 45 T.L.Rama Char and S.K.Panikarr. "Electrodeposition of Zn-Ni alloys from the pyrophosphate baths". Electroplating & Surface Finishing, 1960, **13**(11), 405.
- 46 M.Kurachi, K.Fujiwara and T.Tenaka. "Zn-Ni alloy coatings for steel strip". Proc. Cong. Int. Union Electrodeposition Sur. Finishing, p152, (1973).
- 47 G.B.Rynne. "Zn-Ni alloy electroplating baths". U.S.Pat.4 285 802, (25.8.1981).
- 48 H.Tsuji and M.Kamitani. "Electrodeposition and passivation of bright Zn-Ni alloys". Proc. 69th Annal.Conf., Paper p.2, (June 20-24, 1982).
- 49 R.Noumi, H.Nagasaki and A.Shibuya. "Zn-Ni alloy coatings". SAE, Technical Paper No.820 332, Detroit, (Feb.22 - 26, 1982).
- 50 T.Sauda and T.Kurimoto. "Electrolytic Zn-Ni alloy plating". U.S.Pat.4 249 999, (10.2.1981).
- 51 A.Shibuya, Y.Hoboh, N.Usuki and T.Kurimoto. "Development

- of Zn-Ni alloy plated steel sheet". Trans.Iron and Steel,Jpn., 1983, **23**(11), 923.
- 52 S.A.Watson. "Evaluation of Electrodeposited Coatings of Zn-Ni Alloys on Steel Sheet". Report of INCO Europe Ltd., London, England (Jan. 1982).
- 53 D.E.Hall. "Zn-Ni alloy deposition from a sulphamate bath". U.S.Pat.4 268 364, (19.5.1981).
- 54 T.A.Hirt and R.H.Dillon. "Electrodeposition of corrosion resistant Zn-Ni alloys onto steel substrates". U.S.Pat. 351 713, (28.9.1982).
- 55 Y.Miyoshi, J.Oka and S.Maeda. "Fundamental research on resistance of precoated steel sheet for automobiles". Trans.Iron and Steel, Jpn., 1983, **23**(11), 974.
- 56 S.M.Kochergin & G.R.Pobedimsk. "Use of radioactive isotopes in studies of the conditions of formation of electric alloy". Zhur.Priklad,Vihim, English Transl., 1985, Paper 1413-1414.
- 57 D.V. Subrahmanyam and T.L.Rama Char. "Zn-Co alloy deposition from the pyrophosphate bath". Chem. and Ind., 1963, (1), 69.
- 58 T.L.Rama Char and K.G.Sheth. "Zn-Co alloy deposition from sulphate bath". Chem and Ind., 1967, (2), 189.
- 59 H.Leidheiser, A.Vertes and M.L.Versang. "Mossbauer spectroscopic study of the chemical state of the Co in an electrodeposited Zn-Co alloy". J.Electrochem.Soc., 1981, **128**(7), 1456.
- 60 T.Adaniya. "Effect of addition elements on corrosion resistance and surface properties of electrogalvanized coatings". World Congress of Metal Finishing, 1976, 76

(9th), 1 - 16.

- 61 W.M.J.C.Verberne. "Zn-Co alloy electrodeposition". Trans.Inst.Met.Fin., 1986, **64**, 30.
- 62 H.Leidheiser and T.Suzuki. "Co and Ni cations as corrosion inhibitors for galvanized steel". J.Electrochem.Soc., 1981 , **128**(2), 242.
- 63 T.Adaniya, T.Hara, M.Sagiyama, T.Homa and T.Watanabe. "Zn-Fe Alloy electroplating on Strip Steel". Plating and Surface Finishing, 1985, **73**(8), 52.
- 64 F.W.Salt. "Electrodeposition of Zn-Fe alloys". British patent. 786 418, (1953).
- 65 S.Jepson, S.Meecham and F.W.Salt. "The electrodeposition of Zn-Fe alloys". Trans.Inst.Met. Fin., 1955, **32**, 160.
- 66 V.Sree and T.L.Rama Char. "The electrodeposition of Zn-Fe alloys from the pyrophosphate baths". Plating, 1961, **48**(1), 50.
- 67 S.S. Misra and T.L Rama Char. "Electrodeposition of Zn-Fe Alloys". Met.Fin., 1964, (6), 88.
- 68 T.Aoe, "Electrodeposition of Zn-Fe Alloy". New Materials and New Processes, 1985, **3**, 297.
- 69 M.Nikolova, I.Kristev, J.Cenov and L.Kristev. "Properties of chromate films upon Zn, Zn-Co and Zn-Ni electrodeposited coatings". Bulletin of electrochemistry 1987, **3**(6), 649.
- 70 M.Kamitani and H.Tsuji. "Chromate composition and process for treating Zn-Ni Alloys", U.S.Pat. 4 591 416 May 27, 1986.

- 71 W.Dingley. "Effects and control of Ni and Fe impurities in cyanide Zn plating baths". Proc.Am.electroplater's Soc., 1962, **49**, 155.
- 72 W.E.Pocock. "A survey of chromate treatments". Metal Finishing, 1954 , **52**(12), 48.
- 73 T.Biestek and J.Weber. "Electrolytic and Chemical Conversion Coatings", Portcullis Press Ltd. 1976.
- 74 L.F.G.Williams. "The mechanism of formation of chromate conversion films on Zn". Surface Technology, 1976, **4**, 355.
- 75 N.C.Davies and J.A.Treverton. "An XPS study of chromate pretreatment of aluminium". Metal Technology, 1977, **4**(10), 480.
- 76 C.Barnes, A.J.Bentley, L.G.Earwaker, J.P.G.Farr and J.M.C.Groves. "Nuclear reaction profiling of chromium conversion coatings". Trans.Inst.Met.Fin., 1985, **63**, 120, parts 3 and 4.
- 77 L.F.G.Williams. "Chromate conversion coatings on Zn". Plating, 1972, **59** (10), 931.
- 78 R.F.Reeves and N.J.Newhard. "Surface preparation of aluminium for painting". Industrial Heating 1969, **36**(4), 705.
- 79 T.W.Brown. Light Metal Tech. Report, 1973, **14**, 69
- 80 J.N.Newhard. "Conversion coatings for aluminium". Metal Finishing, 1972, **70**, 49.
- 81 L.F.G.Williams. "The formation and performance of chromate conversion coatings on Zn". Surface

Technology, 1977, **5**, 105.

- 82 J.P.G.Farr and S.V.Kulkarni. "The chromate and dichromate passivation of Zn". Trans.Inst.Met.Fin., 1966, **44**, 21.
- 83 R.E.Van de Leest. "Yellow chromate conversion coatings on Zn: Chemical composition and kinetics". Trans.Inst.Met.Fin., 1978, **56**, 51.
- 84 R.E.Van de Leest and J.Wessels. "Stabilization of Black Chromate Conversion Coatings on Zn". Plating and Surface Finishing, 1980, **67**, 86.
- 85 H.L.Katz, K.L.Proctor and F.Nagley. "Performance of various chromate supplementary films on electrodeposited Zn coatings". Amer.Soc.Testing Materials Proc., 1957, **57**, 203.
- 86 A.Gallacio, F.Pearlstein and M.R.D'Ambrosio. "Effect of heating chromate conversion coatings". Metal Finishing, 1966, **64**, 50.
- 87 L.F.G.Williams. "The effect of chromate content on the corrosion of chromated Zn electroplate on steel". Surface Technology, 1978, **7**, 113
- 88 R.Sard. "Advances in functional Zn and Zn alloy coatings". Plating and Surface Finishing, 1987, (2), 30.
- 89 H.E.Towsend and C.F.Meitzner. "Corrosion resistance of Zn/4% Al and Zn/7% Al alloy coatings compared to Zn and Zn/54% Al alloy coatings". Material Performance, 1983, **22**(1), 54.
- 90 EG & G Instruments. A Division of EG & G Ltd. . "Basics of corrosion measurements". Application Notes Corr-1 and Corr-4, 1982.

- 91 F.Mansfeld and M.W.Kendig. "Impedance spectroscopy as quality control and corrosion test for anodized Al alloys". Corrosion, 1985, **41**(8), 490.
- 92 A.Macias and C.Andrade. "Corrosion of Galvanized Steel in Reinforcement in Alkaline Solutions". Br.Corr.J, 1987, **22**(2), 113.
- 93 M.S.Walker and W.D.France. "New method developed for monitoring automotive cooling system corrosion". Materials Protection, 1969, **8**, 47.
- 94 M. Stern and A.L. Geary. "A theoretical analysis of the shape of polarization curves". Electrochem.Soc, 1957, **104** (1), 56.
- 95 K.B.Oldham and F.Mansfeld. " Discussion on the so-called linear polarization method for measurements of corrosion rates". Corrosion, 1971, **27** (10), 434.
- 96 D.A.Jones. "Discussion on the so-called linear polarization method for measurements of corrosion rates". Corrosion, 1972, **28** (5), 180.
- 97 S.Barnatt. "linear corrosion kinetics". Corrosion Science, 1969, **9**, 145.
- 98 S.K.Roy and S.C.Sircar. "Determination of Tafel Slopes and Corrosion Rates from Cathodic Polarization Curves", Br.Corr.J, 1978), **13** (4), 193.
- 99 B.Oldham & F.Mansfeld. "Corrosion rates from polarization curves - A new method". Corrosion Science, 1973, **13**, 813.
- 100 D.C.Crowe Yaske. "Corrosion rate monitoring in Kraft pulping of process liquors". Materials Performance. 1986, **25** (6), 18.

- 101 M.Dattilo. "Polarization and corrosion of electrogalvanized steel". J.Electrochem.Soc, 1985, **132** (11), 2557.
- 102 N.S.Berk and J.J.Friel. "Application of electrochemical techniques in screening metallic coated steels for atmospheric use", Laboratory Corrosion Tests and Standards. A symposium by ASTM committee G-1, 1983, 143. Bal Harbour.
- 103 H.Feitler. "Instantaneous corrosion rate measurements". Materials protection and Performance, 1970, **9**(10), 37.
- 104 D.W.Siitari, M.sagiyama and T.Hara. "Corrosion of Zn-Ni electrodeposited alloys". J.Iron and Steel Japan, 1983, **23**, 959.
- 105 S.A.Watson. " The throwing power of Ni and other plating solutions". Trans.Inst.Met.Fin., 1960 , **37**, 28.
- 106 M.Stern and A.L.Geary. "Electrochemical polarization". J.Electrochem.Soc., 1957, **104**, 56.
- 107 M.Stern, "a method for determining corrosion rates from linear Polarization data", Corrosion National Association of Corrosion Engineers,(NACE), Sept, 1958, **14**, 440t .
- 108 D.A.Luke. "Notes on throwing power measurements". Trans.Inst.Met.Fin., 1983, **61**, 64.
- 109 F.A.Lowenheim. "Electroplating". McGraw - Hill, Inc., 1978. p.368.
- 110 C.J.Slunder and W.Boyd. "Zn, its corrosion resistance", 1971, Int'l Lead Zn Research Organization, Inc.
- 111 H.Bandes. " The significance of polarization in

- electroplating". Metal Finishing, 1946, (12), 516.
- 112 R.Pinner. "Throwing power and covering power". part 1, Electroplating, Part 1, 1954, (1), 9. and Part 2, 1954, (2), 49.
- 113 D.A.Swalheim "Beneficial effects of polarization". Plating and Surface Finishing, 1985, (2), 16.
- 114 H.Silman. "Zn electroplating: an expanding industry". Electroplating and Metal Finishing, 1975, (2), 8.
- 115 B.S.James and W.R.Mc Whinmie. "The action of quaternary pyridinium addition agents in the electrodeposition of Zn from alkaline electrolytes". Trans.Inst.Met.Fin., 1980, **58**, 72.
- 116 J.Darken. "Recent progress in bright plating from zincate electrolytes". Trans.Inst.Met.Fin, 1979, **57**, 145.
- 117 J.Hajdu, J.A.Zehnder. "Bright Zn electroplating from low cyanide and cyanide-free alkaline solutions". Plating, 1972, **58**, 458.
- 118 T.Adaniya. "Method for manufacturing an electrogalvanized steel sheet excellent in bare corrosion resistance and adaptability to chromating". U.S. Pat. 4048381, 1977, Sep 13.
- 119 P.Delahay. "Potential-pH diagrams of Zn and its application to the study of Zn corrosion". J.Electrochem.Soc., 1951, **98**(3), 101.
- 120 D.A.Jones and N.Ramachandran Nair. "Electrochemical corrosion studies on Zn coated steel". Corrosion, 1985, **41**(6), 357.

- 121 M.R.Lambert, R.G.Hart and H.E.Townsend. "Corrosion mechanism of Zn-Ni alloy electrodeposited coatings". S.A.E Technical paper 831817. Warrendale, Pennsylvania, 1983.
- 122 J.Darken. "Recent progress in bright plating from zincate electrolytes". Trans.Inst.Met.Fin., 1979, **57**, 151.
- 123 C.W.Davies. "Electrochemistry". William Clows and Sons Ltd., 1967, p227.